The Hydrology of Malaria: Field Observations and Mechanistic Modeling of the Malaria Transmission Response to Environmental and Climatic Variability

by

Arne Bomblies

M.S. Civil and Environmental Engineering
University of Colorado

B.S. Chemical Engineering
Cornell University

Submitted to the Department of Civil and Environmental Engineering in partial fulfillment of the requirement for the degree of

Doctor of Philosophy in the Field of Hydrology

at the

MASSACHUSETTS INSTITUTE OF TECHNOLOGY
February 2009

Author ……..
Department of Civil and Environmental Engineering
December 15, 2008

Certified by……
Elfatih A.B. Eltahir
Professor of Civil and Environmental Engineering
Thesis supervisor

Accepted by ……..
Daniele Veneziano
Chairman, Departmental Committee for Graduate Students

The Hydrology of Malaria: Field Observations and Mechanistic Modeling of the Malaria Transmission Response to Environmental and Climatic Variability

by

Arne Bomblies

Submitted to the Department of Civil and Environmental Engineering on December 15, 2008, in partial fulfillment of the requirement for the degree of
Doctor of Philosophy in the Field of Hydrology

Abstract

A coupled HYDrology, Entomology and MAlaria Transmission Simulator (HYDREMATS) has been developed. The model simulates the hydrological and climatological determinants of malaria transmission mechanistically and at high spatial- and temporal resolution, and is valid for semi-arid, desert fringe environments where the mosquito *Anopheles gambiae s.l.* is the dominant malaria vector. This includes much of the most malarious parts of Africa such as the Sahel. The model is validated with several years of field data collected from Banizoumbou village in southwestern Niger. Simulations of the 2005 and 2006 rain seasons in Banizoumbou using measured meteorological data successfully reproduce the observed interannual variability in malaria vector mosquito abundance.

The distributed hydrology model operates at high spatial and temporal resolution, and incorporates remotely-sensed data for land cover and topography to simulate the formation and persistence of the small, temporary pools that constitute the breeding habitat of *Anopheles gambiae s.l.* mosquitoes. An agent-based mosquito population model is coupled to the distributed hydrology model, with aquatic stage and adult stage components. Aquatic stage mosquitoes are allowed to breed in any surface water, but the developing eggs, larvae and pupae die if the pool dries. The model structure maintains the spatial relationships of breeding pools, mosquitoes, and human habitation. For each individual adult mosquito, the model tracks the attributes relevant to population dynamics and malaria transmission, which are updated as mosquitoes interact with their environment, humans, and animals. The model reproduces mosquito population variability at seasonal and interannual time scales, and highlights individual pool persistence as a dominant control of mosquito population dynamics.

HYDREMATS is applied to study the impact of village-scale spatial variability in hydrologic conditions on malaria transmission. Zindarou is a village located only 30 km from Banizoumbou, but hydrologically it is very different from Banizoumbou. The groundwater table around Banizoumbou is about 25 meters below the surface, while the

groundwater table around Zindarou is a few meters below the surface. HYDREMATS reproduces the much higher mosquito populations observed in Zindarou arising from the lush, wet conditions compared to drier Banizoumbou. This result exposes small scale spatial variability in surface and subsurface hydrology as a principal control of village-scale malaria transmission.

Further experiments simulate the effect of climate shifts on Sahel malaria-transmitting mosquito abundance using HYDREMATS. Climate variability and climate change in West Africa often occur in the form of a shift from a wet regime to a dry regime or vice versa. Such a climate shift in the West African Sahel can greatly impact the intensity of regional malaria transmission. To investigate possible outcomes of such shifts, meteorological data from two different Sahel stations are used as alternate climatic forcings for the Banizoumbou model domain. The stations are located north and south of Banizoumbou in Agoufou, Mali, and in Djougou, Benin at 200 km and 400 km in the north-south direction from Banizoumbou, respectively. These data series represent possible climate shift scenarios, based on the observation that a northward or southward translation of Sahelian climate conditions along the north-south gradient has accompanied past climate shifts. A series of simulations investigate individually the effects of precipitation frequency and ambient temperature on anopheles mosquito populations and vectorial capacity. The vectorial capacity with Djougou, Benin conditions exhibited a 25% increase compared to baseline Banizoumbou conditions, whereas the vectorial capacity decreased by 26% with the Agoufou, Mali meteorological conditions. Isolation of temperature contributions to these differences show that in a cooling scenario (to resemble Benin), elasticity of mosquito abundance is 1.3, compared to –8.9 for the shift to hotter conditions found in Agoufou, Mali. Mosquito mortality ultimately limits malaria transmission in shifts to warmer conditions, and parasite extrinsic incubation period (sporogony) becomes limiting at low temperatures. In all cases, changes in precipitation frequency can limit mosquito breeding due to small-scale hydrological processes influencing breeding pool persistence.

Finally, a simple model of human immune response to malaria transmission is built into HYDREMATS. The HYDREMATS representation of acquired immunity acting in opposition to—yet depending on—malaria parasite in the bloodstream explains field observations of very similar malaria prevalence in Zindarou and Banizoumbou despite pronounced difference in vectorial capacity. The results are consistent with various paradoxical observations in the literature of unexpectedly low prevalence with higher biting pressure. HYDREMATS represents acquired immunity as dependent on repeated inoculations of malaria, with a slow loss of immunity in the absence of infectious bites. Because climate variability determines variability in vectorial capacity, in an endemic environment acquired immunity level in a human population has a memory of past climate variability. Model experiments in Banizoumbou evaluating the impacts of climate shifts confirm this.

Thesis Supervisor: Elfatih A.B. Eltahir
Title: Professor of Civil and Environmental Engineering

Acknowledgements

This work was supported by a NOAA Oceans and Human Health Initiative grant, as well as a fellowship from the Martin Family Society of Fellows for Sustainability.

I am indebted to my adviser Elfatih Eltahir who provided me much valuable guidance. The opportunity to work as a graduate student in this dynamic research group was very rewarding and unforgettable. I am very grateful for the hydrology education, the advice, support and trust in me to carry out extensive field research in Niger on behalf of this project.

Also, I would like to express my sincere thanks to Jean-Bernard Duchemin. The mentoring in field entomology, malariology, and logistics of working in Niger were crucial to research success. Equally important to project success was the support as a friend during lonely times in the field. The trip to Filingue, the discussions over coffee, the trips to the market, as well as the various wonderful dinners with his family (especially Christmas 2005) are deeply etched in the memory bank.

Many thanks also to the late Andrew Spielman of the Harvard School of Public Health who patiently taught me the basics. At the beginning of the project, I was completely ignorant of anything biological, let alone entomological. Andy saw this as a good thing and proceeded to patiently and systematically fill my clean mental slate with a basic public health entomology education. That and the inspirational stories of chasing dangerous mosquitoes in remote and inaccessible parts of the world will stay with me forever. Also, many thanks to Tony Kiszewski, Rich Pollack, and Mike Reddy at the Harvard School of Public Health for assistance and advice.

I wish also to thank the third member of my thesis committee, Charles Harvey for his assistance, and also Wassila Thiaw of NOAA for helping make this study possible in the beginning. At Parsons Lab at MIT, I would also like to thank Gayle Sherman for all of the instrumental support over the years. Her work on the sidelines of the project was absolutely critical and much appreciated.

I am very thankful to Luc Descroix of IRD for his invaluable assistance and local Niger hydrology expertise and advice. His kindness, good nature and humor were also very much appreciated during my stays in Niger. I am indebted to Suzanne Chanteau for the opportunity to work out of the CERMES facility in Niamey and use vehicles and other resources, despite her initial aversion to model-based studies involving virtual mosquitoes. Thanks also to CERMES staff and researchers, particularly Ibrahim Issa-Arzika whose tireless field and lab support was much appreciated. Other contributors in Niger were Tinni, Hamza, Modi, Roufai, Sani, Rabiou, Boubacar, Ghibril, etc.

Much thanks to the chiefs and inhabitants of Banizoumbou and Zindarou, Niger for their

participation during the field studies, especially for tolerating those loud, annoying light traps right next to their beds all night once a week.

Much sincere thanks to Anne Thompson, whose special warm companionship has enriched my life here at MIT beyond measure. The adventures and good times we shared over the years were wonderful and unforgettable and provided the balance in life necessary to maintain sanity during this process.

In addition, I thank my friends in Parsons lab, both past and present, for the fun, the interesting discussions, and the fine collegial atmosphere (in no particular order): Becca Neumann, Anke Hildebrandt, Sarah Jane White, Behnam Jafarpour, Lejo Flores, Frederic Chagnon, Jonathan Winter, Marc Marcella, Rebecca Gianotti, Gajan Sivandran, Arne Materna, Gautam Bisht, Teresa Yamana, and the many others not listed.

I am eternally grateful to my wonderful parents whose love and support has always been permanent and unconditional. Also, their globetrotting spirit of adventure has greatly inspired and influenced me. Without such an influence and the inherited love of adventure and desire to explore the world, thirteen months of field work in West Africa would have been long drudgery instead of the exciting adventure in a fascinating part of the world that it was!

Contents

List of figures

List of Tables

Chapter 1: Introduction and literature review

Malaria is a devastating disease that claims millions of lives each year. It is most prevalent in the tropics and in some of the world's poorest countries, where suitable climate conditions allow transmission and low socioeconomic conditions exacerbate transmission and disease burden. The 300 – 500 million estimated annual worldwide cases of malaria (WHO, 2005) cause great suffering and lost productivity. The disease continues to pose a major public health challenge.

Malaria transmission responds clearly to climate and environmental variability. An example of malaria association with seasonal climate variability is illustrated by figure 1.1. The figure depicts weekly malaria incidence at Niger hospitals for three years (2001-2003), and demonstrates a pronounced increase in cases, lagged a few weeks behind the peak of the superimposed Global Precipitation Climatology Project (GPCP; Huffman et al., 1997) monthly average rainfall data for the same years. The correlation of rainfall and malaria incidence is striking, but correlation does not necessarily imply causality. However, as discussed below, several causative pathways linking environmental conditions to malaria transmission have been described, and it is recognized that climate variability—particularly in precipitation—strongly influences malaria transmission. An understanding of the details of the complicated malaria-environment linkages can yield better predictions of the effects of climate variability, long-term climate change and can improve the performance of malaria advance warning systems. It can also determine *a priori* the effects of various environmental management techniques to combat malaria. The underlying motivation of this study is to elucidate these environment/malaria linkages and formalize their representation in a mechanistic mathematical model, validated by field data. A mechanistic modeling link should provide good predictive ability for a variety of scenarios.

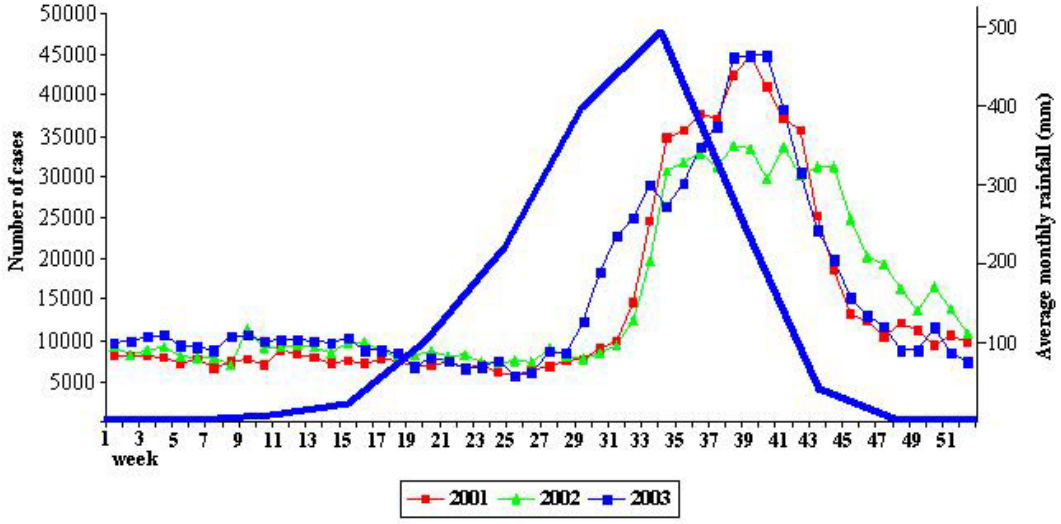

Figure 1.1. Weekly malaria incidence in Niamey, Niger hospitals, and Global Precipitation Climatology Project (GPCP) rainfall data, showing the pronounced increase in malaria transmission following the onset of the wet season.

Malaria is caused by bloodborne protozoa of genus *Plasmodium*, of which four species infect humans. *Plasmodium falciparum, Plasmodium vivax, Plasmodium malariae,* and *Plasmodium ovale* all cause various degrees of disease severity. *Plasmodium falciparum* is the most deadly form of human malaria, and is also the most prevalent in sub-Saharan Africa. The life cycle of the malaria parasite has two distinct stages: a within-host (intrinsic) stage and an outside-host (extrinsic) stage. During the extrinsic stage, the parasite is carried within the body of an anopheles mosquito, and undergoes a metamorphosis to become infectious once the host mosquito takes a blood meal. Mosquitoes of genus *Anopheles* are the sole vectors of malaria, and malaria transmission depends critically on their existence. Without the mosquito vectors, malaria cannot exist, as mosquitoborne transmission is the only mechanism of infection. Figure 1.2 summarizes the various stages of the malaria parasites as they cycle between the mosquitoes and human hosts. Two mosquito bites are necessary for transmission: one to ingest the sexual stages of the parasite (gametocytes) and the second to inject infectious sporozoites into the subsequent bloodmeal host.

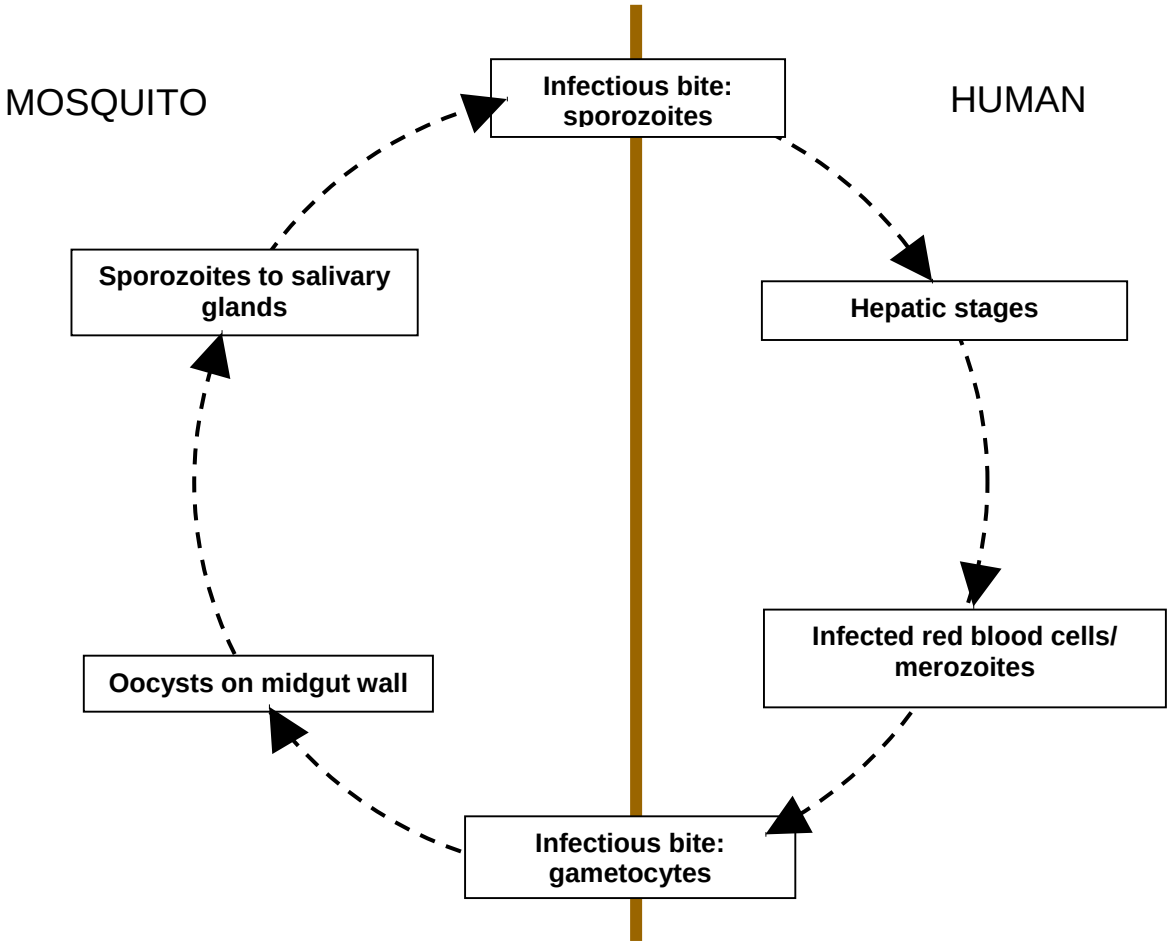

Figure 1.2. The cycle of the malaria parasite between mosquitoes and human hosts.

The primary objective of this study is to develop a calibrated, field-validated coupled hydrology/entomology model which operates at fine spatial and time scales. Using this model, various hypotheses and scenarios can be evaluated, and the effect of climate variability on malaria transmission in precipitation-limited malaria-endemic or -epidemic regions can be explored. Here, we choose to study the Niger Sahel region of Africa. Previous studies relating environmental influences (climate as well as habitat availability) to vector borne disease are reviewed below.

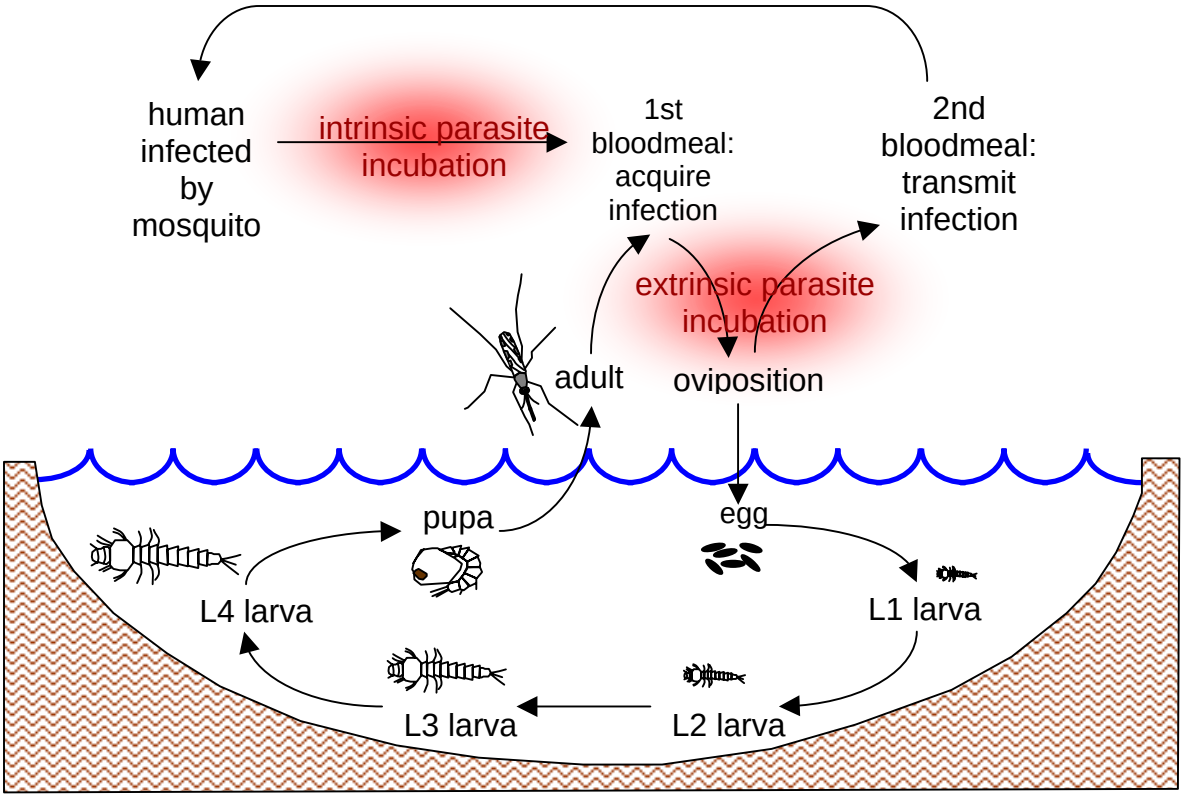

Figure 1.3. Advancement of aquatic stages of mosquitoes, from eggs to different stages of larvae, to pupae and finally adult emergence. The parasite enters the mosquito's body at the first infectious blood meal, which it uses to develop and deposit its first clutch of eggs. Parasite development continues with a degree-day dependence until the mosquito becomes infectious to humans. Transmission occurs when the infectious mosquito takes a second blood meal from a different human. Then, the parasite's intrinsic incubation period begins within the human body. A new mosquito takes a blood meal following the intrinsic incubation period, and becomes infectious to repeat the transmission cycle.

1.1 Mosquito borne disease relationship with climate

The mosquito life cycle depends on the presence of sufficient water. Mosquitoes lay eggs in water bodies, and subsequent subadult (aquatic) stages (egg, first through fourth stage larvae and finally pupae) develop in this aquatic environment until adult mosquito eclosion (emergence). The various stages of subadult development are depicted in Figure 1.3. If suitable water bodies do not form in a certain environment or rainfall is insufficient, then mosquitoes will cease to exist. In addition, total mosquito emergence rate in a population of interest depends on the surface area of suitable persistent water

bodies available to the individual egg-laying mosquitoes. The recognition of this dependence of mosquito abundance on water availability has led many authors to seek relationships of mosquito population dynamics with rainfall variability. For example, Wegbreit and Reisen (2000) sought associations of *Culex tarsalis* with rainfall in Kern County, California, but found that precipitation itself explains only 13% of the variance observed in that mosquito's numbers. Some authors have sought similar spatial and temporal associations for the dominant, most efficient afro-tropical malaria vectors, *Anopheles gambiae, An arabiensis,* and *An funestus*. For example, Minakawa et al. (2002) found that moisture index (ratio of precipitation to potential evaporation) was the climate variable that explained the most variability in *Anopheles gambiae sensu lato* populations. Lindsay et al. (1998) included precipitation limitations in a map defining the climate-predicted ranges of members of the *Anopheles gambiae* species complex in Africa. Other studies seek to extend the associations with climate to vector borne diseases themselves. For example, Singh and Sharma (2002) looked for associations of rainfall anomalies with malaria epidemics in India, but found no clear relationship. Shanks et al. (2002) investigate recent malaria epidemics in the Kenyan highlands by relating local incidence to several climate variables including precipitation. Often, studies seek associations of El Niño/Southern Oscillation (ENSO) events with variability in disease transmission. Many studies have linked ENSO with dengue (e.g. Gagnon et al., 2001; Hales et al., 1996; Hales et al., 1999) and malaria (e.g. Gagnon et al., 2002; Poveda et al., 2001; Bouma et al., 1996; Bouma et al., 1997; Hay et al., 2000). All of these studies recognize the connection of mosquito-borne disease incidence to precipitation variability, due to the requirement for adequate breeding pool availability for mosquito populations to thrive. These studies are all statistical in nature, seeking correlations with observed variables. Correlation does not prove causality, and precipitation correlations sometimes explain only a relatively small fraction of the variability (both spatial and temporal) evident in mosquito abundance or disease risk. Therefore, better representation of mosquito population dynamics may be obtained with the consideration of the regional hydrologic differences that can influence the availability of breeding habitat as well as other climate and environmental factors that may affect mosquito population dynamics.

Early warning systems are another class of model relating disease threat to climate (in addition to non-climate variables such as famine or other indicators of susceptibility). Ongoing research continues to develop and improve these models, concurrently with leading climate simulators that provide model forcing. Recently, Thomson et al. (2006) described recent advances in such a system using multi-model ensembles that adds up to four months lead time to predictions made with observed precipitation alone.

Many attempts have been made to include hydrologic considerations to improve the prediction of mosquito population and disease risk spatial extents. Usually, they involve a proxy for soil moisture, the most common of which is the Normalized Difference Vegetation Index (NDVI). NDVI is a simple numerical measure of photosynthetic capacity and hence energy absorption of plant canopies. It therefore allows distributions of plants to be monitored using multispectral remote sensing, usually from a satellite platform. Vegetation would often be limited by soil moisture availability, and the rationale for NDVI-based studies is that vegetation photosynthetic activity correlates strongly to soil moisture, and elevated soil moisture in turn is related to higher concentrations of suitable vector mosquito breeding sites. Tucker (1985) showed that NDVI as determined from the spaceborne radiometer AVHRR is related to the regional rainfall patterns. This study effectively established NDVI as a suitable proxy for rainfall patterns in parts of Africa. It follows then that NDVI can be an indicator for mosquito breeding as well.

Thomson et al. (1997) correlated NDVI with *Anopheles gambiae* abundance in Africa, and demonstrated that NDVI explains observed variations in mosquito density. Eisele et al., (2003) used NDVI values calculated from satellite data to describe well the spatial variations in entomological parameters in two cities in Kenya. Thomas and Lindsay (2000) used a similar approach, using SPOT satellite data to map areas of intensive anopheline breeding habitat in the Gambia. Diuk-Wasser et al (2004) used an NDVI approach that involves differences in middle infrared reflectance to distinguish areas of

rice agriculture in Mali from other vegetation, and to determine rice crop cohort. Both of these are local determinants of anopheline breeding, as larval productivity is highest in rice-growing areas, and peaks in the early stages of rice crop development. Using a similar approach applied to Connecticut, Diuk-Wasser et al. (2006) showed NDVI as well as many other satellite-derived environmental indicators (e.g. surface water, distance to estuaries, and non-forested areas) to explain variations in light trap captures of the primary vector mosquitoes of West Nile virus in the northeastern United States, *Culex pipiens*, *Aedes vexans*, and *Culiseta melanura*. Many other studies employ similar approaches (e.g. Manguin and Boussinesq, 1999; Nihei et al., 2002; Kuhn et al., and Hay et al., 1998), with varying success.

Satellite-derived proxies for disease vector breeding suitability are informative for delineating areas of higher risk for certain diseases, however the temporal resolution of this approach is limited to the return frequency of the satellite. Moreover, proxies such as NDVI must be related to specific habitat which varies regionally as well as amongst the various disease vectors. Not all green vegetation may indicate pooled water, and not all disease vectors may utilize habitat for which NDVI is a suitable proxy. These limitations must be overcome for detailed spatial and temporal representation of vector abundance and disease risk. Hydrologic models predicting distributed soil moisture response to rainfall can address limitations due to lack of temporal resolution inherent in the satellite-proxy approach. Several models have been developed that correlate predicted soil moisture with vector abundance or disease incidence. An example of such a model is Patz et al. (1998). The authors use a physically-based hydrology model to show that modeled soil moisture yields an improved correlation with malaria entomological inoculation rate (a measure of force of infection), compared to correlations with rainfall alone and correlations with NDVI. Further advances were made by Shaman et al. (2002a). They used a more detailed model using topography, soil, and vegetation data to simulate surface moisture suitable for the breeding of the floodwater breeding mosquitoes *Aedes vexans* and the swamp-breeding *Anopheles walkeri*. This was then related to field-measured abundances of these mosquito species. A negative association with modeled

soil moisture was noted for *Culex pipiens*, which breeds in eutrophic and polluted waters. In this way, modeled soil moisture was able to predict differences in population dynamics of various vector species, based on differential breeding preferences. In a different study, Shaman et al. (2002b) also showed how modeled soil moisture was associated with the amplification and transmission of St. Louis Encephalitis virus (a mosquito-borne pathogen) in Florida.

The models discussed above involved primarily correlation with observed precipitation or modeled moisture. However, temperature also affects malaria transmission in numerous ways. The multitude of complex causal pathways from temperature to malaria prevalence makes correlation with temperature difficult, and more comprehensive biologically-based models become necessary. Development rates of subadult mosquitoes, mosquito eggs, and infectious sporozoites (the infectious stage of the malaria parasite) within the mosquito all depend on ambient temperature. The daily survivability of adult mosquitoes depends strongly on temperature as well. When the temperature-dependent parasite development time in the mosquito (extrinsic incubation period) exceeds the temperature-dependent daily survivability, malaria transmission ceases. This can occur at low temperatures (because of long extrinsic incubation periods) or high temperatures (because of low daily surrvivability). Limits of transmission can therefore be defined by low as well as high temperatures. The temperature dependence of daily survivability was formulated by Martens (1997), and has been incorporated into several models. Craig et al. (1999) have developed a malaria distribution model based on all of the known climatic controls of malaria transmission. The climate-influenced biological contraints listed above are represented, and rainfall limitations are included in a basic manner. The result is a good reproduction of observed data of extents of malaria transmission. Further development of this approach involved transient simulation of mosquito and malaria dynamics, based on climate data time series. A model by Hoshen et al. (2004) simulates malaria transmission in time as well as space, and represents both the within-host stages of the parasite and the climate-influenced mosquito (extrinsic) stages of the parasite. Depinay et al. (2004) developed a model to simulate anopheles mosquito population

dynamics, incorporating many ecological processes such as intraspecific nutrient competition, predation and density-dependent mortality in the aquatic stages, as well as dispersal of adult mosquitoes. Temperature dependencies of larval and pupal development rates are represented in the model using an enzyme kinetics model derived by Sharpe and DeMichele (1977), and thus control adult mosquito eclosion as a function of water temperature. A similar model is used for egg development within the mosquito. In this manner climate-influenced biological limitations on transmission are represented by the model.

Climate change links to malaria have been suggested for many years. Many studies have focused on questions of climate change related to vector borne disease (e.g. Loevinsohn, 1994; Martin et al., 1995; Rogers et al., 2000; Thomas et al., 2004). In the highlands of Kenya, Hay et al. (2002) concluded from attempted associations of disease incidence with long-term meteorological data that climate change was not responsible for highland malaria epidemics in recent years in this temperature-limited environment. Using the same data, Pascual et al. (2005) later concluded that there have in fact been significant warming trends in these highland environments that have recently been plagued by malaria epidemics where malaria transmission is temperature-limited. Indeed, the role of climate change in highland malaria transmission has been hotly debated.

Current models vary in degree of sophistication and predictive ability. Most current models rely on association with a proxy (NDVI, soil moisture, precipitation) to simulate the influence of water availability on malaria transmission. Even the models that represent soil moisture such as Patz et al. (1998) and Shaman et al. (2002a), ultimately link mosquito abundance to water availability with a statistical association. A mechanistic modeling link that explicitly represents the limitation of mosquito breeding by availability of breeding habitat is lacking. A spatially explicit representation of breeding sites, the breeding of individual mosquitoes within those spatially distributed sites, and the various temperature influences on malaria transmission is the next logical step in the progression of models representing malaria transmission. This yields a mechanistic link

between weather events and malaria transmission in addition to the aggregation of climate-influenced biological processes such as daily survivability. The necessary further development considers spatial and temporal variability in surface and subsurface hydrology that may lead to nonlinear responses by mosquito populations, and are impossible to adequately describe with correlative approaches. Such a model structure replaces previous correlative approaches with detailed representation of actual formation and persistence of breeding habitat. This study takes this necessary next step in the progression of models.

1.2 Field site

To inform and validate the proposed model, much field data was collected. Hydrology and entomology data were collected from two representative villages in southwestern Niger, Banizoumbou and Zindarou. The village locations are shown in Figure 1.4. Banizoumbou has about 1000 inhabitants, and Zindarou's population is approximately 500. The reason for selection of these two villages is two-fold. First, they represent typical human population conditions for many of the Sahelian villages, yet they are different in that they are situated in two hydrologically distinct regions. Banizoumbou is located in a semi-arid plateau landscape of tiger bush, millet fields, fallow and bare soil. Subsistence dryland agriculture dominates food production, and local vegetation consists primarily of millet fields near the village. Most of the land is farmed, some areas are left fallow, and the remainder consists of tiger bush shrubland, which is generally more distant from the village and is common near surrounding plateau tops. Banizoumbou villagers farm pearl millet almost exclusively, with small plots of beans, groundnuts, and other crops making up an insignificant portion of the cultivated land. The endorheic nature of the surrounding watersheds and the large depth to the groundwater table result in relatively low levels of surface water ponding. This is in contrast to Zindarou, which is situated in the more lush and fertile abandoned river basin of the Dallol Bosso. Here, the groundwater table is only about one meter below the surface (Leduc et al., 1997), supporting abundant vegetation. The area is characterized by larger, vegetated pools, and substantial surface water/groundwater interactions, as emergence of the phreatic

groundwater table is observed in the form of large flooded areas during the peak of the rainy season from late July through early September. In addition, many shallow unimproved wells dot the area which villagers use to water vegetable gardens. These wells are variable in nature but often contain emergent vegetation and clean, clear water. As such, they present ideal breeding habitat for *An. funestus*, a slightly less abundant yet very dangerous malaria vector which generally prefers to breed in permanent pools of clear water with vegetated fringes (Minakawa et al., 1999).

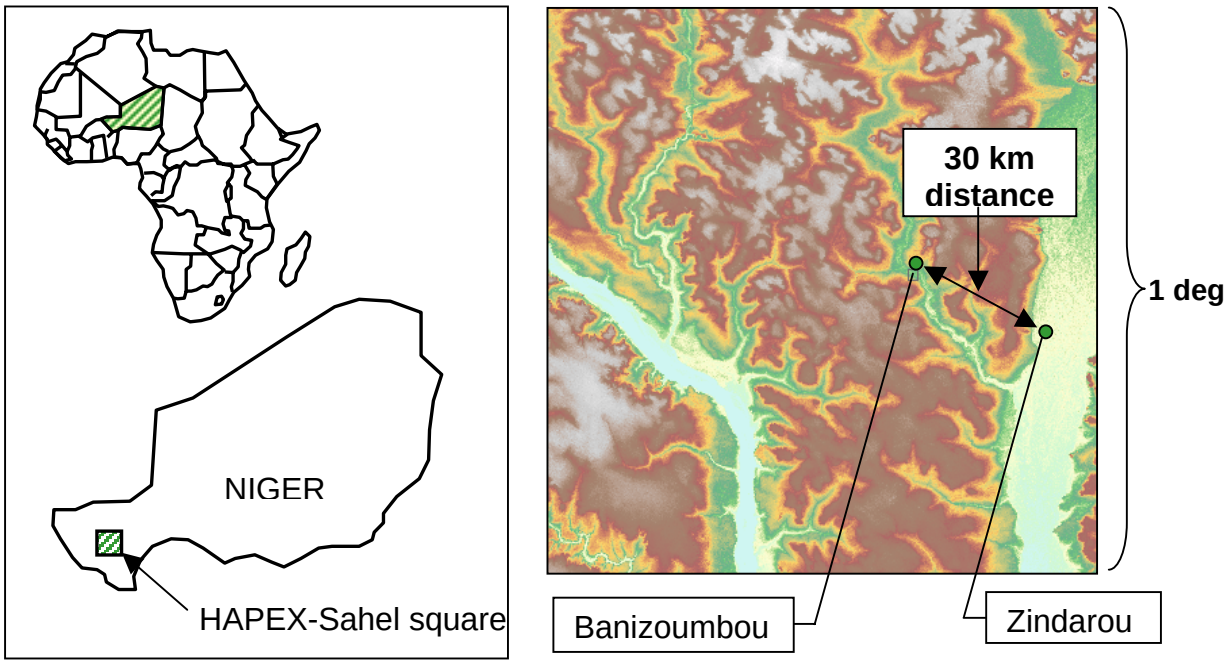

Figure 1.4. The location of the studied villages Banizoumbou and Zindarou, Niger. The right panel depicts topography within the HAPEX-Sahel square degree, the subject of an intensive international hydrology and climatology research project that took place from 1991 until 1993. The Niger River is seen in the bottom left of the domain, and the "Dallol Bosso" relict river basin is seen on the right. Zindarou's location within the Dallol Bosso results in the village's unique hydrology.

The second reason these villages were chosen as a field site is the ongoing intensive field work that has been performed in the region. Bimonthly malaria prevalence surveys are performed by CERMES (Centre de Recherche Médicale et Sanitaire, Niamey, Niger) researchers. Blood smears are taken from many villagers and analyzed for parasites. A

few years of sporozoite rate, parasitaemic, and entomologic data have already been collected, and this data collection will continue for the foreseeable future. In addition, extensive hydrology field work has been performed at the site, during and after the HAPEX-Sahel experiment of 1992. Most relevant to the proposed research are detailed studies of the role of various vegetation and soil types in hydrologic behavior (e.g. D'Herbès and Valentin, 1997). The AMMA (African Monsoon Multidisciplinary Analyses) experiment was conducted between 2004 and 2007. This project included much ongoing multidisciplinary research in the region, facilitating the sharing of data, field resources and expertise.

Regular observations in each village commenced in 2005. A preliminary visit with the village chiefs secured permission to work in the villages. Also, individual homeowners gave permission to place CDC light traps in their homes near their beds to capture host-seeking mosquitoes. Villagers who participated in this manner were periodically rewarded with sacks of millet and rice.

The villages were also instrumented with rain gauges, pyranometers, anemometers, soil moisture probes, various temperature and humidity probes, and were regularly searched for mosquito larvae in water bodies. More details about data collection in each village are presented in subsequent chapters.

1.3 Research objectives

The primary objective of this study was to develop a calibrated, field-validated coupled hydrology/entomology model which operates at fine spatial and time scales. This modeling tool would be used to simulate the effects of interannual climate variability and spatial hydrologic variability on malaria transmission. In addition, it could be used to evaluate the impacts of malaria interventions. This study has addressed modeling deficiencies highlighted above, by providing a mechanistic modeling link between climatic conditions and malaria transmission. All of the known environmentally-driven mechanisms underlying malaria transmission are included in the model, including

hydrologic limitations, and as such it is a useful tool for evaluating village-scale malaria transmission response to environmental perturbations. Beyond model development, primary goals included simulating the effects of inter-annual climate variability, evaluating the effects of spatial variability in hydrology on malaria transmission (by simulating the differences in observed mosquito abundances between the different hydrologic conditions in Banizoumbou and Zindarou), and analyzing scenarios of drastic climatic shifts that periodically occur in the Sahel.

1.4 Introduction to thesis

This thesis is organized into eight chapters. Chapter 2 provides detailed information about field data collection in Banizoumbou and Zindarou. Much data was collected to gain understanding of the local environment as well as to validate the model. Methods of data collection, time spans of data series, instruments used, and other details of field work are presented in Chapter 2. Chapter 3 discusses model development. The hydrology model domain and scale, operation, inputs and outputs are covered in detail. The one-way coupling of the entomology model to the hydrology model is also discussed, as are model inputs, the agent-based entomology model structure, temperature dependencies and other details of the model. Chapter 4 applies the coupled model to Banizoumbou and demonstrates the model's ability to reproduce observed interannual variability in mosquito abundance. Model calibration and validation based on collected field data is also discussed. Chapter 5 covers the model's application to the relatively wet hydrologic environment of Zindarou village to explore the effects of the much wetter conditions on mosquito abundance and malaria transmission, and the simulation results are compared to Banizoumbou simulation results. Conclusions about spatial variability in hydrologic conditions as a determinant of spatial variability in malaria transmission are drawn. Chapter 6 describes model experiments to simulate the impacts of potential major, persistent climate shifts to wetter or dryer conditions on Banizoumbou malaria transmission. Meteorological station data from Mali and Benin are used to force model scenarios for the dryer and wetter scenarios, respectively. Model results show the potential impact of such shifts on the Banizoumbou population's malaria burden. Chapter

7 introduces a simple model of human immunity that plays a key role in relating simulated malaria transmission to malaria prevalence observations. Paradoxical observations of malaria prevalence similarity in Banizoumbou and Zindarou despite large differences in vectorial capacity are simulated using the representation of immunity. Finally, chapter 8 concludes the thesis by addressing several hypotheses that were stated as this research was in the thesis proposal stage.

Chapter 2: Field Data Collection

2.1 Introduction

This chapter presents detailed methods and results of the field work performed in Banizoumbou and Zindarou. All collected field data is included. Some datasets are presented only in graphical form, but the data can be reviewed at web.mit.edu/~eltahir/Public/Niger_data.
Initial field site setup began in June 2005, shortly after initial introductions to the villages and after permissions to work were secured.

My field work activities commenced in June 2005 and continued until January 2006 for the first field season, then resumed in May 2006 through August 2006, and finally July and August of 2007 for a total of thirteen months and three wet seasons in Niger. During these field visits, regularly-collected field data included meteorological data and soil moisture data at datalogger-equipped sites, and adult mosquito abundance at six locations per village both inside and outside houses. In addition, water temperature, water turbidity, anopheles larval abundance, and approximate pool dimensions were noted at each location where pooled water was observed. When I was not in the field, field data collection was continued by Mr. Ibrahim Issa-Arzika of the Centre de Recherche Médicale et Sanitaire (CERMES) in Niamey. Field visits were conducted twice weekly during the wet seasons and twice monthly during the dry seasons, except the early 2005 dry season when more frequent field visits were made.

Figure 2.1 shows the various sampling locations in Banizoumbou, superimposed on a Quickbird panchromatic satellite image at 0.6-meter resolution of the village. Similarly, Figure 2.2 shows the regular field sampling locations in Zindarou, superimposed on a 1-meter resolution Ikonos satellite image of the village. A schematic map of Zindarou is presented in Figure 2.3, which shows locations of shallow garden wells, recurring surface water pools (“Ikonos” and “Southeast Zindarou” pools), the location of the

meteorological station, the locations of the TDR soil moisture stations, and in-situ pool water temperature dataloggers. All of these locations were surveyed with a GPS, and the X and Y axes are UTM easting and northing coordinates (in meters), respectively. The UTM zone is 31N.

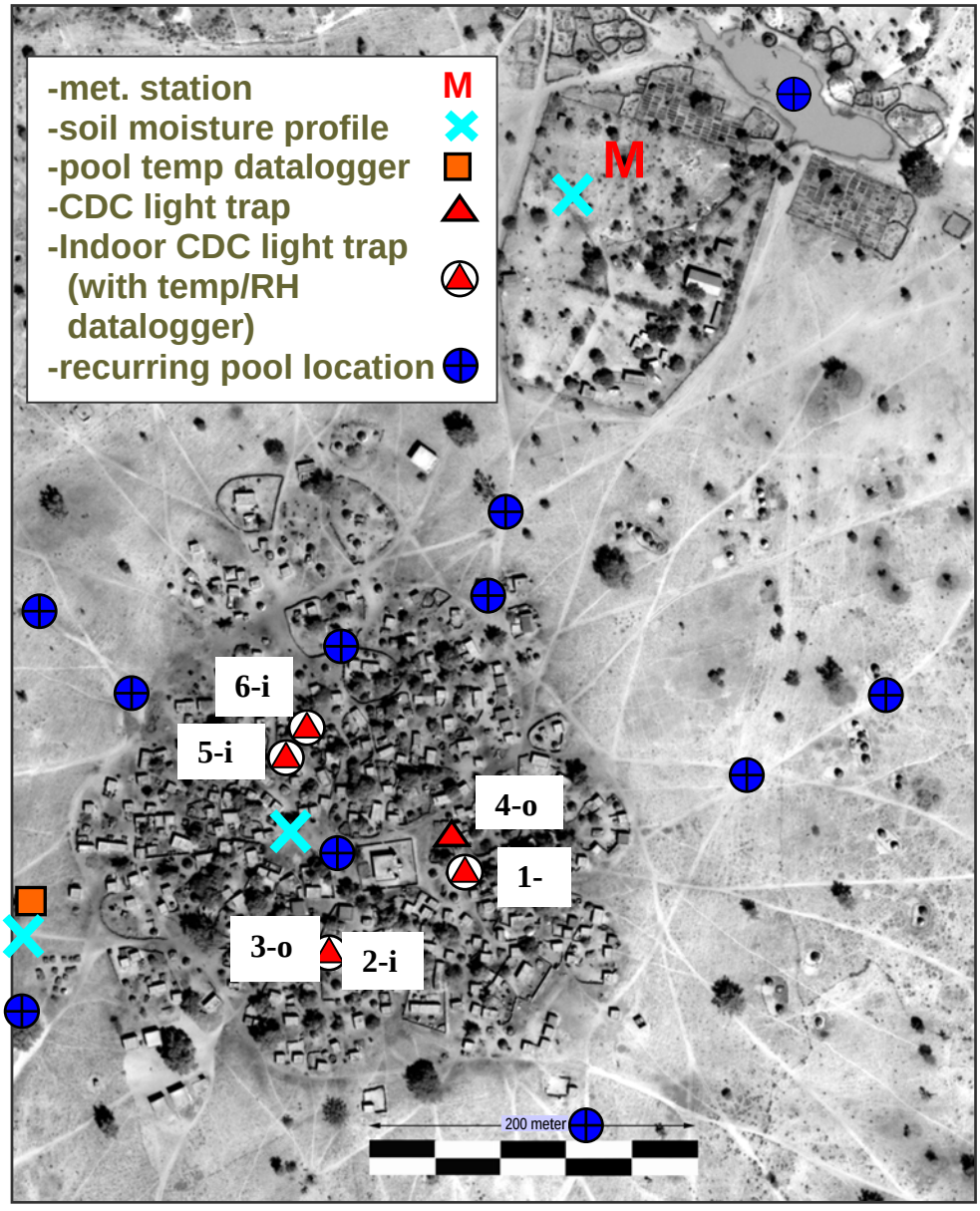

Figure 2.1. The various regular sampling locations in Banizoumbou. Sampling locations are superimposed on a 0.6-meter resolution Quickbird satellite panchromatic image. Light trap locations are labeled as (trap-number)-(o/i) . Outside deployments are labeled with “o” and indoor deployments are labeled with “i”.

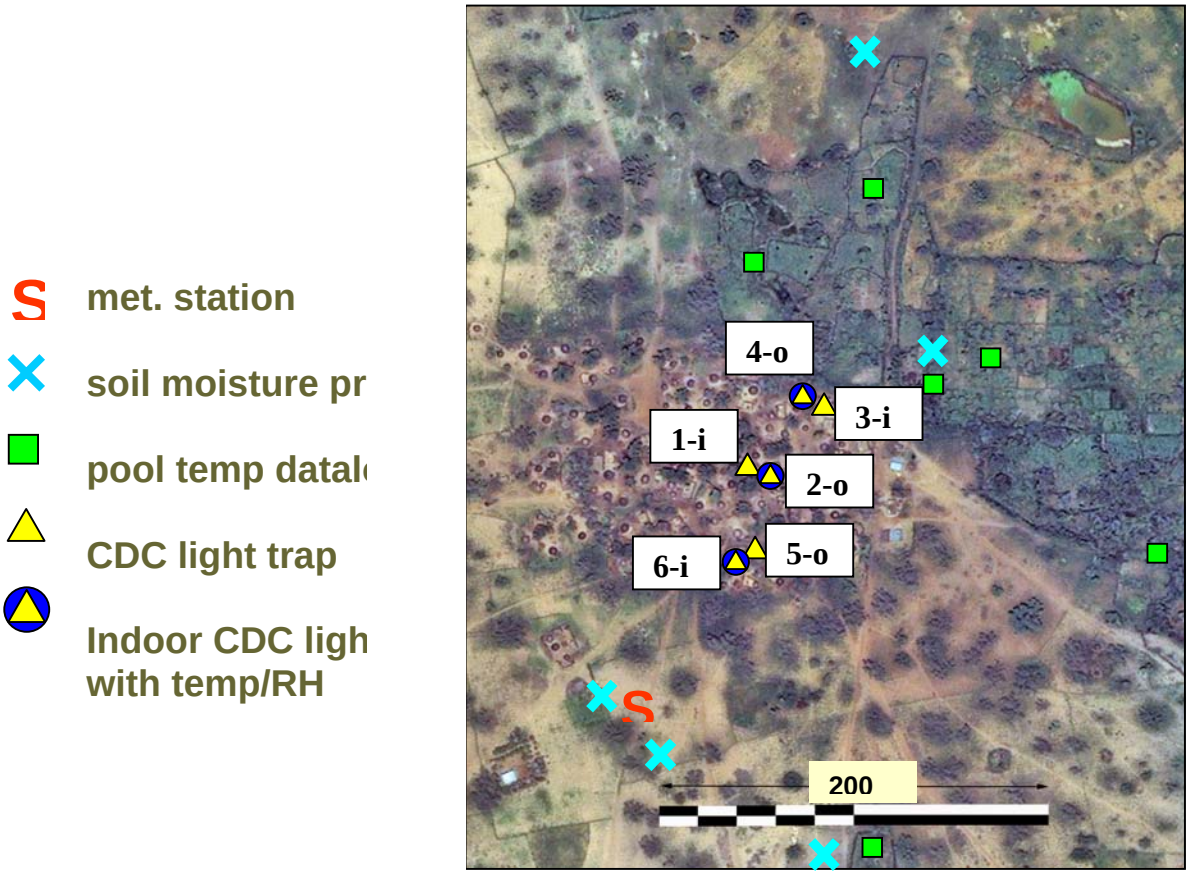

Figure 2.2. The various regular sampling locations in Zindarou. Sampling locations are superimposed on a 1-meter resolution Ikonos satellite panchromatic image. The light trap locations are marked (1-6) as (light trap number)-(i/o). Outdoor deployments are labeled "o" and indoor deployments are labeled "i".

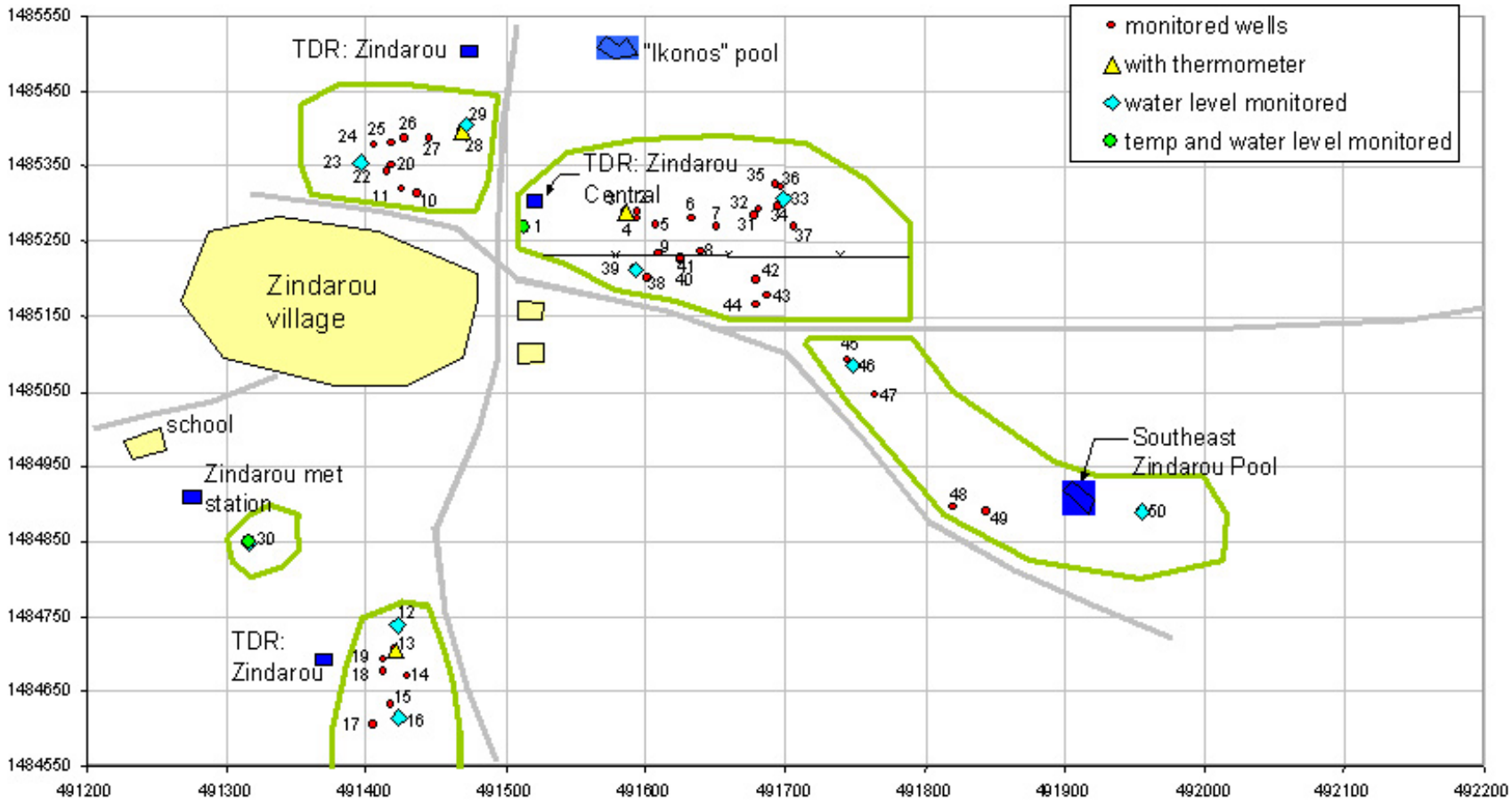

Figure 2.3. Schematic map of Zindarou showing numbered shallow garden well locations, the meteorological station, TDR soil moisture datalogger stations, and in-situ water temperature datalogger sites. The wet garden areas are delineated in green. The X and Y axes are UTM Easting and Northing coordinates (Zone 31N), respectively.

Meteorological stations collected data at 15-minute intervals and soil-moisture (TDR) measurement stations collected data at 30-minute intervals. The temporary pool locations were monitored with regular field visits. After several weeks of initial observations, it became evident where recurring pools tended to form, and these locations were visited and sampled for water temperature and turbidity, as well as larval activity. Often, additional explorations were done surrounding the villages to ensure that no major breeding sites were being overlooked. Field visits were made at least twice weekly during each monsoon season, and twice monthly during the dry seasons on successive days. Field visits always involved two successive days because the adult mosquito abundance had to be sampled overnight.

2.2 Meteorological data

2.2.1 Zindarou

Initial field setup included installation of a meteorological station in Zindarou. Modeling efforts should rely on dependable, accurate and high temporal resolution data sources. The meteorological station at Zindarou measured precipitation, temperature and relative humidity, incoming shortwave radiation, wind speed and direction, and soil moisture at four points in a vertical profile configuration. All instruments were mounted on a 6-foot metal tripod. The tripod was grounded with a 6-foot copper rod. Precipitation was measured using a Texas Electronics TE525 rain gauge, with a 0.254 mm tip and 6-inch orifice. It was mounted on a metal rod approximately two and a half meters from the meteorological station tripod. Temperature and relative humidity were measured with a Vaisala HMP45C-L temperature/RH probe. An RM Young 10-plate gill radiation shield was placed over the probe to protect it from error-producing solar radiation and precipitation. Wind speed and direction were measured with a 05103-L RM Young wind monitor. An LI-200X Li-Cor pyranometer measured incoming solar radiation. It was placed on a long cross-arm extending from the main tripod, and leveled on a flat mounting surface. Finally, four Campbell Scientific CS616 water content reflectometers registered soil moisture below the meteorological station. These were placed at 10cm, 20cm, 50cm and 100cm below the surface in a vertical profile configuration. The 10cm probe was slightly offset from the vertical profile line to ensure that there is no

interference with the 20cm probe. All data were recorded with a Campbell Scientific CR10X datalogger, with 2 megabyte extended memory, which was housed in a locked, weatherproof enclosure mounted on the tripod. The data was periodically downloaded with a laptop. The entire system was powered with a 7 amp-hour sealed rechargeable battery and 12-volt power supply, which was recharged with a 10-watt solar panel and a charging regulator.

The meteorological station was situated in an open millet field at least thirty meters from the nearest obstruction, the tall neem trees surrounding the school (see Figure 2.2). During the monsoon, millet growing near the station can reach heights of about 1.5-2 meters in September and October, and during the rest of the year the land surrounding the station is not vegetated. The meteorological station, including the precipitation gauge were protected from livestock with a chain-link fence.

Zindarou precipitation data is presented in Figure 2.4 for the years 2005-2007. The raingauge integration interval was set at 15 minutes, which is presented in this plot. Instrument resolution was 0.254mm for each tip. Cumulative precipitation for each of the years is compared in Figure 2.5. Cumulative annual totals were 348.7mm in 2005, 459.5mm in 2006, and 287.2mm in 2007. The meteorological station was installed on June 26, 2005, and it is possible that some 2005 precipitation prior to this date was not recorded.

Figure 2.6 shows temperatures measured at the Zindarou meteorological station, and Figure 2.7 shows the relative humidity. Both temperature and relative humidity were sampled every fifteen minutes by the same probe. The measurements showed significant diurnal fluctuations, so a 24-hour average was superimposed on these plots. The 24-hour average temperature affects daily survivability of mosquitoes, and temperature and relative humidity are hydrology model inputs.

Wind speed measured by the Zindarou anemometer is presented in Figure 2.8. Again, a 24-hour average wind speed is superimposed on the plot. Wind direction was also

recorded, and the results are presented in Figure 2.9. The angular histograms depict degrees from north in the azimuth coordinate and number of occurrences in the radial coordinate. The measurements were separated into wet season and dry season histograms, because a general prevailing wind shift was observed as the monsoon commenced, and the opposite shift was seen as the dry season resumed in October. Predominant wind direction during the wet season was south-south-east, at approximately 210 degrees. This was observed to shift to northerly winds from the desert during the dry season.

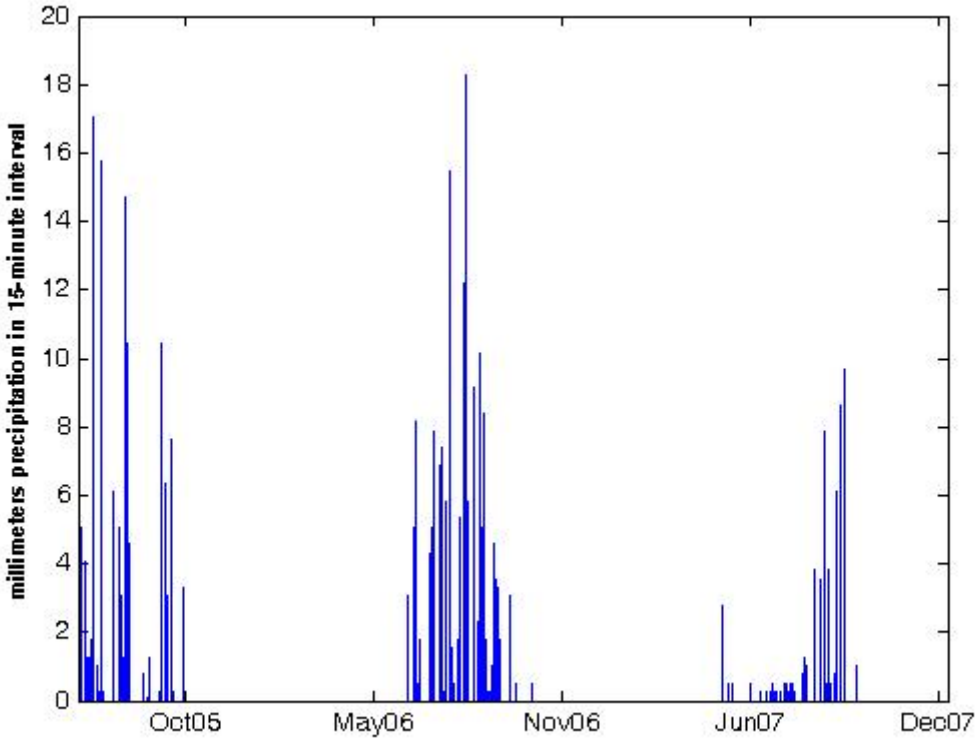

Figure 2.4. Measured precipitation at the Zindarou meteorological station. The station came online June 26, 2005 and has been recording at 15-minute intervals uninterrupted since then.

Pyranometer readings are shown in Figure 2.10. Because of the large intraday fluctuations of the pyranometer data, only maximum values and daily averages are presented in the plot. The data spans the entire period of the instrument's operation: June 26, 2005 through December 31, 2007.

The final dataset stored at the Zindarou meteorological station is soil moisture. Four time domain reflectometry (TDR) probes were placed in a vertical profile configuration, at 10cm, 20cm, 50cm and 100cm below the ground surface. These probes were sampled every two hours for volumetric water content. The measured soil volumetric water content in all four probes is presented in Figure 2.11. The standard TDR calibration given by Campbell Scientific was used to relate frequency to volumetric water content.

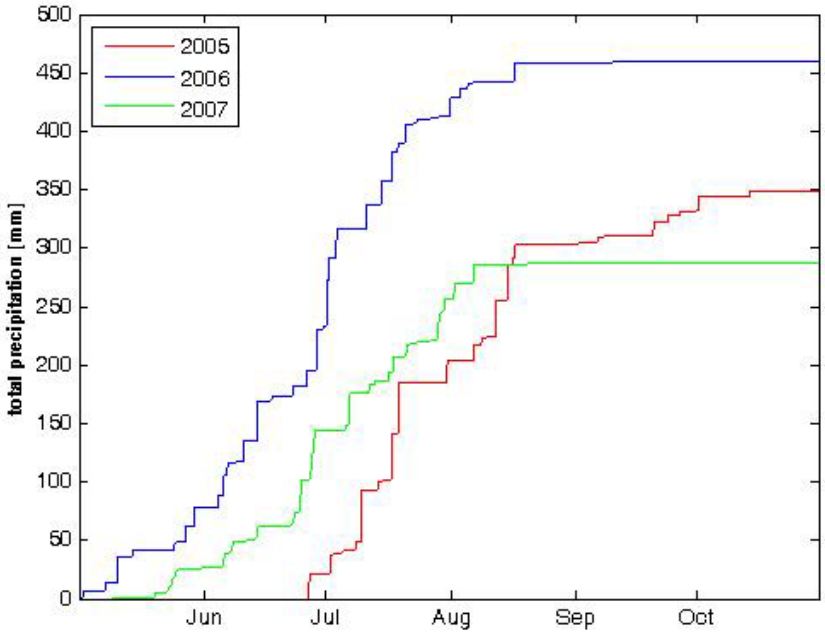

Figure 2.5. Cumulative precipitation measured at the Zindarou meteorological station. Cumulative annual totals were 348.7mm in 2005, 459.5mm in 2006, and 287.2mm in 2007.

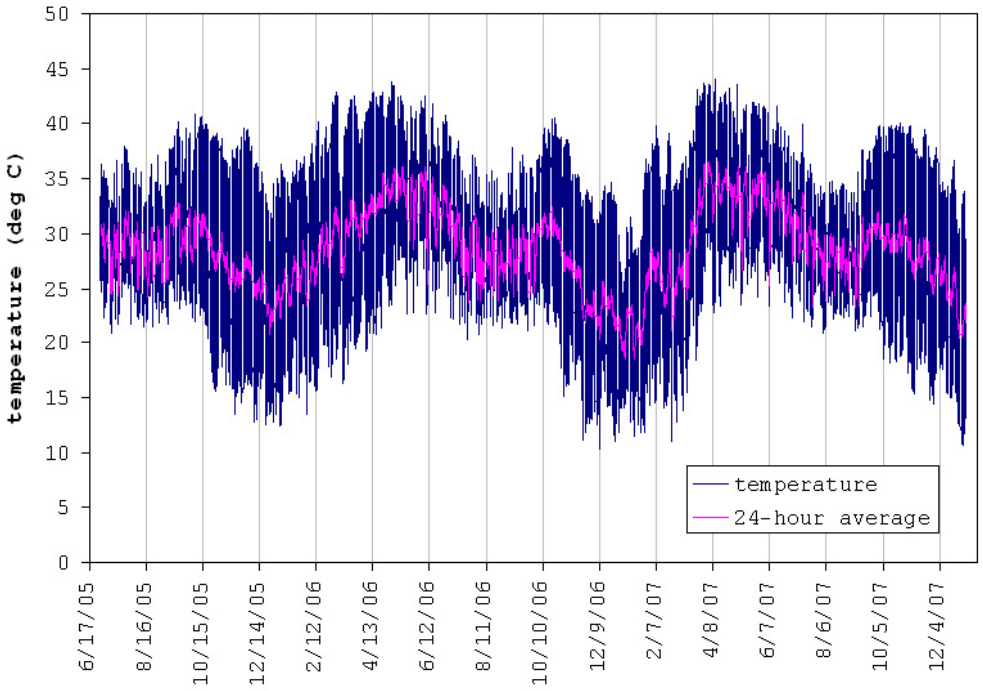

Figure 2.6. Temperatures (degrees C) measured at the Zindarou meteorological station at 15-minute intervals, for the period 6/26/05 – 12/31/07. The 24-hour average temperature (which determines mosquito survivability) is superimposed on the 15-minute measurements.

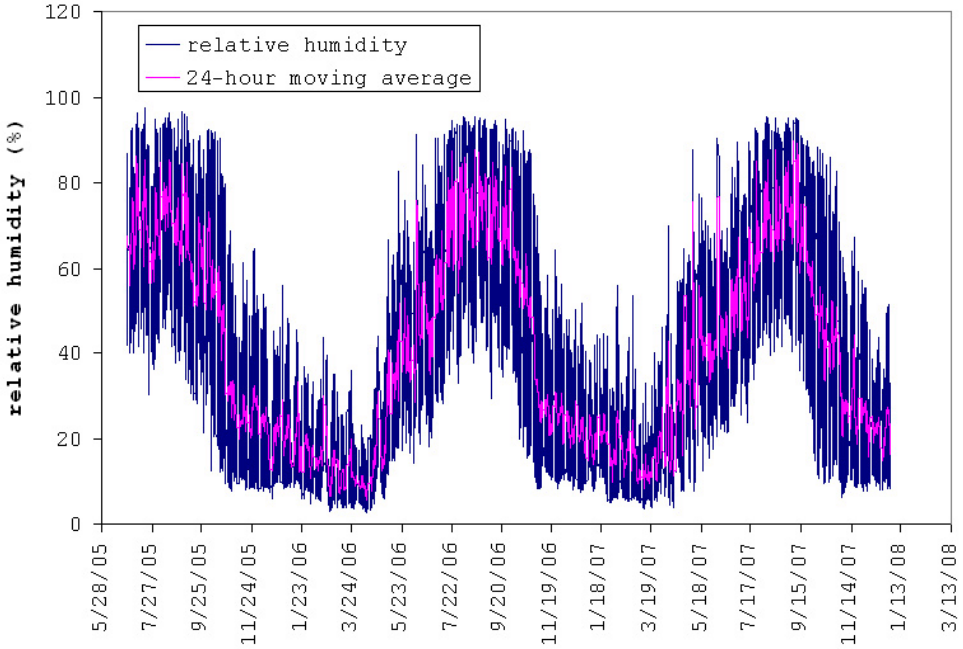

Figure 2.7. Relative humidity measured at the Zindarou meteorological station, over the period 6/26/05 – 12/31/07. The plot includes 24-hour moving average relative humidity.

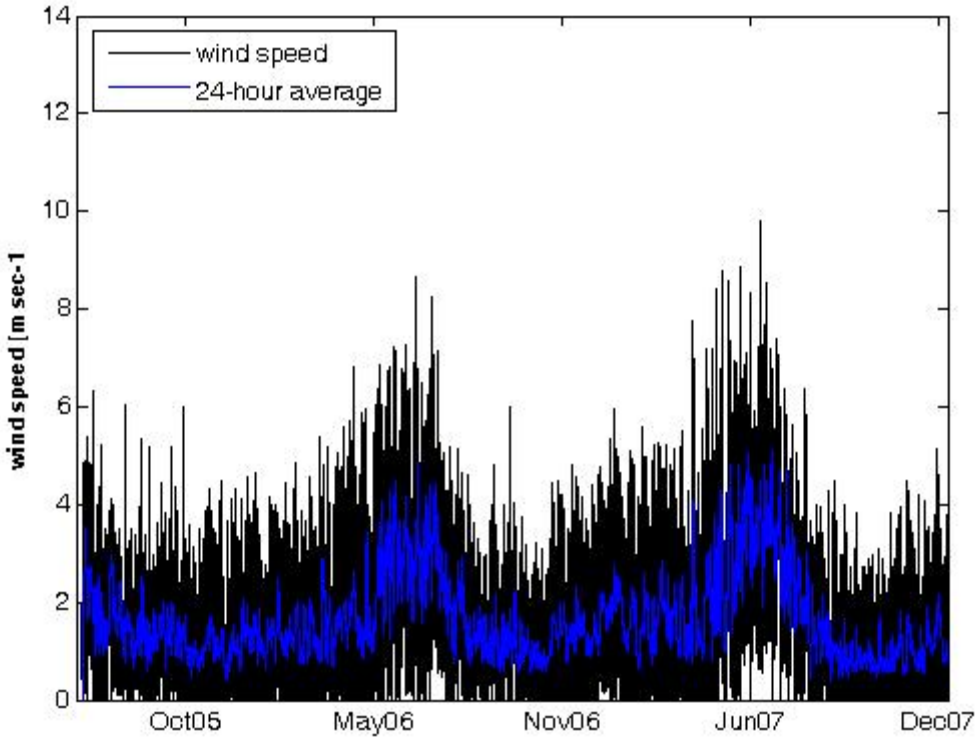

Figure 2.8. Wind speed measured at the Zindarou meteorological station from 6/26/05 until 12/31/07. Both hourly measurements and 24-hour averages are plotted.

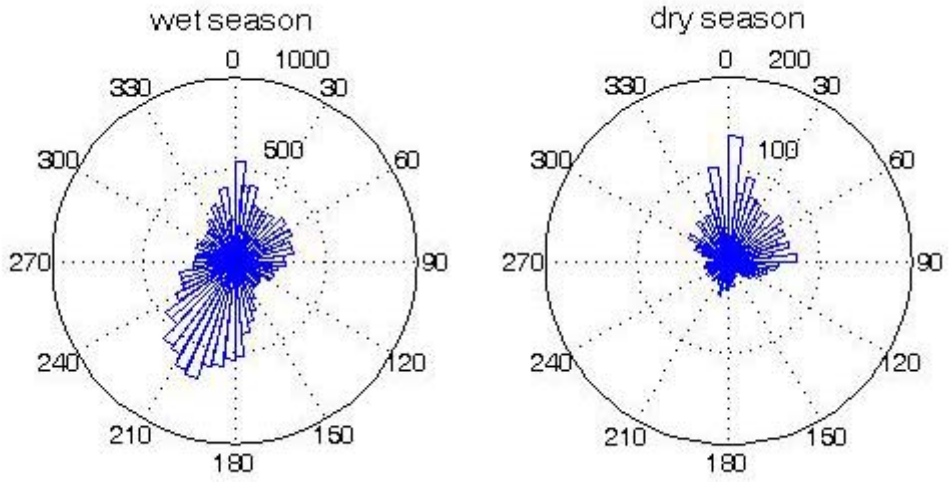

Figure 2.9. Angular histograms of wind directions measured at the Zindarou meteorological station. The record has been divided into wet season (June 1 – September 30) and dry season (October 1 – May 31) periods to illustrate the wind shift from the southwest in the wet season to northerly desert winds in the dry season.

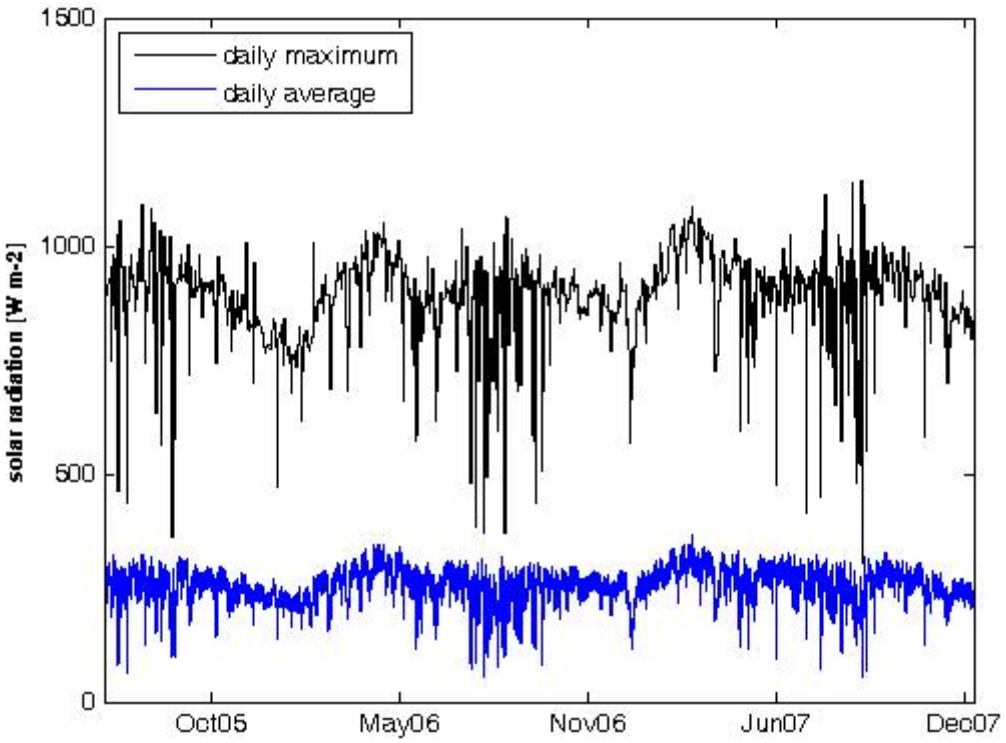

Figure 2.10. Daily maximum and daily average incoming shortwave radiation measured at the Zindarou meteorological station, for the period 6/26/05 – 12/31/07.

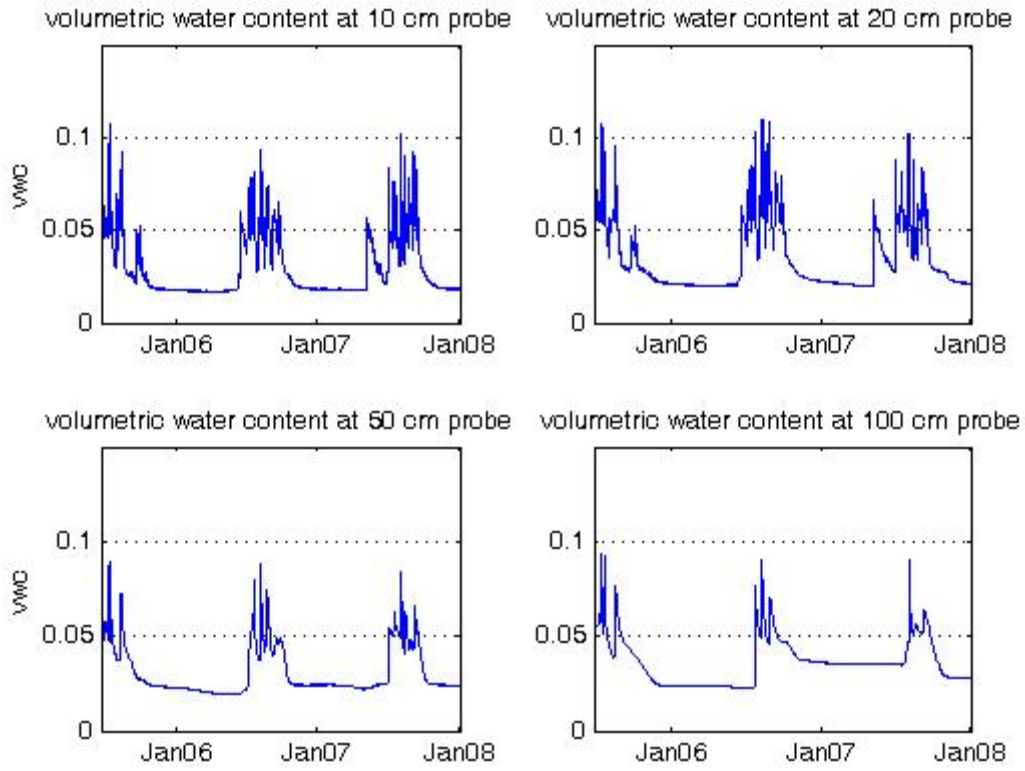

Figure 2.11. Soil moisture (volumetric water content) measured at the Zindarou meteorological station. Probes were inserted into the soil at 10cm, 20cm, 50cm and 100cm below the surface. The record spans the period 6/26/05 – 12/31/07, and measurements were taken every two hours.

2.2.2 Banizoumbou

The Banizoumbou meteorological station was installed by IRD during the HAPEX-Sahel experiment of 1991-1993, and has been operated by IRD since then, including the duration of this study. The station data was periodically obtained from IRD, and is used for modeling purposes. Precipitation was measured at Banizoumbou with a tipping bucket rain gauge, and is presented in Figure 2.12. The data presented spans the period of field observation performed in this study: 6/1/05 – 12/31/07. Cumulative precipitation was calculated, and is presented in Figure 2.13.

Temperature and relative humidity were measured hourly at the Banizoumbou meteorological station. The results for temperature and humidity for the period 6/1/05 through 9/25/07 are presented in Figures 2.14 and 2.15, respectively. A wind vane measured wind speed and direction at the Banizoumbou meteorological station. The results are presented in Figures 2.16 and 2.17 for wind speed and direction, respectively, for the period 6/1/05 – 9/25/07.

2.2.3 Tabular data summaries

Temperature and humidity affect entomological activity in Banizoumbou and Zindarou directly. A summary of the two variables is presented in Table 2.1 for both villages. Precipitation affects mosquito populations very significantly as well. Table 2.2 summarizes rainfall data collected at the two villages.

Table 2.1. A summary of temperature and humidity during the wet season and all year at the Banizoumbou and Zindarou meteorological stations.

		Wet season (June 1 - Sept. 30)			All year		
Banizoumbou		average	maximum	minimum	average	maximum	minimum
2005	temperature (deg C)	28.6	40.7	21.0	29.4	44.3	11.2
	relative humidity (%)	61.7	92.2	20.7	38.4	92.2	4.8
2006	temperature (deg C)	29.3	41.9	20.1	28.7	43.6	8.0
	relative humidity (%)	62.3	93.6	13.8	36.7	93.6	2.2
2007	temperature (deg C)	29.5	41.4	20.1	28.3	43.8	9.1
	relative humidity (%)	61.8	99.0	17.4	37.8	99.0	3.2
Zindarou							
2005	temperature (deg C)	29.0*	40.4*	20.7*	27.9*	41.1*	11.4*
	relative humidity (%)	67.7*	97.6*	21.4*	50.2*	97.6*	6.1*
2006	temperature (deg C)	29.4	42.6	19.5	28.8	44.0	9.2
	relative humidity (%)	63.7	95.9	14.1	37.8	95.9	2.7
2007	temperature (deg C)	29.5	41.8	20.2	28.7	44.5	10.2
	relative humidity (%)	61.9	95.7	15.8	38.3	95.7	3.6

*2005 data begins on June 27, 2005.

Table 2.2 Total annual precipitation in Banizoumbou and Zindarou for 2005 – 2007.

	total precipitation (mm)	
	Banizoumbou	Zindarou
2005	405.5	348.7
2006	478.3	459.5
2007	482.0	287.2

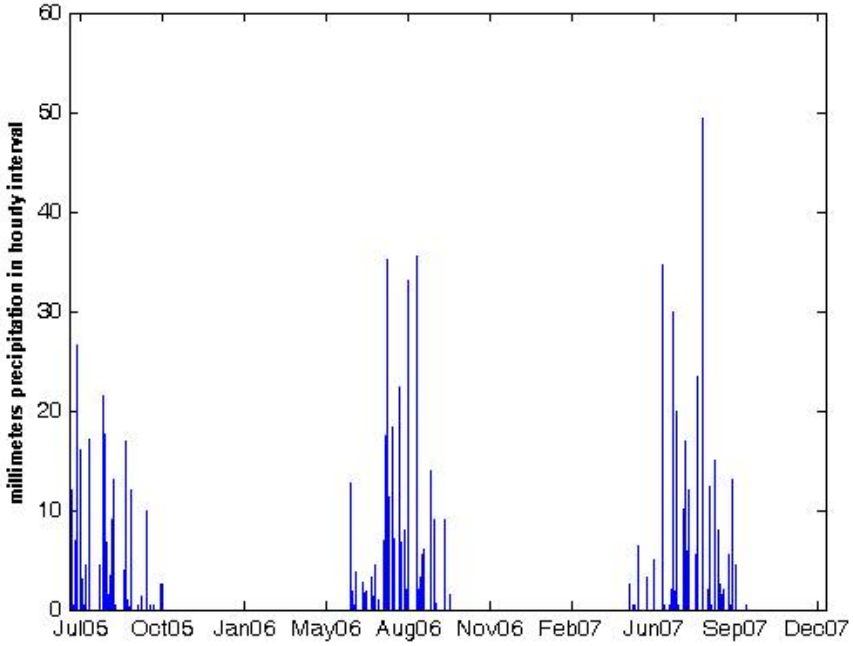

Figure 2.12. Precipitation measured at the Banizoumbou meteorological station, for the period 6/1/05 – 12/31/07.

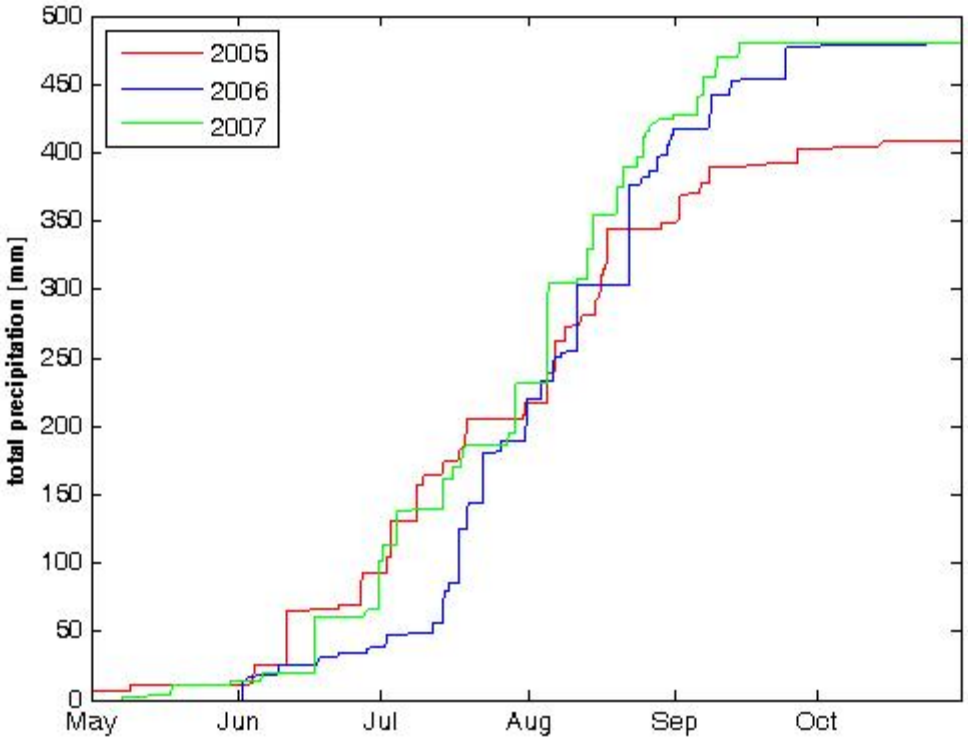

Figure 2.13. Cumulative precipitation measured at the Banizoumbou meteorological station for the period 5/1/05 – 12/31/07.

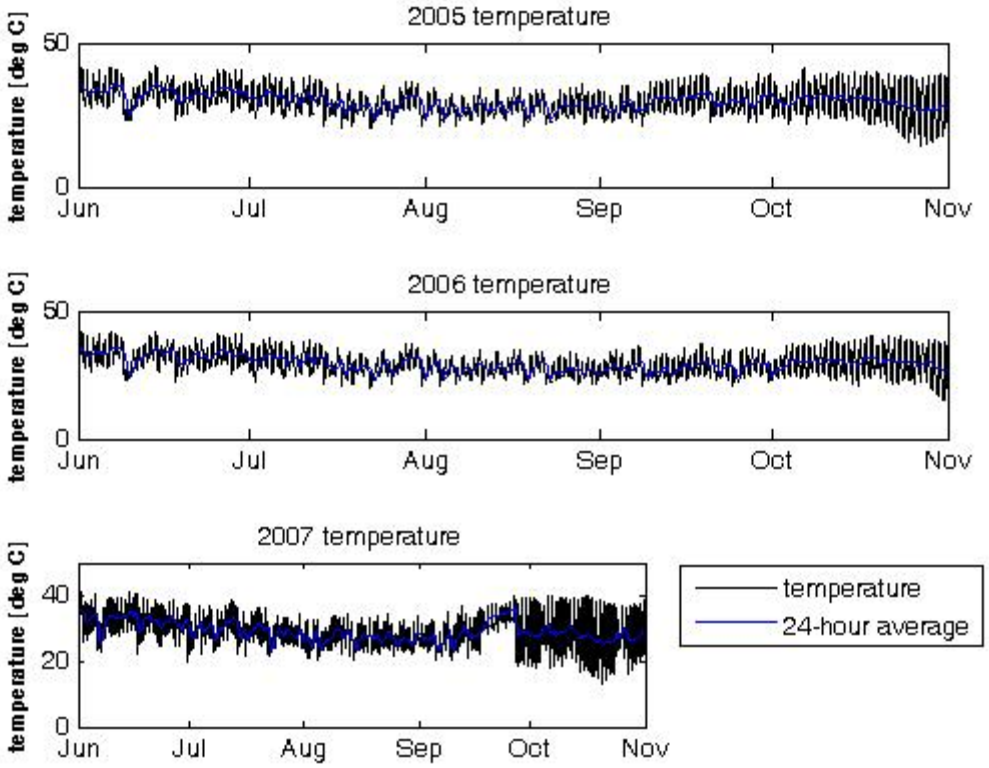

Figure 2.14. Wet-season temperature recorded at the Banizoumbou meteorological station, for the period 6/1/05 – 9/25/07.

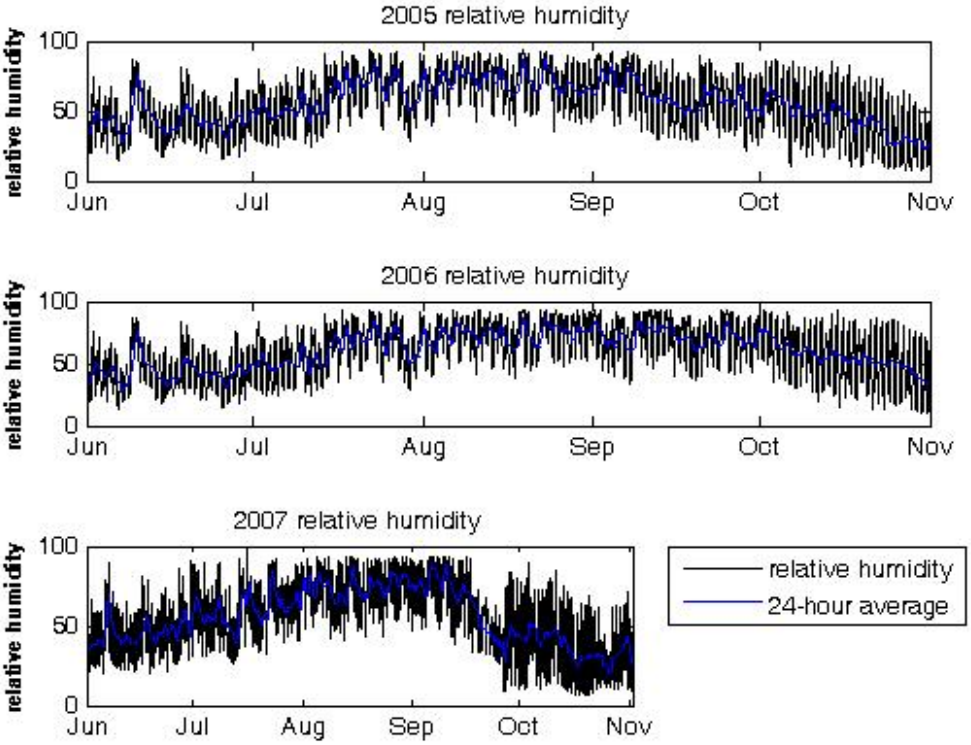

Figure 2.15. Wet-season relative humidity measured at the Banizoumbou meteorological station for the period 6/1/05 – 9/25/07.

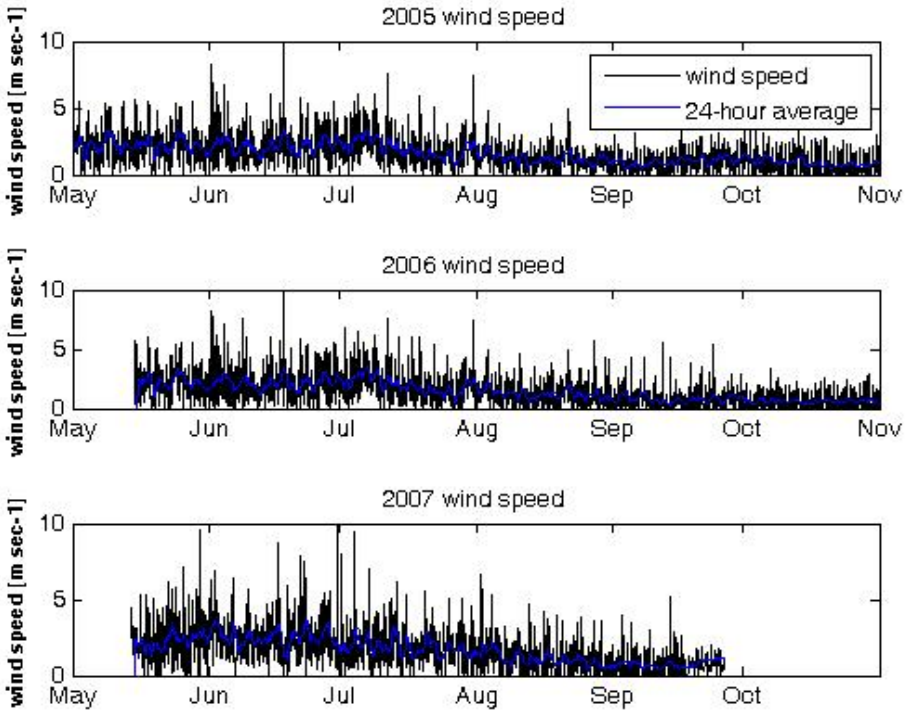

Figure 2.16. Wet-season wind speed measured at the Banizoumbou meteorological station, for the period 5/15/05 – 9/25/07.

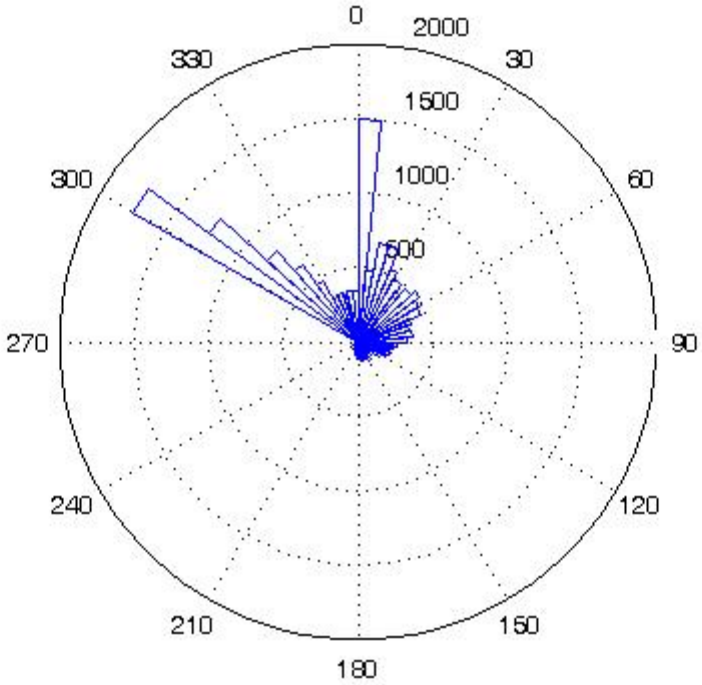

Figure 2.17. Histogram showing wet season wind directions at Banizoumbou meteorological station. The wind vane recording device has malfunctioned, because the registered directions are predominantly northerly. This was confirmed with IRD, who owns and operates the meteorological station.

2.3. Soil moisture data

Besides the profile soil moisture measurements made at the Zindarou meteorological station, three other soil moisture recording stations were installed in Zindarou. These have been labelled “Zindarou south”, “Zindarou central”, and “Zindarou north” for Zindarou, and “Centreville”, “CFTEA”, and “Mare” for Banizoumbou. The locations of these instruments are noted on Figures 2.1, 2.2 and 2.3. Locations of soil moisture measurement in Zindarou were chosen to sample various soil types. Predominant soil types of Zindarou are the sand typical of the region, and a sandy loam which is prevalent in the relict channels of the Dallol Bosso. The meteorological station and Zindarou South TDR stations sampled the sandy soils, and the Zindarou Central and Zindarou North TDR stations both sample soil moisture in the Dallol Bosso channel soil which has much higher fine particle content. In Banizoumbou all TDR stations sampled the very uniform, well-sorted and well-mixed sandy soil that is dominant in the region.

The TDR soil moisture monitoring stations all consisted of four TDR probes (Campbell Scientific model CS625-L water content reflectometers) arranged in a vertical profile configuration identical to that of the meteorological station TDR probe configuration. The data was stored in a Campbell Scientific CS200 datalogger, which was periodically downloaded using a laptop computer. The probes were powered by a 12-volt 7 amp-hour sealed rechargeable battery, which was recharged with a 5-Watt solar panel and built-in voltage regulator. The electronics were housed in a sealed, locked enclosure that was mounted on a tall metal rod inserted into the ground. In addition, a 1-meter copper ground rod was inserted into the soil at each location, to act as a suitable ground for the electronics. Dessicant packs were placed in each of the datalogger enclosures to prevent condensation on the sensitive electronics.

During installation, a 1-meter deep hole was dug, and probes were inserted horizontally at 10 cm, 20cm, 50cm, and 100cm from the soil surface. The 10cm and 20cm probes were slightly offset from the vertical to minimize interference between the two probes as they sample simultaneously. Soil excavated during the installation of the probes was kept in separated piles, so that the hole could be refilled with soil in the original layers. This was done to minimize the impacts of probe installation on any potential natural vertical heterogeneity in the soil profile, although no such heterogeneity was evident when the installation holes were excavated.

Soil moisture measurements were taken at 30-minute intervals. Figure 2.18 shows measured soil moisture at the Zindarou South TDR station. The 100-cm probe shows clearly the effect of rising groundwater levels that saturate the probe during and after the peak of the wet season. During the saturated conditions, the volumetric water content reached 0.27 m^3 m^{-3}, the porosity of the soil sampled at this location. During the relatively dry 2007 rain season, the 100-cm probe did not indicate saturated conditions at 100 cm below the surface.

Figures 2.19 and 2.20 show the measured volumetric water content at the Zindarou Central and Zindarou North measurement stations, respectively. Both of these sites sample a sandy loam soil type with a higher fine particle content than the soils of Zindarou south and the meteorological station.

Figures 2.21, 2.22, and 2.23 show the measured soil moisture for the three Banizoumbou TDR stations. These are labeled “Centre” (Figure 2.21) which is located in the center of the village as shown in Figure 2.1, “Mare” (Figure 2.22) located to the southwest of the village, and “CFTEA” (Figure 2.23) located to the north of the village.

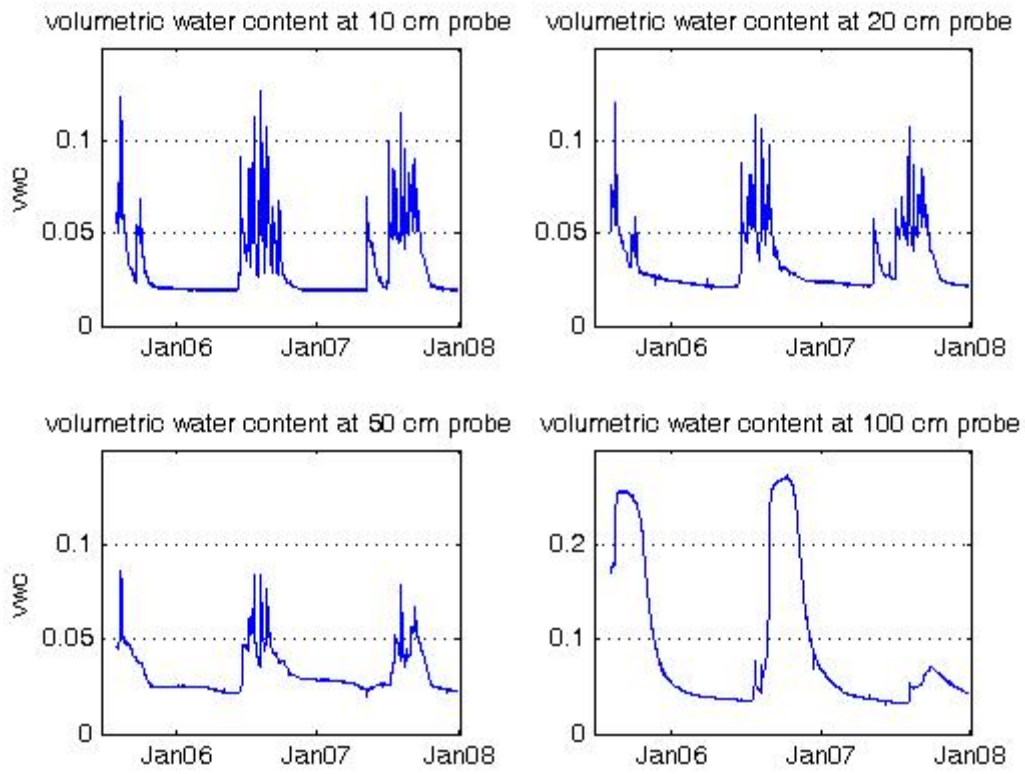

Figure 2.18. Soil moisture (volumetric water content) measured at the Zindarou South TDR station. Probes were inserted into the soil at 10cm, 20cm, 50cm and 100cm below the surface. The record spans the period 8/2/05 – 12/26/07, and measurements were taken every thirty minutes. Note the periods of saturated conditions at the 100cm probe during the wet seasons of 2005 and 2006.

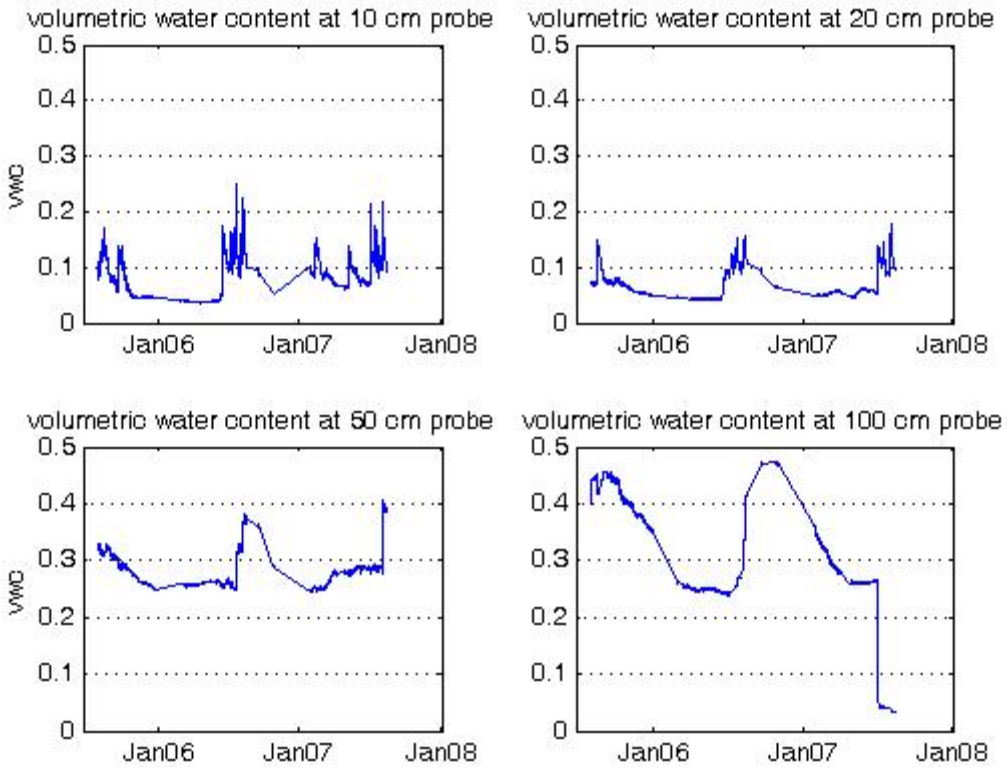

Figure 2.19. Soil moisture (volumetric water content) measured at the Zindarou Central TDR station. Probes were inserted into the soil at 10cm, 20cm, 50cm and 100cm below the surface. The record spans the period 7/30/05 – 8/13/07, and measurements were taken every thirty minutes. Technical difficulties with the probes and technician error caused data gaps in the series, and very erroneous readings in August 2007 before the probes failed.

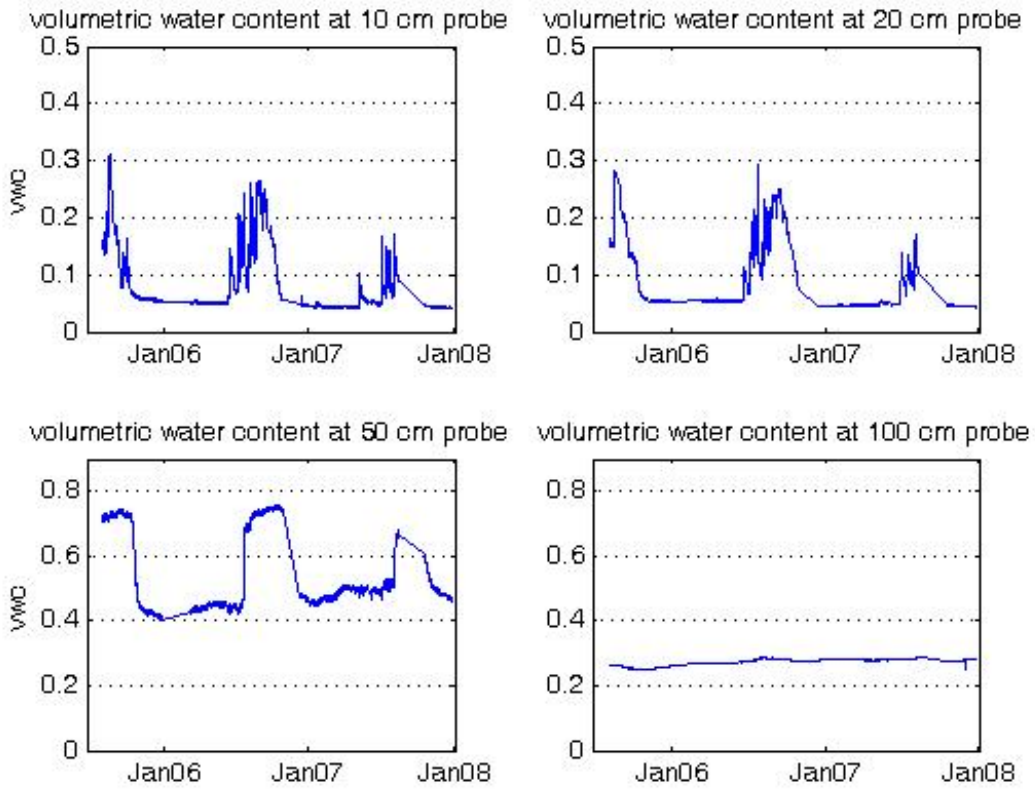

Figure 2.20. Soil moisture (volumetric water content) measured at the Zindarou North TDR station. Probes were inserted into the soil at 10cm, 20cm, 50cm and 100cm below the surface. The record spans the period 8/2/05 – 12/31/07, with a large gap in August 2007. Measurements were taken every thirty minutes.

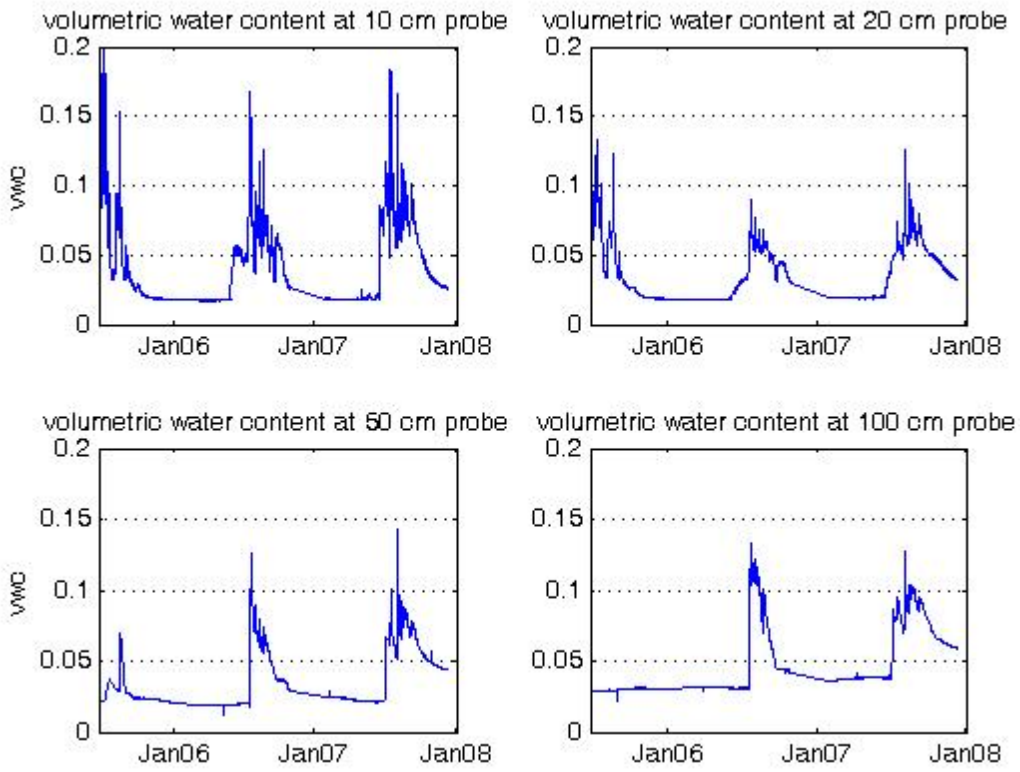

Figure 2.21. Measured soil moisture (volumetric water content) at the site “Centre”, located in the center of Banizoumbou village. Bare, sandy soil is sampled at this site. The period for this record spans June 23, 2005- December 31, 2007.

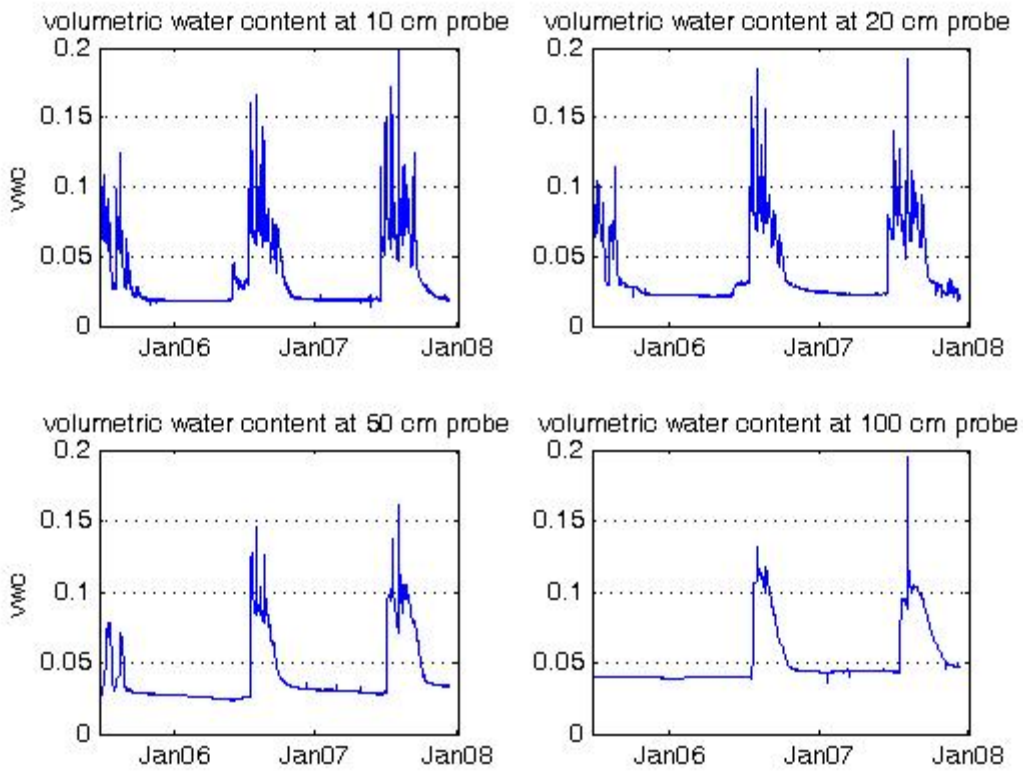

Figure 2.22. Measured soil moisture (volumetric water content) at the site “Mare”, located near a large ephemeral wet-season pool to the southwest of Banizoumbou village. Millet-cultivated sandy soil is sampled at this site. The period for this record spans June 23, 2005- December 31, 2007.

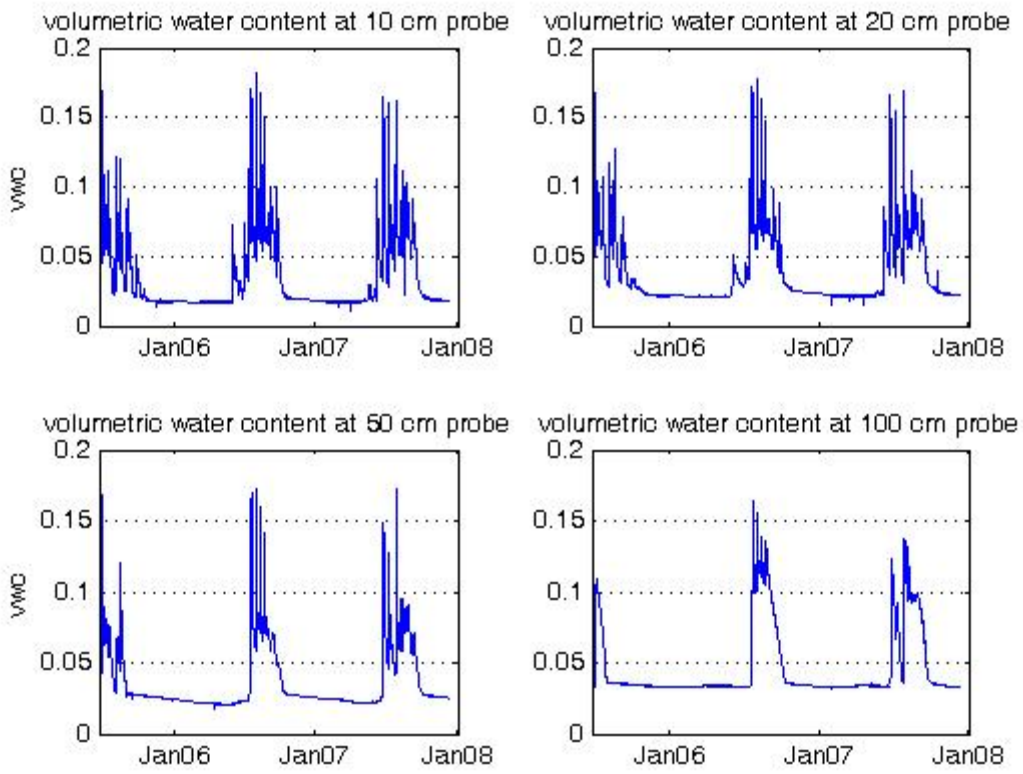

Figure 2.23. Measured soil moisture (volumetric water content) at the site “CFTEA”, located to the north of Banizoumbou village. Sandy soil planted with groundnuts during the wet season is sampled at this site. The period for this record spans June 23, 2005-December 31, 2007.

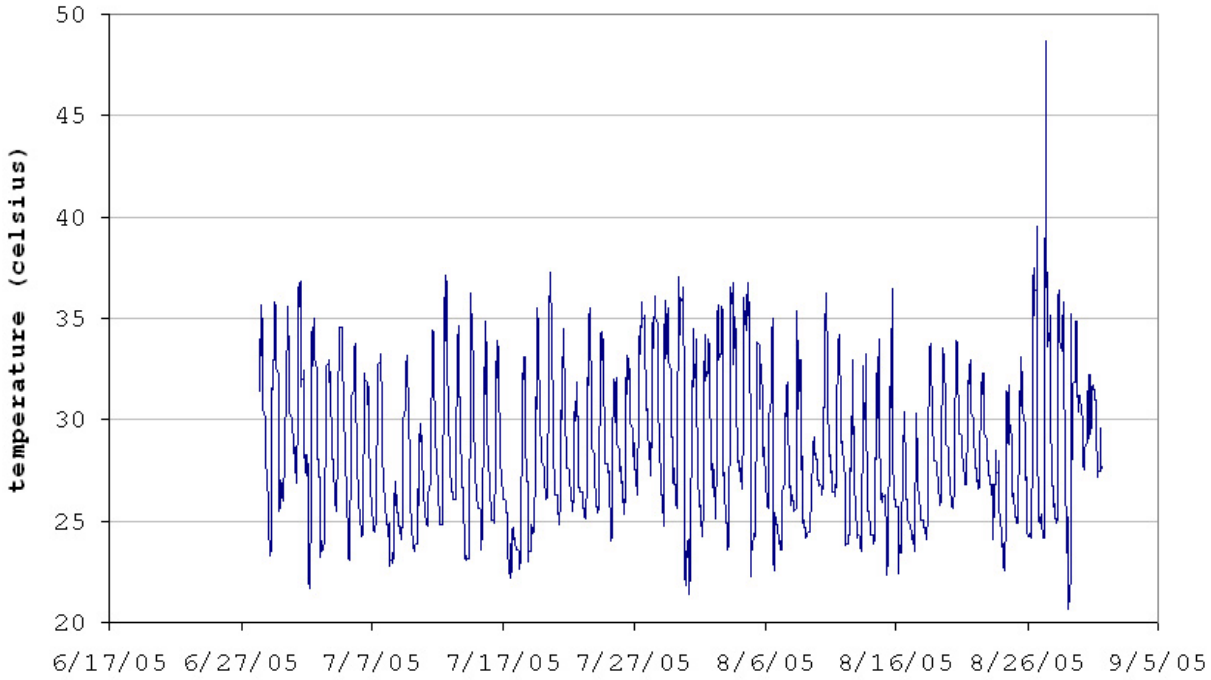

Figure 2.24. Meaured water temperatures in the large pool southwest of Banizoumbou village, named “Mare”. Periodically, the water receded and the probe was dry. An example of dry measurements are around August 28, 2005.

2.4. Water temperature data

Several in-situ water temperature dataloggers were placed in water bodies in Zindarou and Banizoumbou. HOBO WaterTemp Pro (Onset Computer, Bourne, MA) dataloggers were placed in several Zindarou garden wells and a large pool to the southwest of Banizoumbou. Figure 2.24 shows data for the large (but shallow) pool that intermittently forms to the southwest of Banizoumbou (“Mare” pool). A representative sample was chosen for this figure, as the datalogger disappeared repeatedly when it was exposed, likely taken away from the pool by curious children. After the 2005 field season, this in-situ water temperature sampling site was abandoned because the datalogger was repeatedly removed from the dried pool, and subsequently returned by the parents of children who had taken the blinking device home.

Several of the devices were also placed in the shallow garden wells of Zindarou, with generally better sampling results. Figure 2.25 shows the water temperature record from the datalogger placed in well number 30. Garden areas are typically fenced off to prevent animals from entering. This protection of the gardens and wells also minimizes the

number of people who see the datalogger. The garden owners were asked to help ensure that the thermometers remain in place. In most cases in Zindarou, the dataloggers were kept in the pools, but a few dataloggers were lost in Zindarou as well. Figure 2.26 presents the water temperatures measured in Well 16, in the southern garden area (see Figure 2.3). The extreme high and low temperatures registered by this device correspond to the well drying out. In early April, the garden owner dug the well deeper to reach the water table again, and replaced the water temperature datalogger. The resulting turbid, unshaded well had a significantly higher average temperature than the prior shaded, clear conditions.

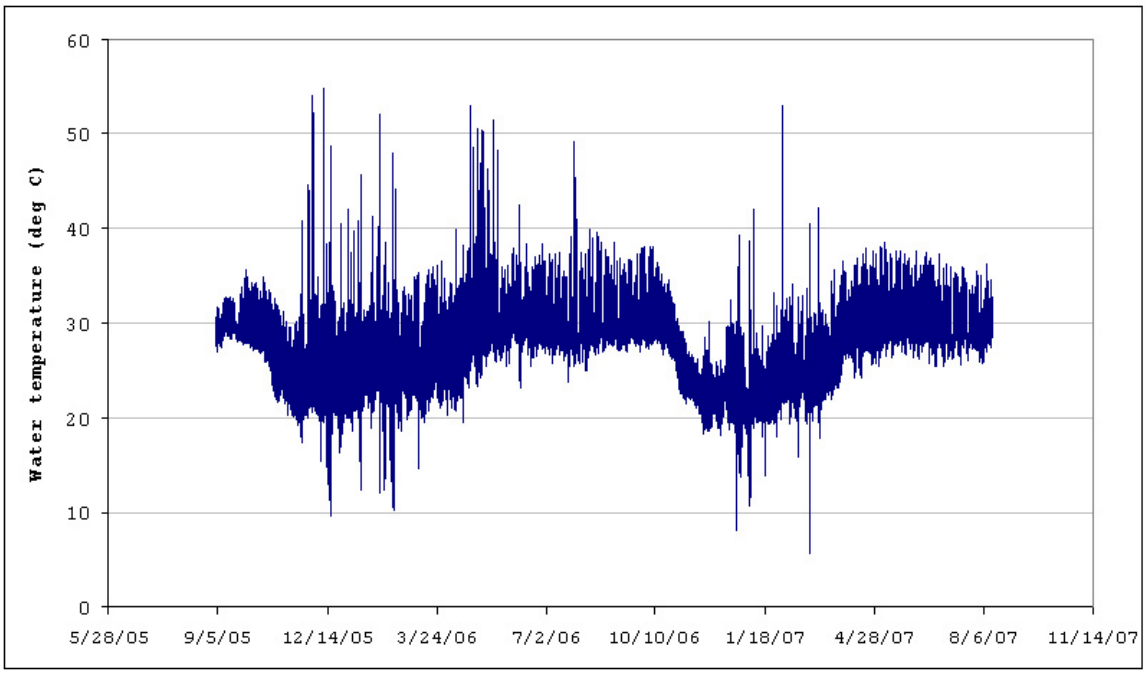

Figure 2.25. Zindarou Well 30 water temperature data. The extreme highs and lows are from periods when the probe was temporarily removed by the garden owner, and not replaced in the pool. The extremes do not indicate very high or low water temperatures.

Figure 2.27 shows measured water temperature in Zindarou well 23. The well did not become dry, but the water level was very low in the 2006 dry season, and the water temperature periodically became very high. Ultimately, this datalogger was lost during the 2006 wet season. Measured water temperature in Zindarou well 46 is shown in Figure 2.28. This datalogger was also lost in 2006. Finally, Figure 2.29 shows measurements

from the water temperature datalogger deployed in Zindarou well 1. This datalogger was also lost, in the 2006 dry season. Table 2.3 summarizes water temperature data.

Table 2.3. Summary of continuous water temperature measurements in Banizoumbou and Zindarou. All measurements were made at hourly intervals. Extremely high maximum temperatures correspond to dry pool bottoms, when the probe was measuring soil skin temperature. Actual water temperatures rarely exceeded 45 degrees.

			temperature (degrees C)			
	Start date	End date	maximum	minimum	average	measurements
Banizoumbou pool	6/28/2005	8/31/2005	48.7	20.7	28.47	6166
Zindarou Well 1	6/28/2005	12/28/2005	38.92	14.84	26.23	17558
Zindarou Well 16	12/28/2005	8/13/2007	69.68	9.9	28.47	14236
Zindarou Well 23	9/16/2005	6/8/2006	45.2	14.55	25.12	6358
Zindarou Well 30	9/2/2005	8/13/2007	54.72	5.69	27.26	17044
Zindarou Well 46	9/16/2005	7/3/2007	49.89	11.47	26.55	15720

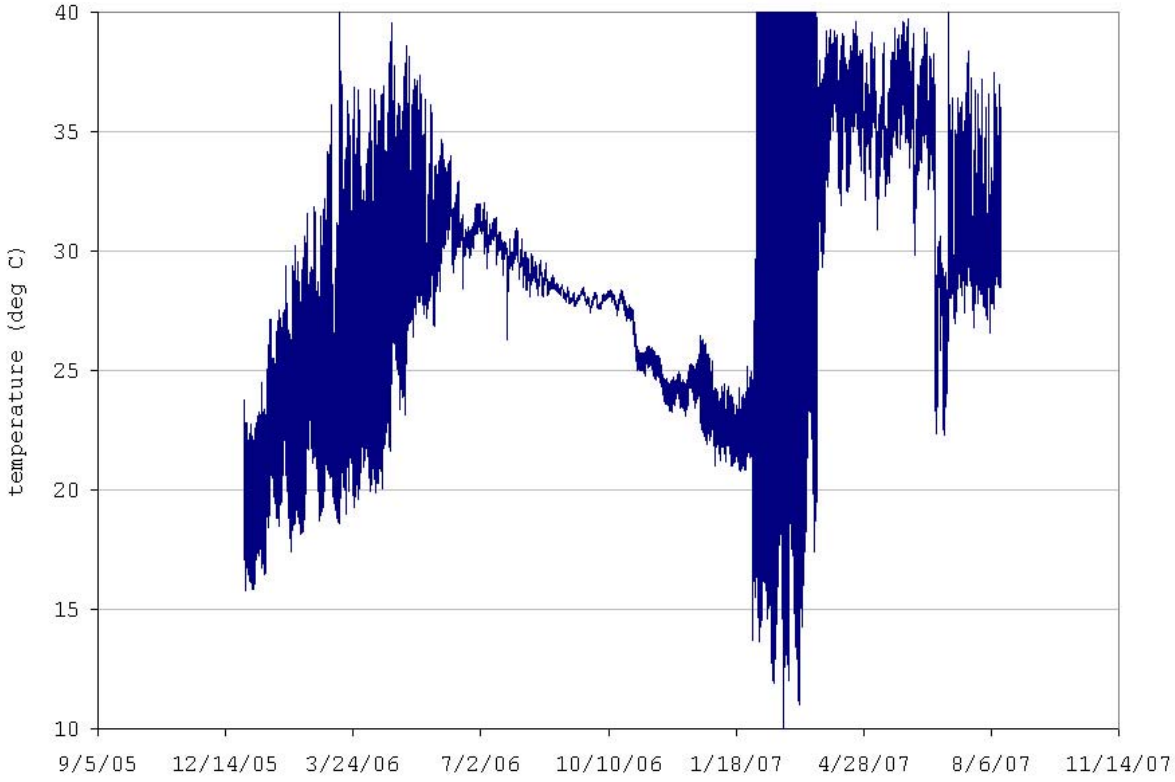

Figure 2.26. Zindarou Well 16 measured water temperature data. The extreme high and low measurements between January 2007 and April 2007 correspond to the datalogger resting on dry soil which reaches very high temperatures during the dry season. In April, villagers dug the well deeper and replaced the datalogger. The resulting turbid, unshaded water had a much higher average temperature than previously.

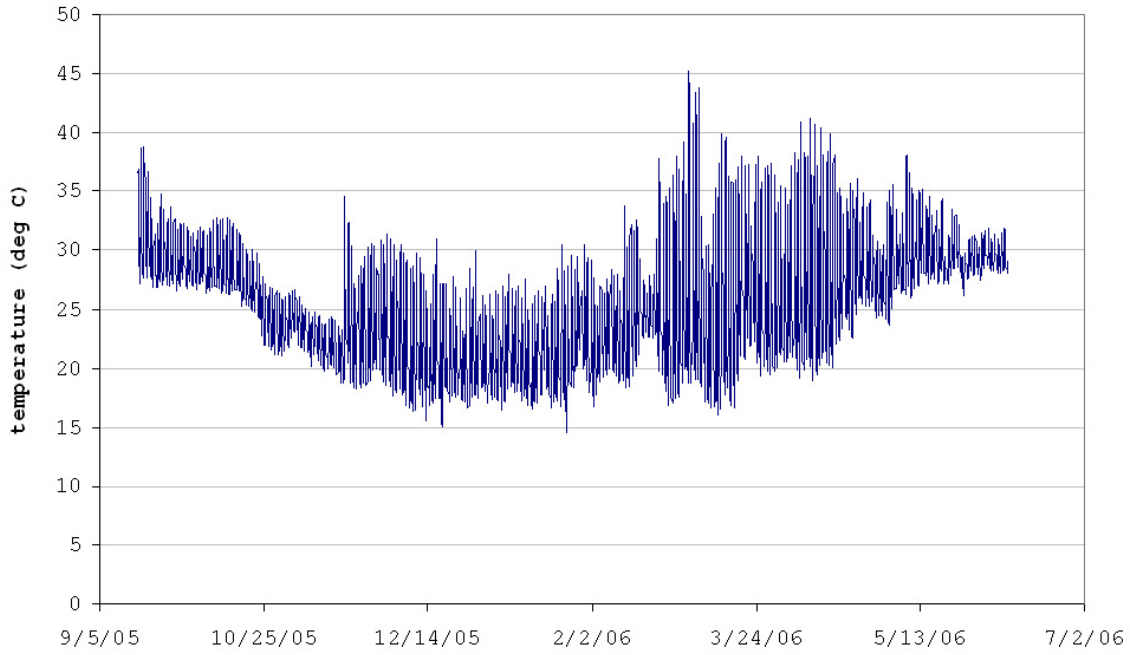

Figure 2.27. Measured water temperature in Zindarou Well 23. The well did not become dry, but the water level was very low in the 2006 dry season, and the water temperature periodically became very high. Ultimately, this datalogger was lost during the 2006 wet season.

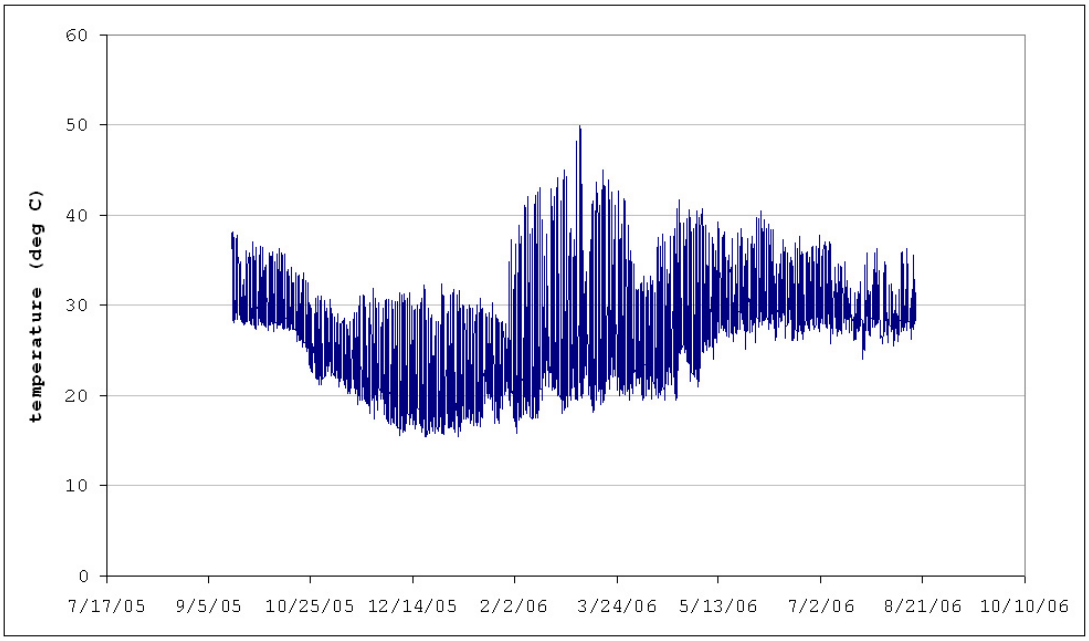

Figure 2.28. Measured water temperature in Zindarou Well 46. Very low water levels in the 2006 dry season led to very high temperatures. A deepening of the well in March 2006 resulted in lower diurnal temperature variability. This datalogger was lost during the 2006 dry season.

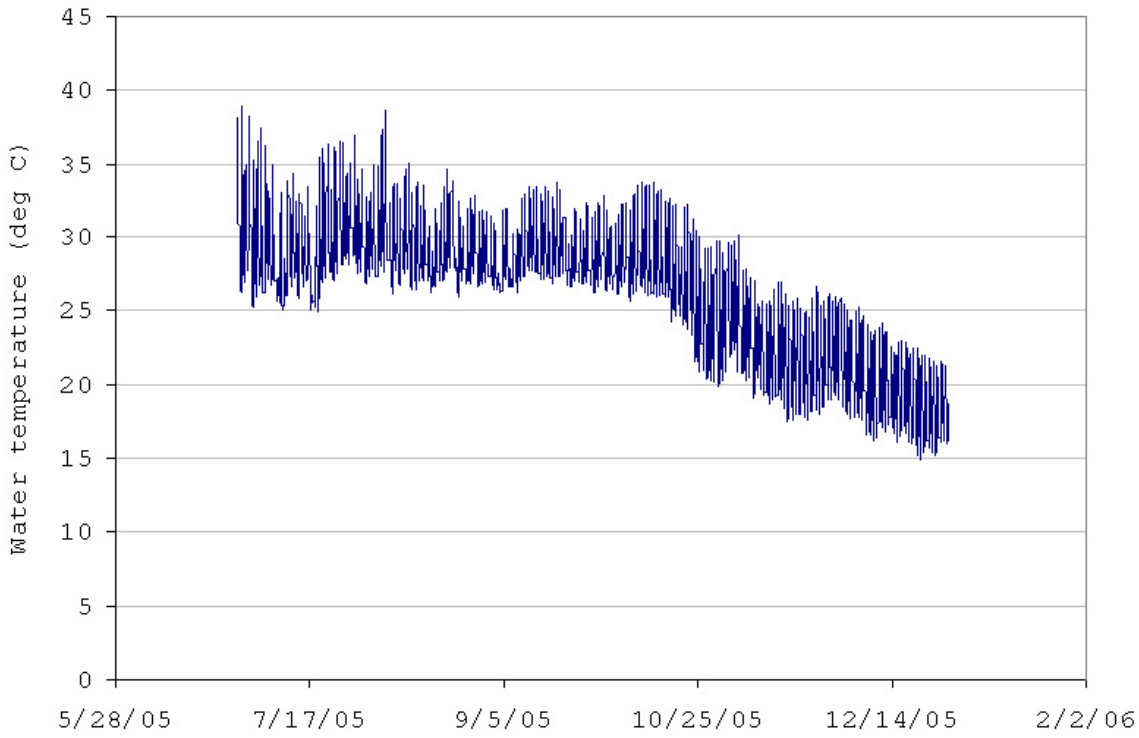

Figure 2.29. Zindarou Well 1 measured water temperature. The temperature datalogger was lost during the 2006 dry season.

2.5 Adult mosquito captures

Six CDC miniature light traps were deployed in each village. Some were placed inside houses next to peoples' beds, and others were placed outside houses. The light traps were set in the evening at 7PM with a freshly charged 6-volt motorcycle battery, and removed at 7AM the following morning after having sampled mosquitoes through the night. The traps were left in place at exactly the same location for all sampling events, and the closed nets were removed and taken to the CERMES lab for mosquito identification and count. The sampling locations are indicated in Figures 2.1 and 2.2 for Banizoumbou and Zindarou, and are marked with an "i" for indoor and "o" for outdoor placements. In addition, the sampling locations are summarized in Table 2.4.

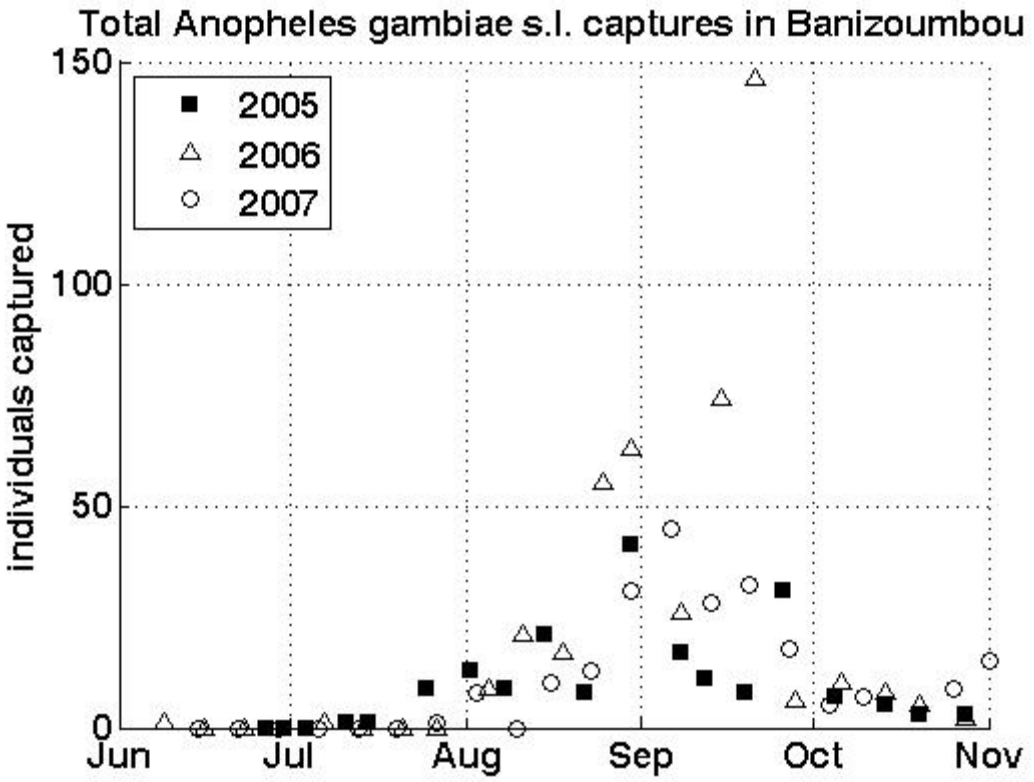

Figure 2.30. Wet season adult *Anopheles gambiae sensu lato* mosquito captures, summed over all light traps, for the 2005, 2006 and 2007 wet seasons.

Table 2.4 Summary of CDC light trap sampling locations.

	description of location	UTM easting	UTM northing
Bani1	inside house, mudbrick house	463212	1495648
Bani2	inside house, mudbrick house	463116	1495597
Bani3	outside house on tree (near Bani 2)	463116	1495597
Bani4	outside house on tree (near Bani 1)	463212	1495648
Bani5	completely thatched house and roof	463109	1495730
Bani6	mud house, thatched roof (near Bani5)	463109	1495730
Zind1	inside house, mud walls, thatched roof	491408	1485210
Zind2	outside on tree (near Zind1)	491407	1485219
Zind3	inside house, mud walls, thatched roof	491438	1485235
Zind4	outside house on rafter, (near Zind3)	491438	1485235
Zind5	outside of house, mud walls, thatched roof	491368	1485143
Zind6	inside house, mud walls, thatch roof (near Zind5)	491368	1485143

The first samples were taken on June 27, 2005 and continued on a weekly basis in the wet seasons, and monthly in the dry seasons. All mosquitoes were removed from each light trap and identified to species. Total captures of each species were counted. Total *Anopheles gambiae sensu lato* mosquitoes in Banizoumbou are presented in Figure 2.30. These mosquitoes were identified only to the species complex level, because *Anopheles gambiae sensu stricto* and *Anopheles arabiensis* are morphologically identical and require genetic analysis for identification. Because of the high number of mosquitoes captured, we did not have the resources to carry out such an identification for all captured anophelines. However, during the 2005 field season, random samples of the total captured mosquitoes were identified by PCR to species level, and the results are presented in Figure 2.31.

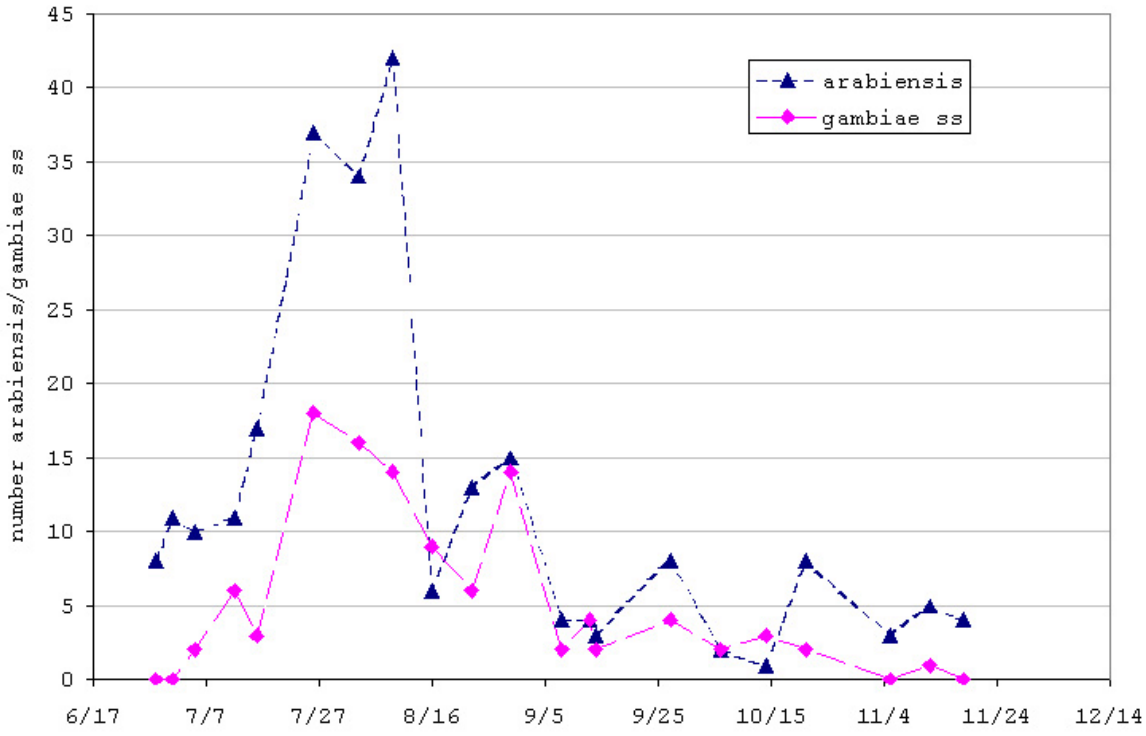

Figure 2.31. PCR analysis results of random samples of *Anopheles gambiae sensu lato* species complex mosquitoes, identified to the species *An arabiensis* and *An gambiae sensu stricto.*

Figure 2.32 shows the total captured *Anopheles gambiae s.l.* mosquitoes in Zindarou for the 2005, 2006 and 2007 wet seasons. The figure shows abundance summed over all traps. Figure 2.33 shows *Anopheles funestus* captures for the same period. Figure 2.34

depicts the same data, but superimposes *An. gambiae s.l.* and *An. funestus*, and includes dry season captures. Figure 2.35 shows all other species captured and identified in the Zindarou light traps. These included *Anopheles rufipes*, *Mansonia spp.*, *Culex spp.*, and *Aedes aegypti*.

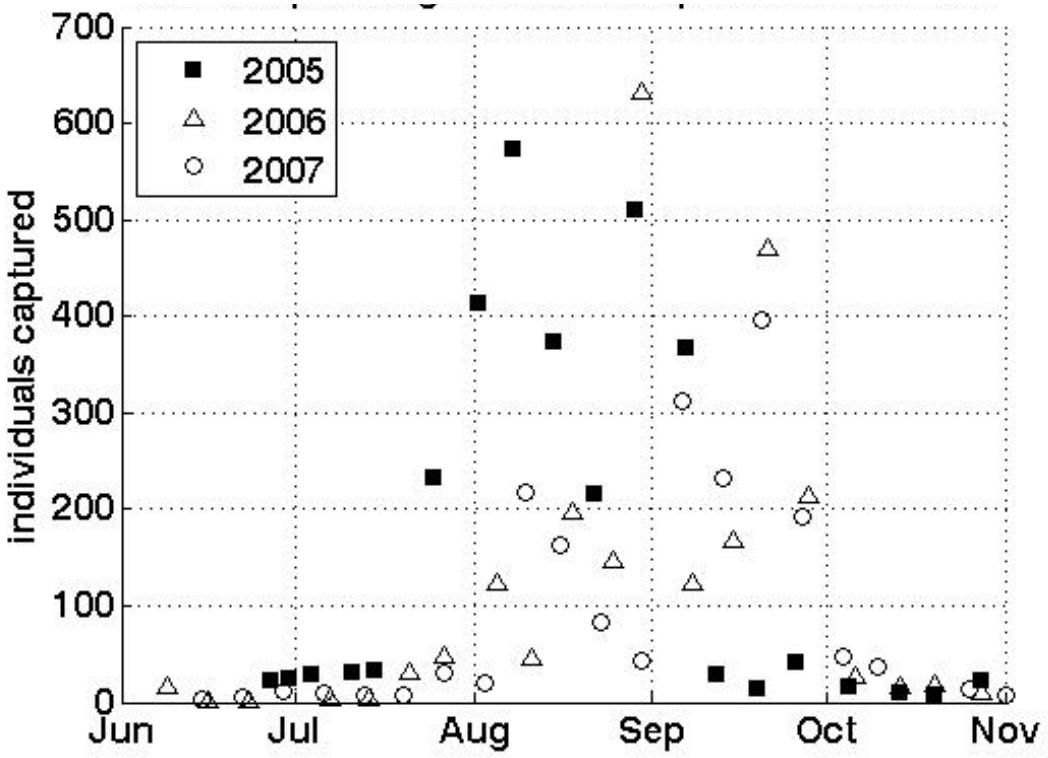

Figure 2.32. Wet season captures of *Anopheles gambiae sensu lato* in Zindarou, summed over all six light traps.

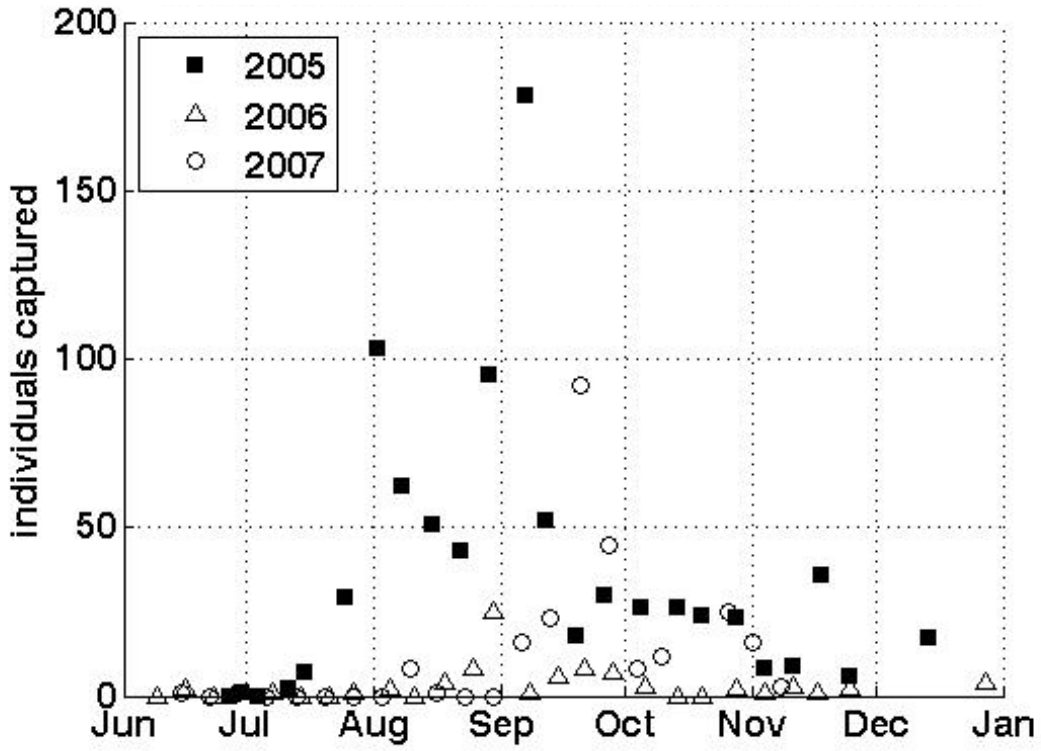

Figure 2.33. Total captures of secondary malaria vector *Anopheles funestus* in Zindarou, summed over all six light traps.

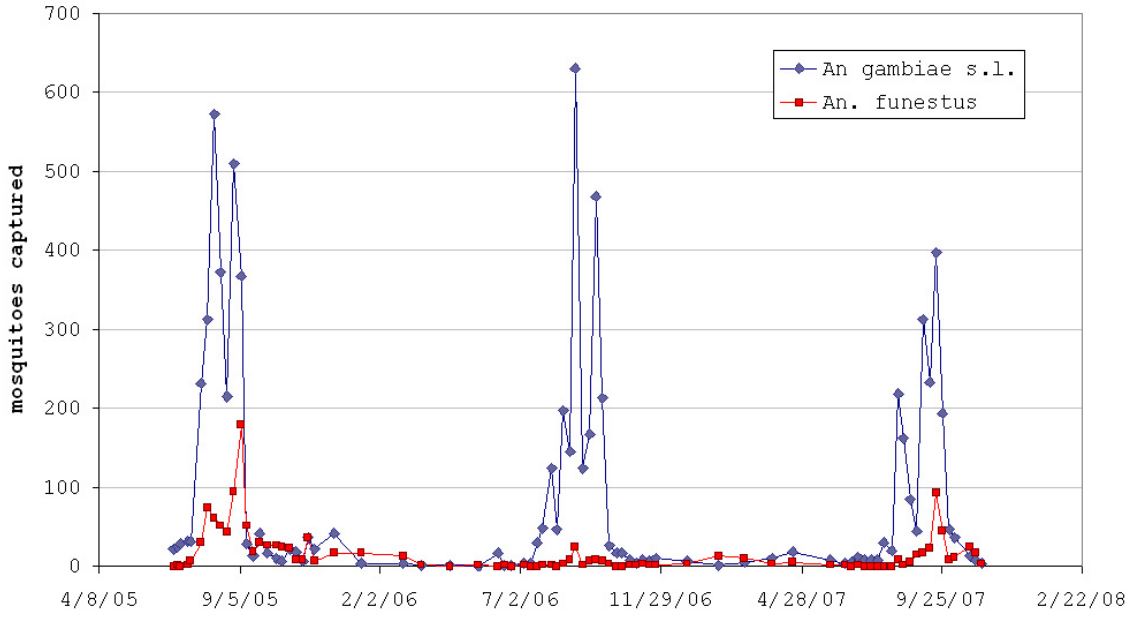

Figure 2.34. Light trap captures of *An. gambiae s.l.* and *An. funestus* in Zindarou spanning the period June 2005 – December 2007. The data are summed over all traps.

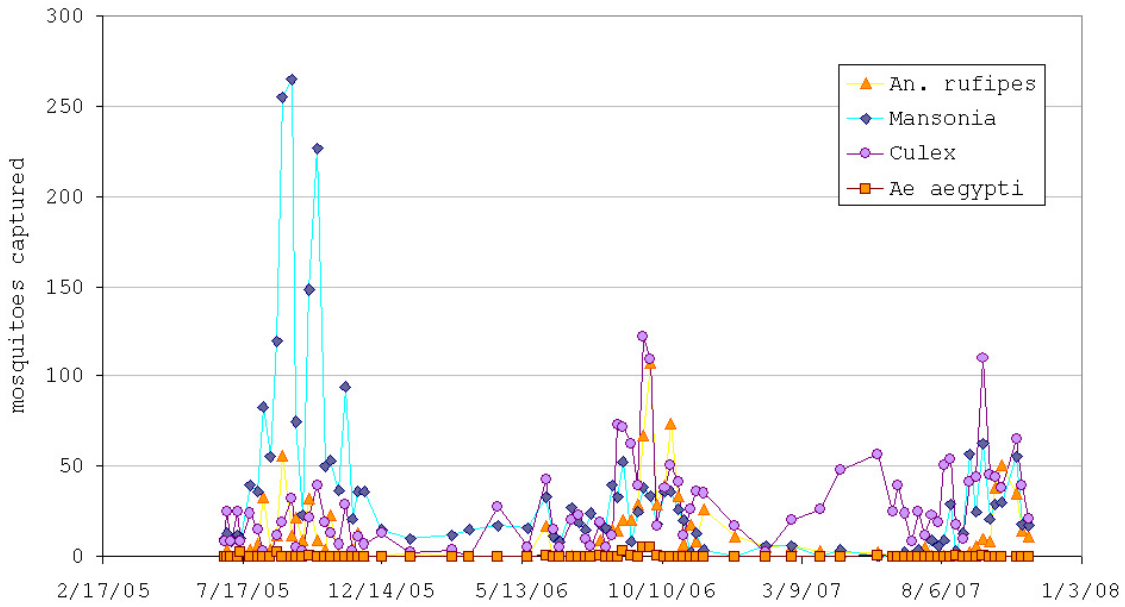

Figure 2.35. Light trap captures of nuisance mosquitoes Zindarou, summed over all traps.

2.7 Larval mosquito counts

The shallow garden wells of Zindarou provide permanent breeding habitat for a variety of mosquitoes, including *An. gambiae s.l.* and *An. funestus*. As shown in Figure 2.3, many wells are near the village in the garden areas to the east and south. None are located directly west of the village and only one (Well 30) is to the southwest in a small isolated garden area. These wells provide gravid mosquitoes abundant opportunities to lay eggs within several hundred meters of Zindarou. The wells are maintained by the villagers, and often when the groundwater level drops after the end of the wet season, villagers dig down to keep the groundwater table exposed. The wells are thus permanent water bodies through this human activity, available to gravid mosquitoes year-round as they choose a place to lay eggs. Therefore, it was recognized that they may be an important component of the entomological system in Zindarou. However, because not all permanent water bodies are utilized for oviposition by *An gambiae* (by far the preferred breeding habitat is small ephemeral rainfed pools) the role of these permanent, grass-lined garden wells was not evident originally and their entomological productivity had to be determined and monitored through the seasons. The wells were monitored for larval activity weekly during the wet seasons and monthly during the dry seasons. A standard dipper was used

to take a sample of well water, and the captured larvae were counted. At each well, ten such dips were made. The maximum of these ten counts was recorded for that well. The count results for wells 1-50 are presented in Figure 2.36. The larval counts have little quantitative value. It became clear while performing these larval surveys that the standard measurement of larvae using a dipper is a highly biased, error-prone and inaccurate measure of pool productivity. This is partly because of the observed spatial clustering of anopheline larvae within pools. Small groups were seen to stay close together, leaving large areas of the pool devoid of larvae and small clusters of high density. Larval counts in the dippers also depended on the ability of the observer to see larvae on the surface. If they were obscured by grass or a deep well, the counts would be significantly lower because the target larvae were not seen. Completely blind dipping results in very low counts. Nevertheless, qualitative information can be derived from these surveys. Through the observations of many larvae, the garden wells were confirmed as important for sustaining year-round malaria transmission in Zindarou. Periodically, samples of anopheline larvae were taken to the CERMES laboratory from the field, reared to adulthood, and identified. This was done to confirm that the important malaria vectors *An. gambiae s.l.* and *An. funestus* were in fact present, and that the counted anopheline larvae were not exclusively the insignificant but common vectors *An. rufipes* or *An. pharoensis*. Table 2.5 shows the results of these samples, which confirm that the dangerous malaria vectors indeed utilize the wells for breeding.

Table 2.5. Identification of anopheline larvae sampled from several Zindarou pools. Larvae were taken to the CERMES lab in small sample bottles, reared to adulthood, and identified to species.

Date	location Label	Identified larvae	general description of site
28-Jul	Well 24	An. pharoensis	grassy, 50% duckweed coverage
2-Aug	Well 38	An. rufipes, An. gambiae	relatively turbid, little grass
8-Aug	Well 16	An. rufipes	80% duckweed coverage
8-Aug	Well 30	6 x An. gambiae	lily pads, no duckweed
22-Aug	Well 47	An. gambiae	some grass
29-Aug	Well 4	An. rufipes	grass and lillies
29-Aug	Well 16	7 x An. pharoensis, An. rufipes	Well flooded; dipped in flooded area
29-Aug	Well 41	An. rufipes, An. gambiae	50% covered by lillies
29-Aug	Well 47	An. rufipes	grassy, murky algae layer
30-Aug	Ikonos	4 x An. gambiae	open, shallow, turbid pool
30-Aug	East	7 x An. gambiae	large pool, grassy edges, shallow
13-Sep	Well 16	2 x An. gambiae	Flooded area
16-Sep	MW24	1 x An. rufipes	uniform, marshy area with abundant vegetation cover; little open water
16-Sep	Pool next to Well 22	1 x An. gambiae, 2 x An. rufipes, 1 x An. funestus	very overgrown, and grassy
19-Sep	Well 23	1 x An. gambiae	grassy, algae floating
19-Sep	Well 26	1 x An. rufipes	grassy, overgrown
19-Sep	Well 45	2 x An. rufipes	open, grassy edges
26-Sep	Well 26	1 x An. gambiae	Grassy
27-Sep	MW24	3 x An. rufipes	uniform, marshy area with abundant vegetation cover; little open water
27-Sep	Ikonos	2 x An. gambiae	open, shallow, turbid pool
27-Sep	Well 8	8 x An. gambiae	open, found a surprising number of larvae clinging to floating debris

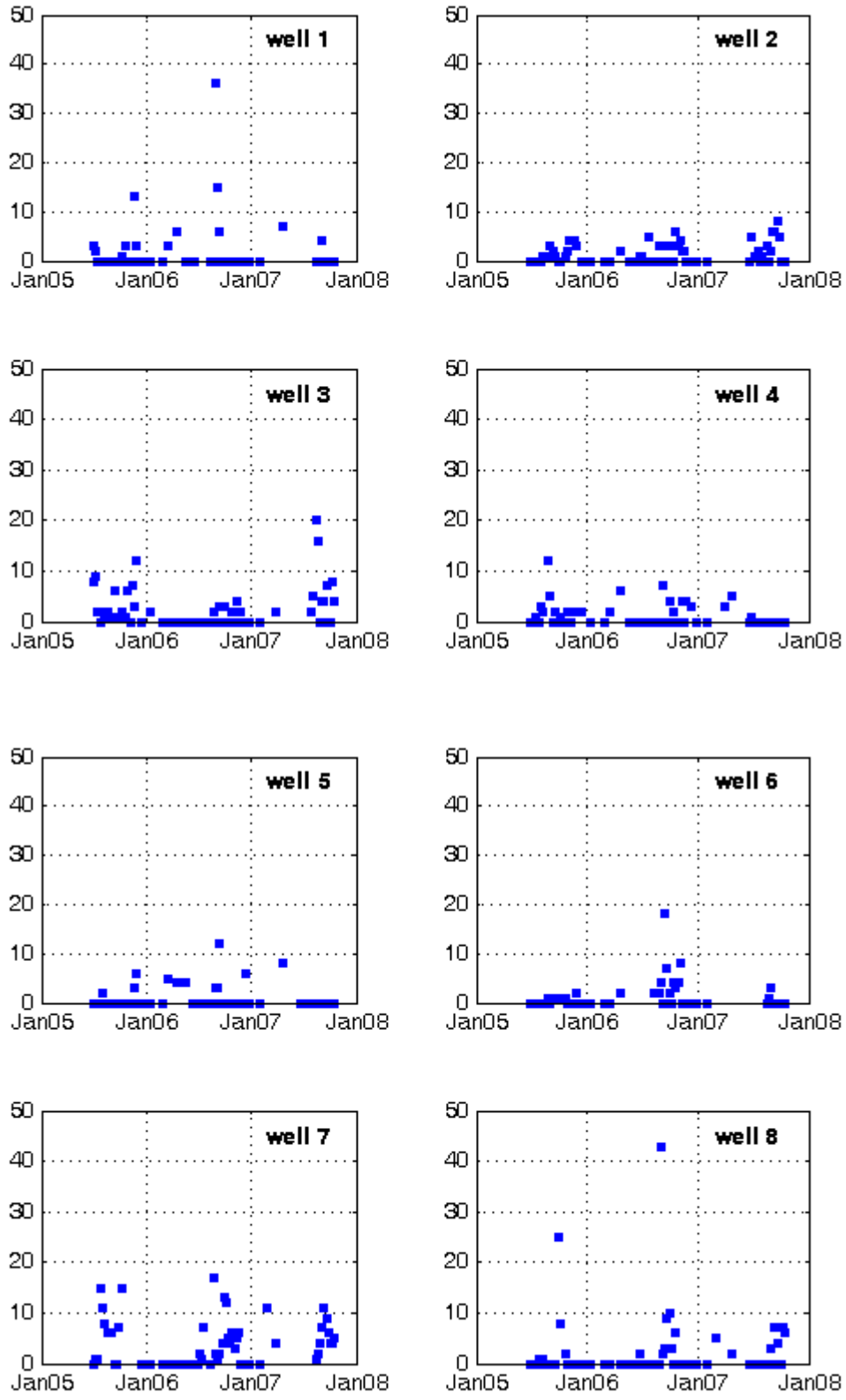

Figure 2.36. Larval counts in Zindarou wells, for the period 6/26/05-12/31/07.

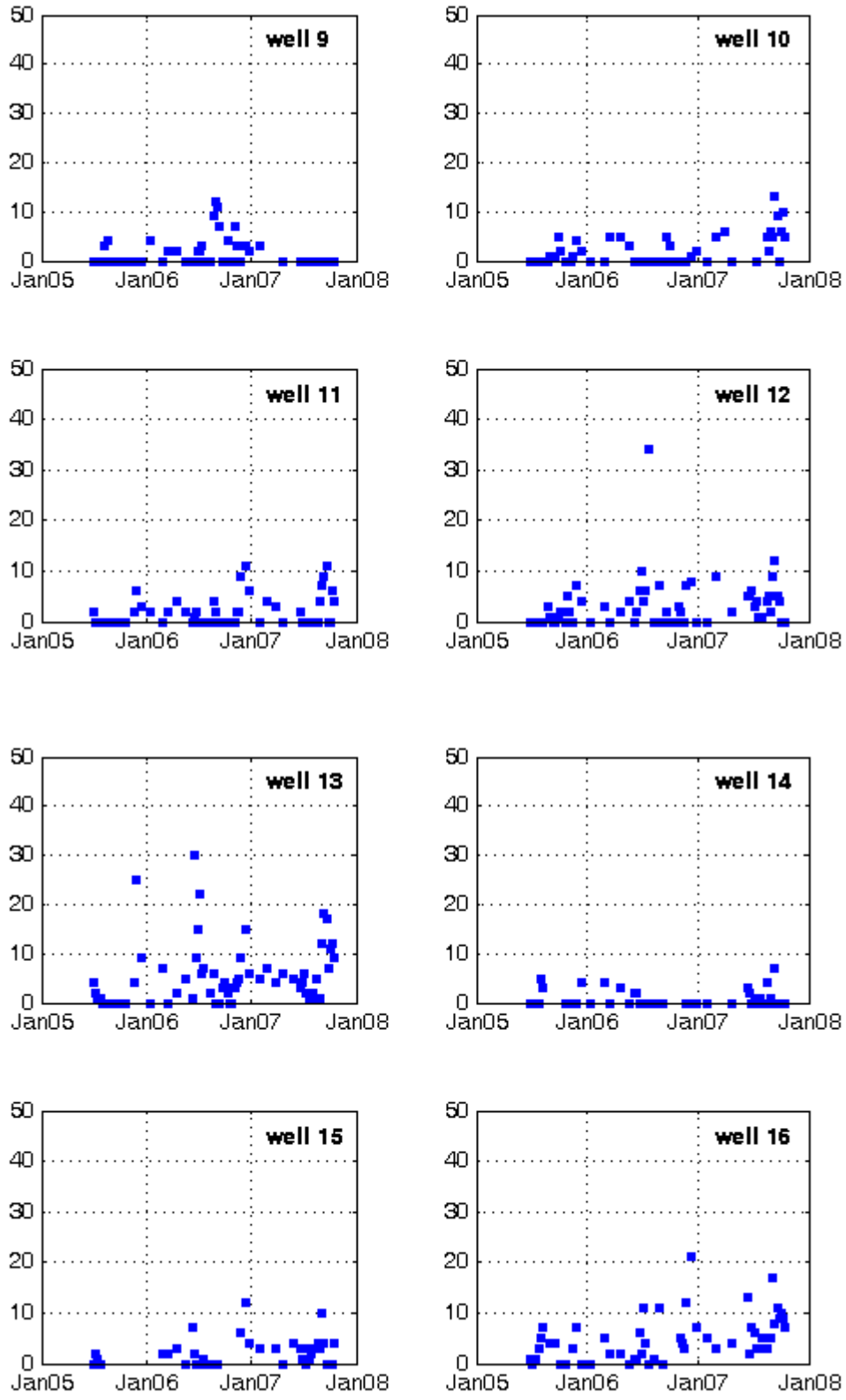

Figure 2.36b. Larval counts in Zindarou wells, for the period 6/26/05 – 12/31/07.

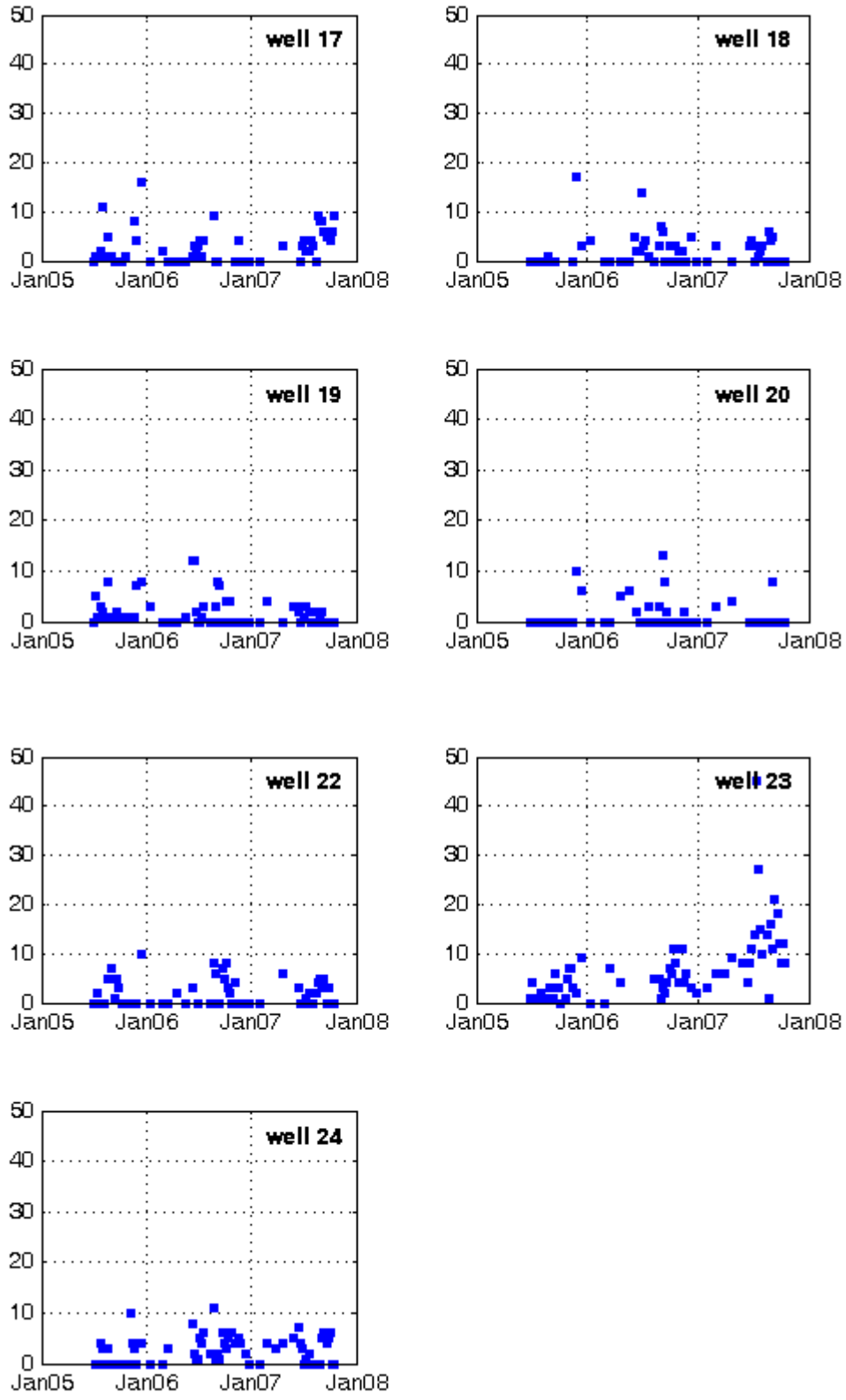

Figure 2.36c. Larval counts in Zindarou wells, for the period 6/26/05 – 12/31/07.

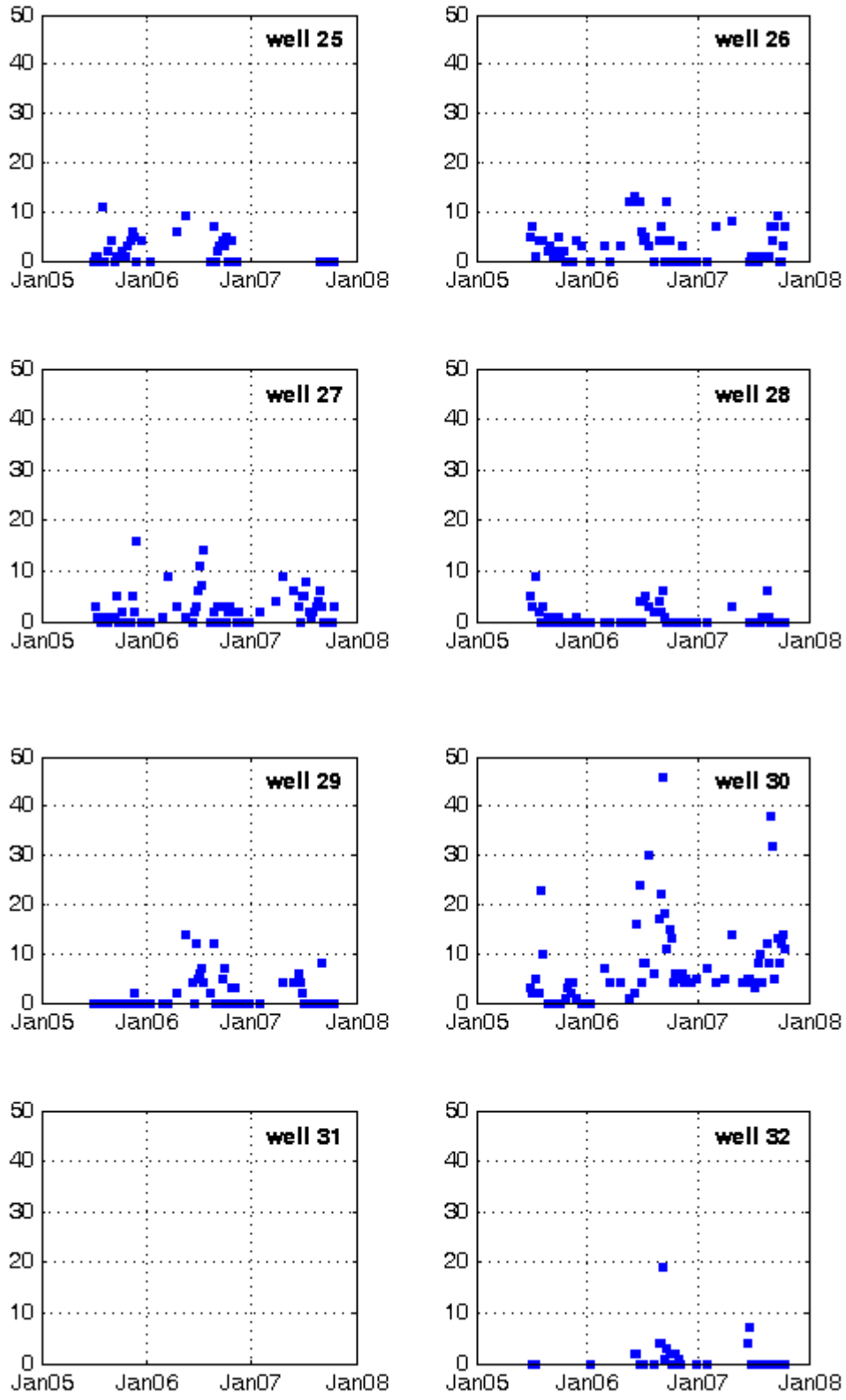

Figure 2.36d. Larval counts in Zindarou wells, for the period 6/26/05 – 12/31/07.

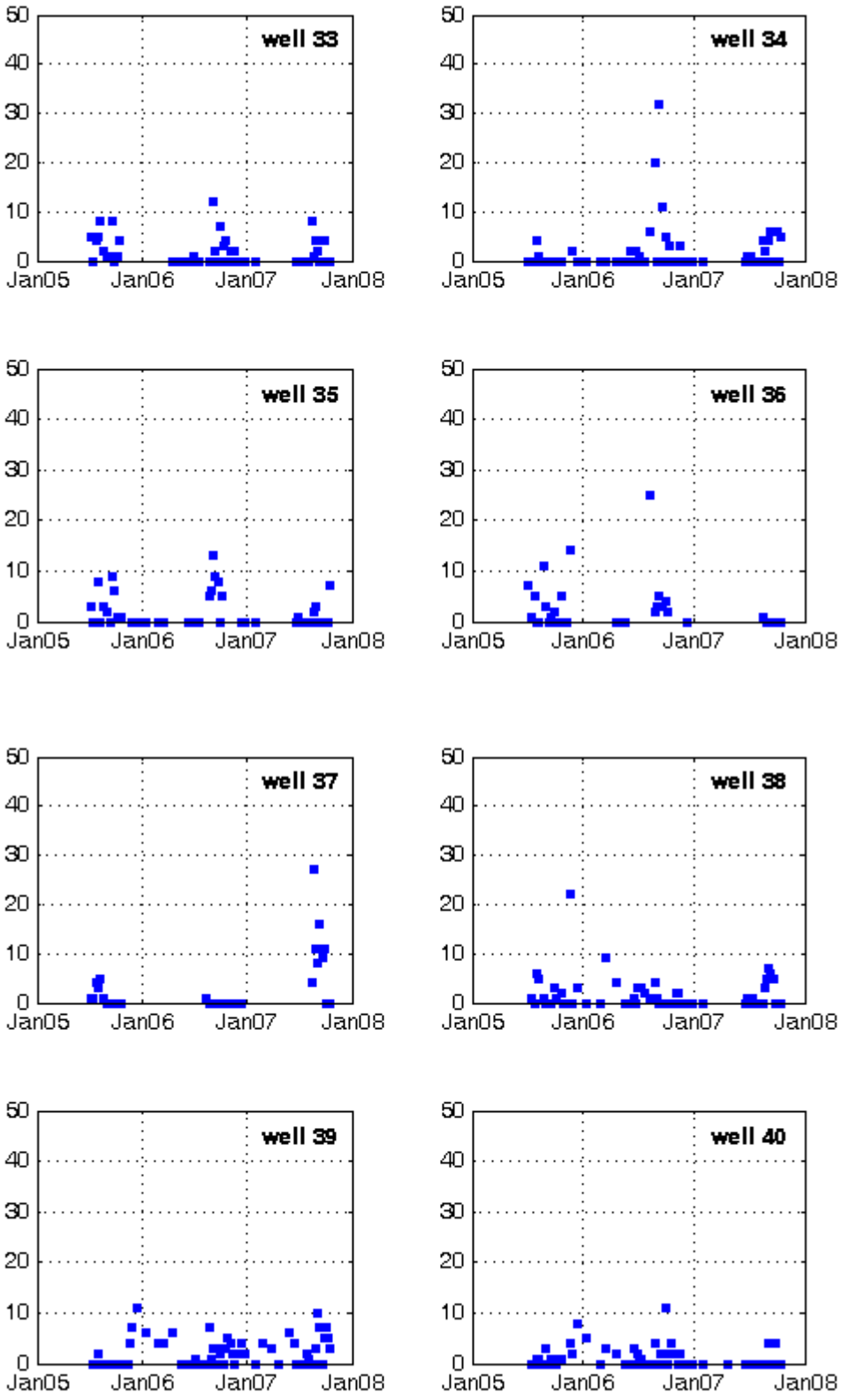

Figure 2.36e. Larval counts in Zindarou wells, for the period 6/26/05 – 12/31/07.

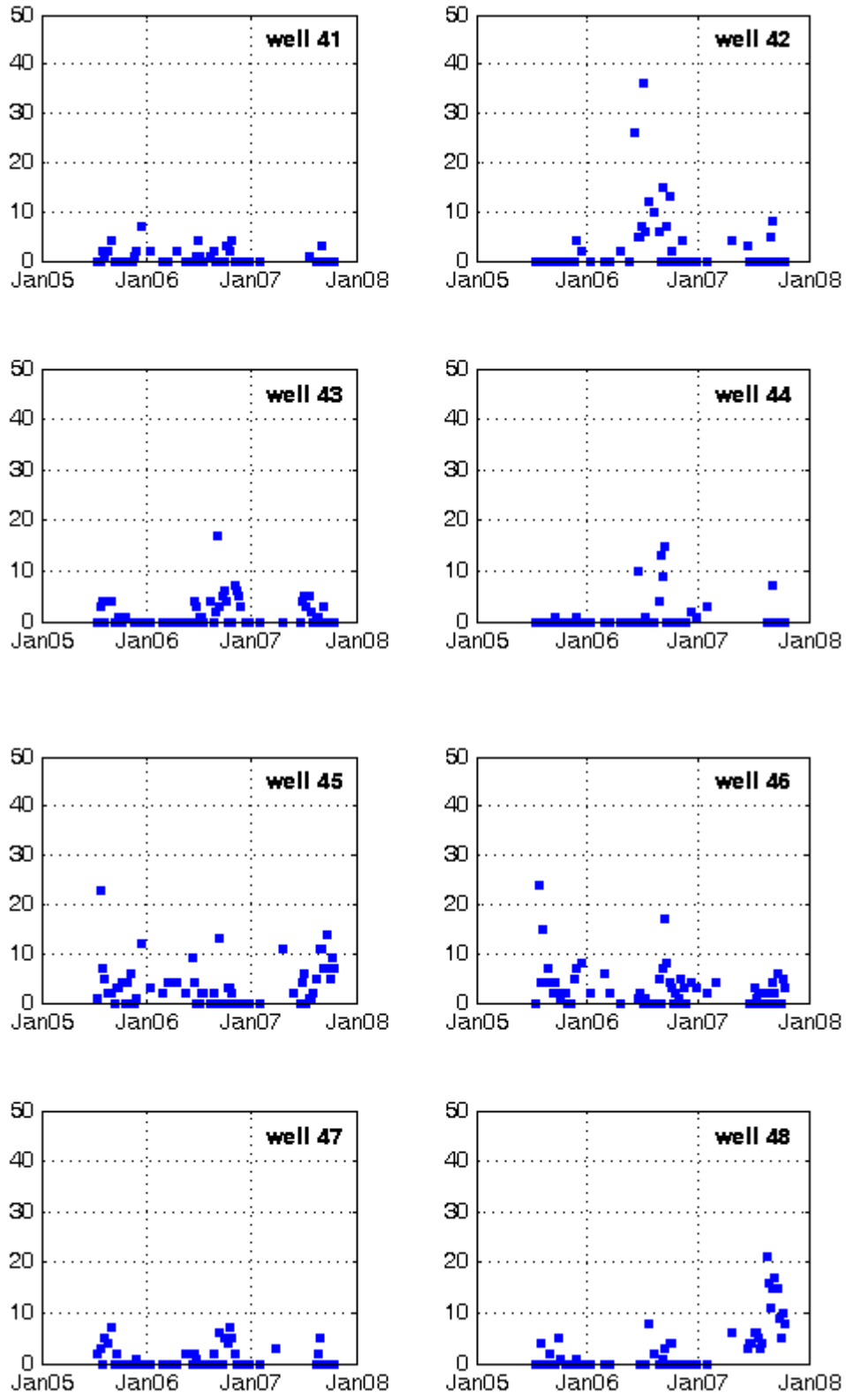

Figure 2.36f. Larval counts in Zindarou wells, for the period 6/26/05 – 12/31/07.

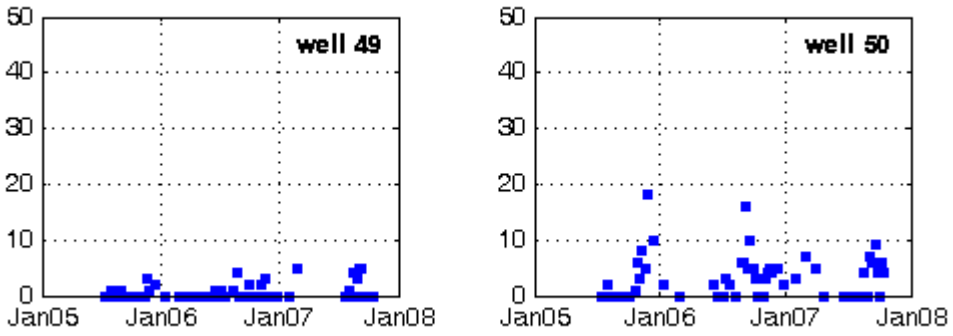

Figure 2.36g. Larval counts in Zindarou wells, for the period 6/26/05 – 12/31/07.

2.8 Water level observations

The garden wells expose the shallow groundwater table. They can therefore be used to monitor the changes in the groundwater table, provided a suitable permanent reference point is established for each well measurement. In some wells, metal rods were pounded into the deepest point within each well. The level was measured from the tops of these rods to the water surface. The elevations above mean sea level of these reference points were measured with a GPS topographic survey, allowing groundwater levels observed at wells to be directly compared. The results are presented in Figure 2.37. Observations of groundwater levels at wells were combined with observations of saturated conditions at TDR probes to obtain the groundwater level fluctuation. Because the observed gradient is near zero, these combined observations are considered representative of the groundwater level in the area immediately around Zindarou.

2.9 Temporary rainwater pools

The temporary pools resulting from rainfall runoff around Banizoumbou and Zindarou were observed to host intensive mosquito breeding activity. After several regular field visits, the locations of regularly recurring pools became evident. These pools were dipped for larvae at each field visit, and explorations were made in and around the villages to seek out possible newly-formed pools. Larvae were counted using a standard dipper using the same method described above for the Zindarou wells (section 2.7). These pools were typically turbid, devoid of vegetation and on the scale of tens of meters in size. In virtually all cases these pools contained abundant larvae during the wet season, however

persistent pools were not always continually occupied by larvae. Figure 2.38 shows the number of counted larvae for each regularly revisited pool. Other pools formed occasionally, but they are not presented here because they were not as consistently present as the pools in Figure 2.38 and rarely productive. Formation and disappearance of the pools presented in Figure 2.38 strongly control mosquito population dynamics in Banizoumbou and Zindarou, as will be discussed in subsequent chapters. Similar to the Zindarou wells, however, larval counts in these ephemeral pools contain little quantitative value, and are used only to gauge pool productivity qualitatively.

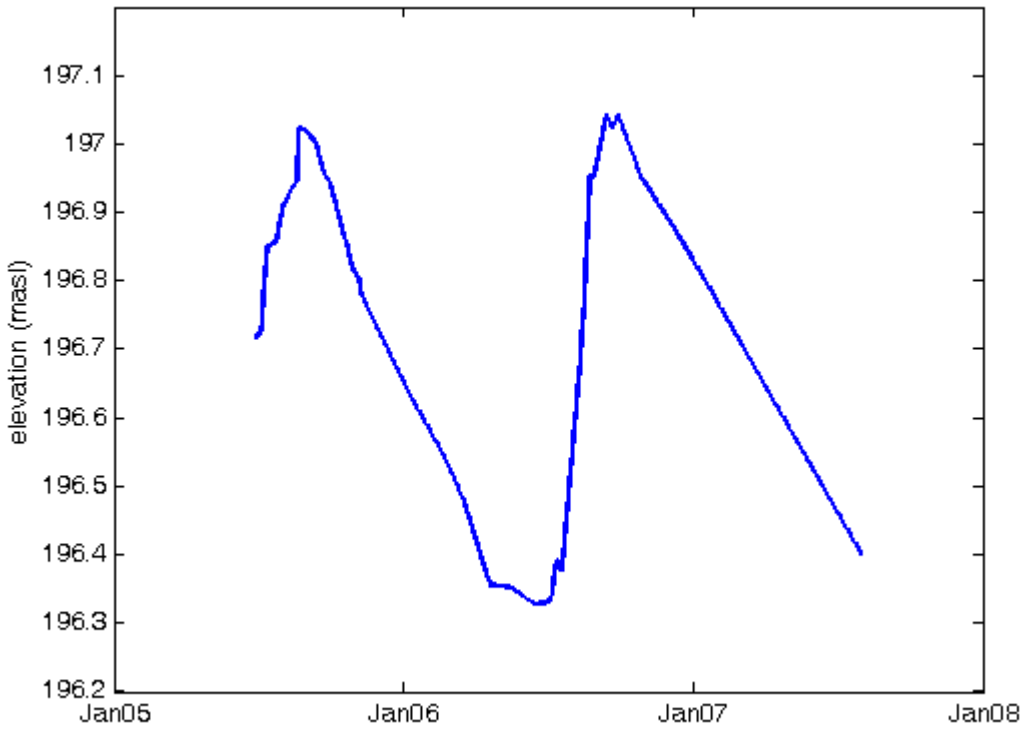

Figure 2.37. Compiled observed groundwater levels and observations of saturated conditions at TDR probes, as a representation of groundwater table fluctuations in Zindarou. The gradient is near zero and these levels are observed to be very close at all wells.

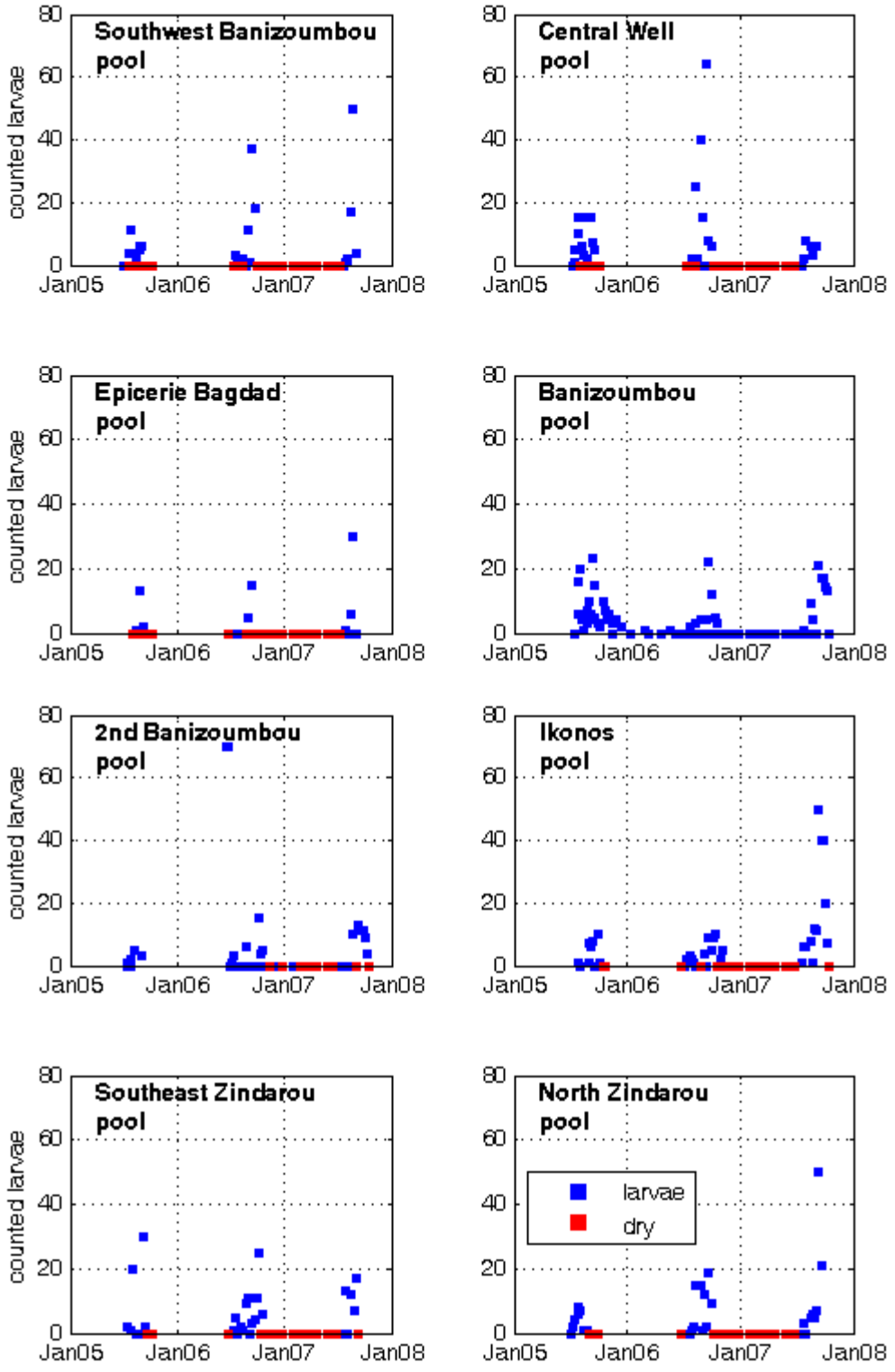

Figure 2.38. Larval counts in several ephemeral pools in and around Banizoumbou and Zindarou. Red markers denote dry pool conditions at the field visit.

Chapter 3 Model Development

3.1 Introduction

3.1.1 Background

Malaria is inextricably tied to water. Because malaria vector mosquitoes utilize water bodies for breeding, malaria cannot exist in regions where environmental conditions prohibit the formation and persistence of such water bodies. Consequently, for regions where water availability limits mosquito populations, hydrology models can provide useful predictive tools for vector mosquito population dynamics, which extends to malaria force of infection. Addressing the inherently cross-disciplinary nature of this problem using numerical modeling techniques at the appropriate spatial and temporal scales should result in an improved understanding of malaria transmission dynamics. We present such a model in this study, applicable to village-scale malaria transmission within African desert-fringe environments such as the Sahel. We then apply the model to Banizoumbou, a typical sahelian village in southwestern Niger.

Malaria burden is particularly severe in sub-Saharan Africa. Sixty percent of the world's 300 - 500 million clinical malaria cases and 80% of worldwide malaria deaths (WHO, 2005) occur in this region. This disproportionately high disease burden in Africa is due primarily to the dominance of *Plasmodium falciparum*, the most severe and fatal form of human malaria, as well as behavioral traits of *Anopheles gambiae* mosquitoes, the principal vectors of the disease in much of the continent. *An. gambiae*'s strong preference for human hosts (anthropophily) makes it an exceedingly efficient vector (White, 1974; Costantini et al., 1996a).

In the African Sahel, monsoonal rainfall collects in small ephemeral pools which dot the landscape after rainfall events (Desconnets et al., 1997). These pools are the preferred breeding habitat of *An. gambiae*. Figure 3.1 shows an example of a typical anopheles-infested rainwater pool near Banizoumbou. In much of the Sahel, such pools are ubiquitous, and are often found to contain many mosquito larvae, especially near human

habitation. The subset of these pools persisting long enough for at least one complete subadult mosquito maturation cycle (7-10 days) facilitates the observed explosive mosquito population growth during the Sahel monsoon (Gillies and DeMeillon, 1968). This seasonal mosquito population peak precedes and causes observed seasonal peaks in malaria incidence, which lag the wet season peaks by several weeks. Figure 3.2 shows malaria incidence data for three years at the clinics in Niger, superimposed on GPCP monthly average rainfall in the same region. In this particular case malaria is endemic (constantly present) but highly seasonal. The dependence of malaria incidence and burden on seasonal precipitation-driven mosquito population dynamics is abundantly clear.

Figure 3.1. A typical rainfed pool which facilitates malaria mosquito breeding. Such pools dot the landscape and can become infested with mosquito larvae. They are the primary controls of population dynamics in the Sahel. Note the proximity to the village in the background.

Due to the lower levels of natural immunity resulting from lack of year-round sustained malaria transmission, zones of unstable malaria transmission such as semi-arid regions or transition zones between malaria-endemic and malaria-free regions are often subject to periodic severe malaria epidemics when environmental conditions shift to favor malaria transmission (Kiszewski and Teklehaimenot, 2004). With its infamous climate

variability, the Sahel is no exception. Because of this unstable and seasonally severe malaria transmission, we focus our effort on modeling environmental conditions typical of the Sahel as a forcing for a mosquito population model.

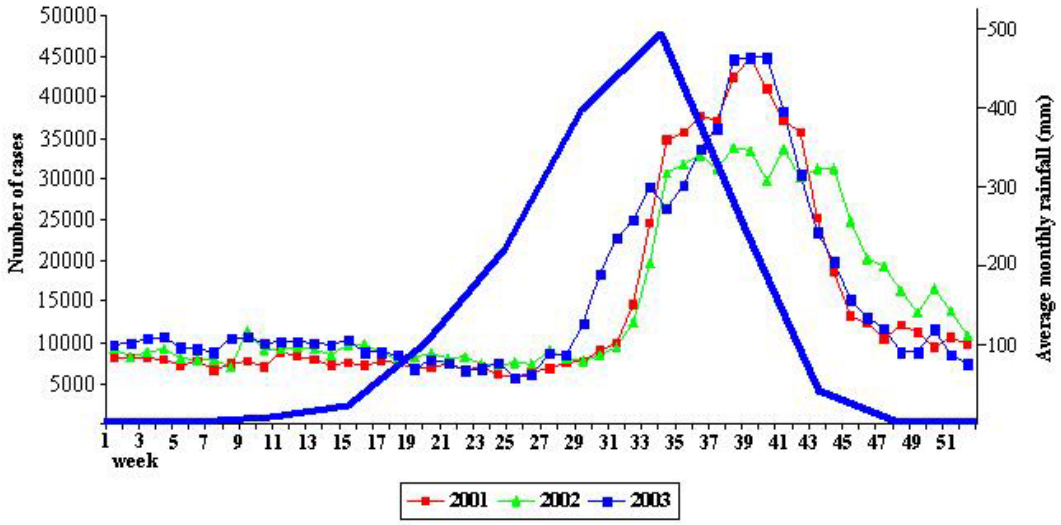

Figure 3.2. Weekly malaria incidence in Niamey, Niger from 2001 to 2003 including GPCP average monthly precipitation data.

In addition to precipitation-driven pool formation, environmental variables can affect the transmission of malaria in several ways. First, the temperature of water bodies (influenced by solar radiation, rainfall, and air temperature) governs the development rate of aquatic stages from eggs to adult emergence. After emergence, because mosquitoes cannot regulate their body temperature, ambient temperature sensed by the adult mosquito strongly affects gonotrophic (egg development) and sporogonic (sporozoite parasite stage development) rates in a degree-day dependence (Detinova, 1962). Furthermore, relative humidity and temperature are thought to influence survivability of adult mosquitoes (Clements, 1963; Craig et al., 1999). Low relative humidity and high temperature may severely stress mosquitoes and cause premature death. The requirement that mosquito longevity exceed the temperature-dependent extrinsic incubation period (parasite development time within the mosquito before it can be transmitted to the next host) restricts malaria transmission to areas with conducive climate conditions. In addition, small-scale variability in these variables associated with micro-habitats (e.g. in

houses, in tree canopies, or other such shelters) may provide refuges sought out by mosquitoes to escape highly stressful ambient conditions such as low humidity, high temperature, or high wind, and may influence survivability and vectorial capacity (Okech et al., 2003). Thus, actual mosquito longevity and sporogonic development may differ from those predicted by coarse-resolution models for mosquitoes occupying micro-habitats. Malaria transmission and force of infection strongly depends on both mosquito longevity and sporogonic development (Ross, 1911; Macdonald, 1957).

Spatial relationships between *Anopheles* breeding habitat, the vectors' human hosts, and favorable microhabitats can also significantly factor into transmission intensity of a human population. Flight distance between productive breeding sites and nearest human habitation can affect mosquito fecundity through lower time required for each gonotrophic cycle (Le Menach et al., 2005; Minakawa et al., 2002), and proximity of predicted breeding pools to sources of airborne nutriment such as maize pollen can strongly influence pool productivity (Ye-ebiyo et al., 2003).

Mosquito population response to environmental perturbations such as climate variability is highly nonlinear. This is due not only to nonlinear hydrologic response to rainfall variability and the threshold temperature and humidity effects outlined above, but also to ecological limitations of nutrient competition and predation, which act in response to exponentially growing populations, in a negative feedback (Sutherst, 2004). The combined effects from all of these factors suggest that simple correlative studies of malaria prevalence with climate variables may not suffice, and a more sophisticated approach is necessary in order to adequately predict system response to perturbation scenarios. The complex system of malaria's dependence on environmental conditions may be best studied using a representative mechanistic model.

The presented model was developed for two primary goals. First, we seek to understand the effects of interannual climate variability on village-scale malaria transmission. Identification of the environmental factors driving seasonal transmission variability is a key to understanding longer-term trends in malaria transmission (Pascual and Dobson,

2005). In the Sahel, anopheles breeding pool persistence (and therefore potential for mosquito breeding productivity) depends as much on precipitation frequency, timing and individual storm hyetographs as it does on cumulative rainfall. Excessive rainfall may flush out breeding pools, but storm return periods significantly longer than typical pool persistence times would result in pool desiccation, total sterilization of all aquatic stage mosquitoes within that pool, and would therefore preclude adult mosquito development (Charlwood et al., 1995). Site-specific microtopography, microclimate, and soil and vegetation type determine pool persistence. Interannual variability in humidity and temperature can affect populations as well, as described above. The model was developed to address effects of the Sahel's pronounced climate variability on malaria transmission and transmissibility, measured by malaria prevalence and mosquito vectorial capacity.

The second purpose of the coupled model development was to construct a modeling framework that allows explicit representation of the spatial determinants of malaria transmission. Differences in pool productivities may be related to a variety of proximal factors, all of which have small characteristic scales, such as nearby human habitation, presence of livestock (which act as an alternate bloodmeal source for anophelines), nearby pollen sources such as maize or millet or microhabitat availability. Mosquitoes' interactions with these spatial determinants and the village inhabitants can be represented using an agent-based approach operating on a small-scale grid. Spatial structure of the population is maintained, which is absent in analytical models with "perfect mixing" assumptions. With such a format, mosquito population structure can be reproduced, observed, and studied in a simulated, virtual field environment. An important extension of this design purpose is that potential local intervention methodologies can be evaluated *a priori*. The model can evaluate a variety of environmental management scenarios, such as the effects of pool removal, draining, larviciding, etc. In addition, specific questions about mosquito population behavior such as dry season survival, or inter-village mosquito migrations can be examined.

Several studies have confirmed association of climate variability and malaria transmission, and some models have demonstrated predictive ability based on malaria/climate associations

using past observations (e.g. Teklehaimenot et al., 2004, Thomson et al., 2006). However, with an associative approach and a coarse spatial scale, these types of models cannot fully untangle the complexities of malaria dependence on environmental variables, and thus may not provide adequate predictive ability to test climate change or intense climate variability scenarios. In addition, because small-scale spatial variations in soil, vegetation type and especially topography influence the degree of pooling for a given rainfall amount, coarse resolution models may be limited in applicability (Thomson et al, 2004). Resolution must be adequately high in order to predict precipitation effects on *Anopheles gambiae* mosquito ecology in the Sahel. Shaman et al. (2002) demonstrated that high-resolution soil moisture modeling that incorporates topographic details yields good correlation of soil moisture states with captured mosquito abundances in New Jersey. However, improvements on malaria models that are based largely on correlations with mosquito abundances or historical incidence data can be made with a mechanistic, first-principle simulation of environment-dependent processes involved, operating at appropriate scales. This should yield predictive ability for response to perturbations beyond the limits of past observations, such as extreme climate variability or climate change. For such a model, hydrology and entomology simulators are necessary intermediates.

We evaluate the effects of climate variability on malaria transmissibility in the Sahel using the presented coupled hydrology/entomology model, forced with 2005 and 2006 field data. The application of this model to Banizoumbou, Niger, will demonstrate the model's utility for studying malaria transmission responses to environmental variability.

3.1.2 Model development

The presented model was developed to evaluate the aforementioned complexities in mosquito population response to climate variables in the Sahel, simulating breeding pool formation and persistence with a distributed hydrology model. Previous hydrology models have successfully correlated soil moisture and mosquito abundance. For example, Patz et al. (1998) showed an improved explanation of variance in *An. gambiae* abundance and biting in Western Kenya using modeled soil moisture, compared to both rainfall alone and normalized difference vegetation index (NDVI). Potential for the use of hydrologic modeling to predict malaria transmission was demonstrated with this study,

however the spatial and temporal resolutions used in the model were low. Improvements on the use of a soil moisture model to predict mosquito abundance were made by Shaman et al. (2002). As previously mentioned, they predicted distributed soil moisture at high spatial and temporal resolution in New Jersey, to correlate with observed abundances of mosquito species *Aedes vexans*, *Anopheles walkeri* and *Culex pipiens*. Ahumada et al. (2004) developed a model to predict population dynamics of *Cx. quinquefasciatus* in Hawaii, as a function of seasonal changes in environmental conditions. These authors successfully predicted temporal population patterns along an altitudinal gradient. Depinay et al. (2004) and Pascual et al. (2006) incorporated temperature-dependent subadult development rates into mosquito population models. We use these prior studies as a foundation for our model development. However, we explicitly represent the distributed pooled water which constitutes anopheles mosquito breeding habitat as well as the soil moisture which governs the formation of this habitat, and link the resulting pooled water locations with a high temporal resolution individual-based representation of mosquito populations interacting with the environment.

Figure 3.3 shows the conceptual schematic and coupling of various model components. Because spatial distributions of pools relative to human habitation are so important and can play a large role in transmission intensity (Le Menach et al., 2005; Minakawa et al., 1999; Minakawa et al., 2002), a gridded region surrounding human habitation forms the model domain and individual pool locations are predicted using fine-scale topography as hydrology model input. Simulated pools in topographic depressions host sub-adult mosquitoes, which emerge as individual “agents” if their host pool persists long enough, and are free to interact with their simulated environment within the model domain based on a set of pre-assigned rules and attributes.

Pool persistence is a key mosquito population control. To inform the presented model, many field observations were made in a region of southwestern Niger considered representative of the Sahel. In this field environment, rainfed pools and their entomological activity were monitored regularly. Pool desiccation kills all aquatic stage mosquitoes (Charlwood et al., 1995). If they manage to emerge before desiccation,

however, mosquitoes will plague humans living nearby. Interaction of simulated mosquito “agents” with immobile human agents facilitates virtual malaria transmission. A geographic information system (third component in the Figure 3.3 schematic) aids the visualization and management of model input and output.

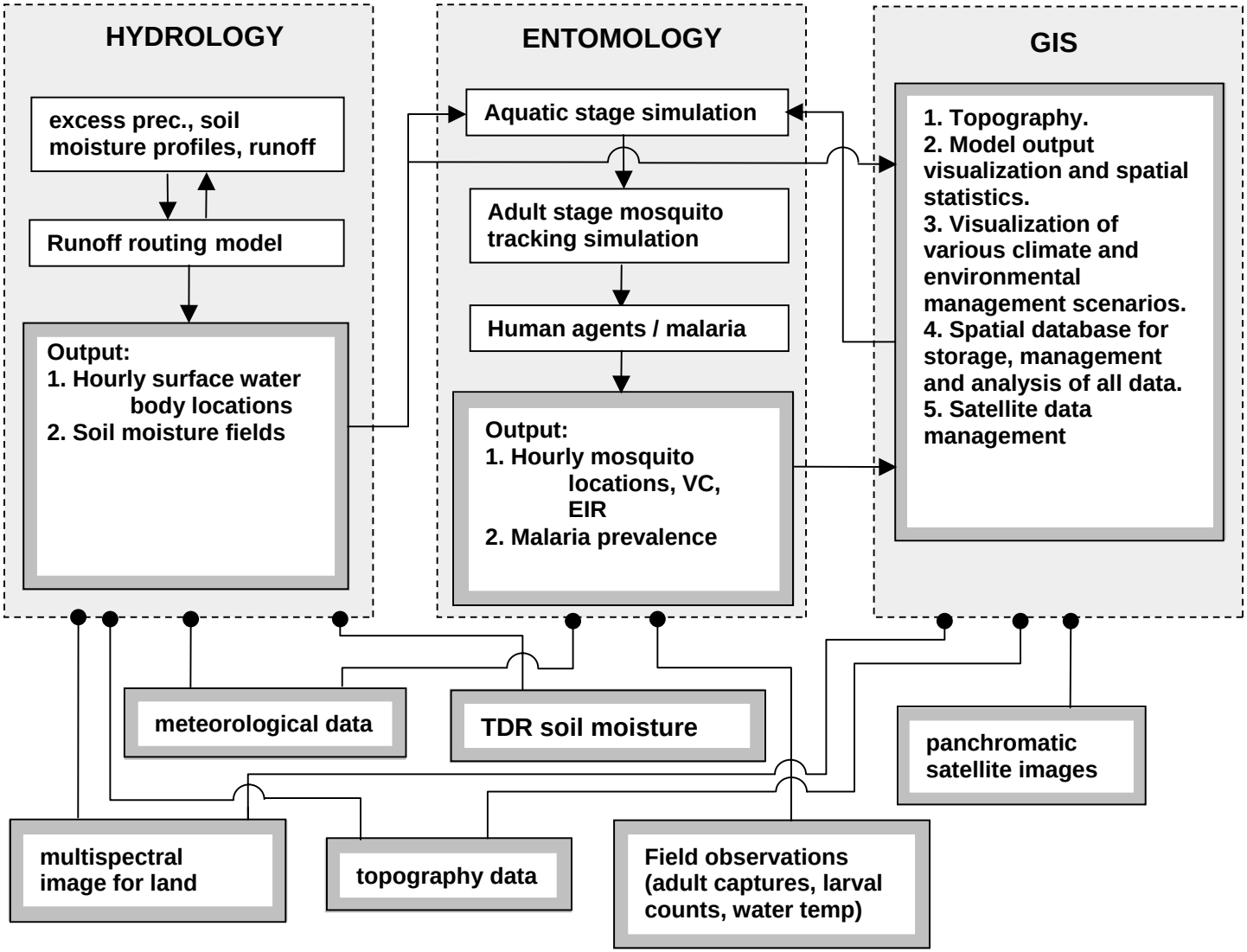

Figure 3.3. Schematic diagram of model setup, with three components. Various inputs into the different components are summarized in the bottom of the figure

3.2 Hydrology model development

3.2.1 Domain and scale

In the Sahel, the ephemeral pools which *An. gambiae* typically exploits for breeding are fed by closed basin catchments of less than 1 km flow length. The resulting pool sizes are typically tens of meters in diameter (Desconnets et al., 1997). In this region, *An. gambiae* exploits these medium-sized pools almost exclusively (Service, 1993). Many references indicate that *An. gambiae* breeds prolifically in very small puddles such as cattle hoofprints (e.g. Minakawa et al., 2004; Mutuku et al., 2006; Service, 1993). While larvae are indeed found in cattle hoofprints in the study area (considered representative of the Sahel), when filled with water these anophelous hoofprints are always directly within a larger-scale topographic depression which collects water, and as such are embodied by the presented model. Hoofprints distant from these topographic depressions never contain water long enough to allow subadult mosquito maturation. There is therefore no need to simulate at scales consistent with animal hoofprints for simulations in the arid Sahel. Moreover, anthropogenic water bodies such as discarded tires, small cans, water storage containers, discarded calabashes, or any other such container do not constitute *An. gambiae* habitat (Service, 1993). While these tiny water bodies have been implicated in the breeding of yellow-fever vector *Aedes* mosquitoes, the local Anopheles mosquitoes virtually never oviposit (lay eggs) there. The same is true for deep wells.

Studies of mosquito dispersal surrounding Sahel villages using marked release and recapture experiments have shown *An. gambiae* populations to cluster around these villages (Gillies, 1961; Constantini et al, 1996b; Taylor et al, 2001), from which some mosquitoes will stray from the village and enter neighboring villages (Constantini et al., 1996b, Taylor et al, 2001). *An. gambiae* dispersal behavior and Sahelian hydrologic characteristics suggest appropriate model domain dimensions of several kilometers square surrounding villages or human populations of interest and a resolution of ten meters. The presented model allows flexible, user-prescribed fine spatial discretization directly surrounding the population of interest for detailed pool resolution, and coarser resolutions away from pool locations in a telescopic grid refinement. Coarse discretization at the pool catchments' upper reaches allows efficient and adequate

overland flow simulation. The existence of small scale pools in distant areas is not expected to influence significantly the village anopheline population, and therefore provides an acceptable compromise which allows both satisfactory overland flow simulation and feasible run times.

3.2.2 Overland flow

Pool formation is simulated by distributed flow routing. A finite difference solution of a diffusion wave approximation to the St. Venant equations determines routed and pooled water for each time step. Run-on onto down-gradient grid cells combines with available precipitation for the next iteration of the unsaturated zone model. In this manner, shallow flow over a spatially variable infiltrating surface is simulated. Flow velocity is represented by Manning's equation with distributed roughness parameter n. The formulation follows that of Lal (1998). The continuity equation for shallow flow is:

$$\frac{\partial h}{\partial t} + \frac{\partial (hu)}{\partial x} + \frac{\partial (hv)}{\partial y} - P + I + ET = 0 \qquad (3.1)$$

where u and v are the flow velocities in the x and y directions, respectively, h is the water depth, P is precipitation, I is infiltration, and ET is evapotranspiration.

The momentum equations for the x and y directions are:

$$\frac{\partial (hu)}{\partial t} + \frac{\partial (u^2 h)}{\partial x} + \frac{\partial (uvh)}{\partial y} + hg\frac{\partial (h+z)}{\partial x} + ghS_{fx} = 0 \qquad (3.2)$$

$$\frac{\partial (hv)}{\partial t} + \frac{\partial (v^2 h)}{\partial y} + \frac{\partial (uvh)}{\partial x} + hg\frac{\partial (h+z)}{\partial y} + ghS_{fy} = 0 \qquad (3.3)$$

where g is the gravitational acceleration, and S_{fx} and S_{fy} are the friction slopes in the x and y directions, respectively. For the diffusion wave approximation, we neglect the first three terms which represent inertial effects. We make the replacement H = h + z for water level above a datum. Equations 3.2 and 3.3 then reduce to

$$\frac{\partial H}{\partial x} = -S_{fx} \qquad (3.4)$$

$$\frac{\partial H}{\partial y} = -S_{fy} \qquad (3.5)$$

Manning's equation relates flow velocity to friction slope and flow depth. For the x-direction:

$$u = \frac{1}{n} h^{\frac{2}{3}} S_{fx}^{\frac{1}{2}} \tag{3.6}$$

where *n* is the Manning's roughness coefficient which determines resistance to overland flow. The y direction velocity is formulated similarly. Following Lal (1998), we reformulate equation 3.6 in terms of H and n:

$$u = -\frac{h^{\frac{2}{3}}}{n\sqrt{S_{fx}}} \frac{\partial H}{\partial x} = -\frac{K}{h} \frac{\partial H}{\partial x} \tag{3.7}$$

$$v = -\frac{h^{\frac{2}{3}}}{n\sqrt{S_{fy}}} \frac{\partial H}{\partial y} = -\frac{K}{h} \frac{\partial H}{\partial y} \tag{3.8}$$

with $K = \frac{h^{\frac{5}{3}}}{n\sqrt{S_f}}$

Equations 3.1, 3.4, 3.5, 3.7 and 3.8 are then solved using the alternate-direction implicit (ADI) method. Lal (1998) found ADI to be the most efficient solver of several common options. At half time steps, the following equations are evaluated sequentially:

$$\begin{aligned} H_{i,j}^{*} &= H_{i,j}^{n} + \frac{\Delta t}{\Delta A}\left[K_{i+\frac{1}{2},j}\left(H_{i+1,j}^{*} - H_{i,j}^{*}\right) + K_{i-\frac{1}{2},j}\left(H_{i-1,j}^{*} - H_{i,j}^{*}\right)\right] \\ &+ \frac{\Delta t}{\Delta A}\left[K_{i,j+\frac{1}{2}}\left(H_{i,j+1}^{n} - H_{i,j}^{n}\right) + K_{i,j-\frac{1}{2}}\left(H_{i,j-1}^{n} - H_{i,j}^{n}\right)\right] + P \end{aligned} \tag{3.9}$$

$$\begin{aligned} H_{i,j}^{n+1} &= H_{i,j}^{*} + \frac{\Delta t}{\Delta A}\left[K_{i+\frac{1}{2},j}\left(H_{i+1,j}^{*} - H_{i,j}^{*}\right) + K_{i-\frac{1}{2},j}\left(H_{i-1,j}^{*} - H_{i,j}^{*}\right)\right] \\ &+ \frac{\Delta t}{\Delta A}\left[K_{i,j+\frac{1}{2}}\left(H_{i,j+1}^{n+1} - H_{i,j}^{n+1}\right) + K_{i,j-\frac{1}{2}}\left(H_{i,j-1}^{n+1} - H_{i,j}^{n+1}\right)\right] + P \end{aligned} \tag{3.10}$$

ΔA is the grid cell area, or $\Delta x \Delta y$. $H^{n}_{i,j}$ is the flow depth at the previous time step, $H^{*}_{i,j}$ is the flow depth at a half time step, and $H^{n+1}_{i,j}$ is the updated flow depth after both x and y directions are solved implicitly. Δt in this formulation is half of the model time step. Infiltration and evapotranspiration are left out of this formulation because they are updated in the unsaturated zone model, in a separate model subroutine.

Topography at very high resolution is a critical parameter for overland flow simulation and prediction of pool formation. Topography determines the cell-to-cell bed slope, which is then used to determine intercell flow potentials (Lal, 1998). The model uses a digital elevation model (DEM) which was derived from a combination of a ground topographic survey and Envisat synthetic aperture radar data (Toutin et al, 2000). In addition to topography, Manning's n in equation 3.6 strongly controls the timing and volume of hydrographs entering topographic depressions. This roughness parameter depends on the vegetation cover and soil type at the grid cell, and influences overland flow velocities.

3.2.3 Land Surface Scheme

The model presented borrows heavily from the land surface scheme LSX of Pollard and Thomson (1995). The model simulates six soil layers and two vegetation layers for a detailed representation of hydrologic processes in the vertical column. LSX simulates momentum, energy, and water fluxes between the vegetation layers, soil, and the atmosphere. Vegetation type and soil type strongly influence soil moisture profile simulation, and spatially variable soil and vegetation properties are used to assign roughness in the runoff routing model. Spatial variability of soil properties is a key determinant of the endorheic behavior observed in typical Sahel catchments (Peugeot et al., 2003).

Vertical soil layer thicknesses are assigned to allow simulation of a low-permeability structural crust commonly observed at the land surface in bare soil and sparsely vegetated areas of the Sahel (d'Herbès et al., 1997). Precipitation at each grid cell is partitioned between runoff and infiltration, based on hortonian runoff processes. The resulting infiltration flux is redistributed in the unsaturated zone with a Richard's equation solver, with soil hydraulic parameters assigned for each layer and grid cell. The Richards equation governs vertical water movement through the unsaturated zone, for which the model uses an implicit solver. The Richards equation is presented in equation 3.11:

$$\frac{\partial\theta(z,t)}{\partial t} = \frac{\partial}{\partial z}\left[K_u(\theta)\frac{\partial\phi(\theta,z)}{\partial z} + K_u(\theta)\right] \tag{3.11}$$

where θ = soil moisture [$cm^3\ cm^{-3}$]

$K_u(\theta)$ = unsaturated hydraulic conductivity [$m\ sec^{-1}$]

$\phi(\theta,z)$ = head value [m]

z = elevation [m]

Several key hydrologic parameters govern the rainfall partitioning into infiltration and runoff. Saturated hydraulic conductivity and porosity are two critical parameters. The soil model subroutine determines unsaturated zone hydraulic conductivity as a function of soil moisture following Campbell's equation (Campbell, 1985):

$$K(\theta) = K_s\left(\frac{\theta}{\theta_s}\right)^{2b+3} \tag{3.12}$$

where θ is the volumetric water content, and θ_s is the volumetric water content at saturation, (porosity) b is a model exponent dependent on soil texture, and K_s is the saturated hydraulic conductivity. The b exponent is introduced in this formulation as a model parameter, and derives from the moisture release equation (Campbell and Norman, 1998):

$$\psi_m = \psi_e\left(\frac{\theta}{\theta_s}\right)^{-b} \tag{3.13}$$

where ψ_m is the matric potential and ψ_e is the air entry potential. Air entry potential and b exponent are two soil parameters which influence unsaturated zone water redistribution, and nominal values are thus assigned based on the observed soil texture in the field following Table 9.1 of Campbell and Norman (1998). In addition, root zone soil water uptake from transpiration is forced by canopy-level climatic variables.

3.2.4 Groundwater level

The model was developed for application in African desert fringe areas, such as the Sahel. In many parts of the Sahel, the unconfined aquifer groundwater level is very deep and exhibits no interaction with the land surface. However, in some locations, particularly in wetlands and rice-growing areas, there may be significant hydraulic connection between the unconfined aquifer and the land surface. Concentrated rainwater in topographic depressions of Niger has been shown to affect groundwater levels by

Leduc et al. (2001). In southwestern Niger, they demonstrated that a decades-long groundwater table rise can be attributed to ephemeral pools being filled for longer periods of time, most likely because of recent land use changes. It is conceivable that the rising groundwater table can create groundwater-fed pools in the future. Such a phenomenon is presently observed in areas of southwestern Niger, where relic channel features of long extinct rivers that once drained the central Sahara contain pools formed by phreatic water table penetration of the ground surface. The resulting pools do not behave the same way as the more typical ephemeral pools. Instead, they appear during the wet season and continue to grow past the monsoon peak, after which the water level begins to recede. This behavior results in much more persistent water bodies than in areas with only rapidly-infiltrating pools. Anophelines exploit these emergent groundwater-fed pools, exacerbating the malaria problems within these areas.

3.2.5 Model inputs

Necessary model inputs come from a variety of sources. The climate data for model forcing can come from meteorological stations in the field, and/or from regional climate model simulations. Meteorologic variable inputs for the hydrology model are temperature and humidity, wind speed and direction, incoming solar radiation, and precipitation. These six variables can be assumed spatially invariant over the model domain, or can be represented as distributed rasters, based on either multiple measurements or assumptions, to account for the existence of mosquito microhabitats. Table 3.1 summarizes all hydrology model inputs.

Table 3.1. Hydrology model inputs

variable	Type	Remarks
vegetation	distributed	supervised classification of multispectral satellite image (eg Landsat)
roughness	distributed	Assigned based on vegetation classification
soil type	distributed	supervised classification, and knowledge of local soil compositions
topography	distributed	Synthetic aperture radar products (eg Radarsat), or other suitable DEM source
precipitation	lumped	from meteorological station or climate model output
temperature	lumped	from meteorological station or climate model output
humidity	lumped	from meteorological station or climate model output
wind speed	lumped	from meteorological station or climate model output
wind dir	lumped	from meteorological station or climate model output
SW radiation	lumped	from meteorological station or climate model output
grid resolution	user-defined	flexible telescopic mesh refinement grid layout to accommodate area of interest
time step	user-defined	different time steps as input for overland flow and unsaturated zone models

3.2.6 Model operation

The hydrology model operates according to the schematic shown in Figure 3.3. The overland flow module operates at a small user-defined time step (nominally one second) while the unsaturated zone model is stepped at a coarser time step (nominally one hour). Vegetation canopy energy and water redistribution calculations are performed at this time step as well. The vegetation module tracks evapotranspiration and root zone moisture uptake for the various vegetation types. This interacts with the model's soil water redistribution component, which tracks both soil moisture and temperature in the vertical column. Routed water depths from the overland flow module are updated for infiltration and evapotranspiration losses at each model time step before being returned to the overland flow routing subroutine.

3.2.7 Model output

Pool depth rasters generated at each model time step (nominally one hour) serve as entomology model input. The loosely-coupled model structure derives from the one-way dependence of entomology on hydrology, as well as the need to calibrate the model components separately. Each output file contains water depths for each model grid cell, based on the user-prescribed grid configuration. Soil moisture profiles are tracked for each grid cell. Volumetric water content time series for user-specified points are also

generated as output to allow hydrology model validation using profile soil moisture measurements such as TDR probes.

3.3 Entomology model development

Malaria response to environmental determinants is simulated using individual mosquito and human "agents". Mobile individual mosquito agents behave probabilistically according to a prescribed set of rules governing dispersal and discrete events (e.g. bloodmeals, egg-laying, etc), in response to their immediate environment. This formulation allows population behavior of both mosquitoes and malaria parasites to emerge based on the individuals' actions. Characteristics of each mosquito such as location and gonotrophic or infective status are tracked through time. At least two bites are required for a new malaria infection, one for the mosquito to acquire the parasite from an infected human, and a second bite from an uninfected human to cause the secondary infection (see Figure 1.3). Interaction with the human population, acquisition of infection, intrinsic and extrinsic incubation periods (parasite development time in humans and mosquitoes, respectively), and infectious bites upon subsequent contact with humans are all simulated in the described manner. Only female mosquitoes are tracked, because male mosquitoes do not take bloodmeals and therefore play no role in malaria transmission. We assume that male availability for mating is not limiting.

3.3.1 Model input

Model input for the entomology component includes pool water levels from the hydrology model output, as well as local meteorological conditions, if they are set to vary spatially. Certain aspects of mosquito behavior depend on relative humidity and temperature, and mosquito dispersal is influenced by wind speed and direction, both for physical displacement when wind is very strong, as well as to direct plumes of CO_2 and human odor from the villages which act as host-seeking cues (Healy et al, 1995, Takken et al., 1999). CO_2-mediated flight behavior is described below. In addition, aquatic stage development rates for the subadult mosquitoes depend on water temperatures (Depinay et al., 2004). Egg development within an adult mosquito, as well as the sporozoite phase of the *plasmodium* parasite depend on ambient temperature (Detinova, 1962; Craig, 1999).

Accordingly, these six variables (air temperature, water temperature, humidity, wind speed, wind direction, distributed water depths) are the primary inputs for the entomology model. Water depth and temperature for each grid cell are predicted by the hydrology model, and the remaining four can be either field measured or supplied by climate models.

The entomology model input variables temperature and humidity can be either spatially invariant throughout the domain, or can be distributed to allow simulation of microhabitats potentially inhabited by mosquitoes. These microhabitats, possibly under shady trees or in houses, can offer comfortable refuges to mosquitoes as an alternative to harsh ambient conditions. The less stressful conditions of suitable microhabitats can decrease mortality and temperature variations and can influence the parasite extrinsic incubation period (Okech et al., 2003). Both of these relevant microhabitat-related processes can affect village-scale malaria transmission. Assignment of distributed temperature and humidity values can be done based on remotely-sensed land cover types. However, in the model application presented here, they are assumed spatially invariant.

3.3.2 Aquatic stage simulation

Aquatic stage, or subadult, mosquitoes advance through several stages between eggs and adult mosquitoes. As shown in Figure 1.3, eggs hatch to become L1, or first stage larvae. They then advance through three more larval stages (instars) as they grow and mature, to finally pupate. Pupae do not feed. They remain in this state for approximately two days before emerging as adult mosquitoes.

Simulation of aquatic stage development relies on a compartmental structure model for each grid cell in which the hydrology model assigns a pool. As long as the pool persists in the simulation, the aquatic stage model will continue to advance. In pools predicted by the hydrology model to disappear, any simulated aquatic stages will be killed in the simulation, as is expected of naturally occurring *An. gambiae* larvae and pupae upon desiccation (Charlwood et al., 1995). Figure 3.4 presents the aquatic-stage model structure, which is embedded within each model grid cell containing water. This model

describes the water temperature-dependent stage progression rates of eggs, larvae, pupae, and emerging adults. Only integer abundances are advanced from a previous stage to the next. Temperature dependence of the progression rates has been observed by Bayoh et al. (2004) and incorporated in the model of Depinay et al. (2004). During each model time step, in pools with subadult mosquitoes, the progression from eggs to larvae to pupae to adults is calculated using Depinay's temperature-dependent model:

$$d_k = r(T_k) \cdot \Delta t_k \tag{3.14}$$

where d is the fraction of individuals in a certain stage progressed to the next stage, T_k is the temperature (K) over time interval k, Δt_k is the time step at interval k, and $r(T_k)$ is the temperature-dependent development rate, given by Depinay et al. (2004) as a function of water temperature and biochemical parameters specific to each subadult stage. For details of the temperature dependence, the reader is referred to Depinay et al. (2004).

As shown in Figure 3.4, each larval instar (L1 through L4) is subject to predation and natural mortality losses. In addition, L4 larvae cannibalize L1 larvae at a rate dependent on L4 larvae abundance (Koenraadt and Takken, 2003). For all stages, predation and natural mortality are model parameters. Pupae are subject to predation losses, but we assume that they do not suffer natural mortality. The development rates between the aquatic stages ($\varepsilon(T)$, $\lambda(T)$, and $\varphi(T)$ for egg, larvae and pupae, respectively, as in Figure 3.4), are represented by r(T) in equation 3.14.

Following Depinay et al. (2004), we limit pool biomass using the ecological carrying capacity, which becomes a model parameter. As an example of nutrient limitations, in past studies mosquito larval abundance and pool productivity has been highly correlated to availability of maize pollen (Ye-Ebiyo et al, 2003). In Figure 3.4, the coefficient C represents competition for limited nutrients in each pool, restricting advancement as the pool biomass approaches the assigned carrying capacity. As in Depinay's model, an intraspecific competition coefficient is defined as:

$$C = \left(\frac{e - w}{e} \right) \tag{3.15}$$

where *w* is the sum of total larval biomass in the pool grid cell, and *e* is the ecological carrying capacity [mg biomass m^{-2}]. Ecological carrying capacity is an assigned model parameter and is assumed to be time-invariant.

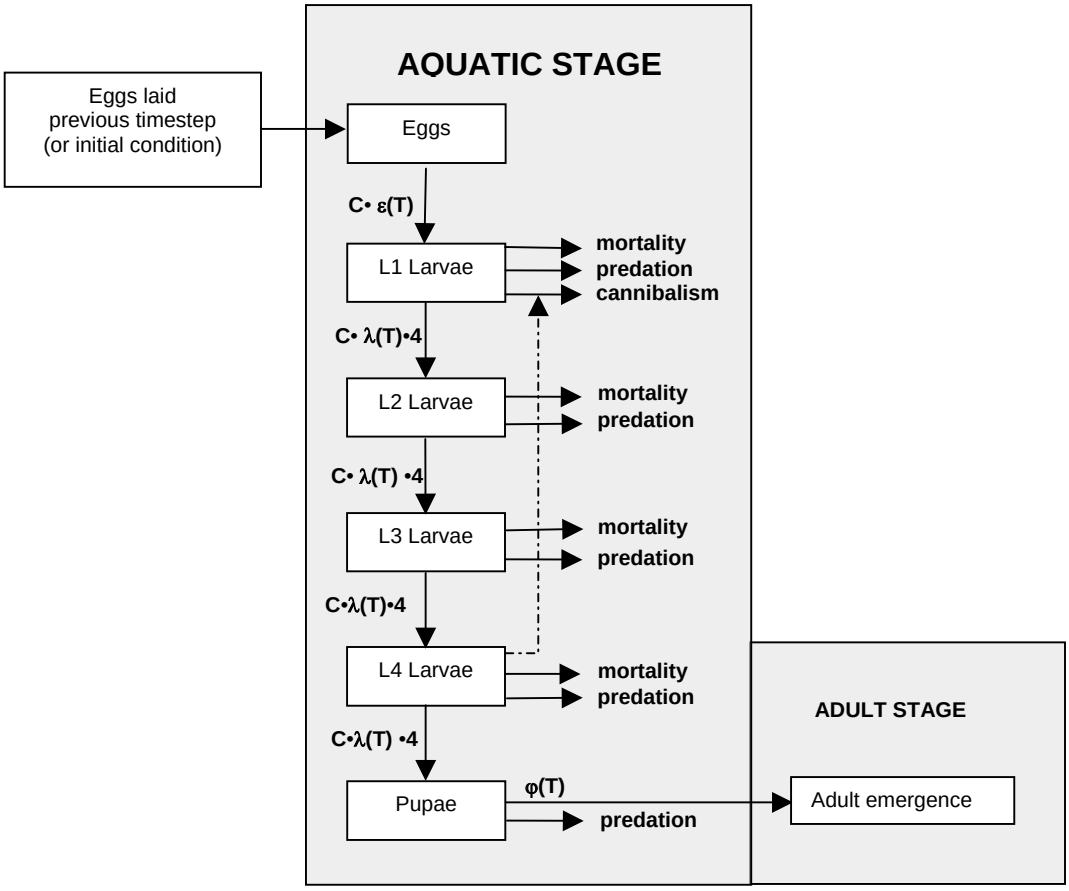

Figure 3.4. Aquatic stage schematic diagram. ε(T) is a temperature-dependent egg development rate, λ(T) is the larvae development rate, φ(T) is the pupae development rate, and C is a coefficient to account for intraspecific nutrient competition.

Several other factors influence larvae. Pool water temperatures in excess of 40 degrees result in death of larvae (Jepson, 1947; Depinay, 2004). In addition, we assume that oviposition does not occur in pools deeper than a threshold depth (Minakawa, 2005). This is consistent with our own observations that wave action (which generally occurs in deeper, larger, unvegetated pools) seems to deter larvae, either by wave action drowning them or by waves discouraging oviposition. Also, deep water in the center of large pools appears to contain virtually no larvae. In the hydrology simulation, shrinking pools will regularly dry out grid cells at the pool edges as the receding water line causes a retreat of

the pool boundaries. As soon as one pool grid cell is predicted to become dry, all subadult mosquitoes are simply moved into the adjacent cells, concentrating larvae and pupae into remaining pool cells. Clearly, this will impact further development of the remaining subadult mosquitoes through the *C* coefficient of equation 3.15. Field observations show high spatial variability in larval density within each pool. Clusters of subadult mosquitoes populate certain areas. In the model, however, larval abundance is constant throughout each pooled grid cell. Within a multi-cell pool spanning several grid cells, the model allows heterogeneity in larval abundances between adjacent cells. This is consistent with field observations of spatial variability in larval abundance.

3.3.3 Adult stage simulation

After emergence from the pools, adult mosquitoes are tracked through space and time using an individual-based approach, in contrast to the compartmental structure of the aquatic stage simulation. Each mosquito simulated to emerge into the model domain has an associated attribute matrix, as shown in Table 3.2. At each time step in the model, after the aquatic routine has been stepped to simulate newly emerging adult mosquitoes in the simulation, the mosquito matrix is updated. Elapsed times since significant events are updated, and X and Y position and behavior of the mosquito are updated based on radial random walk motion, corrected for wind displacement and including representation of CO_2 plumes as a host-seeking cue, as described below.

Table 3.2. Mosquito attribute matrix

	Name	Remarks
1	mosquito ID number	constant throughout simulation
2	X position of mosquito	weighted radial random walk; for both X position as well as Y position, it is determined from a number of anthropological and meteorological tropisms
3	Y position of mosquito	
4	elapsed time since emergence	Δt added each time step
5	blood meal flag	=1 for blood meal, 0 otherwise
6	elapsed time since blood meal	Δt added each time step after blood meal
7	oviposition flag	add 1 each time mosquito oviposits
8	elapsed time since ovipositon	Δt added each time step after oviposition
9	death flag	=1 if death occurs, 0 otherwise
10	infection flag	=1 if mosquito becomes infected, 0 otherwise
11	degree-days since infection	updated each time step
12	mosquito weight	assigned upon emergence based on aquatic crowding conditions

We assume the following sequence of behavioral events: host-seeking, biting, resting, oviposition, and again host-seeking to repeat the cycle until the mosquito dies. This involves several key parameters to simulate accurately the mosquito dispersal and interaction with its immediate environment. Most importantly, the nominal flight velocity per model time step strongly influences the degree of dispersal. Flight velocity is difficult to assign directly, primarily because of generally erratic flight paths. Straight-line velocity measured over a few seconds will differ greatly from averaged flight velocity over one hour. We use a weighted random walk formulation for mosquito dispersal, corrected for CO_2 stimulated host seeking behavior, and a slight correction for wind influence. We assign flight velocity to match predicted dispersal to that witnessed by other authors for *An gambiae*. In a wet region of Tanzania, marked female *An gambiae* mosquitoes were tracked by Gillies (1961), from which he estimated the average flight range of adult *An gambiae* females as between 1 and 1.5 km. In addition, he suggested that the majority of mosquitoes stayed well within that distance of the village. Similar results were observed in Burkina Faso by Constantini et al. (1996b). To be consistent with these recorded dispersals surrounding villages, we assume that hourly effective flight velocity follows a normal distribution centered at a mean of 15 m hr^{-1} and standard deviation of 5 m hr^{-1}. A low effective velocity (compared to straight-line velocity) over one time step integrates periods of short-term resting and flight direction changes. Direction of flight is assumed random outside of a threshold distance from human habitation. We assume that the random component of flight is slightly weighted by a direct flight toward human habitation, to account for visual cues of the mosquito when host-seeking. The effect is a random movement with a varying degree of “pull”, dependent on distance from the houses. The weighting of this visual cue compared to random dispersion is a model parameter.

If an individual mosquito senses a CO_2 concentration of 0.01% above background, it flies up the concentration gradient of the plume (Takken and Knols, 1999). The carbon dioxide plume is dependent on wind speed and direction for the area of interest. We model the CO_2 plume at each time step, with exhaling human and animal agents in the model grid as CO_2 sources. This is done using the gaussian dispersion equation:

$$C_{CO2} = \frac{Q}{2\pi u_w \sigma_y \sigma_z} \exp\left(-\frac{1}{2}\frac{y^2}{\sigma_y^2}\right)\left[\exp\left(-\frac{1}{2}\frac{(z-H_e)^2}{\sigma_z^2}\right) + \exp\left(-\frac{1}{2}\frac{(z+H_e)^2}{\sigma_z^2}\right)\right] \qquad (3.16)$$

where:

C_{CO2} is the concentration of CO_2 [g m^{-3}] at any position *x* meters downwind of the source, *y* meters crosswind of the source, and *z* meters above the ground level,

Q is the carbon dioxide exhalation rate [g sec^{-1}],

u_w is the horizontal wind velocity along the plume centerline [m sec^{-1}],

H_e is the height of the emission plume centerline above the ground [m],

σ_z is the vertical standard deviation of the emission distribution [m], and

σ_y is the horizontal standard deviation of the emission distribution [m].

The horizontal and vertical dispersion is a function of atmospheric stability conditions and downwind distance (Smith, 1968). We assume that stable atmospheric conditions prevail during the nighttime periods of high mosquito activity, due to radiative cooling at the land surface under clear skies. From Smith (1968), the horizontal and vertical dispersions for such conditions are given by:

$$\sigma_y = 0.31x^{0.71}$$
$$\sigma_z = 0.06x^{0.71} \qquad (3.17)$$

Furthermore, we assume a height of 1.0 meter at which mosquitoes sense the plume, and an emission height of 1.5 meters. The source emission of carbon dioxide exhaled is assumed to be 275 ml min^{-1} per human, and that emitted by livestock is estimated at 3925 ml min^{-1} (Kinsman et al., 1995). The concentration of carbon dioxide at each time step and position in the model domain is calculated as the sum of the contributions of all exhaling members of the community. The plume dimensions and directions vary with wind speed and direction, and mosquito activity response to CO_2 cues therefore varies strongly throughout the model domain. The plume is always oriented directly downwind.

Anopheles gambiae s.l. is nocturnal in feeding and oviposition habits (Haddow, 1954). The model simulates the diurnal cycle, and allows mosquito activity only during the evening and

nighttime hours. Anophelines are assumed to rest during the day, either in houses or in nearby vegetation.

Bednet use is represented by a simple parameterization in the model. When a mosquito enters a model grid cell identified as containing human habitation, we assume that there is a certain probability of a bloodmeal being taken. We assume (for now) that this probability is 0.5. In a dense village environment, the population may not be very sensitive to this parameter due to the dense clustering of villagers' houses which provide abundant bloodmeal opportunities. This parameter can be varied spatially or adjusted globally to reflect bednet use in the village.

Figure 3.6 shows adult stage model flow. The model cycles through each individual, assesses the mosquito's gonotrophic and infectious states and updates the mosquito attributes for infection and bloodmeals based on interaction with the environment or human agents at that individual mosquito's location.

3.3.4 mortality

Macdonald demonstrated, using a modified version of Ross's groundbreaking model, that mosquito longevity is the most important variable in malaria transmission (Macdonald, 1957; Ross, 1911). According to the model, a reduction in longevity reduces malaria transmission potential much more than the same percentage reduction in abundance. It is therefore important to simulate probabilistic death at each time step based on all factors influencing longevity. As discussed above, environmental stresses affect mosquito longevity. We assume that longevity is independent of infected state.

The model incorporates a daily survivability based on daily average temperatures. Above a 41 ˚C daily average temperature threshold, anophelines cannot survive. (Craig et al., 1999; Martens, 1997). The survivability dependence on daily average temperature follows the model developed by Martens (1997):

$$p = \exp\left(\frac{-1}{-4.4 + 1.31T_d - 0.03{T_d}^2}\right) \tag{3.18}$$

where p is the daily survivability probability of each mosquito and T_d is the average temperature of the previous 24 hours.

3.3.5 Egg development and extrinsic incubation period

Egg development within the mosquito follows the temperature-dependent model of Depinay et al. (2004) as shown in equation 3.14. For details of the temperature-dependent development rate of eggs within the mosquito, the reader is referred to Depinay et al (2004). Ambient temperature at the mosquito's location regulates this development rate. If the mosquito has finished the full gonotrophic (egg development) cycle, and it encounters a suitable water body, then it deposits a clutch of eggs to add to the subadult mosquitoes of various stages already present in that water body.

Once an adult mosquito takes an infectious bloodmeal and becomes infected, the parasite advancement beyond the midgut and into the salivary glands as infectious sporozoites requires 111 degree-days above 18˚ C (Detinova, 1962). Because each individual mosquito tracks degree-days since infection, infective status depends on a simple comparison of this value to 111. If the mosquito reaches this point, it becomes capable of malaria transmission to humans during subsequent blood meals. Once it has become infectious with sporozoites in the salivary glands, all subsequent bites from the mosquito are capable of transmitting malaria.

3.3.6 Human agents

The model simulates immobile human agents, representing village inhabitants. Several underlying assumptions govern human agent behavior. First, superinfection is not incorporated in the model. Superinfection refers to the acquisition of multiple infections of a single malaria species, which are independently cleared from the host with a first-order recovery rate (MacDonald, 1950). Future research will investigate how human agents can be programmed to acquire superinfection.

Second, the human agents are assumed immobile. While villagers are obviously in reality quite mobile, this may be a reasonable assumption because the mosquitoes actively seek

blood-meal hosts at night (Service, 1993) when villagers are sleeping in their houses. Each model grid cell marked as inhabited (digitized houses from satellite image) contains a finite number of human agents. Unless house survey data allows actual assignment of inhabitant numbers to each house, we assume a constant ten inhabitants per 10 m x 10 m village grid cell. When a mosquito enters a house to seek a bloodmeal, a certain portion of the inhabitants can be assumed protected by bednets, and if that bednet-protected host is targeted by the mosquito for a bloodmeal it will result in the mosquito's death. If desired, repellent effects can also be included through a simple modification.

Human agents track infected status as well as time since infection. Time since infection is tracked for gametocyte (parasite stage in humans which is infectious to biting mosquitoes) development and potential completion of the transmission cycle back to mosquitoes. Following an infectious mosquito bite, we assume that gametocyte development takes two weeks before a biting *Anopheles* mosquito can become infected. This intrinsic incubation period does not depend on ambient temperature, unlike the extrinsic incubation period of the parasite within the mosquito midgut. Human malaria infections are cleared with time. In the model algorithm, a uniform random number is chosen for each individual, which is compared to the preset clearing rate (adjusted for the hourly time step), and human infected status is toggled to negative if the random number is less than the clearance rate. This is a crude representation of human malaria infection, but the model framework as presented can easily be modified should improved algorithms for *in vivo* malaria dynamics become available.

3.3.7 Zoophily – animal agents

A third type of agent can be represented in the model. Animals can act as alternate bloodmeal hosts, but cannot host infections of human malaria. Therefore, the presence of animals can divert potentially infectious bites from humans, with no negative consequence for either humans or mosquitoes. In other words, the mosquito's need for blood is satisfied, while parasite transmission is not advanced. In this way, higher animal densities can moderate malaria transmission intensity in a village. *Anopheles gambiae s.s.* and *An. arabiensis* are predominantly anthropophilic, greatly preferring human blood to

animal blood. There is some variation in anthropophily between the two malaria vectors simulated in the model, with *An gambiae sensu stricto* showing greater preference for human blood meals (Coluzzi et al., 1979) and *An. arabiensis* showing less discriminating behavior. In West Africa, studies have shown *An. arabiensis* to be predominantly anthropophilic, except when near abundant alternative hosts, particularly cows (Coluzzi et al., 1979; Lindsay et al., 1993). However, the degree of anthropophily in *An. arabiensis* can vary significantly by region, as evidenced by a finding of virtually complete zoophily in Madagascar (Duchemin et al., 2001). Exact levels of anthopophilic behavior are unknown in southwestern Niger. In the Sahel, animals are often found within the village at a low density where people keep their livestock near their homes, or near some of the largest water bodies at a higher density. Animal agents' locations are user-prescribed and are assumed immobile. The density per grid cell is a model parameter.

3.4 Summary

We have presented a coupled hydrology/entomology model to predict mosquito population dynamics and malaria transmission response to spatial and temporal environmental variability in the Sahel. It is well known that hydrology strongly controls anopheles mosquito populations and thus influences malaria incidence, and indeed the associations have been demonstrated repeatedly. However, the details of malaria/environment interactions are complex and true predictive ability arises from mechanistic, first-principle simulation of hydrology and entomology processes involved. Here, we have presented a mechanistic, high spatial and temporal resolution representation of pool formation in response to rainfall as well as subsequent pool persistence, coupled to an individual-based entomology model capable of utilizing the pools for breeding. Spatially explicit simulation helps identify and understand the proximal determinants of malaria transmission. Remotely-sensed land cover and topography rasters provide distributed model parameters. In this manner, the presented high temporal- and spatial-resolution distributed model augments existing models by explicitly simulating all of the aforementioned complexities.

The model is suitable for use in desert-fringe, water-limited environments in Africa, where *An. gambiae s.l.* is the dominant malaria vector. This includes all of the Sahel and possibly areas in southern Africa. The model was designed in a flexible way, allowing user-prescribed grid configurations and a wide range of possible mosquito model parameterizations. Model input and output was designed to interact easily with geographic information systems, satellite-derived digital elevation models and land cover rasters. We present a specific example of model application and field validation for Banizoumbou, Niger in Chapter 4.

Chapter 4: Model Application to a Sahel Village

4.1 Introduction

Here, we evaluate the effects of climate variability on malaria transmissibility in the Sahel using the presented coupled hydrology/entomology model, forced with 2005 and 2006 field data. The application of this model to Banizoumbou, a typical Sahelian village, will demonstrate the model's utility for studying malaria transmission responses to environmental variability.

4.2 Study area

Banizoumbou is a village in southwestern Niger (13° 31', 2° 39') of about 1000 inhabitants and is located in a semi-arid plateau landscape of tiger bush, millet fields, fallow and bare soil. Land use and land cover types in Banizoumbou's immediate environs are typical for Niger Sahelian villages. Average annual rainfall in nearby Niamey is 562 mm over the period 1905-1989 (Le Barbé and Lebel, 1997), all of which falls during the single May-October rain season with a peak in August. Because of extended drought, during the period 1968-1990, the average annual precipitation has decreased to 495 mm (Le Barbé and Lebel, 1997). Average annual rainfall in recent years in Banizoumbou is slightly less at 450 mm. The majority of the annual rainfall occurs during the West African monsoon peak between mid-July and late August. The rain tends to fall at a high rate, with a distinctive hyetograph shape consisting of an initial burst of high intensity and short duration rain (squall line), followed by several hours of low-intensity rainfall from the trailing stratiform (Amani and Lebel, 1996).

Regional topography as seen in digital elevation models reveals an extensive drainage network. However, these channels no longer conduct runoff, as they are relics from a wetter period (Talbot, 1980). Pleistocene aeolian sand deposits in the drainages impound water in the channels (Peugeot et al, 2003), confining runoff to small closed-basin catchments, which are typically no more than 1 km in length (Desconnets et al., 1997). Surrounding Banizoumbou, small catchments drain into pools several meters to tens of meters across (Desconnets et al., 1997). Pool inflows are balanced by a change in volume, infiltration, and evaporation, and

levels fluctuate in response to inflows from concentrated runoff. Incidentally, infiltration from these pools is the primary source of recharge to the unconfined aquifer (Leduc et al., 2001). A layer of low permeability clayey soil lines the bottom of these pools (Desconnets et al., 1997). Outside of the pools, homogenous sandy soils with 10-15% fine particle content predominate in the hillslopes and valley bottom ravines, and infiltration capacity in these sandy soils can reach 45 cm/h (Peugeot et al., 2003), however the soils are highly susceptible to crust formation (Hoogmoed and Stroosnijder, 1984). When crust forms, runoff coefficients can increase to 90%, with dramatic consequences for pool inflows (Casenave and Valentin, 1992).

Subsistence dryland agriculture dominates food production, and local vegetation consists primarily of millet fields near the village. Most of the land is farmed, some areas are left fallow, and the remainder consists of tiger bush shrubland, which is generally more distant from the village and is common near surrounding plateau tops. Banizoumbou villagers farm pearl millet almost exclusively, with small plots of beans, groundnuts, and other crops making up an insignificant portion of the cultivated land.

As previously stated, *Anopheles gambiae s.s.* and *Anopheles arabiensis* mosquitoes dominate malaria transmission in Banizoumbou (White, 1974; Jean-Bernard Duchemin, personal comm., 2005). Both of these species are members of the *Anopheles gambiae s.l.* species complex, genus *Anopheles* (the only mosquito genus capable of transmitting malaria) (Gillies and DeMeillon, 1968). The strong anthropophily (human-biting nature) of *Anopheles gambiae s.l.* mosquitoes makes them highly efficient malaria vectors (White, 1974; Coluzzi et al., 1979; Costantini et al., 1998). The less abundant (and less anthropophilic) *Anopheles* species such as *An. pharoensis* and *An. rufipes* play only a very minor role in Banizoumbou malaria transmission (Muriu et al., 2008; Appawu et al., 2004). The highly anthropophilic vector *Anopheles funestus* has never been captured in Banizoumbou and is assumed absent.

4.3. Field data

Hydrology and entomology data were collected from Banizoumbou starting in the 2005 wet season and continuing through the 2006 monsoon. Regular field observations of many

hydrologic and entomologic variables were made. In addition, we logged meteorologic variables at Banizoumbou for model input. These data were collected at a meteorologic station located just outside of Banizoumbou village, in a sparse millet field. Meteorologic variables are considered invariant over the model domain. Table 4.1 summarizes the field data collected in Banizoumbou, and data collection locations for the study area are superimposed on a Quickbird satellite image of the village in Figure 4.1.

Table 4.1. Field observations taken in Banizoumbou spanning the period June 2005 – November 2006.

variable	**sensor or observation mode**	**sampling frequency**	**sampling locations**
adult anopheline abundance	CDC light trap	weekly in wet season	6
larval abundance	standard dipper	at least weekly	each pool
pool dimensions	visual estimate	at least weekly	each pool
precipitation	tipping bucket rain gauge	hourly	1 meteo station
temperature	temperature/humidity probe	hourly	1 meteo station
relative humidity	temperature/humidity probe	hourly	1 meteo station
solar radiation	pyranometer	hourly	1 meteo station
wind speed	anemometer	hourly	1 meteo station
wind direction	wind vane	hourly	1 meteo station
water temperature	HOBO watertemp pro	hourly	1
soil moisture	TDR probes buried	hourly	3 (4 sensors each loc.)

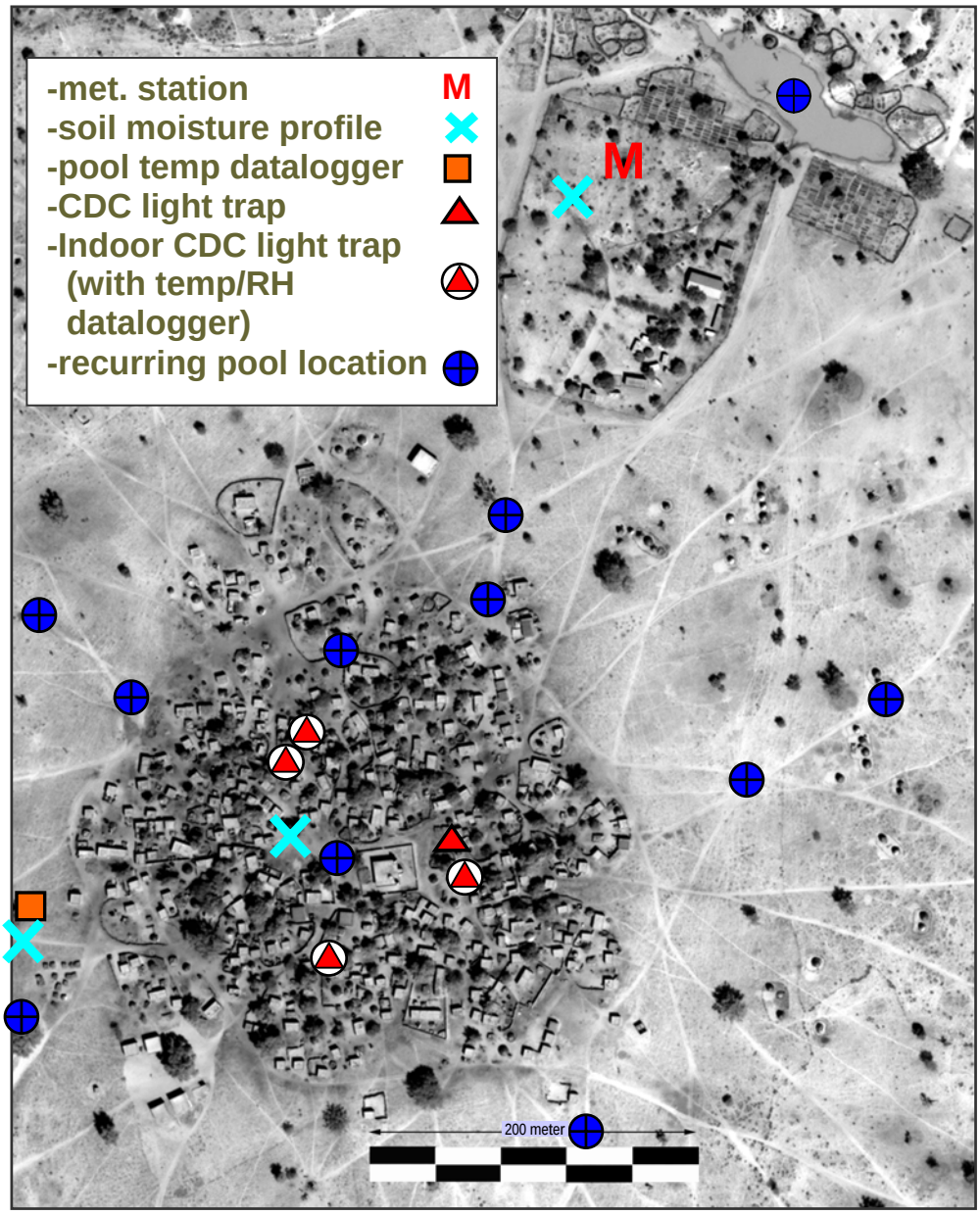

Figure 4.1. Sampling locations in Banizoumbou, Niger.

4.3.1 Adult mosquito abundance

We monitored adult mosquito abundance weekly at six locations throughout Banizoumbou using CDC miniature light traps. These traps attract insects with a small 6-volt incandescent bulb, and force insects near the bulb into a collecting net using a small fan. Figure 4.2 shows a CDC light trap at an outdoor sampling location in Banizoumbou. The depicted sampling location is at "Bani3", just south of the center of the village. Figure 4.3 shows a captured *Anopheles gambiae s.l.* mosquito from such a light trap, and Figure 4.4 is a photograph of

technician Ibrahim Arzika identifying mosquitoes from light trap captures the day after the overnight operation of the traps. Trends in abundance follow trends in light trap captures, but absolute abundance values are difficult to establish using light traps. Sampling locations include four indoor and two outdoor light trap placements. The outdoor locations are outside the houses containing two of the light traps. Three of the sampled houses are mud-brick constructions with closed eaves and corrugated steel roofs, and one is built completely of thatch. Sampling locations remained unchanged throughout the June 2005 to November 2006 field observation period. For each sampling event, light traps were set with a freshly charged 6-volt motorcycle battery, and started at 7 PM and stopped at 7 AM the following morning. The trap aperture was closed before the battery was removed. In the morning, the traps were removed, and all captured mosquitoes were separated from the other trapped organisms. All mosquitoes of genus *Anopheles* were identified to the species level, while other mosquito types were identified to the genus level. Light trap captures commonly included *Anopheles gambiae s.s.*, *An. arabiensis*, and rarely *An. rufipes* and *An. pharoensis. Mansonia*, *Culex* and *Aedes* mosquitoes were also commonly caught at all locations. Figure 4.5 (top frame) shows the *Anopheles gambiae s.l.* captures in Banizoumbou, summed over the six light traps operating in the village.

The weekly CDC light trap mosquito capture data presented in Figure 4.5 displays a pronounced dependence on lunar phase. The four indoor-placed traps showed only slightly less inter-weekly variability with the moon phase than the outdoor traps. The trap capture peaks are all within several days of a new moon, and the low captures correspond to full moons. Similar well-defined lunar cycle effects on anopheles mosquito light trap captures have been noted many times before (e.g. Horsfall, 1943; Pratt, 1948). Moonlight competes with light trap bulbs as an attractant and mosquito flight stimulant, and on the brightest moonlit nights, moonlight may reduce the effective trap capture area dramatically because mosquitoes at some distance from the trap no longer resolve the bulb in the bright ambient light conditions. The reverse is true on moonless nights, when the light trap bulb attracts mosquitoes from a greater distance because the effect of the moon as a light source interfering with the light trap's illumination is no longer present. We account for the effects of lunar phase as follows. The light trap effective capture area is the annular area surrounding the trap

where bulb illumination exceeds background illumination from the moon. The illumination of a light trap bulb (lux) is given by (Bowden and Church, 1973):

$$B = \frac{L}{D^2} \qquad (4.1)$$

where L is the bulb intensity (lumens) and D is the radial distance from the trap (in meters).

Figure 4.2. An outdoor CDC light trap placement in Banizoumbou. This is location "BANI3".

Figure 4.3. An *Anopheles gambiae sensu lato* mosquito captured in Banizoumbou. This one could be either *Anopheles gambiae sensu stricto* or *Anopheles arabiensis*. For exact identification, PCR analysis is necessary.

Figure 4.4. Identification of light trap captures. Here, Ibrahim Arzika of the CERMES inspects a captured mosquito. Each individual mosquito must be analyzed with a microscope to determine its species.

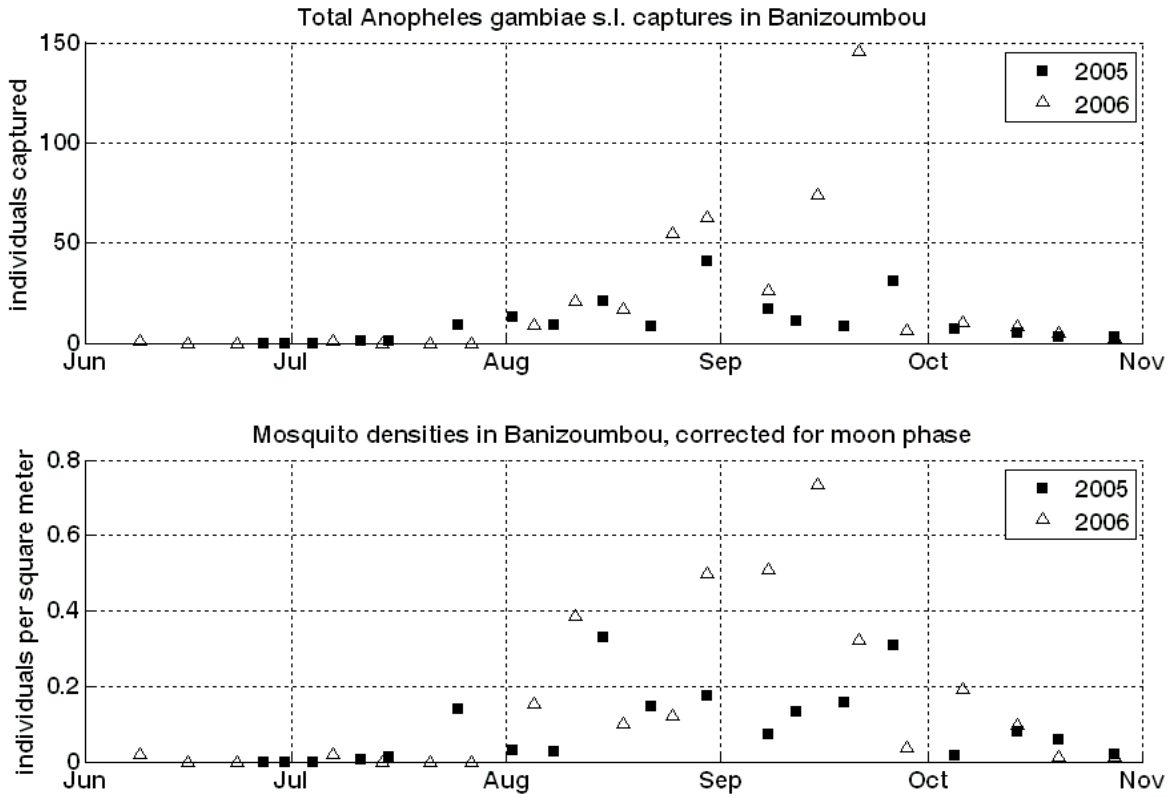

Figure 4.5. *Anopheles gambiae s.l.* adult mosquito captures, summed over six light trap sampling locations in Banizoumbou (top), and calculation of mosquito areal density to remove variability attributed to lunar phase effects (bottom).

The value of D for which B matches the ambient moon light defines the radial extent of trap influence (Service, 1993). Moonlight intensity is assumed to follow a sinusoidal pattern, with a maximum of 0.7 lux at full moon. A further sinusoidal correction to light intensity accounts for the proportion of each night with the moon above the horizon. At first quarter and last quarter the moon is only visible for half of the night.

The expected catch in the trap's effective area can be expressed as the product of effective area and areal mosquito density:

$$M = \delta \cdot \pi D^2 \qquad (4.2)$$

where M is the catch (mosquitoes) and δ is the density of mosquitoes (mosquitoes m^{-2}). Mosquito density is assumed independent of lunar phase and fluctuations in density are assumed attributable to environmental variables.

Solving for δ, the relation becomes

$$\delta = \frac{B \cdot M}{\pi \cdot L} \qquad (4.3)$$

Background moonlight decreases to near zero at new moon, which according to equation 4.1 causes an unrealistically large D. We limit the possible effective radius of influence to 12 meters to prohibit unrealistically low densities. Figure 4.5 (lower frame) shows the corrected light trap captures, reformulated as areal mosquito density, independent of lunar phase.

4.3.2 Ephemeral pool observations

We visited Banizoumbou at least twice weekly throughout each wet season to gather data. Soon after beginning regular sampling, it became evident where persistent and entomologically productive pools formed. Each field visit involved inspection of these pool locations and a search for larvae. If water was present, then dimensions were estimated and larvae were sought. Standard entomologic dippers were used for larval counts, and the maximum of ten successive dips was recorded. Otherwise, the location would be recorded as "dry" for that visit, and the pool considered devoid of larvae. In addition, we recorded water temperature, time of day, and turbidity at each sampling location, for each visit. Water temperature was measured in one ephemeral pool for several weeks using a HOBO Watertemp pro datalogger (Onset Computer, Bourne, MA), until the sensor disappeared, likely picked up by curious passersby. In this manner, we carried out systematic monitoring of frequently recurring and persistent pools. Also, after large rainfall events, we conducted surveys to seek new pools which had not existed previously.

The largest, most persistent pools in Banizoumbou did not always contain the most larvae and pupae. The establishment of predators after a certain period of pool existence can explain this counterintuitive observation. In addition, as previously mentioned, large pools tend to have small waves which may interfere with oviposition and the comfort of larvae at the pool shores. We observed the most larvae and pupae in newly-formed, medium sized (approx 20 - 30 meters) pools.

4.3.3 Meteorology measurements

Precipitation, incoming shortwave radiation, temperature, humidity, wind speed and wind direction were sampled and recorded hourly at the Banizoumbou meteorological station (see location in Figure 4.1). The sensors are all at the same station site, and measurements are recorded using a Campbell Scientific CR10X datalogger.

4.3.4 Soil moisture measurements

We deployed three sets of four time domain reflectometry (TDR) soil moisture probes in and around Banizoumbou. These sensors measure volumetric water content at half-hour intervals, and the resulting values are recorded in dataloggers for periodic download. These data are used for parameterization of the unsaturated zone hydrology model. The measurements began on June 23, 2005. Volumetric water content is measured at 10 cm, 20 cm, 50 cm, and 100 cm from the surface in a vertical profile configuration. Diverse land cover types were chosen for TDR sensor locations: millet field, fallow field, and bare, compacted soil in the center of Banizoumbou village. These represent three of the predominant land cover types assigned to the model domain from remote sensing data.

4.4. Model inputs and grid

4.4.1 Parameterization- hydrology model

As previously discussed, our modeling objective at Banizoumbou is to simulate the pool water volume resulting from overland flow entering topographic depressions yielding suitable mosquito habitat, and the persistence of these pools after formation. This objective requires an accurate simulation of rainfall partitioning into runoff and infiltration at the soil surface, for determination of both the total runoff water entering a depression and the soil water dynamics in the unsaturated zone over the model domain. Soil moisture, which has significant "memory", will strongly influence runoff generation in the subsequent storm. This requires accurate parameterization of the unsaturated zone hydrology model to reproduce the temporal behavior of soil moisture in the vertical soil column as observed by the in-situ soil moisture sensors.

The model was calibrated for 2005 field data, and was subsequently verified with 2006 field data. The hydrology model was calibrated primarily for the vadose zone, but soil crusting was also represented. From the Richard's equation (Equation 3.11) and Campbell's formulation for soil water retention (Equations 3.12 and 3.13), the flexible, soil type-dependent model parameters are the air entry potential (ψ_e), saturated hydraulic conductivity (K_s), Campbell's curve fitting exponent (b), and porosity (θ_s). These four parameters for each discrete soil layer completely parameterize unsaturated zone water redistribution according to Campbell's model. With the addition of soil root zone uptake, all of the major determinants of soil moisture are modeled. This assumes homogeneous conditions in each layer and no lateral movement. Both of these assumptions are consistent with field observations of uniform sandy soils throughout the model domain. We assign parameter values to match model output to field observations, constrained by results of previous field investigations into soil characteristics at the site (Peugeot et al., 2003; Vandervaere et al., 1997). Initial parameter assignments were made based on typical values for the sandy soils of Banizoumbou and published values, and were refined using a Gauss-Newton method. The objective function for this optimization is formulated as a least squares minimization, as shown in Equation 4.4:

$$F(x) = \sum_{t=1}^{m} [y_t - h_t(x)]^2 \qquad (4.4)$$

where y_t = observed soil moisture value at time t

h_t = simulated soil moisture value at time t, dependent on input parameters contained in vector x.

$F(x)$ = objective function value, as a function of parameter vector x.

m = total number of time steps

In the Gauss-Newton method, an approximation to the computationally expensive Hessian matrix is used, followed by a line search for a new estimated parameter set, for each iteration. This gradient-based methodology results in identification of local optima. We encountered the well-known topographic complexity of this objective function (Lambot et al., 2002), and therefore began the Gauss-Newton search with published values for K_s and θ_s, and typical values for sand for ψ_e and b. A local optimum was found near these initial parameter values. While it was not evident if this local optimum was

also a global optimum, within allowable ranges of parameters, Figure 4.6 represents the optimum. Figure 4.6 shows hydrology model fit with TDR soil moisture profile data at the "CFTEA" measurement site in Banizoumbou. Hydrology model parameterization is summarized in Table 4.2.

Table 4.2. Banizoumbou hydrology model parameters: Saturated hydraulic conductivity (K_s), porosity (θ_s), Campbell's "b" exponent (b), air entry potential (Ψ_e), and Manning's n (n). We use published parameters (when possible) for nominal values, which have been fine-tune using a Gauss-Newton parameter estimation technique.

	subsoil	**surface crust**		
	all classes	**millet field**	**Fallow**	**pool bottom**
K_s	5.0×10^{-2} mm sec^{-1} (†)	5.5×10^{-4} mm sec^{-1}	1.9×10^{-3} mm sec^{-1} (†)	1.7×10^{-4} mm sec^{-1}
θ_s	0.3 (†)	0.25	0.3 (†)	0.3
b	2.9	6.0	6.0	7.6
Ψ_e	-0.98 J kg^{-1}	-2.84 J kg^{-1}	-2.84 J kg^{-1}	-3.63 J kg^{-1}
n	N/A	0.12 (‡)	0.17 (‡)	0.05

† Vandervaere et al. (1997)

‡ Desconnets et al. (1996)

The hydrology model operates on a rectangular grid. For the simulations at Banizoumbou presented here, we set up a 100 cell by 100 cell model domain centered on the village. The inner region of 10-meter square cells is made up of 50 cells square, surrounded by ten 20-meter width cells on each side, then ten 40-meter width cells on each side, and finally five cells around the outside of 80-meter width. Thus, the total model domain has dimensions 2.5 km x 2.5 km.

A land cover class was assigned to each cell. This was done by supervised classification of a Landsat 7 multispectral image (Boyer, 2003). In the vicinity of Banizoumbou, the dominant land cover types of millet field, fallow field, and tiger bush shrubland were identified and assigned to each grid cell to parameterize root zone hydrology, transpiration, and surface roughness.

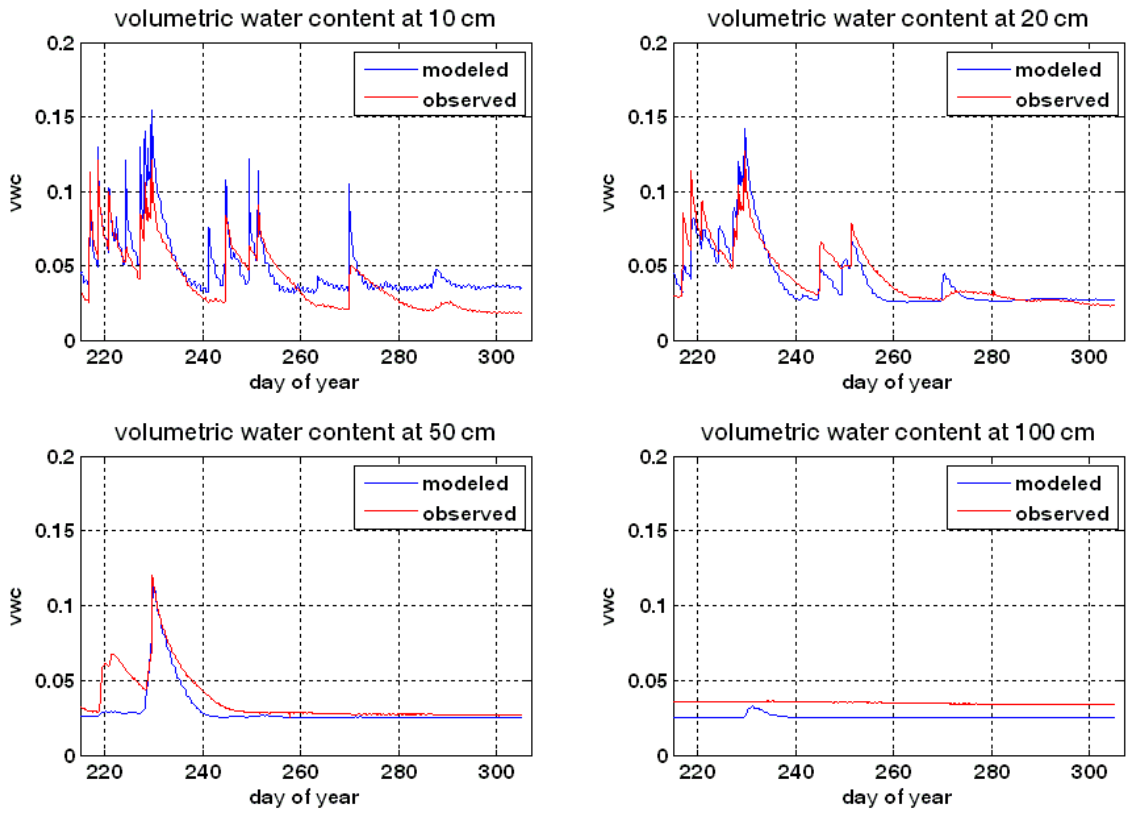

Figure 4.6. Model soil moisture output (volumetric water content) compared to measured soil moisture at a millet field 500 meters north of Banizoumbou, for the period 1 August – 10 November 2005.

4.4.2 Parameterization- entomology model

Table 4.3 summarizes entomological model parameters for the Banizoumbou simulation. Subadult stage model parameterization generally follows that of Depinay et al. (2004). The subadult model parameter values presented in Table 4.3 are chosen based on other published models without field verification at Banizoumbou (e.g. ecological carrying capacity). Model parameterization was constant between the two years, so potential errors in some parameters are equally applied to the two years. A sensitivity analysis was performed for each parameter in Table 4.3 and its influence on peak mosquito abundance represented in the table.

Based on field observations of presence of cows, goats and sheep near residences in Banizoumbou, we simulate one animal per village grid cell as a source of blood meals. Because we do not distinguish between *An. gambiae s.s.* and *An. arabiensis* as mosquito agents in the model, we assign a 10% chance of a bloodmeal being taken, should a blood-

seeking mosquito encounter an animal. This value reflects the dominance of anthropophilic *An. gambiae s.s.* and the greater availability of human blood meals. Outside of village areas, for modeling purposes we assume there are no animals available for blood meals. This is supported by our observation that during the malaria transmission season, villagers prevent animals from roaming freely because they damage crops.

In December 2005, Niger was the subject of a nationwide insecticide-treated bednet (ITN) distribution program. All families with children under 6 in Niger were given a free ITN from the program (Loewenberg, 2006). In Banizoumbou, we noted that 20% of all households were protected by an ITN as a result of the December 2005 bednet distribution. The permethrin-treated bednets have a knock-down killing effect on mosquitoes attempting to feed on a sleeper under the net, and the resulting dramatic reduction in average daily survivability of a mosquito population makes ITNs highly effective for malaria control. We simulate the presence of bednets in 2006 by killing a percentage of host-seeking mosquitoes entering houses with bednets and attempting to feed. Not all mosquitoes simulated to enter an ITN-protected household will die. Because generally not all sleepers in the house are covered by an ITN, we assume that 80% of attempted bloodmeals are successful, because a repellent effect of the bednet may divert bites from protected individuals to unprotected inhabitants. The rest of the attempted bloodmeals result in the mosquito's death. ITN protection in houses is assigned randomly within the village so that the observed 20% coverage is attained. Mosquitoes that are in a village grid cell but are not seeking bloodmeal hosts are assumed to be flying past the houses and not entering, and are therefore not subject to the ITN's knockdown effect.

For the entomology model, effective flight velocity was the primary calibration parameter. This varied the dispersal, and resulted in mosquito populations clustered around the village with dispersal similar to previous dispersal observations taken in Burkina Faso (Costantini et al., 1996b). The other parameters were prescribed based on published values or arbitrarily.

Table 4.3. Entomology model parameterization.

aquatic stage simulation

Variable	nominal value	units	reference	sensitivity*
cannibalism rate	0.0008	hr^{-1}	7	medium
number of eggs lain per oviposition	150		4	low
egg death rate	0.001	hr^{-1}	none	very low
weight of first-stage larvae	0.02	mg	none	low
weight of stage 2 larvae	0.16	mg	none	medium
weight of stage 3 larvae	0.30	mg	none	medium
weight of stage 4 larvae	0.45	mg	none	low
lag time for predators to establish	240	hr	2	low
carrying capacity of pools	300	mg m^{-2}	2	low
larvae death rate	0.005	hr^{-1}	6	very low
maximum predation rate for larvae	0.006	hr^{-1}	2	medium
pupae predation rate	0.005	hr^{-1}	none	very low

adult mosquito simulation and human individuals

Variable	nominal value	units	reference	sensitivity
human infection clearing rate	0.0005	hr^{-1}	6	very low
degree days above 18ºC necessary for sporozoites	111	deg-day	3	very low
probability that a mosquito takes a bloodmeal	0.07		none	low
average mosquito flight velocity	15	m hr^{-1}	1	low
time required for gametocyte development	336	hr	6	very low
weighting of random walk vs. straight line	0.2		none	medium
resting time	24	hr	none	medium
threshold distance for visual cues	15	m	5	low
utilization probability of water	0.95		none	low

references:

1. Costantini et al. (1996b)
2. Depinay et al. (2004)
3. Detinova (1962)
4. Detinova and Gillies (1964)
5. Gillies (1980)
6. Hoshen and Morse (2004)
7. Koenraadt and Takken (2003)

*parameter sensitivity gauged by maximum simulated abundance

4.5. Results

4.5.1 Hydrology

We simulate hydrology in Banizoumbou, Niger, for the 2005 and 2006 wet seasons. The 2005 wet season precipitation totaled 411.5 mm, and the 2006 wet season yielded 478.3 mm of rain, a 16% increase over the previous year. Much of the 2005 rainfall was unusually early and

more sporadic than in 2006, when heavy rains started in mid-July and continued into September. The sporadic nature of the 2005 rainfall with greater between-storm durations allowed many pools to desiccate completely during the monsoon. This was not observed in 2006, and mosquito populations reflected this difference. Some 461 adults were captured in 2006 compared to 193 in 2005, a 140% increase. In both years we sampled the same locations with the same frequency, and the dramatic difference in observed mosquito populations evidently results from climatic variability between the two years.

Figure 4.7 shows sample hydrology model results, superimposed on a 0.6-meter resolution panchromatic Quickbird satellite image of Banizoumbou Village. The two frames show water depth in the model domain (left) two days after the 47-mm precipitation event of August 11, 2006, and (right) one week after the storm. No additional precipitation occurred during the week following this storm. In the succession of frames, water loss to evaporation and infiltration lowers the pool water levels. In this particular example, simulated evaporation flux in one depicted pool ranges from 0.1 to 5 mm d^{-1}, depending on temperature and humidity conditions. This is consistent with estimates by Desconnets et al. (1997) for a nearby pool in a similar village. As previously noted, pool infiltration rates depend on water level, because the low-permeability substratum of clay-clogged sand in the pool bottoms inhibits pool infiltration losses up to a certain threshold pool water level (Desconnets et al., 1997). When the water level extends into sandy areas surrounding the pool, infiltration rates are high. Conversely, when it retreats to the clayey area, infiltration slows. We observe this characteristic in Banizoumbou pools, and therefore larger pools are assigned a lower top-layer saturated hydraulic conductivity based on observed extents of clayey surface. As expected, water level recession rates for the example presented in Figure 4.7 are high because of the high infiltration rates occurring beyond the clayey zones. Infiltration at sandy pool edges dominates. Persistent, remnant pools in the clayey area are evident in the second frame.

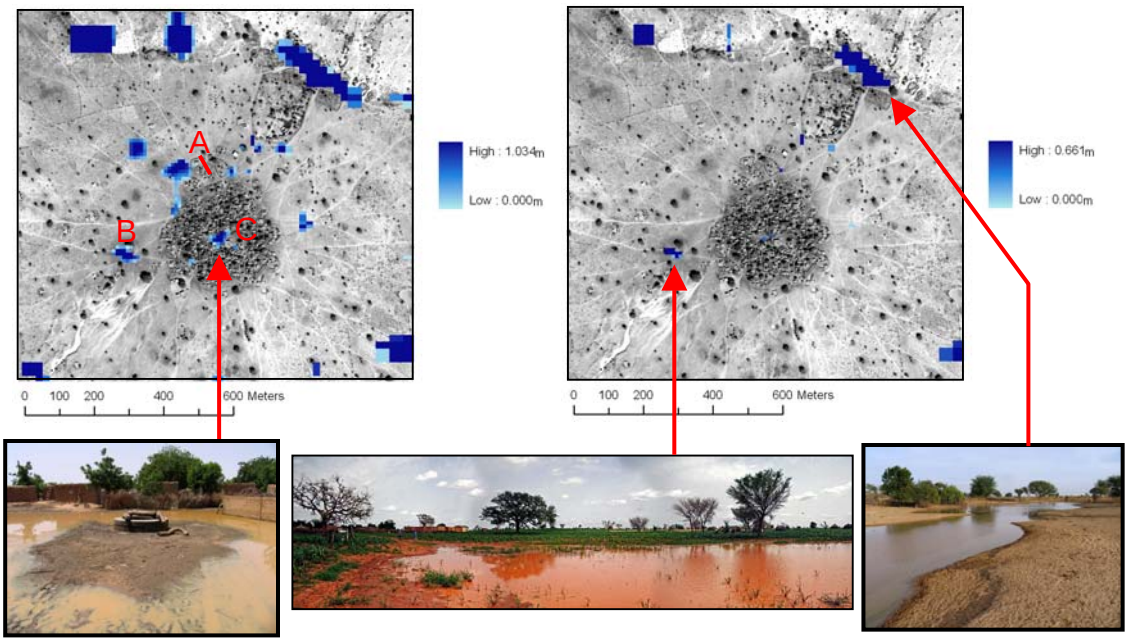

Figure 4.7. Two sample model output rasters for a sub-area of the model domain, focused on Banizoumbou village. Each frame shows water depth above the ground surface in response to the 47-mm precipitation event of August 11, 2006, superimposed on a Quickbird satellite image. The frames represent water depths two days after the storm (left), and one week after the storm (right). Photos of the real pools corresponding to selected model-predicted pools are presented. The photos do not necessarily correspond to the same times as the model output in this figure. The locations "A", "B", and "C" identify locations of data presented in Figure 4.8.

The persistent pooled areas are the most problematic because they allow uninterrupted mosquito breeding. Figure 4.8 plots modeled maximum pool depth over the 2005 wet season for three recurring productive pools of varying sizes. The plot includes depth estimates, which were calculated from a depth-area relationship using field-measured pool surface areas. The depth-area relationships were generated from very high resolution bathymetry data collected by topographic survey in December 2005, at approximately one meter resolution in the dry pool bottoms. Pool surface area measurements, made at each field visit with either a tape measure or a handheld GPS unit, contain some measurement error, estimated at about 10%, which would be carried over to the depth measurements as well. The southwest pool is shown in the photo of Figure 4.7. Pool size estimates and derived depths are reasonably well-

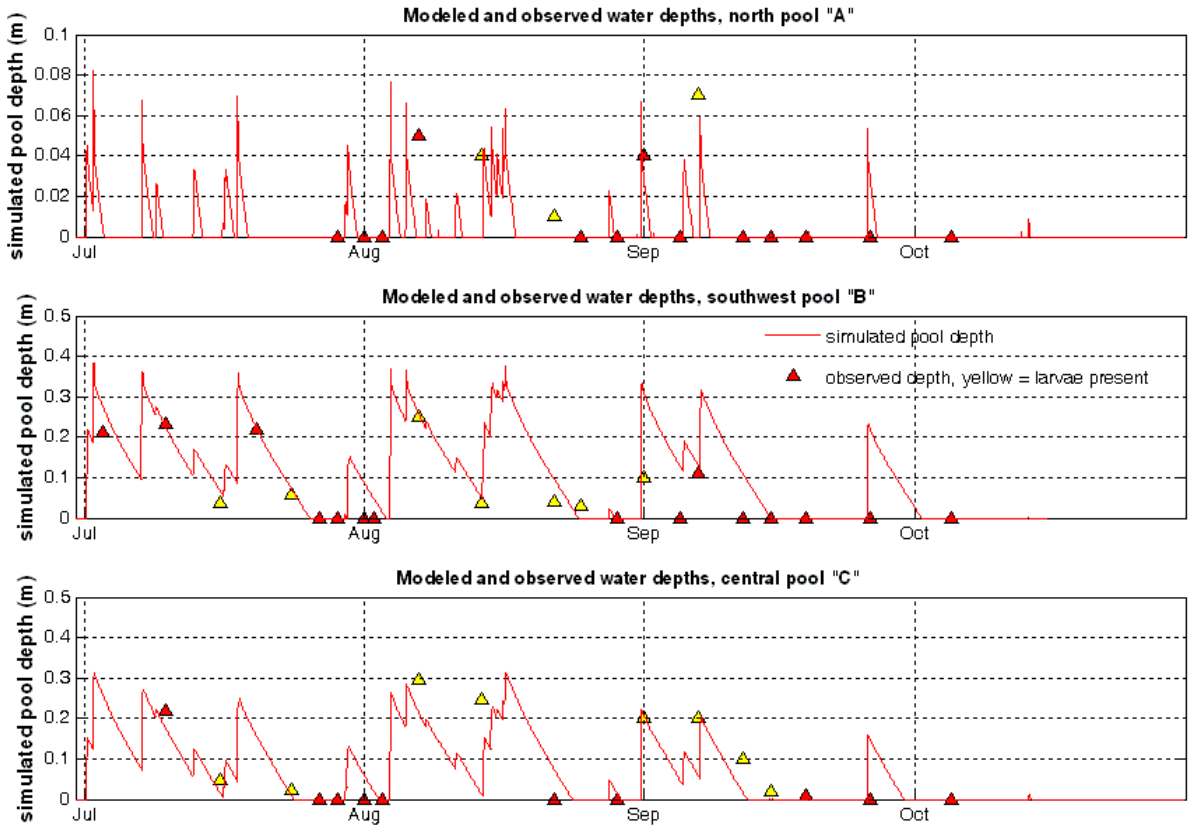

Figure 4.8. Simulated pool water levels for the 2005 rainy season at three pools in Banizoumbou (labeled “A”, “B”, and “C” in Figure 4.7), and larval presence at each field visit.

matched by the simulated pool depths for this sample of Banizoumbou pools. Notable deviations are evident in the southwest pool in September, which are not seen in the central pool. The primary reason for this disparity is the difference in land cover types within the catchments of each pool. The central pool, located in the center of Banizoumbou, catches water only from bare soil within the village, whereas the southwest pool catchment encompasses mostly cultivated millet fields. From field observations, crop height varies rapidly during the late growing season period, which is expected to result in a decrease of surface crusting from lower raindrop impact speeds and an increase of Manning’s roughness parameter *n* from a greater vegetation density. Moreover, greater root zone uptake in the near-surface soil layers could be partly responsible for this, although such a signal is not evident in soil moisture measurements taken in millet fields. These temporal changes associated with

crop growth are not incorporated in the hydrology model, and the result is an overprediction of pool depths in the southwest pool late in the growing season. The northern pool (labeled "A" in Figure 4.7), illustrates typical behavior of the smaller, more ephemeral pools surrounding Banizoumbou. Observations at this site are consistent with the simulated depths, except for one field visit in late August. In this case, pool surface area (about 10 m^2) was less than the model resolution, so failure to reproduce observed pool depth resulted from resolution limits. However, due to their small overall size and highly ephemeral nature, resolution issues highlighted by the behavior of this pool are not expected to drastically influence entomology model results. We observed rapid pool drying after reaching such low levels. Observations of larval presence in the pool is shown on Figure 4.8, shown as yellow depth points. These observations are for all larval instars, and in some cases only tiny first stage larvae were observed after rewetting of a dried-out pool. Red points indicates an absence of larvae at that field visit.

Larval counts were measured as the number of larvae caught in a standard dipper, and do not necessarily reflect abundance in the pools, because of clustering of the larvae. Certain areas of the pools typically had high larval density, whereas other sections of the same pool often had very low densities. Because of this problem, larval counts are not included on this plot and are replaced by an indication of larval presence at each field visit. When pools become completely dry, all larvae in those pools die. In this semi-arid, hot and sunny region, mud rapidly dries, so potential interstorm survival of larvae in wet mud is unlikely. After desiccation, therefore, a pool will not yield adult mosquitoes for at least several days, until any deposited eggs in the rewetted pool have hatched and advanced through all of the subadult stages. The timing of adult emergence as allowed by persistent yet ephemeral pools, as shown by Figure 4.8, underscores the importance of precipitation timing. Sparse rainfall in short-duration low-intensity storms will not yield pools persistent enough to allow long uninterrupted periods of adult emergence. Therefore, this limitation in rainfall frequency, amount, and intensity will strongly affect population dynamics as shown in Figure 4.8 and the low 2005 mosquito capture data. Figure 4.8 is one example of pool behavior during the 2005 wet season. All pools in the simulation have similar dynamics in response to water inflows, and if sufficiently persistent the pools will control adult mosquito emergence comparably.

4.5.2 Entomology

Emergent adult mosquitoes entering the model domain as mobile agents are faced with a series of environmentally-influenced decisions. Carbon dioxide levels above background levels attract individual mosquitoes to human habitation, where they take human bloodmeals and make malaria transmission possible. Visual cues may also play substantial roles in host-seeking behavior. After biting and resting, mosquitoes seeking oviposition sites disperse from the village, and may utilize pools that they encounter. These behavioral processes suggest that close proximity to productive water body locations is an indicator of malaria risk, because mosquito densities are greater in houses near pools. This is indeed the case. Minakawa et al. (2002) observed that in a village in Western Kenya, 94% of captured anophelines were in houses within 300 meters of the nearest productive breeding pools, 67% were in houses within 200 meters, and 36.3% were in houses within 100 meters of the nearest productive breeding site. Similar trends of decreasing biting rate with distance from breeding site are seen in data from the WHO Garki Project in Nigeria (Molineaux and Gramiccia, 1980). Not enough houses were sampled in our study to draw similar conclusions in Banizoumbou. However, modeling results show a very similar effect. From the 2005 simulation, 99.6% of the simulated indoor-resting anophelines were in houses less than 200 meters from the nearest productive breeding pool, 93% less than 150 m, and 67% were found less than 100 meters from the nearest breeding habitat. These simulation results show a similar trend to that reported by Minakawa et al. (2002), however quanititative differences of simulation results with those of Minakawa are likely related to a different layout of the village as well as a different configuration of pools within the village. Figure 4.9 shows sample model output for one arbitrary time step during the peak of the 2005 transmission season. Dense clustering around the northeastern section of the village is compared to the southeast corner, where relatively few mosquitoes are seen. For this time step, average mosquito indoor resting density is plotted against distance from the nearest productive breeding site in Figure 4.10, showing the expected decrease as distance from breeding sites increases. Few houses are more than 250 meters from the large, very productive pool near the well in the center of Banizoumbou. A major implication of spatial variability in mosquito density is the increased malaria transmissibility at certain locations within the village.

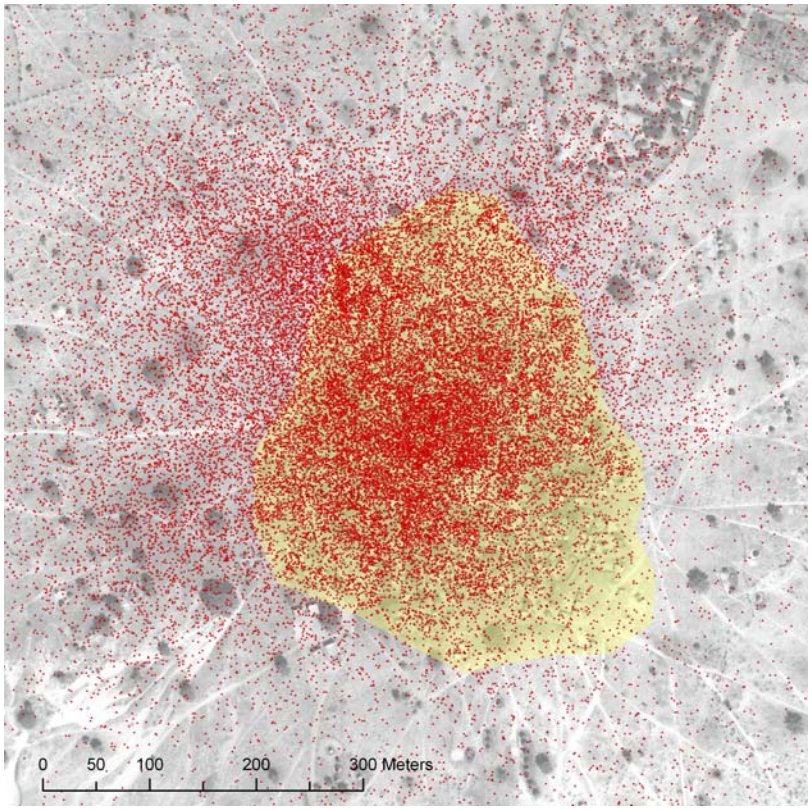

Figure 4.9. Example model output at an arbitrary timestep. The figure shows individual mosquitoes in red, superimposed on Banizoumbou Village (yellow buildings).

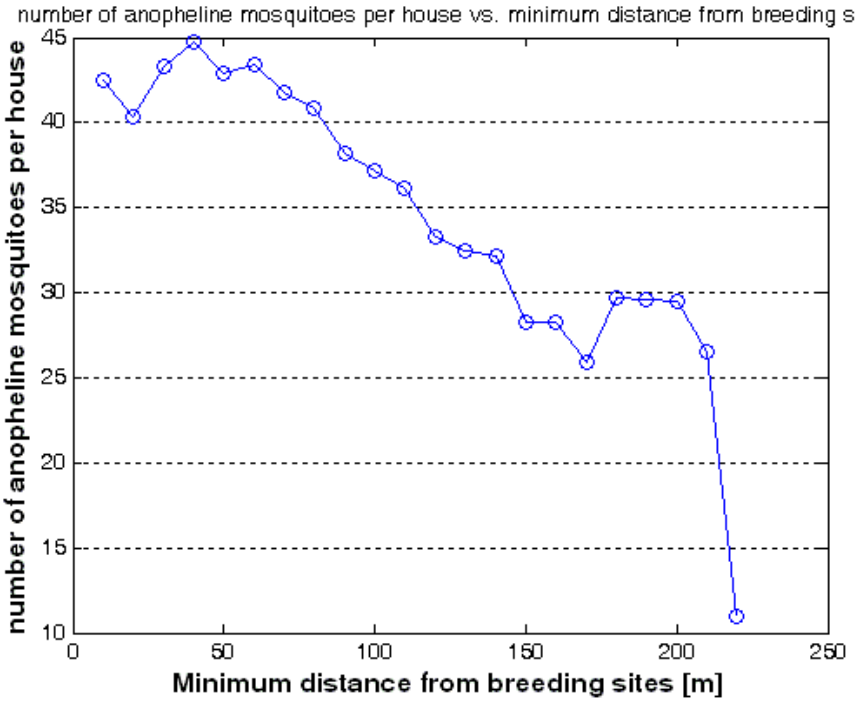

Figure 4.10. Model-predicted indoor resting density (mosquitoes per house) for the model output depicted in Figure 4.6.

4.5.3 Mosquito population dynamics

Simulated mosquito abundances are compared to observed trends using CDC light traps in Figure 4.11. The simulated mosquito abundances represent the total number of live mosquitoes over the whole model domain for each hourly time step. The result shows a general replication of trends and relative abundances (i.e. a strong wet-season peak in each year), however the simulated trends do not match the observed trends exactly on a weekly basis. It is likely that much of the discrepancy arises from limitations of CDC light trap use. As previously discussed, it is difficult to relate catch numbers to abundance, primarily because of lunar phase effects. We have attempted a correction for lunar phase. However, the resulting comparison indicates that either additional measurement error in CDC light traps or the lack of highly specific details within the model governing the exact hourly behavior of simulated mosquitoes are sources of additional error. Nevertheless, light traps are valuable tools for measuring relative changes in abundance (Service, 1993). As such, we compare cumulative simulated mosquitoes to cumulative mosquito captures in Figure 4.12. Relative differences in observed abundance between the two years are highlighted here. Model parameterization is unchanged between the two runs, except for the inclusion of ITNs. The increase derives solely from climatic variability between years, as ITNs would act to reduce abundances in 2006, compared to 2005 when they were absent from the village. The precipitation difference is a 16% increase between the two years, which is relatively small when compared to the more than doubling of mosquito populations. We attribute increased abundance to timing of rainstorms and resulting pool persistence. In 2005 the first rain fell in late April, which is unusually early for the area, and was spread out temporally with much of it in the form of local convection thunderstorms. Larger, organized mesoscale convective systems dominate precipitation in the peak of the monsoon and tend to yield more rain. These systems were more prevalent in 2006 than in 2005, which may partly explain the difference.

In order to evaluate the sensitivity of predicted mosquito population dynamics to variations in individual parameters, we varied each model parameter by 5% and quantified the resulting response in mosquito population. The maximum seasonal abundance was used as a basis for comparison. Resulting model sensitivities are added as a column in Table 4.3. A multiplier of 1.05 was applied to each parameter, and the resulting effect on the mosquito abundance was

assessed. Those parameters for which the predicted abundance increased 5% or less are denoted as having “low” impact, and those parameters for which the predicted abundance increased between 5% and 10% in response to the 5% parameter perturbation are denoted as having “medium” impact. We consider sensitivity of model outcome to parameters with a greater than 10% response of mosquito abundance to the 5% parameter perturbation as having a high impact. None of the model parameters in Table 4.3 matched this description.

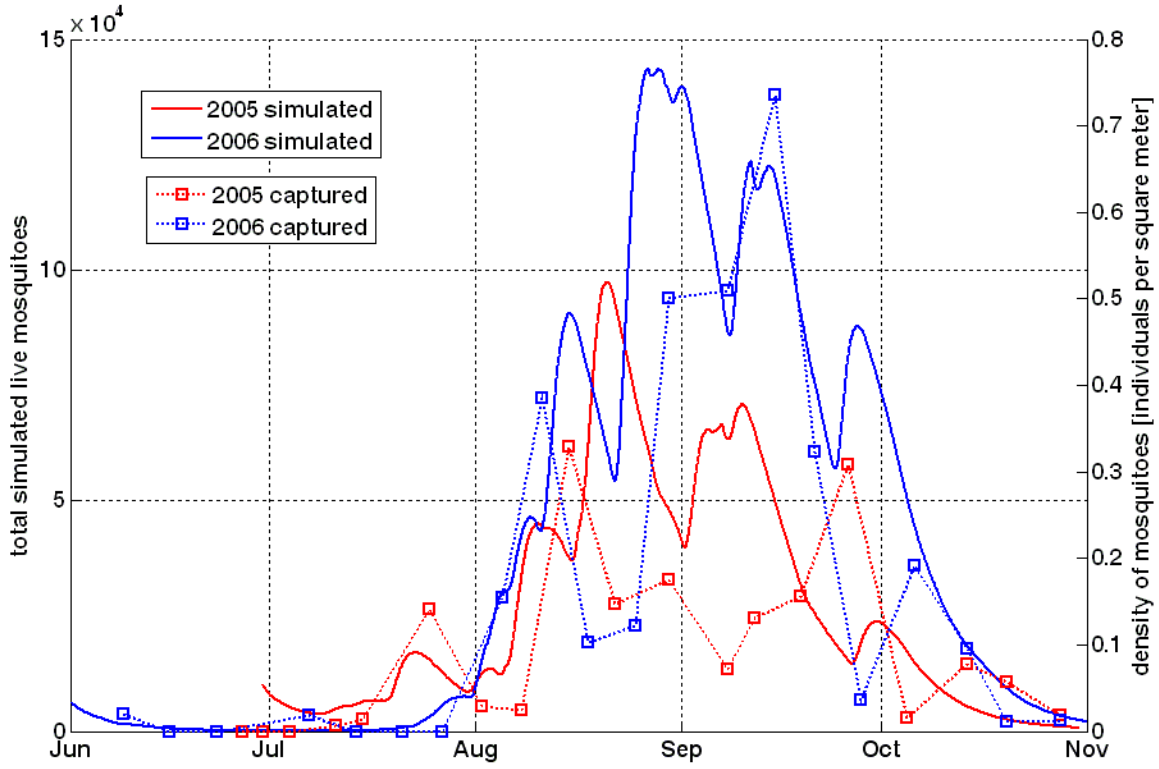

Figure 4.11. Simulated adult mosquitoes over the whole model domain in 2005 and 2006, compared to light trap captures in 2005 and 2006.

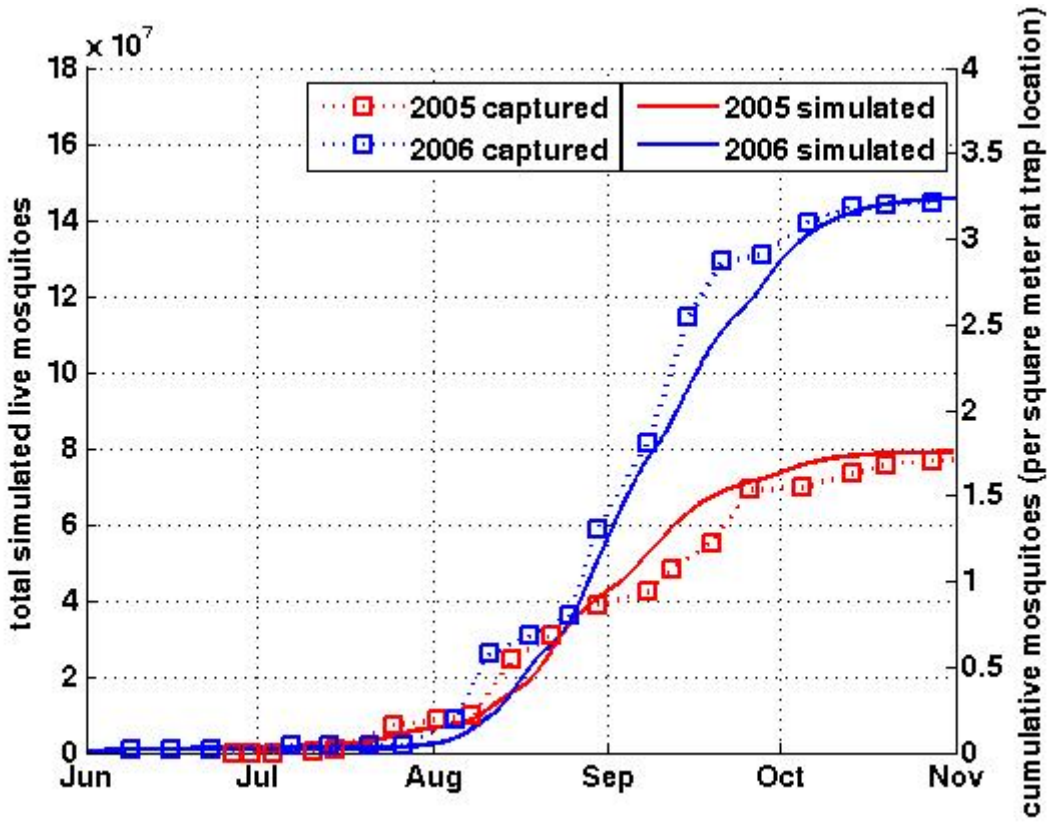

Figure 4.12: Cumulative mosquitoes, observed and model output.

4.5.4 Malaria transmission

The agent-based model simulates mosquito populations and their carriage and transmission of malaria parasite. Much focus in this paper has been on entomology simulation, primarily because model output can be compared to the entomological field data collected at Banizoumbou. In this chapter, we do not compare model simulations to malaria prevalence data. However, as previously discussed, many major steps in the malaria life cycle are represented: gametocyte development, uptake by bloodfeeding mosquitoes, parasite development within the mosquito to the sporozoite stage, and subsequent inoculation of a human upon taking a second bloodmeal, provided the sporozoites are mature. As such, time series of malaria prevalence can be generated by the model. Predicted malaria prevalence for 2005 is presented in Figure 4.13. Malaria transmission simulation in no way influences the entomology simulation, so errors in malaria-related model parameters cannot affect the entomology model results. As previously mentioned, neither superinfection nor immune response as a function of inoculation rates are represented in the model.

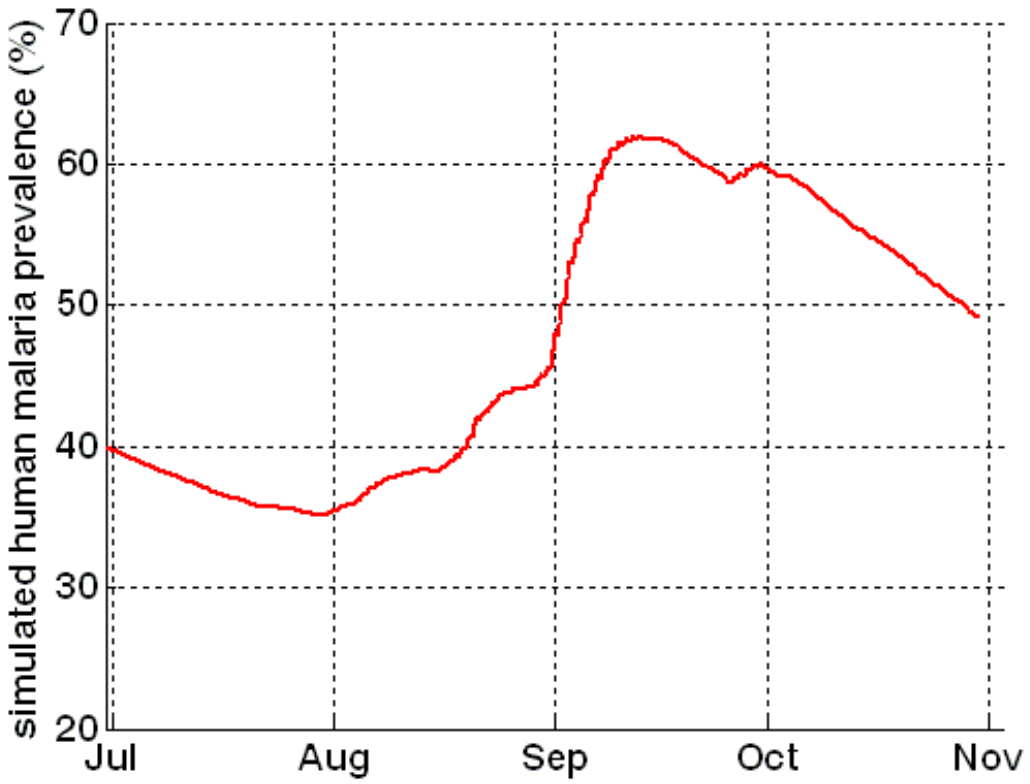

Figure 4.13. Model-predicted malaria prevalence.

4.6. Discussion

In a water-limited environment such as the Sahel, land surface hydrology controls malaria mosquito population dynamics. In the case of Sahel malaria transmission, we have shown that high resolution modeling yields credible, mechanistic modeling links of climate variable inputs to village-scale malaria transmissibility through hydrology and entomology model components. A variety of perturbations can be evaluated with the completed model. For example, land use changes, environmental management alterations, as well as climate variability and change scenarios can be explored by varying the inputs.

Using the weekly CDC light trap catches in Banizoumbou as a comparison, the model has proven successful in simulating the variability of mosquito populations at seasonal and interannual time scales, however at shorter time scales the model has limited ability to replicate trends in observations made by CDC light traps. We attribute this limitation to two

factors. First, CDC light traps are not perfect sensors of absolute abundance at the sampling location, as discussed previously. Second, the assumption of spatial uniformity in atmospheric forcing may also influence spatial population distributions. Random error resulting from this assumption may be partially responsible for the discrepancies between simulation results and observations at weekly time scales. The potential importance of microhabitats for providing sheltered areas within houses, tree canopies or other vegetation may be an important factor regulating short time-scale mosquito behavior. As presented, the model does not incorporate possible mosquito behavior leading to the utilization of such areas in which they are protected from adverse meteorological conditions. In response to microhabitat availability, resting behavior or flight paths may in fact deviate from the assumptions of fixed resting times and radial random walk which are presently incorporated into this model. Error resulting from such assumptions in the model, combined with random error in light trap measurements, likely result in the difference between observations and simulation results. At longer time scales, random errors are averaged out, resulting in better model correspondence to observations at seasonal to inter-annual time scales.

As has been presented in this study, effects of interannual climate variability on malaria-transmitting mosquito population dynamics are evaluated within this modeling framework. An example of real interannual variability at Banizoumbou has been presented and has shown the importance of both timing and amount of precipitation for mosquito breeding, emphasizing the need for simulation at temporal scales which resolve individual storms. Hortonian runoff generation and overland flow over an infiltrating land surface into topographic depressions, as well as subsequent pool level recession are short time-scale processes. The timing of pool recession until desiccation exerts strong controls on mosquito development. For these reasons, imperfect matches of observed and simulated mosquito abundances at short time scales do not diminish the value and need for simulation at short time scales.

Similar to climate variability evaluations, climate change scenarios can be simulated by changing climate inputs to the model. In chapter 6, we explore climate shift scenarios which can act as surrogates for climate change. However, climate change occurs over a long time scale, and so model assumptions of stationary and unvarying human populations may not

completely reflect human adaptability to changes, but aside from this caveat, mechanistic modeling links between climate change and malaria transmission can be achieved using the presented model.

4.7 Conclusion

The presented model provides a spatially explicit representation of Anopheles mosquito population interactions with humans and natural environments. It provides an organized, structured, and mechanistic means of representing known environmentally-sensitive causations of malaria transmission. We have calibrated the model using observed field data from 2005, and have predicted 2006 hydrologic and entomologic conditions with the calibrated model. Distributed hydrology yielding favorable Anopheles mosquito breeding pools is successfully modeled in detail. The model effectively reproduces observed mosquito population dynamics at seasonal and interannual time scales, as well as spatial distributions of clustering near breeding pools and human habitation. However, at weekly time scales, limitations of the model become evident. It does not perfectly reproduce weekly CDC light trap measurements made at several locations within the village. This may reflect both deficiencies in CDC light traps as a short time-scale sampling method, as well as possibly some unknown short time-scale mosquito behavior governing exact distributions which the model does not include. Nevertheless, comparisons of time-integrated model output with observations confirm that climate variability controls on mosquito populations were successfully simulated. A 16% increase in rainfall between 2005 and 2006 was accompanied by a more than doubling in anopheline abundance, which the model reproduced. The presented model is also capable of tracking the acquisition and transmission of malaria parasite, and the temperature-dependent extrinsic incubation period. Future research will continue to develop the model and its applications.

Chapter 5: Banizoumbou and Zindarou comparison study

5.1 Introduction

Malaria transmission in the Sahel typically fluctuates seasonally and peaks following onset of the wet season rains in May or June. Figure 3-2 depicts weekly malaria cases at the hospitals in Niger for three years. The pronounced increase in malaria incidence lags the monsoon, which lasts until early October. Global Precipitation Climatology Project (GPCP; Huffman et al., 1997) weekly reanalysis rainfall data is superimposed on this plot to show the association (with slight lag) with rainfall. As discussed in previous chapters, the small-scale, ephemeral pools that dot the Sahel landscape after rainstorms facilitate the prolific mosquito breeding that brings about the seasonal transmission increase. Pool persistence depends on local hydrology (soil type, vegetation type, overland flow yields from each pool's catchment), and strongly influences mosquito abundance. Through this mechanism, hydrology affects malaria transmission in the water-limited Sahel regions.

Water-limited savannah environments such as the Sahel exhibit spatial variability in hydrology associated with the local dominance of either trees or grasses. This is largely due to topographic effects and applies to a region of climatic conditions spanned by the very dry conditions in the north and the uniformly wet conditions in the south (Kim et al., 2004). Spatial variability of malaria transmission is associated with the availability of surface water for mosquito breeding. In regions south of the Sahel, wet conditions prevail and water availability does not limit mosquito populations. North of the Sahel it is too dry for mosquitoes to breed. Both of these extreme bounds of the Sahel exhibit low spatial variability of hydrology and malaria transmission. The Sahel therefore represents a maximum in spatial variability of malaria transmission.

Banizoumbou and Zindarou, Niger, are separated by only 30 km, however they represent two drastically different hydrologic environments. Banizoumbou is typical of the Sahel:

dry savannah conditions prevail and vegetation is dominated by wet-season millet crops and tiger bush shrubland. Soil is predominantly sand (about 90%), and natural water bodies are exclusively rainfed pools that rapidly lose water to evaporation and infiltration. The groundwater table is about 25 meters below the surface. In contrast, Zindarou has a much wetter environment due to the presence of a shallow groundwater table which is approximately 1 meter below the ground surface at the peak of the monsoon. As the monsoon progresses, the rising groundwater table penetrates the land surface in topographic low points, creating large water bodies that persist for many weeks, and recede after the cessation of rains in September. The shallow groundwater is the legacy of a major river system draining what is now the central Sahara (Talbot, 1980). Zindarou is situated in the floodplain of this abandoned river, which is known as the "Dallol Bosso". Relict braided channel features are identifiable in satellite images, and these features typically constitute the low points allowing the surface expression of groundwater. Extensive and prolonged mosquito breeding results from this hydrologic phenomenon, and consequently Zindarou is plagued with many more anopheles mosquitoes than other villages during the wet season.

Because of the proximity of Banizoumbou and Zindarou, and the major differences in their hydrologic characteristics, we have studied these villages' environments and mosquito dynamics to understand the role of hydrologic variability in malaria transmission. The short distance between the villages (30 km) controls for spatial climate variability, and in both villages malaria transmission is seasonal and water-limited due to mosquito dependence on water bodies. The goal of this study is to characterize the hydrologic differences leading to observed discrepancies in malaria mosquito abundance between the two villages, using a mathematical model (HYDREMATS). The model reproduction of observed differences between the villages highlights the role of hydrologic variability as a spatial determinant of malaria transmission. We simulate the mosquito abundance in the two villages using only climate input (precipitation, temperature, humidity) and soil type, vegetation type and topography data.

5.2 Field observations

We collected mosquitoes at Banizoumbou and Zindarou weekly during the 2005 and 2006 wet seasons, and monthly during the dry seasons. During each field visit, CDC light traps were placed at six locations in each village. Each trap was powered with a freshly charged motorcycle battery, and was started at 7PM and stopped at 7AM the following morning. Mosquitoes were separated from the catch and then identified to species using a microscope. In Banizoumbou, light traps yielded only *Anopheles gambiae sensu lato* mosquitoes (the species complex which comprises sibling species *Anopheles gambiae sensu stricto* and *Anopheles arabiensis*). In Zindarou, light traps also showed *Anopheles gambiae s.l.* to be the most abundant species. Due to resource limitations, we did not distinguish sibling species *Anopheles gambiae sensu stricto* from *Anopheles arabiensis*, because they are morphologically identical and require genetic analysis for identification beyond the species complex level. Many *Anopheles funestus* were also caught albeit in much lower numbers. Due to its anthropophily (preference for human blood meals over animals), *An. funestus* is a highly efficient malaria vector (Gillies and DeMeillon, 1968). Other captured anophelines included *An. rufipes* and *An. pharoensis*, however total captures for these species were very low even in Zindarou, and because of lower anthropophily they are considered only minor vectors of malaria (Costantini et al., 1998). We therefore assume that they play a negligible role in Zindarou malaria transmission and omit them from the study. In each village, three of the traps were placed inside three houses near the inhabitants' beds, and three others were placed outside of the same three houses. The sampled houses were constructed of mud brick walls with a thatch roof, or completely of thatch. All sampled houses have open eaves and open doorways.

Total mosquito captures in Zindarou and Banizoumbou are shown in Figure 5.1. The wet conditions of Zindarou allow significantly higher abundances, and Zindarou mosquito populations persist well into the dry season due to the permanent shallow groundwater wells. It is thought that temperature-induced mortality severely limits mosquito populations in the hot dry season (March – May).

Meteorological stations were operating in both Zindarou and Banizoumbou for the duration of the study. Temperature, humidity, incident solar radiation, and wind speed and direction were sampled every 15 minutes in both villages, and recorded in dataloggers. In addition, soil moisture was monitored at three sampling sites in each village, with four time domain reflectometry (TDR) probes at each station sampling volumetric water content in a vertical profile configuration. These soil moisture values inform unsaturated zone hydrology and provide a calibration target for simulated soil moisture. Section 2.2.1 summarizes Zindarou meteorological measurements during the study period, and section 2.2.2 summarizes Banizoumbou meteorological measurements.

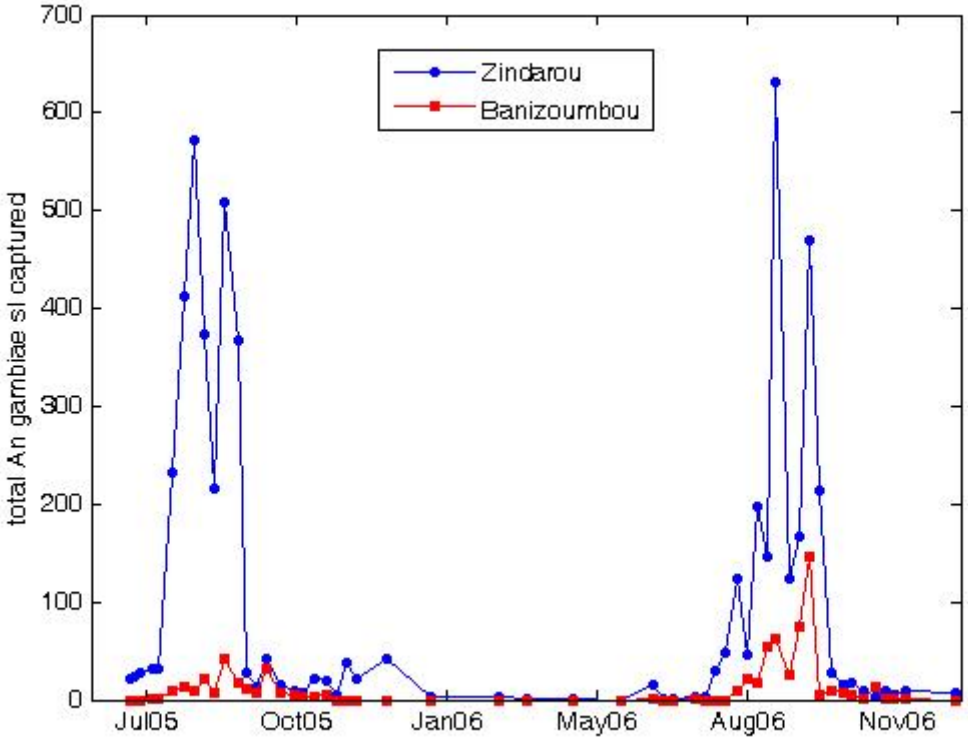

Figure 5.1. Total captured *Anopheles gambiae s.l.* mosquitoes captured in Banizoumbou and Zindarou in the period June 2005 – December 2006.

All surface water bodies were regularly monitored for anopheles mosquito larval activity using a standard dipper. For each dip, the anopheles larvae were counted and the maximum number per dip was recorded. Because Banizoumbou light trap captures included only *An. gambiae s.l.*, we assumed that all anopheles larvae seen in Banizoumbou pools are *An. gambiae s.l.* In Zindarou, however, several other types of

anopheline mosquitoes abound, as previously discussed. Various types of aquatic habitat are present in Zindarou, including permanent shallow garden wells, long-duration (multi-week) surface expressions of groundwater as well as short-duration (multi-day) rainfed puddles similar to those found in Banizoumbou. All of these Zindarou water bodies regularly contained *An. gambiae* larvae in addition to the other anophelines. Larval samples were taken and reared to adulthood. These are listed in Table 2.5, and were used to confirm various habitat usage by *An gambiae*. Because virtually no sizeable water bodies in Zindarou were consistently devoid of larvae, and because larval surveys are generally not a good measure of absolute abundance (see discussion in section 2.7), little emphasis is placed on the numbers from the larval counts. Instead, the larval counts are valuable as qualitative indicators of pool productivity, and were used to justify the inclusion of all open water bodies (except small anthropogenic containers such as bowls) in the Zindarou simulation.

Table 5.1. Zindarou hydrology model parameters: Saturated hydraulic conductivity (K_s), porosity (θ_s), Campbell's "b" exponent (b), air entry potential (Ψ_e), and Manning's n (n). We use published parameters (when possible) for nominal values, which have been fine-tuned using a Gauss-Newton parameter estimation technique.

	Subsoil		**crust**	
	millet fields & fallow	**garden area**	**millet & fallow**	**pool bottom**
saturated hydraulic conductivity K_s	5.4×10^{-2} mm sec^{-1}	1.7×10^{-2} mm sec^{-1}	3.3×10^{-4} mm sec^{-1}	3.8×10^{-4} mm sec^{-1}
porosity θ_s	0.25	0.44	0.38	0.48
Campbell's "b" exponent	1.3	1.85	6.0	7.6
Air entry potential Ψ_e	-0.07 m	-0.08 m	-0.29 m	-0.37 m
Manning's n	N/A	N/A	0.12	0.05

Many references cite very small depressions such as cattle hoof prints and tire ruts as primary anopheline breeding habitats (e.g. Minakawa et al., 2004; Mutuku et al., 2006; Service, 1993). In Banizoumbou and Zindarou, we encountered such micropools, but in all cases they have been directly beside larger, saturated topographic depressions and as

such their existence is embodied in the model structure. Cattle hoof prints and tire ruts were also seen at some distance from such depressions, however the persistence of these micropools is far too low to allow development of mosquitoes. Without exception the micropools were seen to disappear several hours after rainfall. With regular, comprehensive surveys, we never observed late-stage larvae or pupae in cattle hoof prints or tire tracks, except when located at the saturated edges of larger pools. In Zindarou as in Banizoumbou, there is therefore no need to simulate at spatial scales consistent with such microdepressions.

In Zindarou, the seasonal groundwater rise increases the extent of surface water availability for mosquito breeding in topographic low points. When the groundwater table is higher than the ground level of these topographic low points, large areas of open water form. An example is depicted in Figure 5.2. The presence of such extents of shallow open water is a fundamental difference in the hydrology of Zindarou compared to Banizoumbou. The water level fluctuations are incorporated into a version of HYDREMATS tailored to the Zindarou hydrologic environment. Some field observations of groundwater level fluctuations were made to inform the model development and to serve as a calibration target. Villagers maintain their shallow hand-dug garden wells to water dry-season vegetable crops, and keep them deep enough to at least reach the groundwater table year-round. The garden wells are therefore permanent, however the large areas of surface groundwater expression are seasonal. We placed metal rods in the middle of some of these wells to provide a stationary reference for monitoring water level fluctuations. During times of heavy garden well use in the dry season, however, the metal rods were frequently disturbed, negating their intended purpose. Eventually after one season most of the rods were removed and we did not replace them because they proved intrusive to the villagers. One well has a concrete casing which provided a useful, permanent, non-intrusive measurement reference. Groundwater level rise is also evident in some TDR soil moisture measurements. The lowest probe, at 1 meter depth, registered saturated conditions during the peaks of the wet 2005 and 2006 monsoons, but not during the low rainfall 2007 monsoon. The reference for each of these measurement points was surveyed using a high-accuracy differential GPS system. From all of these measurements,

a compiled groundwater level time series was produced (Figure 5.3). Well measurements show a very flat groundwater table surrounding Zindarou, and the groundwater level in Figure 5.3 is therefore assumed to be applicable over the entire 2.5 km square model domain surrounding Zindarou.

Figures 2.1 and 2.2 depict the sampling locations in both Banizoumbou and Zindarou, including meteorological and entomological observation sites. Figure 2.3 shows the well locations in Zindarou, relative to the village.

Figure 5.2. An example of surface expression of groundwater in Zindarou, at a topographic low point. This is the “Ikonos” pool of Figure 2.3. The name derives from the pool’s easy identification from an Ikonos satellite image.

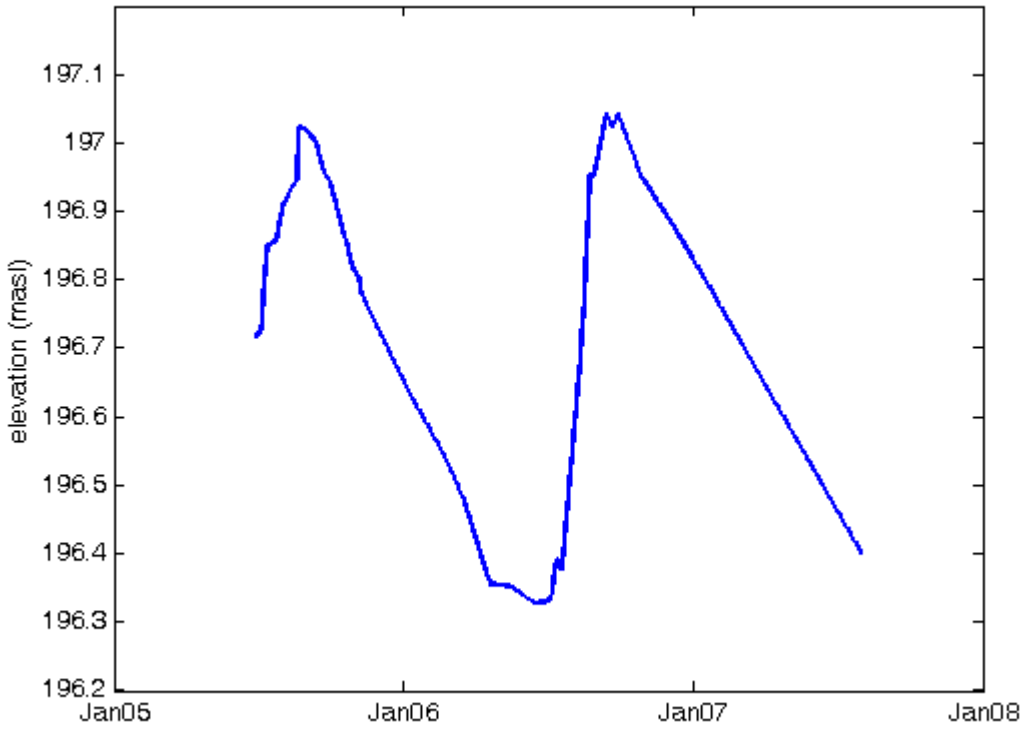

Figure 5.3. Compiled domain-wide groundwater fluctuations spanning the 2005 and 2006 wet seasons.

5.3 Modeling Methods

5.3.1 Model structure and domain

We apply the validated, field-tested model HYDREMATS to Banizoumbou and Zindarou. HYDREMATS is a coupled hydrology and entomology model that simulates in very high spatial and temporal resolution the formation and persistence of the types of pools that facilitate the breeding of *Anopheles gambiae s.l.* mosquitoes. Within HYDREMATS, water, energy, and momentum balances in two canopy layers and multiple soil layers are performed by a modified version of the Land-Surface Exchange model (LSX) of Pollard and Thompson (1997). An overland flow routing component was added to route predicted runoff using a two-dimensional solution to the shallow flow equations. Spatially-distributed roughness, parameterized by Manning's *n*, retards overland flow. At each model grid cell and for each model time step, infiltration and evaporation losses are predicted, and differences in runon from upstream cells and runoff

to downstream cells results in a change in water depth. The infiltrating land surface regulates the amount of runoff available for pooling in the topographic low points, and pool-bottom infiltration further controls pool persistence.

The 2.5 km x 2.5 km model domain around Banizoumbou was chosen based on maximum expected extent of mosquito dispersal around the village. For the same reason, as well as computational efficiency, a similar model domain was chosen surrounding Zindarou (2 km x 2 km). Figure 5.4 shows the model grid superimposed on an Ikonos satellite image of Zindarou. Zindarou village is located at the center of this figure, and the discretized model domain shows elevations applied to each model grid cell. Grid cell elevations are from a 50-meter resolution digital elevation model derived from Envisat satellite synthetic aperture radar data. The model grid does not have the same very fine discretization as the center of the Banizoumbou grid, because in the center of the model domain near Zindarou, no rainwater pools of comparable size were noted. Only shallow garden wells and a few small saturated areas nearby large groundwater-induced surface water bodies were of this size. The garden wells were represented in the model as stationary, permanent small water bodies. Because they are smaller in size than the computational grid elements for Zindarou (50 meters square), water depth values at ten meters square were superimposed on hydrology model output to represent their existence. The wells were often smaller than ten meters square, but this is the minimum allowed pool size in the model.

Hourly predictions of breeding pool locations and the pool water temperatures provide the input for the entomology component of HYDREMATS. These pools facilitate the breeding of anopheles larvae and eventual eclosion as adult mosquitoes, provided the pool persists long enough for temperature-dependent development to complete. After emergence, simulated adult mosquitoes interact with their environment and disperse in the model domain in an agent-based model structure. Interactions with village inhabitants and water bodies for oviposition (egg-laying) allows mosquito population dynamics and malaria transmission to be tracked. After pools have received eggs from a gravid female, the predicted temperatures determine the pool-specific advancement rate of aquatic-stage

development from egg to larva to pupa and finally adult mosquito. The reader is referred to chapters 3 and 4 for more details.

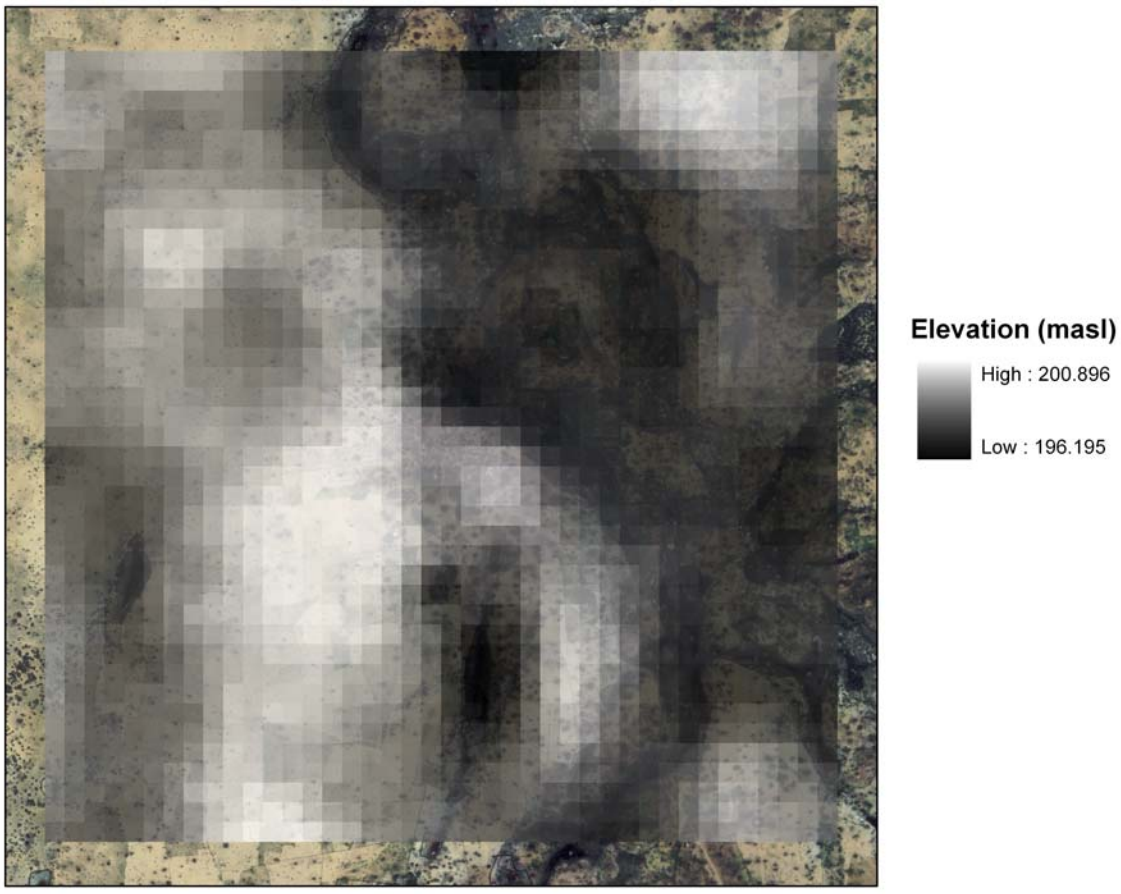

Figure 5.4. Model domain, discretization, and topography for the 2 km x 2 km area surrounding Zindarou. The model domain is superimposed on an Ikonos image of the Zindarou environs. Grid cells are 50m square. Zindarou village is located at the center of this model domain.

5.3.2 Adaptation of the entomology model to the Zindarou environment

While the decrease of Banizoumbou mosquito populations following cessation of rains clearly coincides with the disappearance of primary breeding pools (Figure 5.1), the decline of the Zindarou anopheline populations did not coincide with the disappearance of surface water available for mosquito breeding. Large areas of surface water persisted into November as the groundwater table slowly receded, but the persistent pools did not produce large numbers of anophelines after early September. Clearly, other factors limited mosquito development and eclosion. Limitations may include competition for

reduced nutrient sources, and heavy predation after complex ecosystems have become established in the pools. Larvae primarily feed on algae and bacteria (Walker et al., 1993; Gimnig et al., 2002) and respond strongly to available pollen (Ye-Ebiyo et al., 2000). During rain seasons, local residents farm pearl millet extensively. Millet pollen is thick and rich and may provide an important source of nutriment for aquatic stage anophelines during the peak of the transmission season. After the end of the rains in early to mid September, millet pollen production ceases (Clerget et al., 2007), abruptly ending supply of what may be the dominant source of nutriment for mosquito larvae. Competition for decreasing nutrients in the late rain season could therefore be a serious impediment to subadult mosquito development after local pollen production stops. In order to simulate this effect, a decrease in ecological carrying capacity was included in the HYDREMATS simulation representing Zindarou. Ecological carrying capacity was reduced from 1500 mg m^{-2} to 150 mg m^{-2} in order to represent the drastic reduction in food supply.

Predation can also seriously affect mosquito populations, and constitutes a significant proportion of larval mortality (Service, 1977). Soon after the formation of pools following rainstorms, *An gambiae* lays eggs which rapidly develop into adults. However, after this initial cohort of mosquitoes emerges, predators become established with some delay. This frequently results in a decline from initial population peaks as predators begin to regulate the population (Service, 1977; Depinay et al., 2004). Predation is represented in HYDREMATS as a logistic function with a delay of several weeks to reach the maximum allowable predation rate. Both lag and maximum predation rates are model parameters.

Entomology model parameterization for Zindarou is the same as Banizoumbou (Table 4.5), except for the variable ecological carrying capacity in the Zindarou simulation. The same reduction of carrying capacity in the Banizoumbou simulation would not affect the mosquito populations, because the Banizoumbou pools disappear due to lack of rain in mid-September, roughly at the same time as the reduction of Zindarou carrying capacity. In addition, predator lag was increased to 3000 hours for attainment of maximum predation rates of 0.06 hr^{-1}. This change in parameterization is based on observations of

more complex ecosystems with high predator abundance (mostly predatory aquatic beetles) in the persistent and permanent pools of Zindarou, compared to the more ephemeral, ecologically simple pools of Banizoumbou. In Banizoumbou, pools disappear much more frequently, and predators have little time to become established before the pool dries. Rewetted pools reset the predation rates, and therefore the high predation rates of Zindarou are not seen in Banizoumbou.

5.3.3 Adaptations of the hydrology model to the Zindarou environment

Distributed soil parameters are assigned based on previous studies performed in the area (e.g. Desconnets, 1997) as well as model calibration. Assigned soil parameters are summarized in Table 5.1. Example soil moisture model results are depicted in Figure 5.5 with each figure pane representing a different soil layer at the Zindarou South measurement site. Soil moisture measured by the TDR probes is compared to the model-predicted soil moisture. The 100-cm TDR probe shows the influence of the groundwater table rise, which is reproduced by the model.

The seasonally fluctuating water table in Zindarou is simulated using a modified version of the unsaturated zone hydrology model within LSX. The one-dimensional Richards equation governs vertical water redistribution:

$$\frac{\partial\theta(z,t)}{\partial t} = \frac{\partial}{\partial z}\left[D(\theta)\frac{\partial\theta(\theta,z)}{\partial z} + K_u(\theta) \right] \tag{5.1}$$

Campbell's model (Campbell, 1985) is used for soil water retention:

$$K(\theta) = K_s\left(\frac{\theta}{\theta_s}\right)^{2b+3} \tag{5.2}$$

and

$$\psi = \psi_e\left(\frac{\theta}{\theta_s}\right)^{-b} \tag{5.3}$$

so

$$\frac{\partial \psi}{\partial \theta} = -\psi_e b \left(\frac{\theta}{\theta_s} \right)^{-b-1} \frac{1}{\theta_s} \tag{5.4}$$

and

$$D(\psi) = -K_s \psi_e b \left(\frac{1}{\theta_s} \right) \cdot \left(\frac{\theta}{\theta_s} \right)^{b+2} \tag{5.5}$$

where $K(\theta)$ is the unsaturated hydraulic conductivity, K_s is the saturated hydraulic conductivity, θ is the volumetric water content, θ_s is the porosity, ψ is the matric potential, ψ_e is the air entry potential, b is Campbell's fitting exponent, and $D(\psi)$ is the diffusivity.

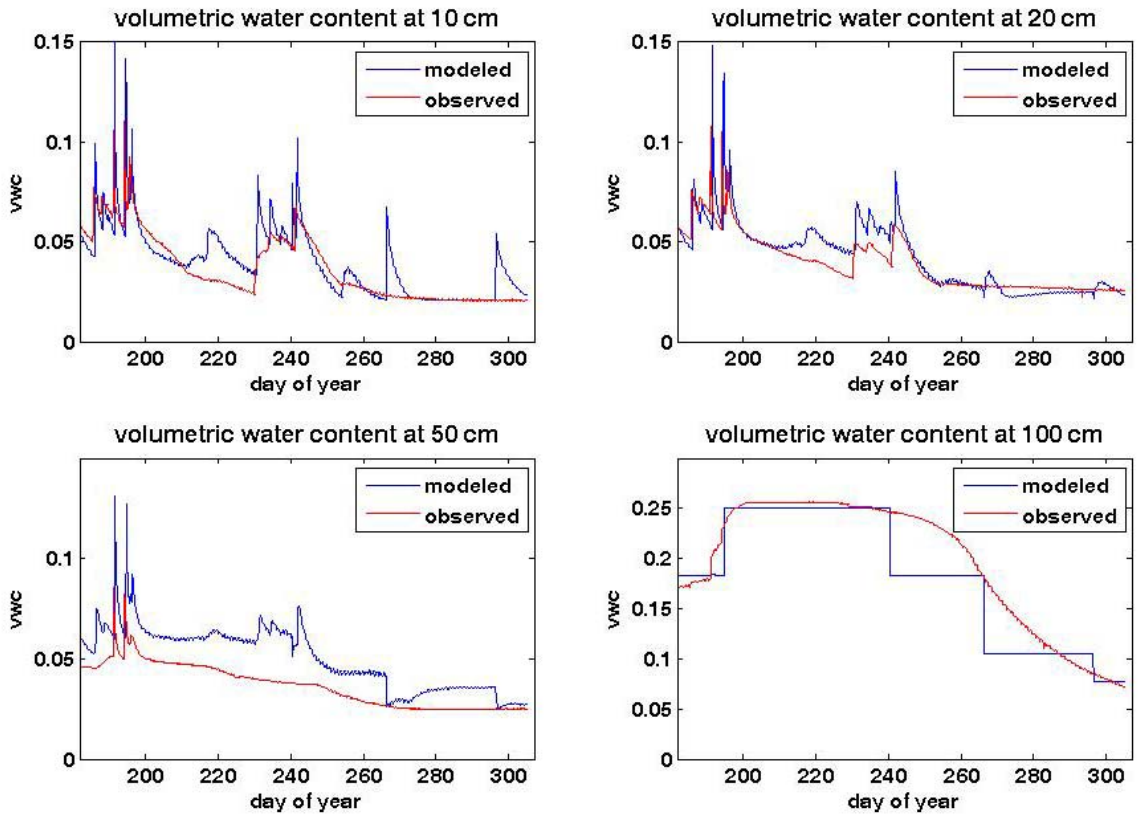

Figure 5.5. Soil moisture simulated and observed values at the Zindarou South TDR recording site, for the 2005 rain season. The influence of the groundwater table rise is evident in the 100cm probe, as the volumetric water content reaches saturation for about six weeks. The modeled soil moisture reproduces the trend, but has a step shape because of the vertical soil discretization.

In HYDREMATS, the unsaturated zone model of LSX has been expanded to include representation of a groundwater table, following the formulation of Yeh and Eltahir (2003) for simulations in shallow groundwater aquifers in Illinois. For solution of equation 5.1 in the unsaturated zone, the gravity drainage (Neumann type) boundary condition at the lower soil layer of LSX has been replaced by a Dirichlet-type boundary condition representing saturated conditions of the groundwater table. At the boundary of the saturated and unsaturated zones, the difference of gravity and diffusion terms in equation 5.1 determines net recharge into (or out of) the aquifer for each time step. For each time step, the aggregate net recharge integrated over the model domain determines water level change and hence updated groundwater level for the subsequent time step. In this manner, water table fluctuations are simulated. Air entry potential ψ_e and Campbell's *b* exponent were used as calibration parameters for groundwater level. Groundwater behavior was matched to the curve of combined observations represented in Figure 5.3.

The formulation of Yeh and Eltahir (2003) was modified to allow the groundwater table to penetrate the surface and allow pooling. This involved coupling with the overland flow routine added to LSX (see chapter 2) to combine surface water bodies formed by groudwater table rise with pooled water from overland flow. The diffusion wave formulation of overland flow routing represents backwater effects, allowing large pooled areas to form when overland flow meets surface-penetrating groundwater.

Necessary model input data included topography, vegetation and soil types. These were assigned by supervised classification of a Landsat 7 multispectral image (Boyer, 2003). Field investigations of soil type (90% sand) and detailed verification of vegetation informed the model as well. Topography was surveyed in April 2008 using a highly accurate differential GPS system, at very fine spatial resolution that allowed us to generate a 10-meter digital elevation model.

5.4 Results

5.4.1 Hydrology

Figure 5.6 compares results of the groundwater simulation to the observed water levels. Discrete measurements of water levels at groundwater wells, observations of saturation and subsequent dry down at buried TDR probes, and observations of extents of groundwater-fed pools were compiled into a combined representation of groundwater level. Observations were frequent and numerous during the 2005 wet season, but little data was available for defining domain-wide groundwater behavior during the ensuing dry season. Only the concrete-lined well number 8 (see Figure 2.3) provided periodic measurements of groundwater table locations. Buried TDR probes registered the dry-down, and slow dessication of the large swampy areas around Zindarou in November and December provided clues about the extent of groundwater table recession during the dry season. However, compared to the wet season when many areas showing surface penetration of groundwater existed and were measured, observations of groundwater behavior in the dry season are sparse. The simulated groundwater table fluctuations are superimposed on the observed groundwater level, showing good agreement in the 2005 rain season and less good agreement during the dry season. However, due to the deficiency of reliable measurements throughout the region as well as the inconsequence of groundwater levels when there are no areas of surface penetration, divergence of simulated groundwater level from observations is considered acceptable during the dry season. Peak groundwater levels match interpolated observations well, and due to relatively shallow topography, pooled water surface area is sensitive to maximum rise of the groundwater table. Therefore, the accurate model reproductions of Zindarou groundwater levels shown in Figure 5.6 signal good model representation of surface water availability for mosquito breeding.

Figure 5.7 shows surface water area in the model domain over the simulation period. Total water surface area summed from various sources (groundwater-saturated zones, shallow garden wells, and overland flow) is represented in this plot. Water surface area from overland flow (often submerging much of the model domain for one time step as

water is being routed to the topographic low points) disappears rapidly compared to groundwater-supplied marshes, which provide the longer-duration surface area.

5.4.2 Mosquito abundance and malaria transmission

As discussed in chapters 3 and 4, it is difficult to relate light trap mosquito captures to absolute mosquito abundance. Because light traps effectively represent relative abundances, however, the interannual difference in simulated mosquitoes can be compared to the interannual difference in observed (captured) mosquitoes, assuming that the light trap samples a constant proportion of the active mosquitoes in the village. Figure 5.8 shows 2005 and 2006 simulated cumulative and observed mosquito abundance in Zindarou compared to simulated cumulative and observed mosquito abundance in Banizoumbou for the same two years.

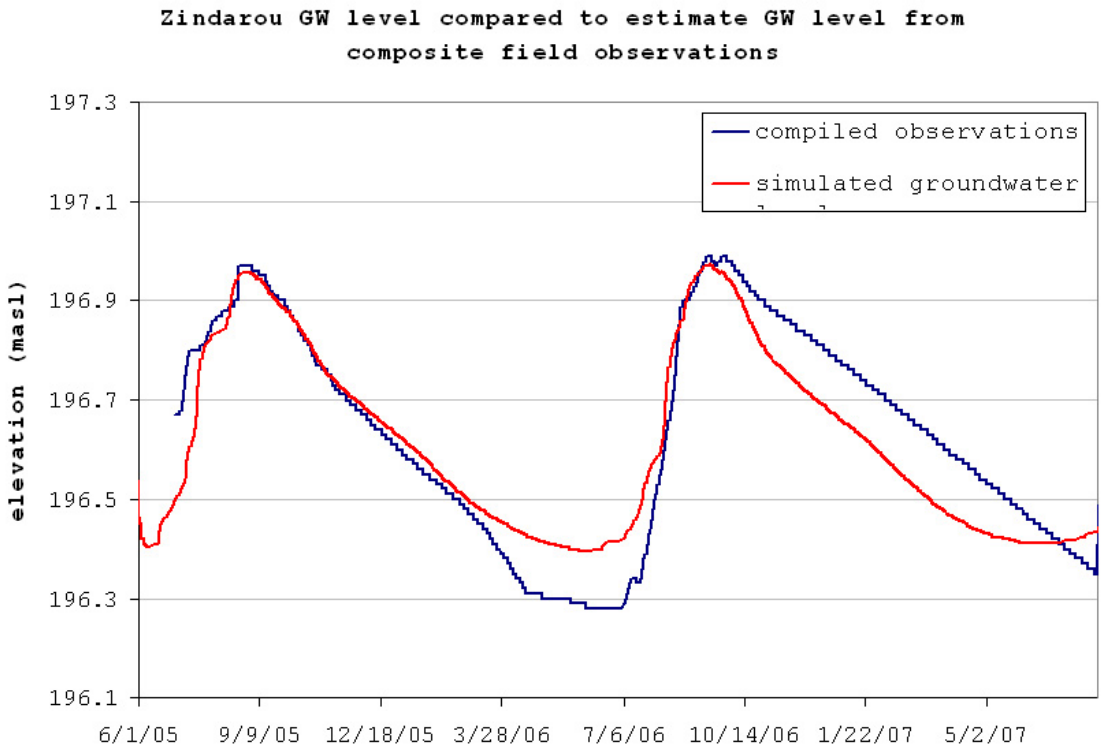

Figure 5.6. Comparison of observed and simulated groundwater levels in Zindarou. Near the wet season groundwater peaks, the observed groundwater level contains many measurements, whereas during the dry season measurements are sparse.

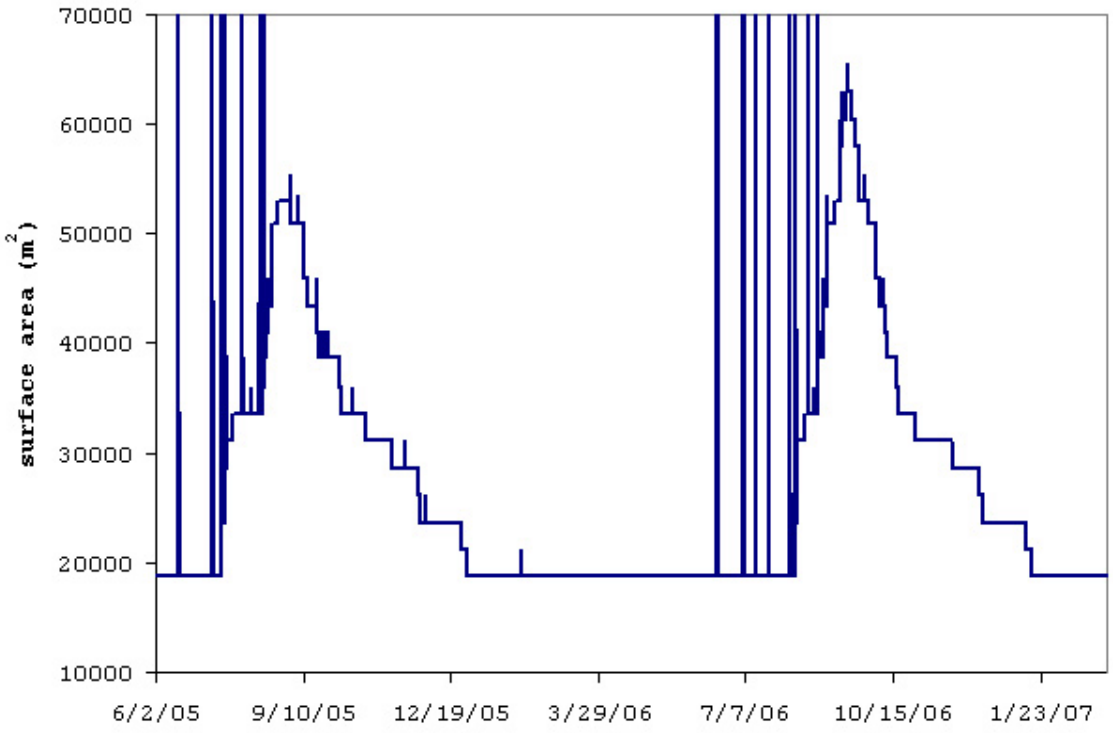

Figure 5.7. Simulated surface area of water (m^2) over the entire Zindarou model domain. There are many areas with year-round surface water, including wells, ditches and swamps.

The correct timing of mosquito abundance peaks depends on sufficient availability of nutrients for which larvae are competing. The match of observed and simulated relative abundances depicted in Figure 5.8 depends on the timing of changes in carrying capacity, indicating that strong reductions in nutrient availability may be responsible for the observed population decrease in the late wet seasons.

Vectorial capacity is a measure of malaria transmissibility that depends on mosquito abundance, temperature-dependent mosquito longevity, and temperature-dependent extrinsic incubation period. Equation 5.6 shows the formulation of vectorial capacity.

$$C = \frac{ma^2 p^n}{-\ln(p)} \qquad (5.6)$$

where m = abundance term (mosquitoes per human)

a = number of bloodmeals per vector per day

p = daily survival of vectors (0 – 1)

n = extrinsic incubation period of parasite

Vectorial capacity can be interpreted as the number of secondary infections resulting from one primary infection, and represents the degree to which malaria vector mosquitoes spread disease. With this interpretation, it follows that values of vectorial capacity above 1 represent stable malaria transmission, and vectorial capacity below 1 would result in insufficient transmission. Due to many infections acting as "dead-ends", the disease would soon die out in the population, provided the vectorial capacity stays below 1.

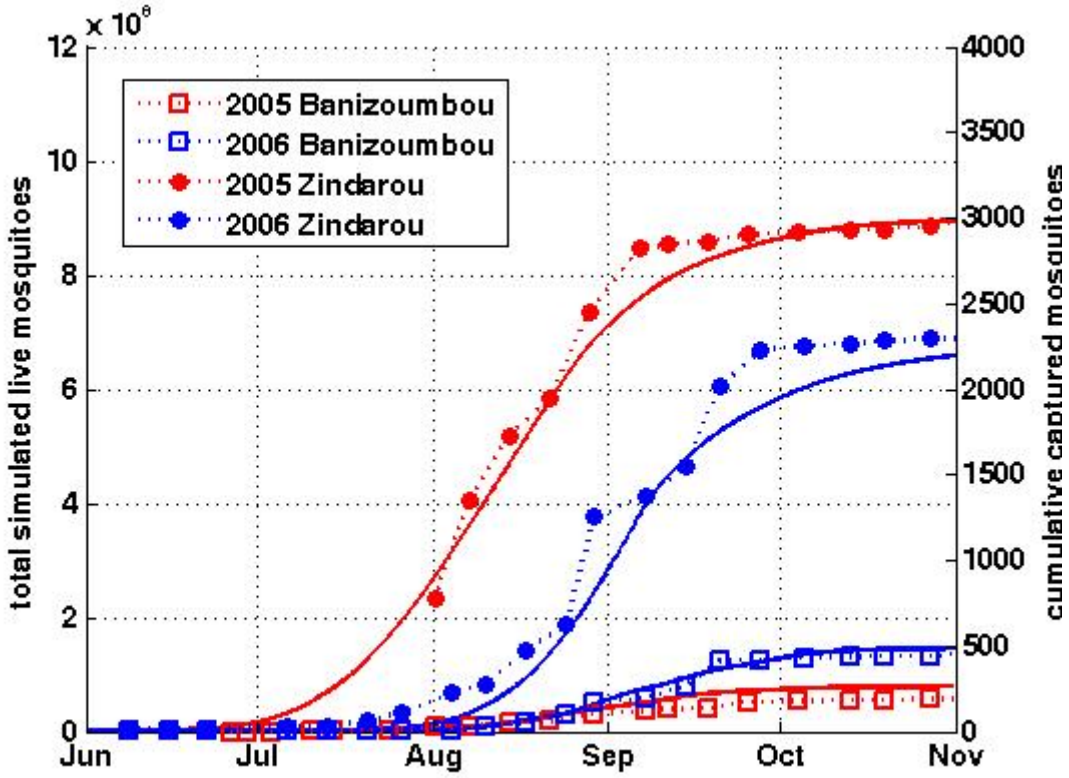

Figure 5.8. Cumulative simulated and observed mosquitoes in Banizoumbou and Zindarou. Close fits of simulation results to observations show that the model reproduces the inter-village differences in mosquito abundance as well as the interannual variability in abundance between the villages.

The calculated vectorial capacities for the Zindarou and Banizoumbou environments are presented in Figure 5.9. As seen in the figure, Zindarou has year-round stable malaria transmission, with seasonal variability. In contrast, vectorial capacity in Banizoumbou drops below 1 during the dry seasons, indicating a seasonal interruption in malaria transmission. In Banizoumbou, stable transmission occurs between July 10 and September 13, 2005 and again between July 22 and October 19, 2006. In the dry seasons, parasites in the human hosts provide a reservoir for re-infection once vectorial capacity exceeds 1 the following wet season. The major differences in cumulative mosquitoes dominating the variability in vectorial capacities arise from the large, persistent pools of Zindarou.

5.5 Discussion

The main focus of this study has been the role of hydrologic spatial variability in determining variability in malaria transmission. Banizoumbou and Zindarou Villages are only 30 km apart, but are hydrologically very different. Although Zindarou's location in the abandoned Dallol Bosso river valley makes the hydrology anomalous for the Sahel,

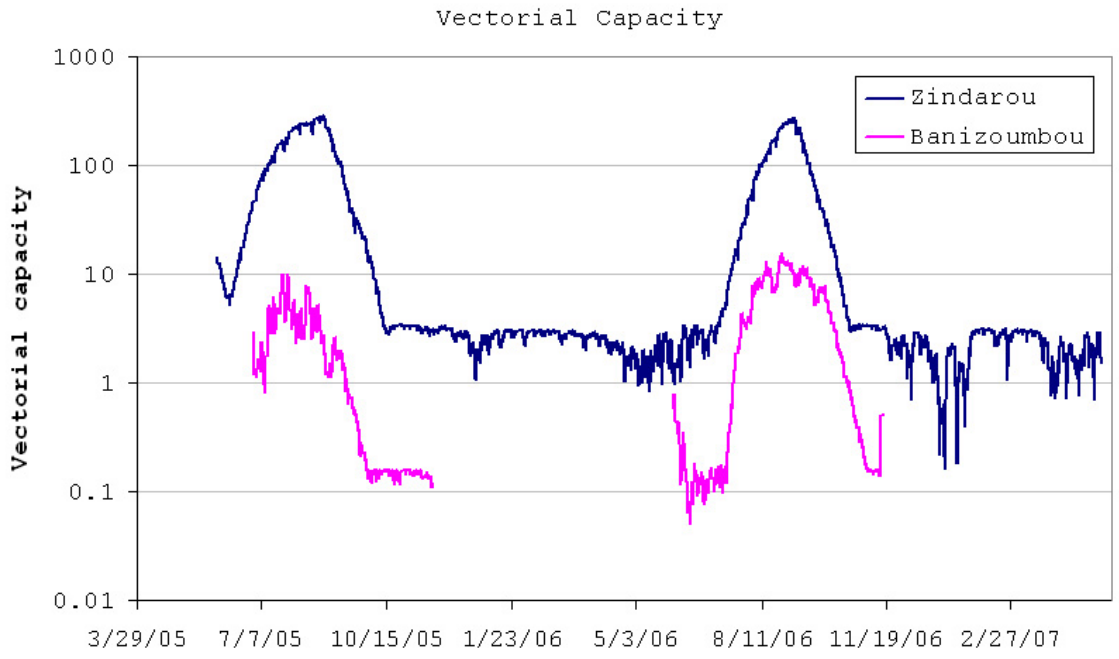

Figure 5.9. Simulated vectorial capacity in Banizoumbou and Zindarou. The vectorial capacity in Banizoumbou is zero for a portion of the dry season.

the pronounced difference in hydrologic conditions between the two villages is conducive to modeling studies aimed at exploring observed spatial variability in anopheline abundance. Besides the contrast in surface water availability for breeding mosquitoes, the differences between the villages are minimal. It is therefore expected (and observed) that potential confounding variables such as climate or vector behavior do not vary significantly between the two villages. In this way, surface water availability and pool persistence that is more typical of wet environments such as the equatorial forests of West Africa can be observed in close proximity to the typical Niger Sahel environment, represented by Banizoumbou. HYDREMATS has reproduced both the interannual variability in mosquito abundance observed in the two villages and the differences in abundance observed between Banizoumbou and Zindarou. The only difference in the simulations was the climatic forcings, topography, land cover type, and subsurface hydrologic environment. The analysis emphasizes the role of hydrologic variability as a determinant of malaria transmission in the region. The order of magnitude difference in vectorial capacity between the two villages and levels of dry season transmission occur despite the same average precipitation covering both sites. Spatial malaria transmission models regularly apply average precipitation values to large areas to predict mosquito response to rainfall (e.g. Craig et al., 1999). Clearly, such models lacking hydrologic detail may contain limitations at the scale of individual villages due to the coarse spatial (and temporal) scales, as demonstrated in this study.

Malaria early warning systems also often operate at low spatial and temporal resolution. These systems use the detection of anomalous conditions in sea surface temperature, seasonal climate forecasts as well as regional vulnerability assessments to predict epidemic conditions in areas susceptible to malaria epidemics, with varying degrees of success. Within the framework of these early warning systems, the consideration of small-scale hydrologic conditions governed by topography, soils, and groundwater behavior may prevent false warnings and may provide better predictive ability for true malaria epidemics.

Different modes of limitation on mosquito abundance were noted in the Zindarou simulation. Large-scale pools resulting from surface expression of groundwater persist well into the dry season, and do not ultimately disappear until November. Identification of adults reared from sampled larvae confirmed that *An. gambiae* breeds in these pools. However, the observed rapid decline in Zindarou anopheline populations long before the pools disappear indicates that other significant processes regulate subadult mosquito development and emergence as adult mosquitoes. As discussed, both nutrient availability and predation may limit mosquito development. With a combination of reduced nutrient input (through a reduction in ecological carrying capacity) and an increase in predation, the model reproduced the reduced emergence of adults following the end of rains in mid-September. The results highlight the importance of understanding local ecological limiters of mosquito development, such as the input of nutrients that sustain anopheline populations. Observations in Ethiopia of *Anopheles arabiensis* larval development showed that maize pollen availability strongly controls subadult development and adult mosquito emergence where pools and maize plants were close together (Ye-Ebiyo et al., 2000). These observations of maize pollen effects on larval development may translate to the rich pollen produced by local pearl millet cultivation in the Niger Sahel and be responsible for the drastic observed declines in mosquito populations.

Relative humidity declines may also be an important control of mosquito populations. HYDREMATS presently does not incorporate relative humidity into calculations of mosquito mortality. However, low humidity may severely stress mosquitoes and may intensify the seasonal decline in mosquito numbers (Ijumba et al., 1990). Figure 5.10 shows the adult *Anopheles gambiae* mosquito captures in Zindarou combined with a plot of the relative humidity measured at the Zindarou meteorological station. Seasonal declines in mosquito activity do not exactly coincide with the annual humidity drop signaling the retreat of the monsoon, yet may still affect daily survival probability of the late season mosquitoes adding to their population decline. In addition, the potential impact on daily survival probability could influence vectorial capacity in the Zindarou dry season. The relationship of relative humidity to daily survival has not been quantified, and therefore was not included in HYDREMATS.

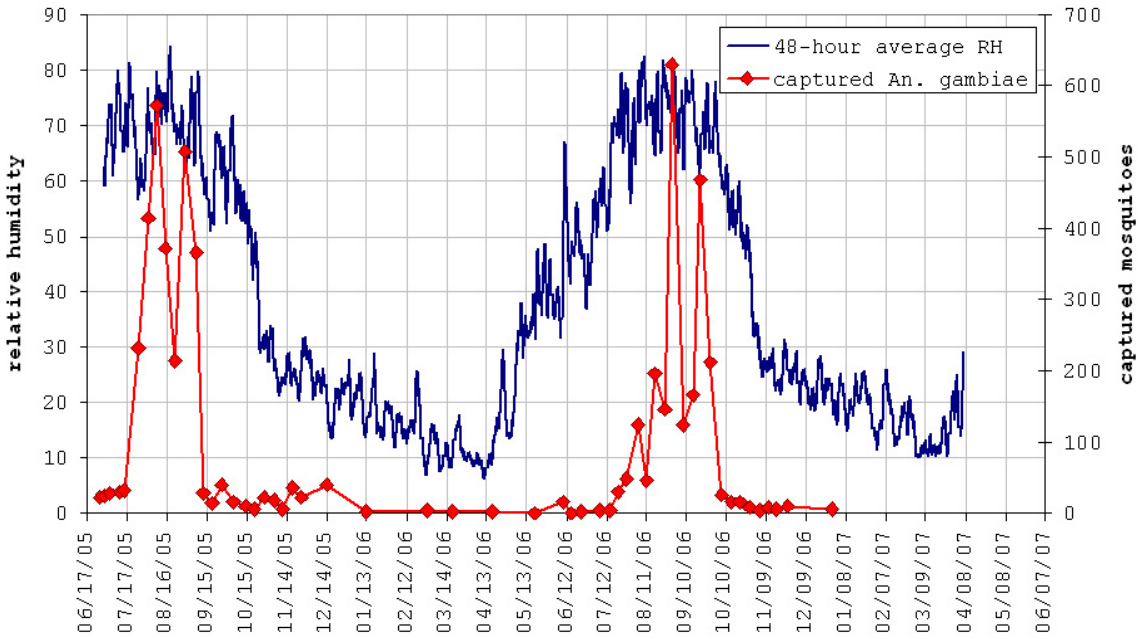

Figure 5.10. Captured *Anopheles gambiae* mosquitoes in Zindarou, and 48-hour average relative humidity (%).

5.6 Conclusion

Spatial hydrologic variability controls local, village-scale mosquito abundance and vectorial capacity in areas of seasonal malaria transmission such as the Niger Sahel. The example of Banizoumbou and Zindarou in this study showed that a distance of only 30 km between the two study foci can have dramatically different anopheline abundance and vectorial capacities, and that these differences were solely explained by hydrologic variability. This result has major implications for efforts to predict malaria risk using climate models. The mismatch of climate model grid cell size (typically ~100 km) and the characteristic scale of hydrologic variability that influences village-scale malaria transmission in areas such as the Sahel suggests that malaria risk predicted by climate models (as components of early warning systems) may contain significant errors. Accurate and reliable assignment of village-scale malaria risk from such models may be impossible because of this scale discrepancy. Moreover, the result suggests that high resolution distributed representation of hydrology may dramatically improve the predicted outcome of malaria transmission response to variable climate forcings. Topography, vegetation, soil type differences as well as shallow groundwater behavior

must all be incorporated at appropriate scales in order to accurately evaluate malaria transmission at the village scale using coarse resolution climate models.

While pool persistence limits mosquito abundance in Banizoumbou, in wetter environments such as represented by Zindarou, different modes of limitation regulate abundance particularly in the late wet season. Nutrient availability and predation may be significant controls in the late transmission season, as is evidenced by drastic decline in late season observed mosquito populations despite the persistence of groundwater-fed pools beyond the end of the rains. The difference in pool persistence resulting from spatial hydrologic variability will influence local modes of mosquito population limitations. High-resolution model representation of spatial hydrologic variability and resulting differences in pool persistence should therefore yield accurate predictions of mosquito population control mechanisms as a function of climate forcing. The result should further emphasize the need to replace correlative linkages of climate forcing with mechanistic ones. Consideration of such nonlinearities in the mosquito population response to climate variability should improve predictive ability and prevent false warnings stemming from coarse resolutions of climate models.

Chapter 6: Assessment of climate shift impacts on malaria transmission in the Sahel

6.1 Introduction

Malaria transmission is partially controlled by environmental conditions, and environmental variability may largely explain spatial and temporal variability in malaria transmission intensity. This is partly because the *Anopheles* mosquitoes responsible for malaria transmission depend on surface water availability for breeding habitat. Favorable precipitation patterns and land surface hydrology allow these breeding habitats to form and persist. Strong temperature dependencies of parasite and vector development rates and vector mortality also influence malaria endemicity (Depinay, 2004; Martens, 1997). Therefore, significant social and economic influences on malaria notwithstanding, climate variability presents a dominant control of malaria transmission variability. An understanding of the nature of malaria transmissibility response to climate shifts can enhance the prediction of epidemics and the effects of longer-term climate change. In this chapter, we explore the linkage of malaria transmission with climate shifts in the West African Sahel, using a validated, mechanistic mathematical model, HYDREMATS (HYDRology Entomology and MAlaria Transmission Simulator).

In some regions, such as desert fringe environments, the availability of suitable breeding pools limits mosquito abundance. Temperature also influences malaria transmission through temperature-dependent larval, egg, and parasite development rates, as well as mosquito longevity (Depinay, 2004). Increased temperature results in faster development of eggs within the mosquito, parasite within the mosquito (extrinsic incubation), and larval stages. However, subadult (larval-stage) mosquitoes suffer thermal death beyond a threshold temperature of 40º C (Jepson et al., 1947). In addition, adult mosquito longevity is reduced with increasing temperatures (Martens, 1997). Consequently, in regions where the average temperature is either sufficiently low or sufficiently high, parasite development time within the mosquito (extrinsic incubation period) exceeds the average lifespan of the mosquito, clearly preventing endemic malaria in these areas (Craig et al.,

1999). This temperature limitation defines boundaries of endemic zones, which are further restricted by hydrologic suitability for breeding habitat formation and microclimates (Thomson et al., 2004). Areas outside of these malaria conducive regions are free of sustained, endemic malaria transmission. However, these areas may experience periodic epidemics as climatic conditions temporarily shift to favor malaria transmission (Kiszewski et al., 2004). Such a shift in climate conditions may include temperature fluctuations affecting development rates, or rainfall pattern changes resulting in altered mosquito breeding habitat availability.

In the Sahel of West Africa, a strong north-south rainfall gradient separates the Sahara desert from the wet equatorial forests near the coast of the Atlantic. The Sahel is roughly bracketed by the 100mm isohyet to the north, and the 600mm isohyet to the south over only a few hundred kilometers (See Figure 6.1). Within this zone, the rainfall gradient is approximately 1 mm km^{-1} (Lebel et al., 1992). Northward migration of the Intertropical Convergence Zone (ITCZ) during the West African monsoon (May – October) is responsible for virtually all of the rainfall in this region, but the annual maximum northward extent of the thunderstorm belt associated with this seasonal pattern displays high interannual variability, largely driven by fluctuations in sea surface temperature in the Atlantic Ocean (Lamb, 1978; Giannini et al., 2003). The impact of this interannual climate variability on human populations is perhaps most evident by its effect on agricultural activity in the Sahel. Individual years of below-average rainfall have resulted in devastating famines, most recently in 2005 in Niger, which was a direct result of very low precipitation in the 2004 monsoon.

Climate and ecological conditions in the Sahara desert and the Sahel occasionally undergo dramatic shifts from dry to wet regimes and vice versa (Wang and Eltahir, 2000; Claussen, 1998). Three notable examples of such “regime changes” in Sahel climate have drastically altered climate patterns and affected vegetation and rainfall. The first occurred about 6000 years ago during the middle Holocene. This shift caused an abrupt 500 km northward movement of rainfall contours as well as associated vegetation (Irizarry-Ortiz

et al., 2003; Hoelzmann et al., 1998). Following this shift, about 5500 years ago a sudden transition from wet to dry conditions occurred in the Sahel, and the last involved the onset of a persistent, multi-decadal drought beginning in the late 1960s (Foley et al., 2003). All three of these climate shifts have translated isohyets along the precipitation gradient, and have demonstrated remarkable persistence. The magnitudes of the changes that caused past climate shifts were probably very similar to those observed occasionally in modern times (Nicholson, 2000). Therefore, such climate shifts constitute the climatological basis for our analysis. For a specific site in the Sahel and for a specific period, a good representation of potential climate conditions arising from shifts to dry (respectively wet) conditions may be the concurrent conditions found north (respectively south) of the site for the same period. For a specific period, two locations along the north-south rainfall gradient would exhibit climate differences comparable to those of two different climate regimes at a stationary site. Therefore, we assume that effects of drastic climate shifts on malaria transmission can be studied by comparing model results forced by climate data sets from various locations along the Sahelian climatological gradient.

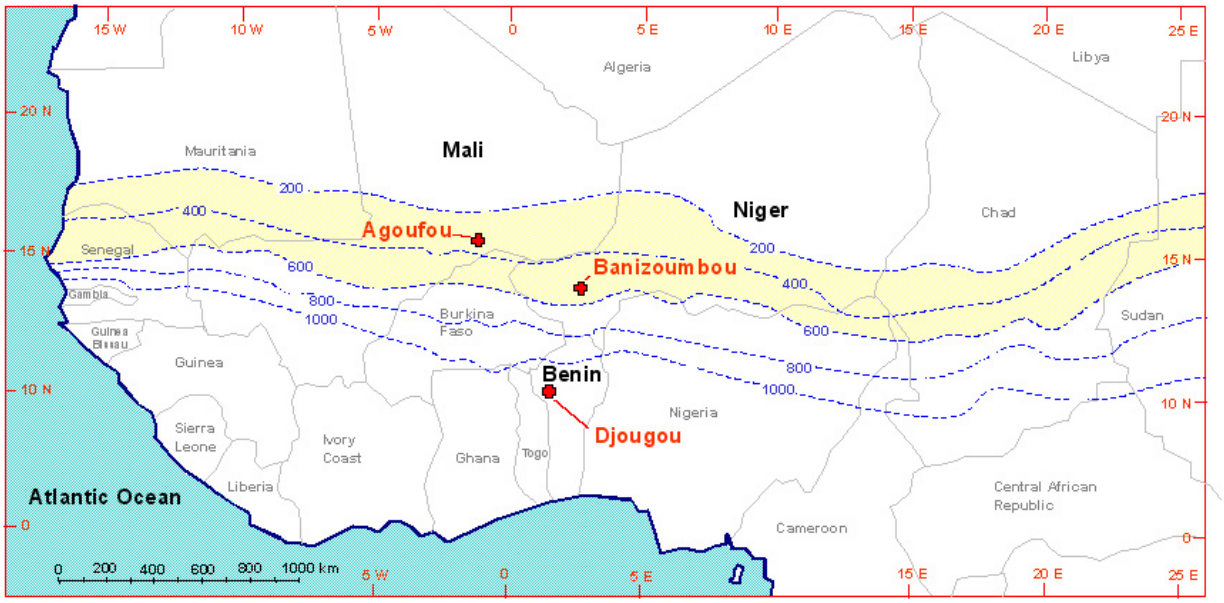

Figure 6.1. Locations of Banizoumbou, Niger; Agoufou, Mali; and Djougou, Benin. The figure also shows the rainfall gradient of the sahel. Isohyets are labeled with annual average millimeters of rain.

6.2 Modeling methods

In this chapter, we explore the effects of interannual climate variability on Sahel malaria transmission using a distributed hydrology model coupled to an agent-based entomology and malaria transmission model, (HYDREMATS). This model was designed to represent the formation and persistence of the typical rainfed pools which allow the breeding of *Anopheles* mosquitoes, and individually represent mosquitoes as they interact with their natural and human environments. Characteristics relevant to malaria transmission are tracked for each mosquito and human. Model inputs are precipitation, temperature, humidity, radiation, and wind speed and wind direction time series. Corresponding output is water depths for each hourly time step of the simulation for each rectangular model grid cell, and mosquito abundance.

HYDREMATS forms a mechanistic modeling link between climatic forcing and the resulting entomological response (for which hydrology is a necessary intermediate) and gets around limitations of correlative approaches linking environmental conditions to malaria. The model facilitates highly detailed studies of population response to various perturbations. The hydrology component of the model incorporates distributed soil and vegetation types to simulate rainfall-runoff transformation, infiltration, and over land flow towards topographically low points. With this spatially explicit structure, applied at high spatial- and temporal-resolution, HYDREMATS can predict entomological response to rainfall of variable intensity, frequency and duration and accounts for antecedent moisture conditions. This is a powerful capability for understanding malaria response to rainfall in environments of water-limited mosquito population dynamics, such as the Sahel.

As discussed in Chapter 4, HYDREMATS has been field validated using two years of intensive hydrological and entomological field observations in southwestern Niger. In this study, we apply HYDREMATS to the location of these field observations (Banizoumbou, Niger), and assume that the model calibration is valid for all of the scenarios presented.

6.2.1 Representation of climate variability in the Sahel

We assume that climate shifts in the Sahel can be represented as a seasonal north-south translation of the seasonal isohyets and isotherms. For a certain location in the Sahel, climatic conditions in dry periods resemble typical climatic conditions for locations further north. Conversely, for the same location the climatic conditions in wet periods would resemble the typical climate conditions of locations further south. Meteorological station data records were taken from the African Monsoon Multidisciplinary Analyses (AMMA) project database, for two sites: Djougou, Benin, and Agoufou, Mali to represent wet and dry shifts, respectively. These were used to compare with model results from simulations using in-situ meteorological data recorded at a station directly in Banizoumbou.

The Banizoumbou weather station (13.53°N, 2.66° E) was installed by ORSTOM (present-day IRD, Institute de Rechereche pour le Développement) of France, and has been collecting data for several years during the AMMA project, beginning in 2004. Long-term precipitation climatology, however, is better considered at nearby Niamey because of a much longer record. Over the period 1905-1989, the average annual rainfall in Niamey is 562 mm (Le Barbé and Lebel, 1997). Rainfall occurs only during the May-September monsoon, which peaks in August. Extended drought during the period 1968-1990 decreased the average annual precipitation to 495 mm (Le Barbé and Lebel, 1997). Average annual rainfall in recent years in Banizoumbou is slightly less at 450 mm. For simulation purposes we use Banizoumbou meteorological data.

Djougou, Benin (9.705° N, 1.667° E) is a large market town in north-west Benin, at 430 meters elevation. Average rainfall in Djougou is 1258 mm over the 25-year period 1978-2003 (Weller, 2003). Rainfall records in Djougou and Banizoumbou display a significant difference, as a result of the steep rainfall gradient in the Sahel. Djougou is located 420 km south of Banizoumbou in the north-south direction, along the precipitation gradient. In contrast, Agoufou, Mali is located at 15.34° N, 1.48° W, and is 197 km north of Banizoumbou in the north-south direction along the precipitation gradient. Agoufou is still within the Sahel bioclimatic zone, however the long-term average annual rainfall is

only 370 mm (Baup et al., 2007). Agoufou is at an elevation of about 310 meters above sea level (Baup et al., 2007). Table 6.1 summarizes variations in the climate data for the three sites.

Table 6.1. Summary of 2005 and 2006 climatic differences at Banizoumbou, Niger; Agoufou, Mali; and Djougou, Benin.

	Banizoumbou Niger	Agoufou Mali	Djougou Benin
Altitude (masl)	250	290	454
Latitude	13.54º N	15.30º N	9.69º N
Longitude	2.67º E	1.48º W	1.66º E
2005 precip (mm)	405	153.7*	1325
2006 precip (mm)	478	345.3	951
2005 monsoon Temp (ºC)	28.6	29.0	25.1
2006 monsoon Temp (ºC)	29.1	30.83	26.0
2005 rel humidity	44% (!?)	46.60%	71.90%
2006 rel humidity	61.40%	49.90%	71.60%
2006 avg days between events	2.6	2.5	1.45
2006 number of events	48	54	126
2006 average event rainfall	10.0	7.0	7.5

* some data missing

D'Amato and Lebel (1998) found that inter-annual rainfall variability in the Niger Sahel depends primarily on the number of precipitation events per rain season. A weak correlation of individual event magnitude with annual rainfall was found to be not statistically significant, suggesting the primary mode of inter-annual rainfall variability is event frequency instead of magnitude (D'Amato and Lebel, 1998). Because hydrologic response to rainfall events depends strongly on antecedent moisture conditions, rainfall frequency may play a major role in pool persistence. If soil and pools have sufficient time to dry out between rain events, impacts of the subsequent rainfall on ponding will be diminished because of higher infiltration and lower runoff. In order to assess the contribution of rainfall frequency to variability in mosquito abundance, we isolate the effects of rainfall frequency by scaling 2006 Agoufou and Djougou precipitation series to Banizoumbou 2006 seasonal total rainfall (478 mm). This new, synthetic precipitation series is then applied to the Banizoumbou environment. Temperature, humidity, and

seasonal total rainfall distribution remain unchanged in this scenario. The number of rainfall events registered at the three measurement sites in 2006, the average interstorm period, and the average event rainfall are summarized in Table 6.1.

Temperature and relative humidity vary among these three sites as well. During the 2006 wet season, the Banizoumbou meteorological station registered an average temperature of 29.1º C and an average relative humidity of 61.4% for the five-month period May-September. In Djougou, average temperature and relative humidity for the same period were 26.0 º C and 71.6%, respectively, and in Agoufou, the same variables were 30.8º C and 49.9%, respectively. Agoufou, Mali has slightly warmer and drier conditions than Banizoumbou, and as expected Djougou, Benin is cooler and more humid. Temperature variability is also more pronounced in Agoufou. These variables are summarized in Table 6.1.

6.2.2 Hydrology

For a detailed description of HYDREMATS, see Chapters 3 and 4. The model represents land surface hydrology at high spatial and temporal resolution, to yield hourly predictions of pooled water formation and persistence at 10-meter grid scale. The model borrows heavily from the Land Surface Transfer model LSX (Pollard and Thompson, 1995). Following LSX, the model simulates two vegetation layers and six soil layers, but applies the water, energy and momentum calculations at a high resolution for the small model domain sizes. Cell-to-cell overland flow has been added. The model simulates runoff generation from each grid cell in the model domain, with distributed land surface characteristics (vegetation type, soil type, Manning's roughness) determining runoff. This runoff is then routed over the infiltrating land surface into the topographic low points using an implicit finite difference solution of the overland flow equations. Temperature, humidity and solar radiation influence the transpiration and soil evaporation rates, and thus influence soil moisture. Soil moisture in turn influences energy partitioning into latent and sensible heat, which affects soil temperatures, and finally soil temperatures influence soil evaporation as well as the temperature of runoff arriving in topographic low points. Water temperatures in ponded areas are thus simulated, and are used in the

entomology model to determine the subadult (aquatic-stages: egg, larva, pupa) mosquito growth rates within individual pools.

6.2.3 Aquatic stage entomology

Each model grid cell predicted to contain pooled water is capable of hosting subadult mosquitoes. The presence of subadults depends on a gravid female mosquito laying a clutch of eggs in the pool, as well as constant persistence of pooled water. A compartmental model simulates the temperature-dependent advancement of mosquito larvae from one stage to the next, with intraspecific competition simulated with an assigned carrying capacity regulating advancement rates. Pupae mature into emergent adult mosquitoes, which enter the model domain as independent individuals free to interact with their environment.

6.2.4 Vectorial capacity

Vectorial capacity is a measurement that represents the daily rate of infective bites received by a single human host. Vectorial capacity can be interpreted as a malaria transmissibility, because it relates characteristics of the mosquito vector population (such as abundance and daily survival probability) to potential disease spread, without information about actual parasite presence within the population. The expression for vectorial capacity is:

$$C = \frac{ma^2 p^n}{-\ln(p)} \tag{6.1}$$

where m = abundance term (mosquitoes per human)

a = number of bloodmeals per vector per day

p = daily survival of vectors (0 – 1)

n = extrinsic incubation period of parasite

Environmental conditions affect the abundance term which depends on breeding habitat persistence, the daily survivability term which depends on daily average temperatures, and the extrinsic incubation period (development time of parasite within the mosquito) for which Detinova (1962) noted a degree-day dependence on temperature.

6.2.5 Mosquito mortality

Mosquito mortality depends on daily average temperature, according to Martens (1997). High temperatures stress the mosquitoes, and thereby decrease the daily survival probability. A decrease in the daily survival probability results in a population-scale decrease in mosquito abundance. This temperature-dependent decrease in mosquito abundance opposes the effects of increased development rates of aquatic stage mosquitoes, which result in greater adult mosquito emergence. The Martens model is reproduced here:

$$p = \exp\left(\frac{-1}{-4.4 + 1.31T - 0.03T^2}\right) \tag{6.2}$$

where p = daily survival probability (0-1)

T = temperature (degrees C)

Equation 6.2 is shown graphically in Figure 6.2.

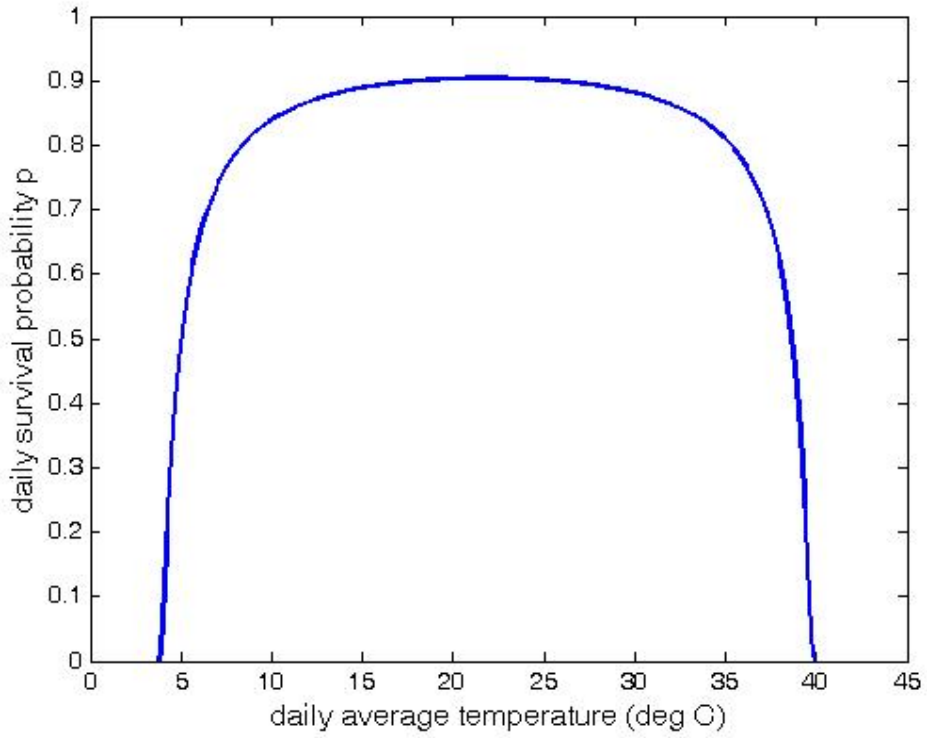

Figure 6.2. Graphical depiction of equation 6.2, which represents daily survivability as a function of daily average temperature.

6.2.6 Sporogonic cycle

The sporogonic cycle length (*n* in Equation 6.1) represents the time required for development of infectious sporozoites within the mosquito salivary gland. Once sporozoites are fully developed, the mosquito becomes infectious and transmission can occur. Detinova (1962) reported that 111 degree-days above 16º C are necessary for *Plasmodium falciparum* sporozoite development, resulting in the following representation:

$$n = \frac{111}{T - 16} \tag{6.3}$$

where *n* is the length of time in days for sporozoite development, and T is the ambient temperature in degrees C. Equation 6.3 is plotted as a function of temperature in Figure 6.3. The asymptotic rise at 16º C clearly indicates that malaria incubation at this temperature and below is impossible, and that near 16º C incubation period far exceeds typical mosquito lifespans of several weeks.

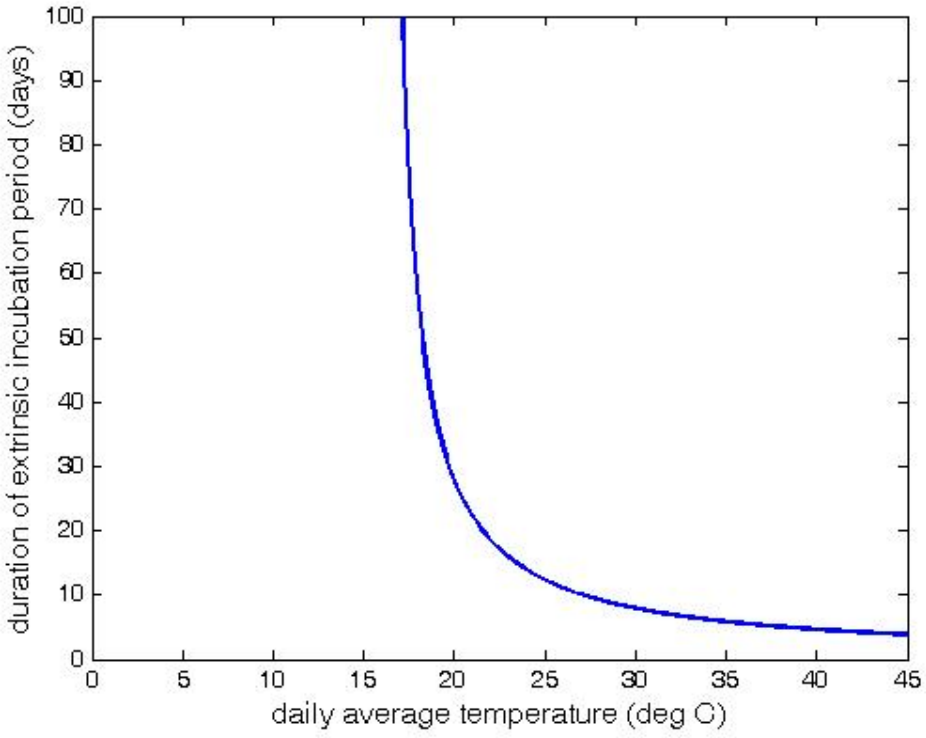

Figure 6.3. The relationship between average temperature and the duration of extrinsic incubation period, in days (equation 6.3).

Climatological limitations of malaria transmission have been previously modeled by Craig et al. (1999). Using equations 6.1-6.3, they define limits of areas in Africa suitable to *Plasmodium falciparum* malaria transmission based on the temperature-limited development of mosquitoes and malaria parasite within the mosquito midgut. To explore the effects of climate shifts in the Sahel on malaria transmission, we employ the same models (equations 6.1-6.3) describing temperature limitations on biological development. However, our mechanistic hydrology modeling approach allows the prediction of breeding pool response to changes in precipitation patterns that typically accompany climate shifts. More accurate prediction of mosquito abundance following climate shifts should be possible with this approach.

6.3 Results

Several simulations were performed to evaluate the effects of climate variability on mosquito population dynamics. First, meteorological data from Djougou, Benin, was applied to Banizoumbou to evaluate the effects of more humid, higher-precipitation conditions typical of several hundred kilometers south of Banizoumbou. Data measured during the 2006 monsoon was applied to the same model grid as the baseline simulation in Banizoumbou. Similarly, precipitation, temperature, humidity and solar radiation data recorded at the Agoufou, Mali meteorological station were applied to the Banizoumbou model domain to gauge the effects of hotter, drier conditions. Simulated mosquito abundance responses to the variable climate forcings are shown in Figure 6.4. The cumulative mosquito abundances for this scenario are presented in Figure 6.5. Clearly, mosquito abundance responds strongly to the combination of favorable precipitation and temperature conditions of Djougou, Benin. Cumulative abundance increases by 127% if meteorological conditions of Djougou are applied to Banizoumbou, and decreases 34% if the drier, hotter conditions of Agoufou are applied. Maximum abundance increases by 52% for the Djougou meteorological data, and decreases by 24.6% for the Agoufou station data. Finally, Figure 6.6 presents the simulated vectorial capacity for the climate shift scenarios. Maximum vectorial capacity in the wetter, cooler Djougou climate conditions increased by 25% relative to the 2006 Banizoumbou baseline. In contrast, maximum vectorial capacity decreased by 26.2% for the Agoufou, Mali scenario with

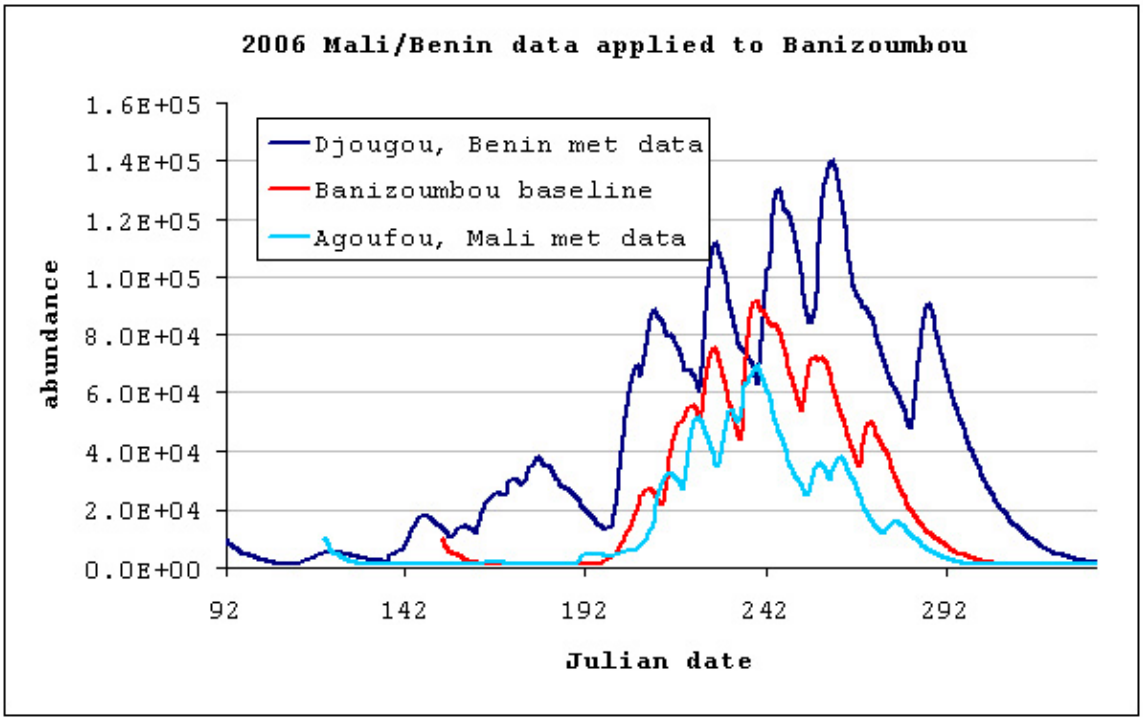

Figure 6.4. Simulated mosquito abundance for the meteorological station data from Djougou, Benin and Agoufou, Mali applied to the Banizoumbou model domain.

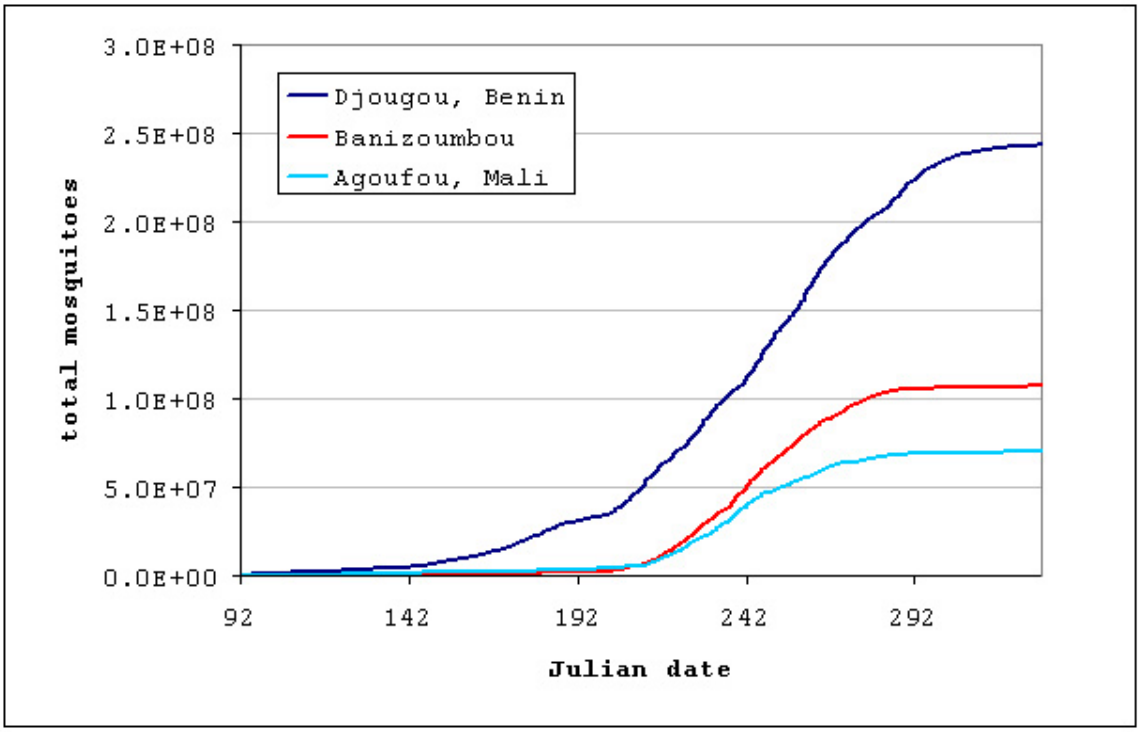

Figure 6.5. Cumulative simulated mosquitoes, for all meteorological station data from Agoufou, Mali and Djougou, Benin applied to Banizoumbou.

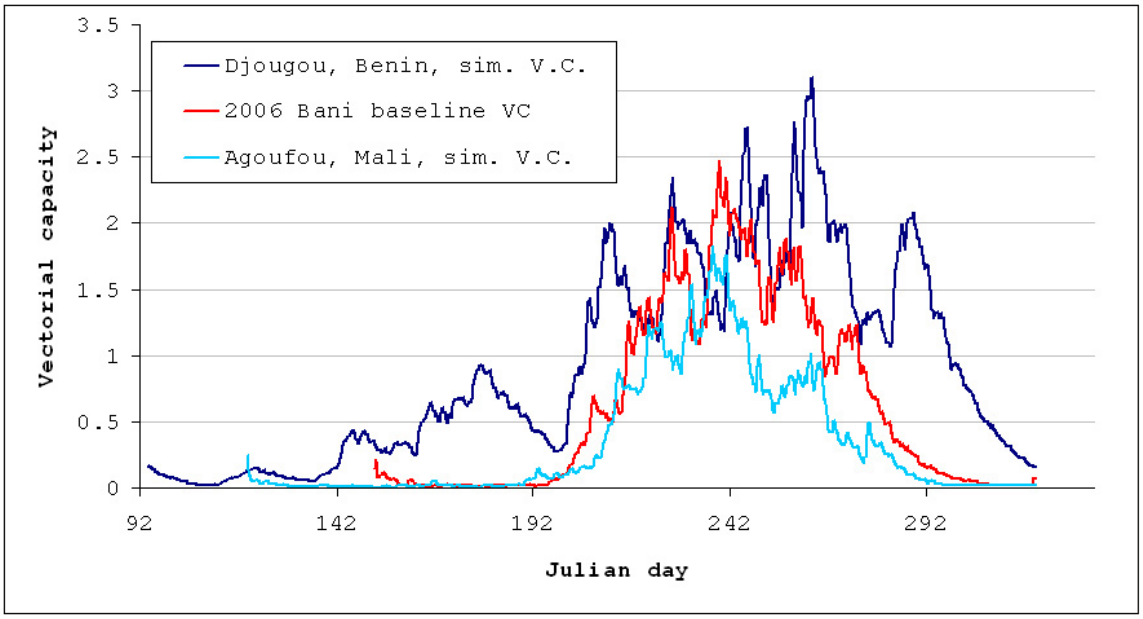

Figure 6.6. Simulated vectorial capacities for all meteorological station data from Agoufou, Mali and Djougou, Benin applied to Banizoumbou. We assume a = 0.2 bloodmeals per mosquito per day, constant in all simulations.

respect to the baseline scenario. For the Djougou, Benin scenario, the increase of vectorial capacity is lower than the increase of mosquito abundance because of the temperature dependence of sporogony. Days required for sporozoite generation (*n* term in Equation 6.1) increases dramatically at lower temperatures, reducing vectorial capacity. At the lower temperatures typical of Djougou, Benin, the temperature dependence of daily survivability is not very strong (Martens, 1997).

Next, the effects of individual climate variables were determined by isolating them in several test scenarios. First, only Djougou temperature was applied to the Banizoumbou environment, holding precipitation and other meteorological variables (wind speed, wind direction and solar radiation) constant. The same was then done for Agoufou temperature. The results of these simulations are presented in Figure 6.7, which shows simulated mosquito abundance. Maximum abundance increased by 9.3% when Djougou, Benin temperatures were applied to Banizoumbou, and decreased by 23.6% using temperature series from Agoufou, Mali. Simulated cumulative mosquitoes are shown in Figure 6.8. In this case, Djougou temperatures resulted in a 15.7% increase in cumulative mosquitoes, compared to a 22% decrease in cumulative mosquitoes using Agoufou temperatures.

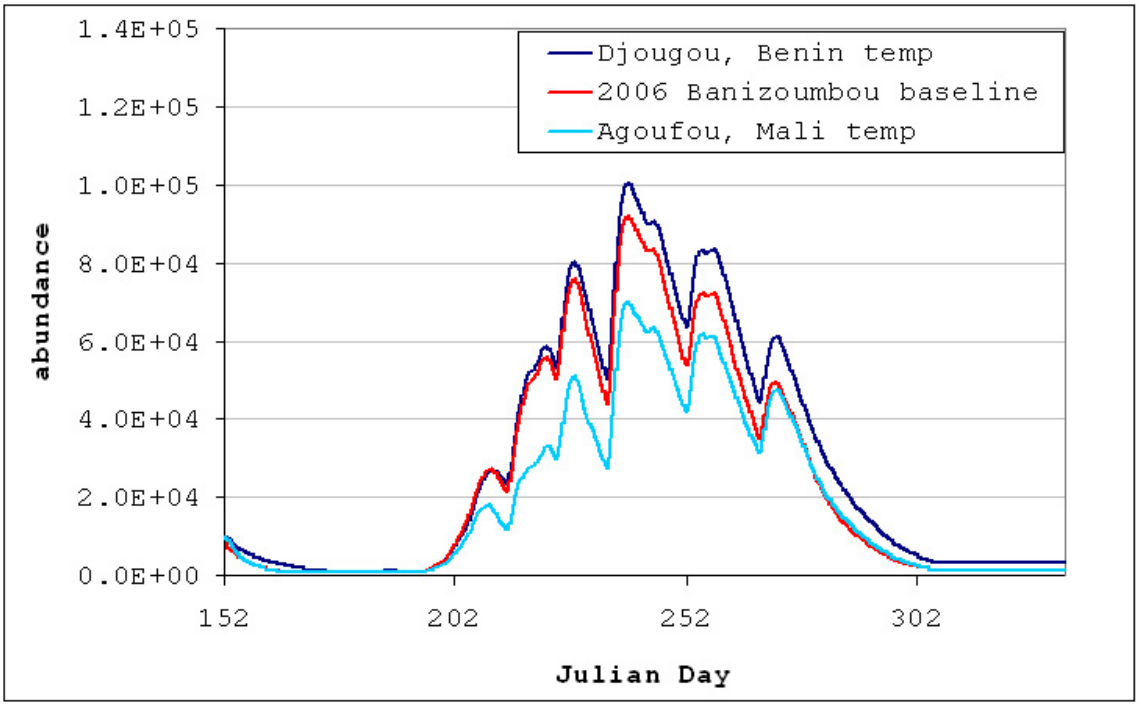

Figure 6.7. Simulated mosquito abundance, using only temperatures from Agoufou, Mali and Djougou, Benin applied to Banizoumbou's model domain.

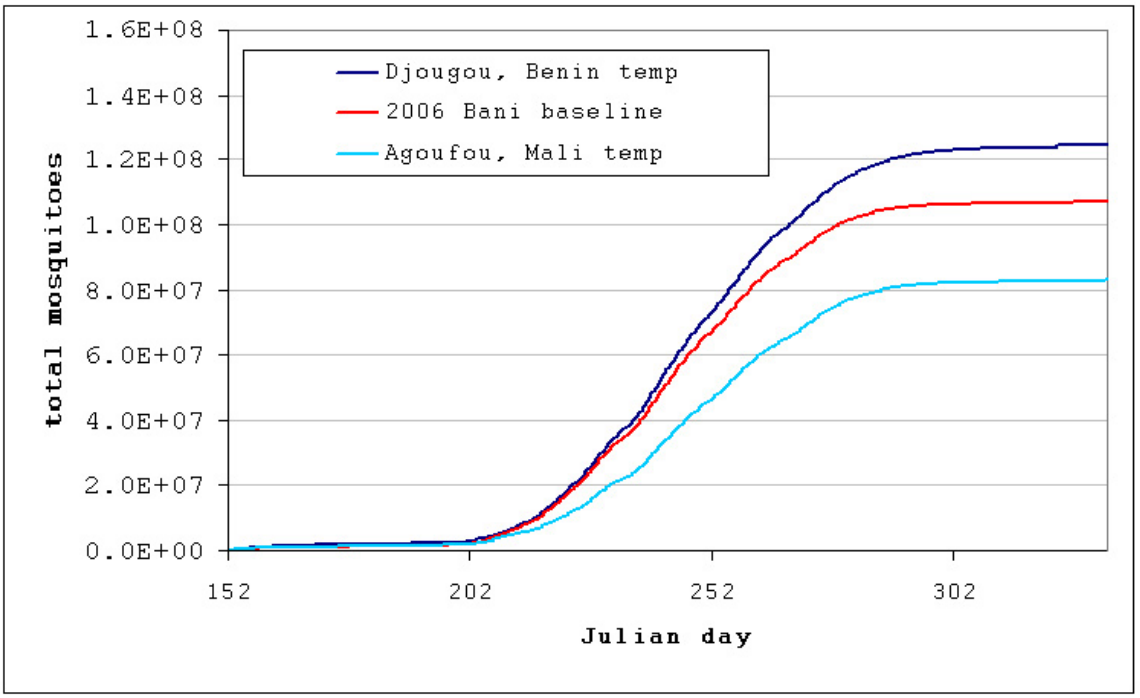

Figure 6.8. Cumulative simulated mosquitoes applying only Agoufou, Mali and Djougou, Benin temperature records to the baseline simulation.

From Table 6.1, 2006 average temperatures in Agoufou were only 0.7º warmer than Banizoumbou, compared to a 3.3º difference between Banizoumbou and Djougou temperatures. The pronounced temperature-dependent daily survivability of the Martens (1997) model (Equation 6.2) is responsible for this drastic decrease using the warmer Agoufou temperatures. The daily survivability decreases much more rapidly at higher temperatures that occasionally occur in this part of Mali than at more moderate temperatures typical of Banizoumbou and Djougou, Benin. Figure 6.9 shows a histogram of 24-hour average temperatures calculated using Djougou, Agoufou, and Banizoumbou temperature series. The few 24-hour average temperature events in Figure 6.9 above 38º C cause the daily survival to drop to around 60% in Agoufou, compared to the relatively constant 90% daily survival between 16º and 32º C. The simulation operates at an hourly time step, but simulated mosquitoes respond to daily average temperature. Hourly mosquito survivability is derived from the daily survivability, which is calculated using Equation 6.2 with the average temperature of the previous 24 hours. The minor increase in abundance resulting from higher subadult development rate at elevated temperatures is overshadowed by the effect of decreased survivability. Due to the dominant influence of average temperature on survivability, climate conditions of Agoufou, Mali, largely control abundance by temperature-decreased longevity, for at least part of the transmission season.

The effects of higher temperatures on vectorial capacity are more pronounced than the elevated-temperature effects on abundance alone, due to the nonlinear dependence of vectorial capacity on daily survivability and the temperature dependence of extrinsic incubation period *n*. Maximum vectorial capacity for this temperature variation experiment is shown in Figure 6.10. Maximum predicted vectorial capacity decreases for both scenarios. Agoufou temperatures caused a 28.2% decrease in maximum vectorial capacity, whereas Djougou temperatures caused a 12.7% decrease in maximum vectorial capacity. Here, the temperature dependence of sporogony becomes evident once again. Similar to the high 24-hour average temperatures exhibited by the Agoufou temperature record, Figure 9 shows several days of daily average temperatures below 23º C in

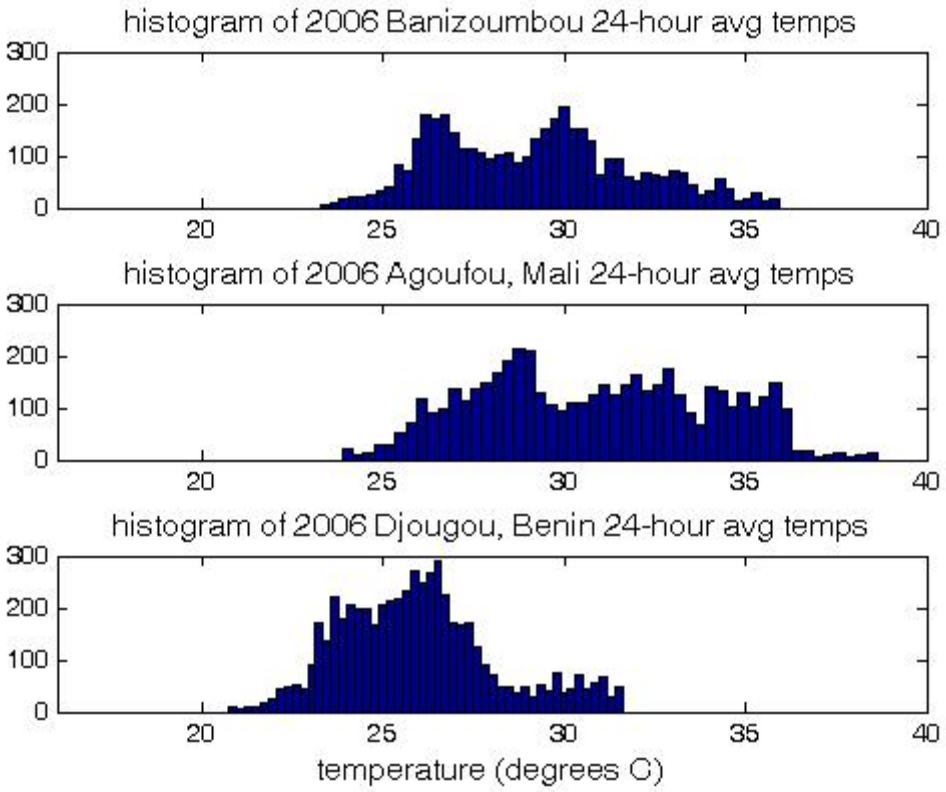

Figure 6.9. Histograms showing daily average temperature distributions for 2006 temperature rain season (May-October) records in Banizoumbou, Niger, Agoufou, Mali, and Djougou, Benin.

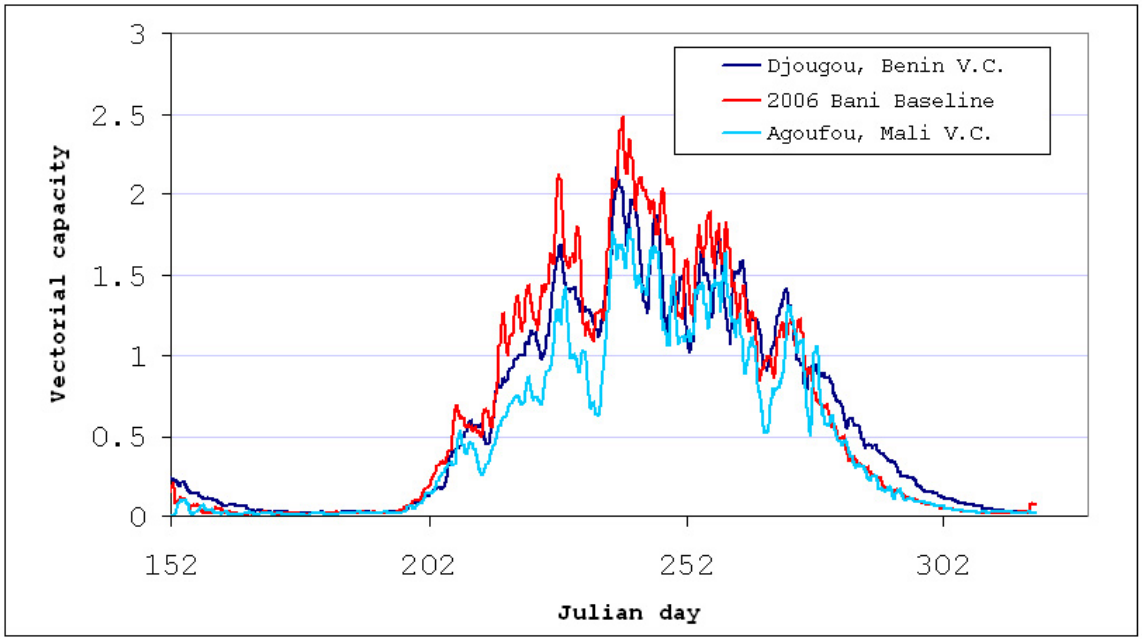

Figure 6.10. Simulated vectorial capacity trends, applying only Agoufou, Mali and Djougou, Benin temperature records to the Banizoumbou baseline simulation.

Djougou. At these temperatures, sporogony advances slowly, and the durations often exceed mosquito lifespans. At low temperatures, sporozoite development time *n* (Equation 6.3) becomes large rapidly as temperature decreases, compared to the much less pronounced variation of *n* at temperatures above 25ºC. This low sporozoite development rate is the reason vectorial capacity decreases in Djougou relative to Banizoumbou, despite the increase in mosquito abundance. The minor effect on vectorial capacity of increased longevity at lower temperatures is overshadowed by the effects of lowered *n*, because the longevity dependence is not very steep at these temperatures.

Finally, precipitation affects pool formation and persistence not only by total amount, but also by the frequency. Average interstorm periods in the 2006 monsoon vary from 1.45 days in Djougou, to 2.5 days in Agoufou and 2.6 days in Banizoumbou (Table 6.1). Higher frequency of rainfall events is expected to keep pools more consistently filled, however a high frequency of low rainfall events may not be sufficient for maintaining productive breeding habitats. We evaluated the effects of frequency by scaling Agoufou and Djougou rainfall series to Banizoumbou total precipitation such that all three precipitation series sum to the 2006 Banizoumbou total precipitation (478 mm). In this way, effects of variations in precipitation frequency were isolated while keeping total seasonal precipitation constant. Temperature series were left unchanged from the Banizoumbou baseline conditions. The results for mosquito abundance and cumulative mosquitoes for this scenario are presented in Figures 6.11 and 6.12, respectively. In this experiment, maximum abundance increased by 11.2% when Agoufou, Mali scaled precipitation was applied to Banizoumbou, and decreased by 24.4% when Djougou, Benin scaled precipitation was applied to Banizoumbou. Cumulative simulated mosquitoes were increased by 8.3% using the Agoufou synthetic scaled precipitation record, and decreased 38% using the Djougou precipitation. Because Djougou, Benin experienced more precipitation events during 2006 than Agoufou, Mali, the scaling process reduced the magnitude of each event in Djougou, and raised the magnitude of each event in Agoufou to result in the total of 478 mm of rainfall recorded in Banizoumbou.

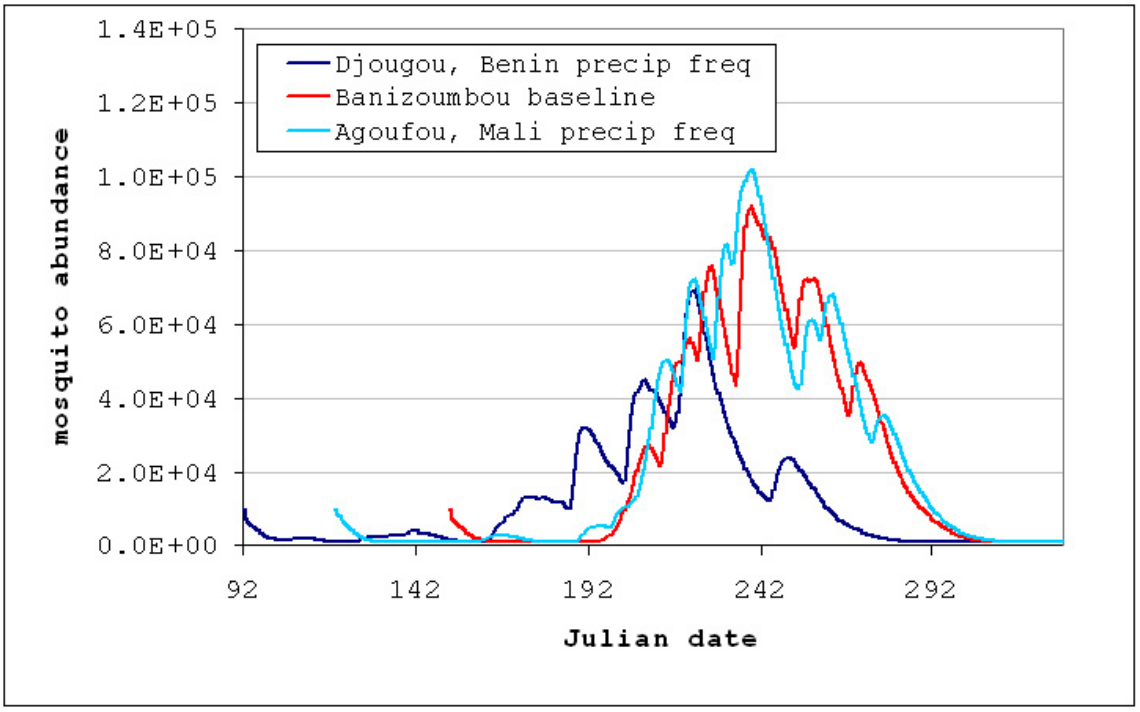

Figure 6.11. Simulated mosquito abundance using scaled precipitation records from Agoufou, Mali and Djougou, Benin applied to Banizoumbou. Total seasonal precipitation equals that of Banizoumbou, but storm frequency varies.

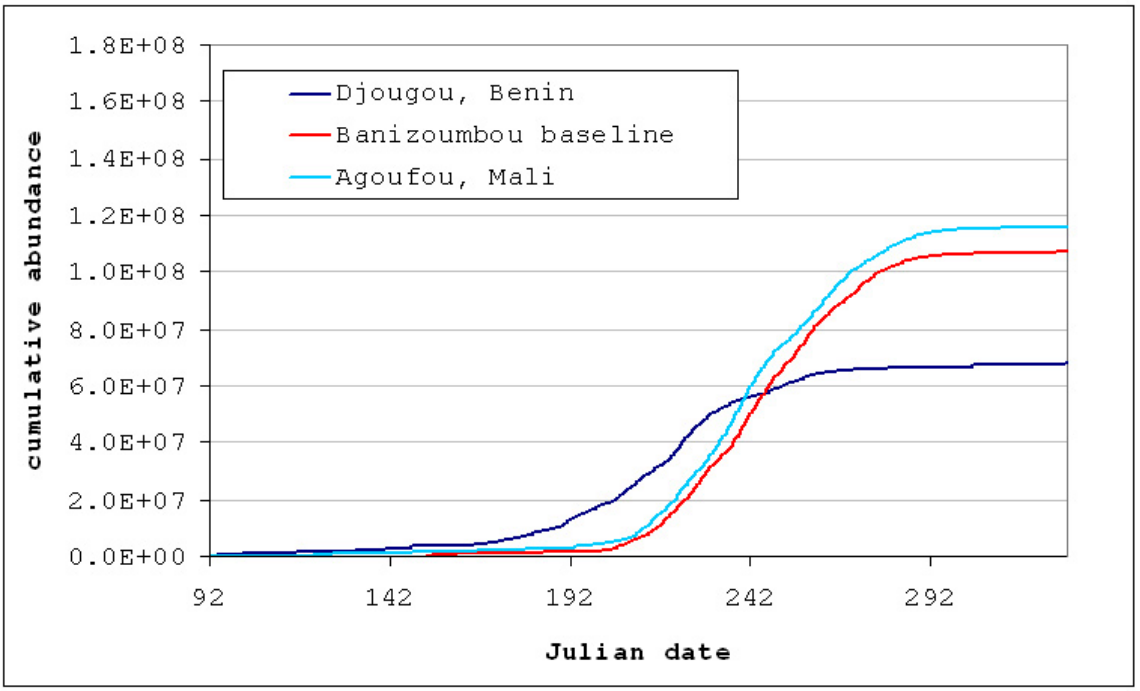

Figure 6.12. Cumulative simulated mosquitoes using scaled precipitation records from Agoufou, Mali and Djougou, Benin applied to Banizoumbou.

The results from this scenario demonstrate the controls of local hydrologic response to rainfall on mosquito population dynamics. HYDREMATS assumes that subadult (aquatic-stage) mosquitoes die if their breeding pool dries out before they emerge as adult mosquitoes. Therefore, any pool dessiccation results in a reduction of abundance by killing a cohort of developing subadult mosquitoes. Soil and vegetation types influence the infiltration losses from a pool, and partitioning of rainfall into infiltration and runoff depends strongly on soil moisture. Soil moisture responds to precipitation events, the frequency of which can determine emergence or death for aquatic-stage mosquitoes. Water depths of a large, highly productive pool in the center of Banizoumbou are presented in Figure 6.13, for the synthetic precipitation series of Agoufou, Mali (top) and Djougou, Benin (bottom). The frequent drying-out events in the Djougou scenario contrast markedly to the uninterrupted periods of water in the pool in the case of Agoufou precipitation applied to Banizoumbou. Due to this hydrologically-determined pool persistence, the synthetic Agoufou precipitation series allows more adult mosquito emergence, resulting in the higher overall mosquito abundance for this scenario, despite the later start of mosquito breeding evident in Figure 6.12. Thus, the importance of precipitation frequency and distribution through the wet season becomes evident. Vectorial capacity differences are not presented here because only the abundance term of the vectorial capacity is changed as a result of the scaled precipitation series. The temperature series recorded at the Banizoumbou station is used in all simulations. Percent changes in maximum vectorial capacities are therefore identical to the percent changes in maximum abundance.

6.4 Discussion

We have used a very high resolution, mechanistic modeling tool to simulate malaria transmission response to climate shifts in one specific village: Banizoumbou, Niger. Banizoumbou is a very specific environment. Certainly the configuration of various soil types and topography dictating pool locations at Banizoumbou is unique, but nevertheless it is instructive to note the strong controls that hydrologic processes exhibit on the abundance term of the vectorial capacity equation. Mosquito populations respond favorably to long periods of uninterrupted pool persistence, because many cohorts of

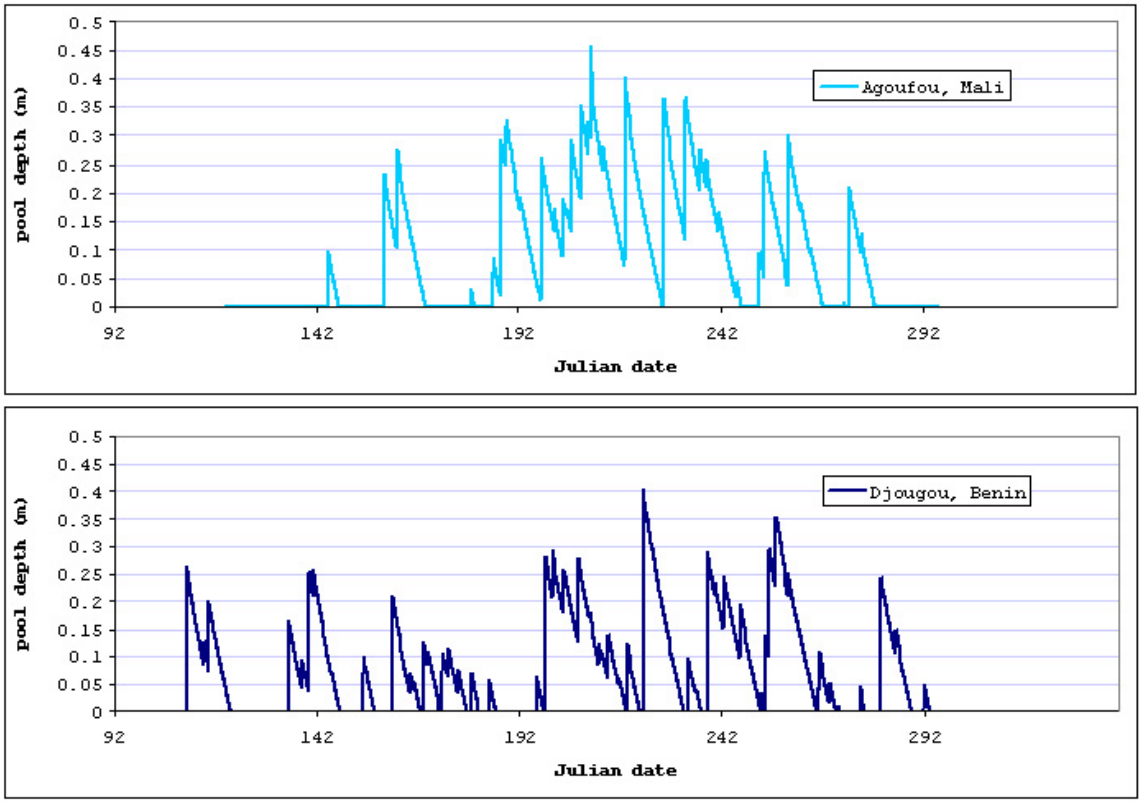

Figure 6.13. Water depths at a dominant pool in the center of Banizoumbou, for the scaled precipitation series from Agoufou, Mali (top) and Djougou, Benin (bottom) applied to the Banizoumbou model domain.

subadult mosquitoes can emerge without suffering fatal desiccation. Dry pools result in complete sterilization. We have demonstrated how manipulations of rainfall series to alter the frequency and number of events—but maintaining the same total annual precipitation—can lead to dramatic differences in pool persistence and therefore mosquito abundance. Because the number of rainfall events and the event frequency are often the primary manifestations of precipitation variability in the Sahel, the implications of such precipitation changes resulting from climate shifts on malaria transmission becomes evident. Increased event frequency associated with a shift to wetter conditions will increase abundance more than a simple linear correlation with rainfall would suggest, and for decreased event frequency the opposite is true because of more frequent pool dry-outs. The general dependence of mosquito abundance on small-scale hydrology

will be common to all water-limited villages in the Sahel, in which the dominant malaria vectors breed in ephemeral rainfed pools.

Modeling results also reveal that the temperature changes which accompany climate shifts can limit malaria transmission by either slowing the development of parasite or decreasing the survival probability of mosquitoes, depending on whether the shift is to wetter conditions or dryer conditions. Not all temperature changes associated with future climate shifts will necessarily involve temperature limitations in malaria transmission, however, and the various causative pathways linking temperature and malaria transmission would have different relative magnitudes depending on average temperatures attained during the climate shift. These include aquatic stage development rate (increase with temperature), survival (decrease with temperature), sporogonic cycle (increase with temperature), as well as the number of influences on hydrology which are relatively minor (e.g. evapotranspiration rates). The two non-linear processes necessary for malaria transmission to occur (pool persistence exceeding mosquito development time, mosquito lifespan exceeding extrinsic incubation period) are shown schematically in Figure 6.14. The dominant environmental variables influencing these processes are included in the figure.

Due to the complexity of the many environmental causations (primarily precipitation and temperature) leading to malaria transmission, it is difficult to predict impacts of changes without resorting to numerical models. Predictions of malaria transmission response to climate change should be made very cautiously for the reasons demonstrated in this chapter. Even though HYDREMATS embodies all of the important environmentally-influenced processes affecting malaria transmission, a few potential changes are not simulated. First, the longer-term vegetation changes that result from and provide positive feedback for Sahel climate shifts may affect local hydrology enough to alter pool persistence and influence runoff volume entering topographic low points. As previously discussed, persistence of pools is a dominant control of mosquito abundance in the Sahel. Partitioning of incident rainfall into runoff and infiltration and surface roughness will change in response to changes in vegetation cover. These processes will affect pond

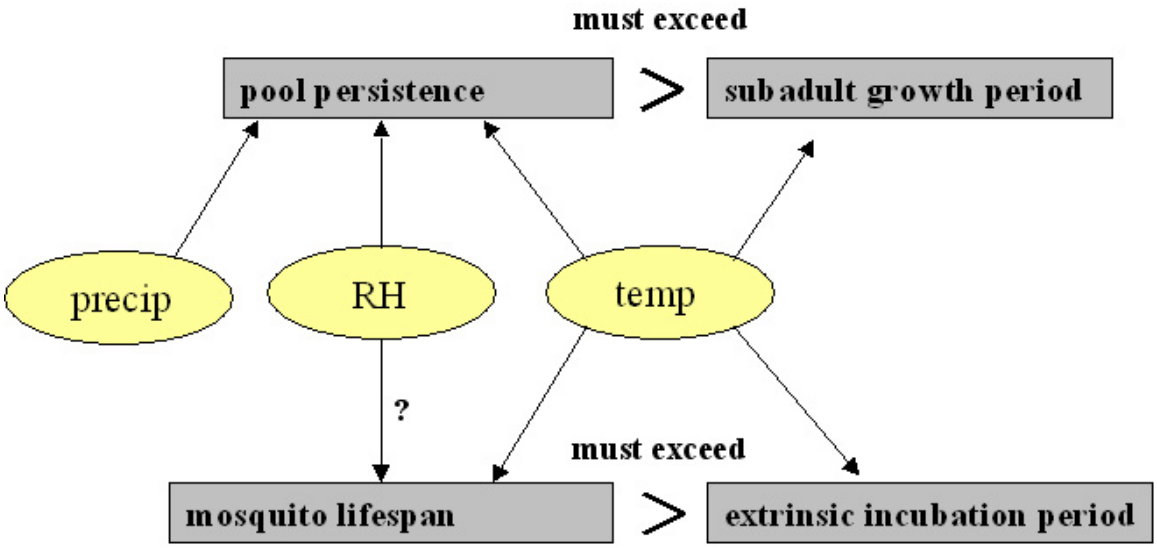

Figure 6.14. Schematic diagram showing the two nonlinear processes defining environmentally-influences conditions necessary for malaria transmission. Pool persistence must exceed mosquito subadult growth periods, and mosquito lifespans must exeed the malaria parasite's extrinsic incubation period. The controlling variables are also included.

formation, and roughness length of the vegetation cover will affect transpiration rates. Moreover, vegetation changes resulting from climate shifts will provide positive feedbacks to the climate shifts. Second, human populations are very adaptable and will adjust to changes in climate. In the model experiments we assume a static human population. Most Sahel inhabitants are subsistence farmers, who would be forced to adapt to climate shifts in order to grow enough food to survive. Such social influences are not considered and may affect malaria transmission.

6.5 Conclusion

Taken together, modeling results indicate various modes of control on malaria transmissibility in terms of vectorial capacity which may result from climate shifts in the Sahel. Changes in rainfall patterns and precipitation frequency associated with climatic shifts affect mosquito abundance nonlinearly, due to small-scale hydrologic processes influencing pool persistence. To illustrate this, we have demonstrated that Agoufou, Mali and Djougou, Benin 2006 hourly rainfall series scaled to the 2006 Banizoumbou rainfall total have resulted in wildly different simulated mosquito abundances. This is due to the

importance of persistent pools for uninterrupted breeding. From this result, the importance of mechanistic modeling of the hydrological links between climate and malaria transmission becomes evident when predicting the impacts of climate shifts.

A shift towards cooler, wetter conditions such as the drastic shift of 6000 years ago in the Sahara may dramatically increase mosquito abundance, however our modeling results indicate that the increased malaria transmissibility is not simply proportional to the precipitation increase. The cooler, wetter conditions increase the length of the sporogonic cycle, damping a large vectorial capacity increase otherwise brought about by increased mosquito survival and greater overall abundance. In contrast, a shift to hotter, dryer conditions results in much lower daily survival probability for adult mosquitoes leading to drastically lower vectorial capacity. Decreased abundance stemming from fewer newly-formed breeding pools compounds this reduction in malaria transmissibility. Therefore, strong climate shifts in either direction may limit malaria transmission by different biological limitation mechanisms. Due to the complexity of the climate/hydrology/disease transmission system, climate shifts may affect vectorial capacity in a number of ways that are impossible to predict without the use of mechanistic predictive models such as HYDREMATS. For the presented reasons, Sahel climate shifts toward wetter, cooler conditions are generally predicted to exacerbate malaria transmission, but not simply as a correlation with precipitation increase may indicate. In contrast, climate shifts toward hotter, dryer conditions are expected to yield lower malaria transmission conditions than would be predicted by changes in rainfall.

These results of this study have important implications for predictions of malaria response to climate change. We have shown that temperature changes alone can either increase or decrease malaria transmission, depending on the magnitude and direction of the temperature change and the initial temperature value. Malaria does not necessarily become more intense with warming. Climate change, however, involves a combination of changes in precipitation amount and precipitation frequency in addition to temperature changes, as well as other changes less important to malaria transmission. The sensitivity of malaria transmission to precipitation event frequency as well as precipitation amount

has been demonstrated in this study, and nonlinear hydrologic responses to changes in precipitation were implicated for this sensitivity. Therefore, in order to draw conclusions about malaria transmission, climate change scenarios involving changes in precipitation must specify changes in both precipitation totals and frequency of precipitation events (or average event magnitude). Otherwise, significant uncertainty and errors may result.

Chapter 7: Malaria parasite transmission and the effects of immunity

7.1 Introduction

7.1.1 The need for parasite and immunity representation

Variability in malaria transmission derives from numerous environmental and climatic determinants, but parasite dynamics are also influenced by the effects of human immune response to the parasite in the bloodstream (Molineaux, 1988). In this study, malaria transmission has thus far been addressed only in terms of vectorial capacity and mosquito abundance. However, HYDREMATS also tracks actual malaria parasite transmission in the mosquito/human host system by allowing individual agents of both types to host the malaria parasite.

The human body responds to malaria infection with two types of immune response, innate and acquired immunity. The innate immune system responds in a non-specific manner to any foreign bodies within the blood, and does not confer long-lasting protection (Alberts et al., 2002). The acquired immune response response in a highly specific manner to pathogenic challenges, but depends on a history of inoculations in order to mount effective attacks on future inoculations (Alberts et al., 2002). The immunity model in HYDREMATS simulates only acquired immunity, which takes longer to develop than the innate response. In HYDREMATS, innate immunity to malaria is neglected. Acquired immunity requires repeated challenge with the parasite to confer partial protection against severe disease and recurrent infections, and is represented in a simple manner.

Humans gain semi-protective acquired immunity to malaria by receiving infectious bites. The resulting partial immunity regulates the density of parasites within the blood, but also depends the on the presence of parasite (Struik et al., 2004). Therefore, human immunity is expected to be a significant factor in shaping malaria propagation through the human/mosquito transmission cycle by a negative feedback mechanism. It follows that

for accurate model representation of parasite in the transmission system, effects of human immunity must be considered. The human acquired (adaptive) immune system, however, is exceedingly complex, involving a variety of effector mechanisms targeting various stages of the *Plasmodium* life cycle. The HYDREMATS formulation of immune response to malaria does not represent physiological details. Instead, it uses a very simple aggregation of all immune processes into a single lumped representation of immunity. This chapter presents the HYDREMATS formulation of *Plasmodium falciparum* transmission and immune response in human hosts.

Neither vectorial capacity nor mosquito abundance are true indicators of actual malaria transmission, because neither measure contains information about actual parasite presence in the vector/host system. For example, significant local populations of anopheles mosquitoes bite humans in Cambridge, Massachusetts, and the city therefore has a non-zero vectorial capacity during the warm summer months. Yet, malaria has not been endemic in Cambridge for much of the 20^{th} century, and the only cases of malaria in Massachusetts are either imported from the tropics or secondary cases resulting from an imported case. Linkages between entomological activity and malaria burden can be measured in terms of force of infection. One standard measure of force of infection is the entomological inoculation rate (EIR) which is the number of infectious bites a person receives per year. This measure depends on the mosquito sporozoite rate (the proportion of mosquitoes infected with sporozoite stage of parasite), and thus contains information about parasite presence within the system. In low- to medium-transmission environments, there is a linear relationship between EIR and malaria incidence (Beier et al, 1994). Because EIR depends on the sporozoite rate in mosquitoes, and because this sporozoite rate is itself a function of human malaria prevalence, EIR is also expected to be indirectly affected by immune suppression of parasite in humans.

Malaria prevalence gives a better indication of the population's malaria infection status than vectorial capacity or mosquito abundance alone. However, the development of immunity may complicate the use of prevalence as an indicator. The human immune response to malaria is highly complex and not perfectly understood, but it is clear that

acquired immunity protects against severe disease, and continuous, low-level parasitemia in the bloodstream protects against further infections (Bruce-Chwatt, 1963; McGregor, 1987). Acquisition of immunity depends on a history of infectious bites (Struik et al., 2004). The effect is also noted in areas of unstable transmission where immunologically naïve people are suddenly challenged with malaria infection as a result of changing climatological conditions, changing environmental conditions or migration. These people rapidly develop symptomatic and often severe malaria infections (Struik et al., 2004). In areas of endemic transmission, severe malaria disease is confined to children under 5 years of age and pregnant women (Snow et al., 1999). This is because by age 5, children in these areas have developed enough immune protection, and are no longer at high risk of severe and fatal disease. Beyond this age, low-level parasitemia persists without symptomatic malaria. However, in areas of epidemic malaria without the emergence of protective immunity, the age structure of disease incidence shifts to include adults of all ages (Snow et al., 2002; Struik et al, 2004). Prevalence in children up to 5 years of age may be an indicator of local transmission intensity, but even so, acquired immunity may play a role in shaping prevalence trends. Beier et al. (1999) noted a non-linear relationship of prevalence with EIR, with steadily rising prevalence levels in the low EIR range (below ~100), and leveling prevalence at EIR values above about 200 infectious bites per person per year. In this range, increases in prevalence are low compared to the increase in EIR. At EIR values in the 200 – 400 (infectious bites per person per year) range, without immunity, entire populations should be infected with malaria parasite in short time. Presumably, the relatively steady 80% prevalence observed in this high EIR range reported by Beier et al. (1999) reflects the protective effects of acquired immunity.

Gupta et al (1999) noted that immunity protection against severe malaria may be attained after only one or two bites in areas of intensive transmission, and that severe malaria cases were less frequent in children in high-transmission environments compared to areas with lower rates of infection (Gupta et al., 1999). This seemingly paradoxical trend was attributed to immunity acquired as an infant when protection from maternal antibodies was still effective. Several other cases of increased mosquito abundances associated with lower human parasite prevalence have been reported (e.g. Diuk-Wasser et al., 2005;

Snow et al., 1997; Gupta et al., 1999). These results have been attributed to several potential causes, but it is thought that human immunity may play a significant role in explaining these observations. In Mali, Diuk-Wasser et al. (2005) noted a decrease in malaria prevalence in villages with intensive irrigation and higher mosquito abundance. They suggested intraspecific competition of subadult mosquitoes for limited nutrients as an explanation. The adult mosquitoes would be smaller, shorter-lived, and thus the vectorial capacity would be depressed. However, it seems plausible that in addition to the increased nutrient competition resulting from larval crowding, acquired immunity played a role in lowering the prevalence in many of these observations.

Field observations by the CERMES in Zindarou and Banizoumbou have revealed prevalence trends consistent with observations in Mali. CERMES staff took bimonthly blood samples from children under 5 in each village, and noted very comparable prevalence in both villages, despite the order of magnitude difference in vectorial capacity (Jean-Bernard Duchemin, personal communication, 2005). This data is presented in Figure 7.1. For the period August 2003 – November 2005, average prevalence is 0.39 in Zindarou and 0.41 in Banizoumbou. The prevalence fluctuated seasonally, and average values were very similar between the two villages. The much higher vectorial capacity of Zindarou corresponds to a slightly lower observed prevalence than Banizoumbou. In order to explain these observations, parasite transmission and human immunity are introduced in the model.

7.1.2 Acquired immunity and past climate variability

The level of acquired immunity depends on a history of infectious mosquito bites, because an individual's immunity is boosted by each infectious bite. The number of infectious bites per person per day in a malaria-endemic area increases as vectorial capacity increases. If climate conditions at a village shift to result in a higher vectorial capacity for that village, the increased rate of infectious bites should stimulate immune responses, rapidly increasing immunity level in both individuals and at the population scale. Acquired immunity helps individuals resist subsequent infections, and the resulting population-scale immunity reduces the level of parasite transmission within the system.

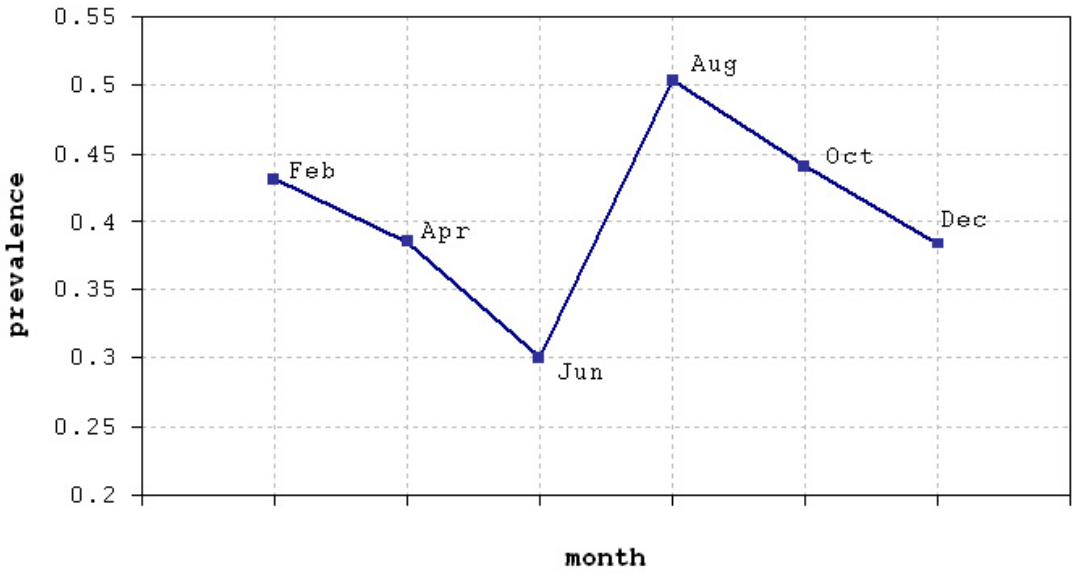

Figure 7.1. Observed average prevalence in Banizoumbou, for 2004 and 2005. (source: Jean-Bernard Duchemin/ CERMES Niger data)

One individual's immunity makes his neighbor less likely to get an infectious bite because the individual does not act as a source of parasite for vector mosquitoes. Immunity thus acts in opposition to—yet depends on—malaria transmission. Increased biting rate should have a negative feedback effect on population-scale parasite prevalence, and may result in prevalence comparable to that before the climate shift. However, the effect of the climate shift will be reflected in the increased population immunity. A climate shift to lower vectorial capacity conditions should have the opposite effect: lower biting intensity will gradually allow immunity to wane, but over a long time period of several years. Individuals in such an environment enjoy some protection from severe disease, but must be reinoculated in order to maintain the low-level parasitemia necessary for immunity. If they are not reinoculated, the non-immune population is susceptible to a resurgence of malaria, or a malaria epidemic.

In summary, population-scale immunity level varies with changes in transmission intensity brought about by climatic variability, and because immunity persists for many years, population-scale immunity reflects past climate conditions. The memory exhibited by the acquired immunity influences susceptibility to reinfection at the individual scale

and epidemics at the population scale. Moreover, it can be affected by interventions that prevent infectious bites from occurring, such as the use of insecticide treated bednets.

7.2 Model representation of parasite transmission

HYDREMATS includes a representation of infected status for both types of model agents: humans and mosquitoes. Infected status is included in the attribute matrix of both mosquito and human agents, and contact between a sporozoite-infected, host-seeking mosquito and a human host can result in an inoculation. Simulated individual mosquitoes are able to acquire parasite infection if they ingest an infectious bloodmeal, and the infectious stage of the mosquito-borne parasite—the sporozoite—forms after 111 degree-days above 16 degrees C. At this point, the mosquitoes are able to transmit a new infection to the next human bloodmeal host, completing one cycle of transmission. If animal hosts are chosen for a bloodmeal instead of humans, no transmission occurs but the mosquito remains infectious. Once infected, mosquitoes remain infected for life, and once the parasite has reached the sporozoite stage within the mosquito, it remains in this stage for the duration of the mosquito's life. In contrast, human agents clear the parasite with a rate of 0.0001 per hour. This corresponds to an expected duration of positive parasitemia state of one year. The long persistence of parasite in the blood does not necessarily mean the person is ill for the entire time. On the contrary, many partially immune people with low-level parasitemia exhibit few if any disease manifestations (Bruce-Chwatt, 1963; McGregor, 1987). However, individuals with little or no acquired immunity may develop clinical malaria if challenged with an inoculation, and may suffer long illness or death.

7.3 Model representation of human immunity

Human immunity is represented by the variable *a*, which varies from 0 (immunologically naïve) to 1 (completely immune). Each day, the immunity (*a*) of any human agent that has received at least one infectious bite during the previous 24 hours is raised by 0.2, regardless of that human agent's infected status. Immunity is then lost at 0.1% per day. These parameters are loosely based on observations made by Snow et al. (1997) and Gupta et al (1999), who observed that few infectious bites are needed to afford protective

immunity against severe malaria. They were also chosen based on the malaria prevalence observations made in Banizoumbou by CERMES (Figures 7.1 and 7.2). The model was calibrated to generally match average observed prevalence and seasonal fluctuation in measured prevalence. The parameters for this model may reflect genetics of the host population. Long co-existence of human populations in Africa and *Plasmodium falciparum* may result in selective pressure influencing the physiological immune response to challenge by malaria parasite. The Duffy negative trait conferring genetic immunity to *Plasmodium vivax* malaria among many African populations is an example of such an adaptation (Horuk et al., 1993).

Each time a human agent is subjected to an infectious bite, the probability of infection is:

$$P = 1 - a \qquad (7.1)$$

A uniform random number is sampled and compared to P to determine if the human agent has acquired the parasite from the infectious bite. An immune human agent may

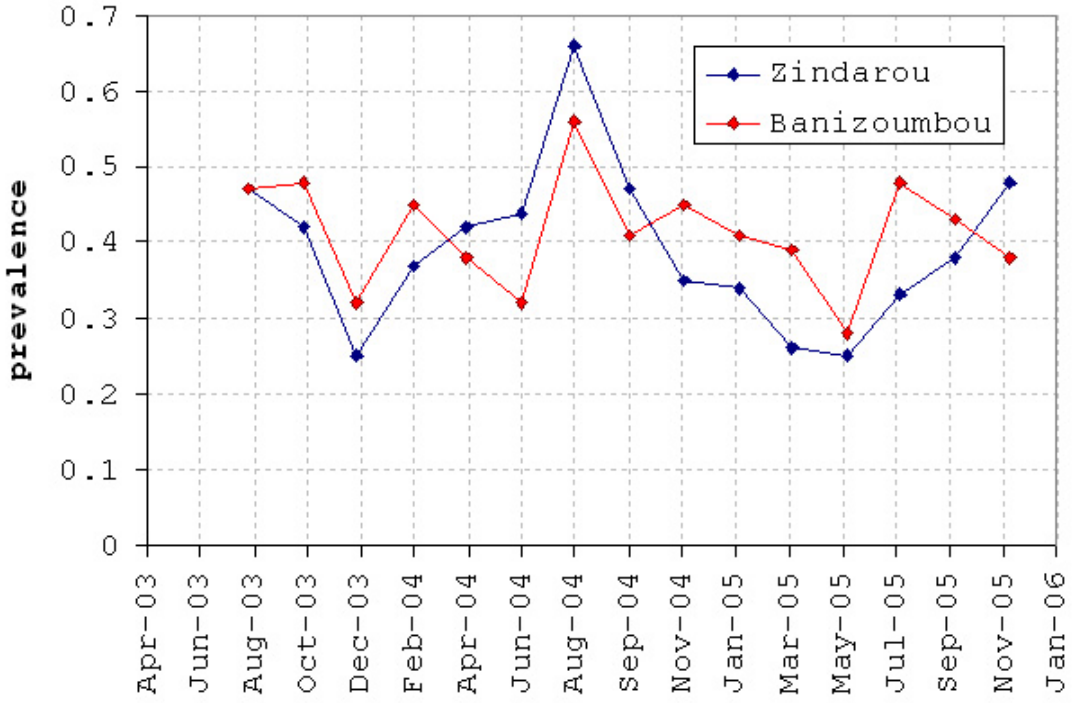

Figure 7.2. Observed prevalence in Banizoumbou and Zindarou, for the period August 2003 – November 2005. (source: Jean-Bernard Duchemin/ CERMES Niger data).

not be a source of infection for biting mosquitoes, even though such individuals may harbor low levels of parasitemia (Struik et al., 2004). Infective gametocytes are assumed to be too low density to allow human-to-mosquito transmission in immune individuals. With this formulation, malaria prevalence depends on resistance acquired over several years of repeated inoculations within a population. We stress that this is a very simple representation of a very complex and highly developed human immune response to malaria parasite. The variety of effector mechanisms of immune response to malaria infection are conveniently lumped together into one "immunity" process represented by a single variable *a*, ignoring the exact details of the multitude of individual processes involved in the immune system. Nevertheless, the model representation of immunity allows the effects of immunity on malaria transmission to be incorporated into the model in a flexible and representative manner. This formulation allows simulated prevalence to be compared to observed prevalence.

7.4 The role of immunity in malaria response to climate shifts

Chapter 6 addressed the response of mosquito populations and malaria transmission to climate shifts. Major climate shifts were simulated using climate data recorded at sites north and south of Banizoumbou along the north-south rainfall gradient. Climate shift scenarios that could affect Banizoumbou in the future were simulated using present-day climate forcings measured at Agoufou, Mali, and Djougou, Benin. Vectorial capacity was higher in the scenario in which Banizoumbou climate shifts toward the cooler, wetter conditions of present-day Benin. The vectorial capacity rise was due predominantly to the increased mosquito abundance resulting from greatly increased rainfall. However, as discussed above, due to the effects of immunity it is not immediately evident if this rise in abundance and vectorial capacity should correspond to greatly increased prevalence as well. Decreased vectorial capacity was observed in Banizoumbou using the hotter, drier present-day Agoufou climate conditions. The resulting prevalence in this scenario is also somewhat uncertain without investigation using the presented immunity model.

Modeling results are presented in Figure 7.3. The top frame shows mosquito abundance for the three climate scenarios, applied to the Banizoumbou model domain. Climate

conditions for 2006 for each scenario are repeated for eight years in order to simulate the steady-state response in prevalence to each climate shift scenario. With a repetition of the same climate forcing for many years, the net effect (in terms of prevalence) resulting from opposing influences of immunity and malaria transmission is shown in the lower frame of Figure 7.3. Malaria prevalence for all three scenarios is seen to reach a steady state, and remarkably, the simulated prevalences are very similar. The model predicts a somewhat paradoxical result consistent with the "anophelism without malaria" observations in the literature: an increase in vectorial capacity due to a shift in climate forcings does not result in a major rise in overall prevalence. The prevalence resulting from the shift to wetter conditions is slightly higher than the baseline Banizoumbou scenario, but the difference is small compared to the differences in vectorial capacity. Also, the reduction in vectorial capacity that would be expected from a shift to the hotter, drier climate conditions of Agoufou, Mali, still results in the model-predicted prevalence very similar to the Banizoumbou baseline condition. This is because of the effects of immunity. Without these effects opposing malaria infection, increased vectorial capacity would raise the malaria prevalence of the Banizoumbou population and vice versa. These results suggest that at steady state malaria prevalence is largely independent of climate. However, natural variability is inherent to any climate. Hence, malaria prevalence always reflects the climatic forcing. In general, the effects of human immunity would result in spatial distribution of prevalence that is smoother than that of vectorial capacity. On the other hand, considering a single location, immunity should amplify the temporal variability in vectorial capacity resulting in higher variability of prevalence (larger coefficient of variation).

Figure 7.4 presents the immunity level *a* for each of the three simulations. Effects of simulated climate shifts are evident in this figure. Immunity responds strongly to increased biting pressure resulting from Djougou, Benin conditions, and stays high compared to the Banizoumbou baseline simulation. The high vectorial capacity relative to the baseline means individuals are frequently challenged with malaria parasite in this simulation, and the high rate of inoculation is reflected in the high levels of immunity. Because this immunity prevents an uninfected individual human from becoming infected,

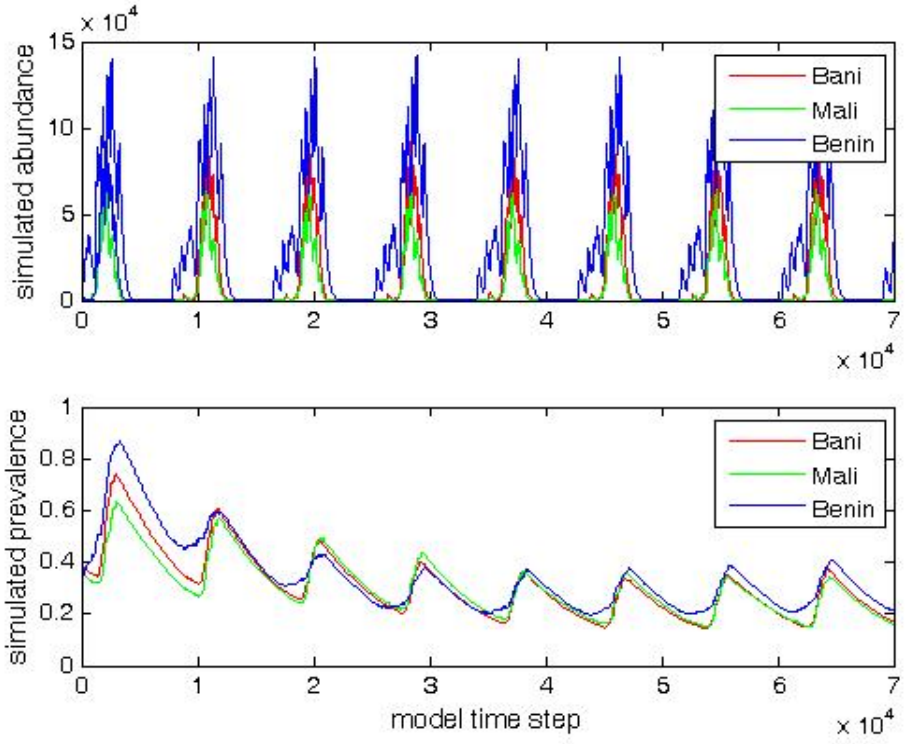

Figure 7.3. Simulated mosquito abundance for 2006 climate forcings from Banizoumbou; Agoufou, Mali; and Djougou, Benin applied to Banizoumbou and repeated eight times (top), and associated modeled malaria prevalence over the same simulation period (bottom).

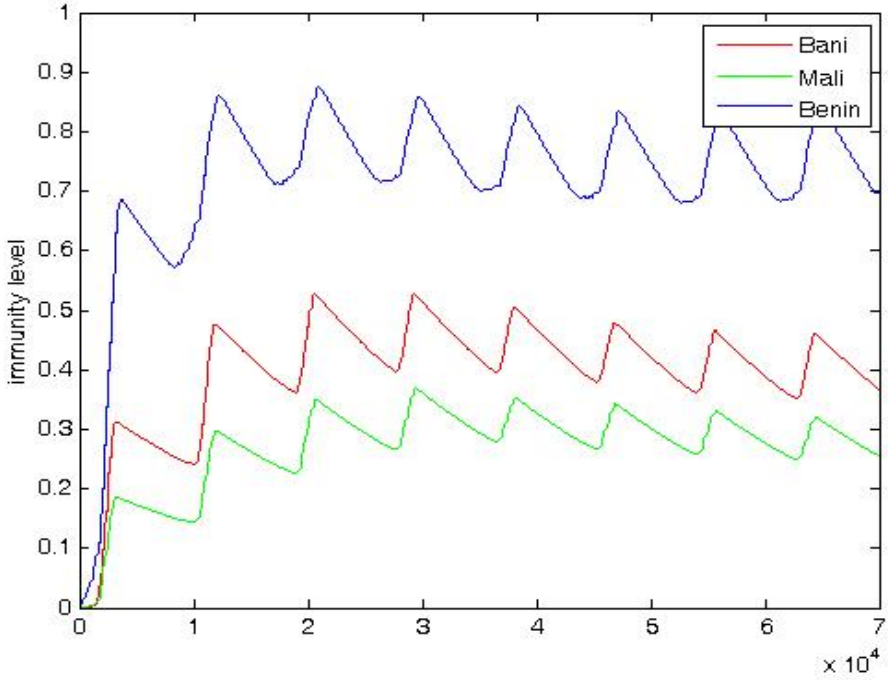

Figure 7.4. Simulated average immunity in Banizoumbou for 2006 climate forcings of Banizoumbou (baseline); Agoufou, Mali; and Djougou, Benin repeated eight years.

resulting overall prevalence is reduced. The opposite is true for the simulation involving Agoufou, Mali climate forcing. In this case, the reduced immunity from lower EIR and vectorial capacity allows more inoculations to result in new infections, thus raising the prevalence rate to be comparable with the baseline scenario. The low acquired immunity of the Agoufou, Mali simulation represents conditions typical of desert fringe areas, making such areas with marginally immune populations subject to serious epidemics.

Increased biting rates associated with the higher vectorial capacity resulting from a shift to Djougou, Benin conditions should also influence the age distribution of malaria prevalence. With such a climate shift resulting in increased biting and greater exposure to malaria, the expected age of children's first infectious bite and acquisition of protective immunity sufficient to prevent severe malaria episodes may drop significantly. If the expected age of protective immunity attainment is shifted low enough to overlap with the period of maternal antibody protection during the first six months of life, then model results would support the proposed mechanism of Snow et al (1997) for explaining the paradoxical observations of lower severe malaria with higher transmission rates in Kenya. HYDREMATS does not presently simulate the age of human agents.

7.5 Simulation of prevalence in Banizoumbou and Zindarou

In Chapter 7 the effects of spatial variability in hydrology as a determinant of malaria transmission were examined and simulated based on intensive field observations at the villages of Banizoumbou and Zindarou, Niger. These two villages are located only 30km apart, yet vectorial capacities in the villages differ by an order of magnitude. This is explained by the vastly different hydrologic conditions of Zindarou, which result from a shallow groundwater table remaining from a large abandoned river system. The shallow groundwater table has numerous surface expressions during the wet season, offering breeding anophelines a large, persistent expanse of surface water for oviposition and resulting larval development. The resulting difference in mosquito abundance leads to the large, order of magnitude difference in vectorial capacity.

The hydrologically determined difference in vectorial capacity between Zindarou and Banizoumbou can lead to significant differences in acquired immunity, similar to the immunity differences in simulation results from the Banizoumbou climate variability scenarios. The prevalence measurements taken by CERMES (Figure 7.2) show very similar prevalence in Banizoumbou and Zindarou, and therefore indicate higher immunity in Zindarou associated with the greater biting pressure, compared to Banizoumbou. Without the mitigating effects of immunity, higher vectorial capacity would cause malaria prevalence in Zindarou to be far greater than prevalence in Banizoumbou. HYDREMATS simulations in Zindarou have therefore included representation of malaria transmission and human immune response, in order to approximate the observed prevalence in the two villages. 2006 climate forcing, recorded at the Zindarou meteorological station, was repeated for several years in order to achieve a steady state in malaria prevalence and immunity. Prevalence results of this simulation are shown in Figure 7.5, and are compared to simulated 2006 prevalence in Banizoumbou. The start of the simulation shows a rapid rise in prevalence to near 100%. This is because the simulated population has no acquired immunity and biting pressure is such that virtually everyone becomes infected because they all receive infectious bites. However, the rapid rise in immunity resulting from these same infectious bites causes the prevalence to fall back to levels in the 30-40% range, near the measured values in Zindarou. The rapid initial rise in prevalence with no protective immunity illustrates the potentially devastating consequences of subjecting immunologically naïve populations to high force of infection. Such a change could arise from migrations, land use change, or severe climate variability. Figure 7.6 shows the immunity level *a* associated with the Zindarou simulation. As expected, immunity rapidly rises after the start of the simulation, and reaches a steady-state after several years of simulation. Immunity is clearly higher in Zindarou than in Banizoumbou, as is expected with the higher vectorial capacity.

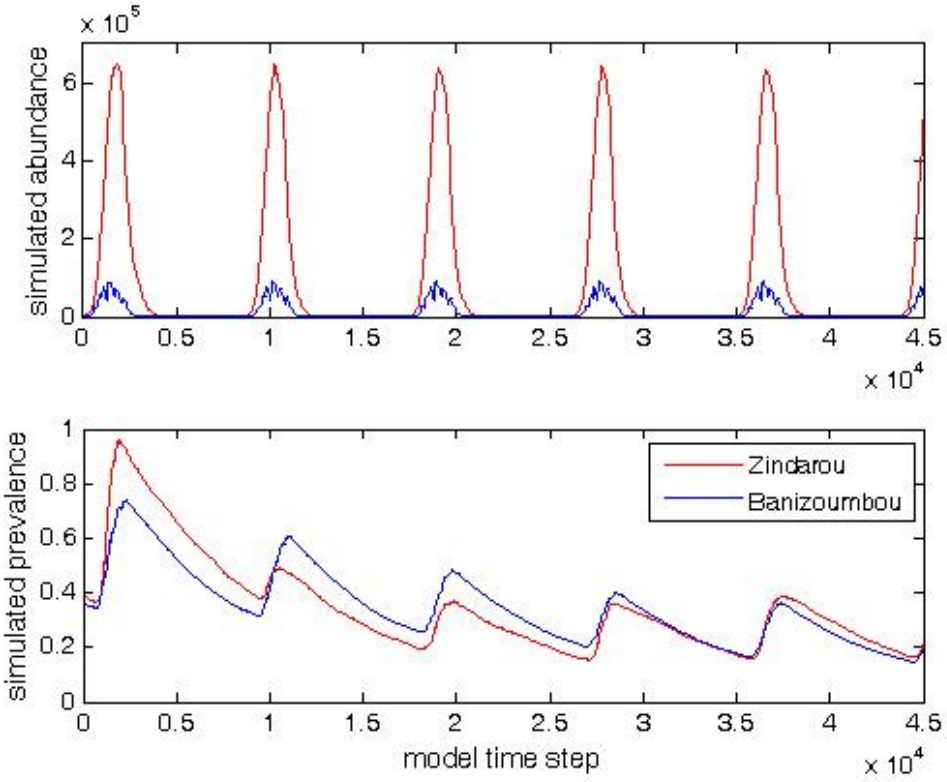

Figure 7.5. Prevalence in Zindarou vs prevalence in Banizoumbou. The top frame shows modeled mosquito abundance in each of the villages. In this simulation, 2006 climate forcing was repeated five times.

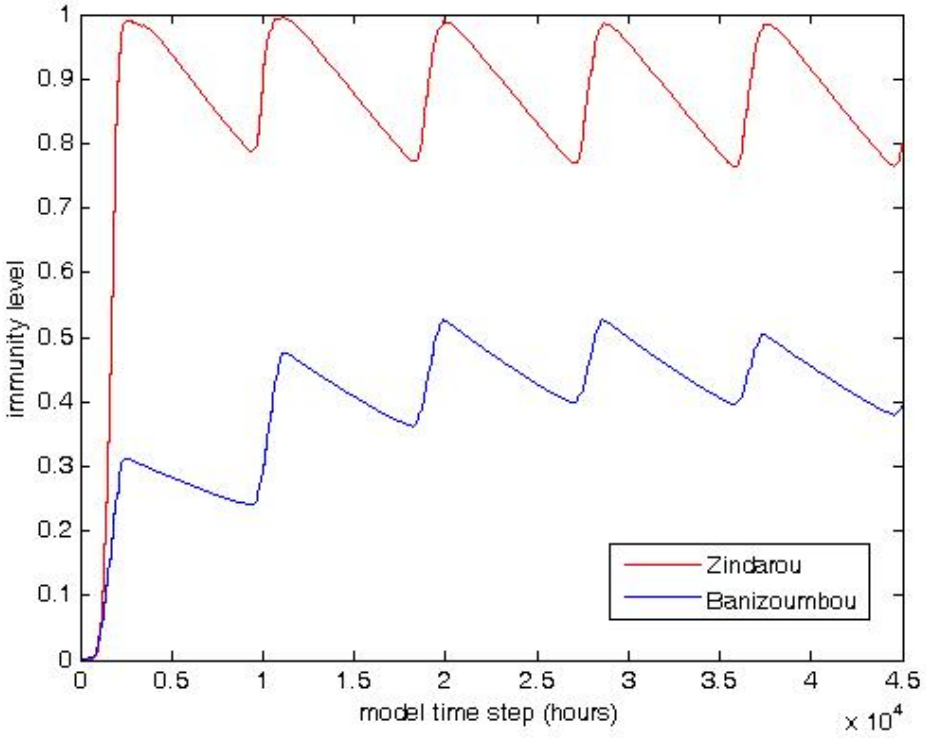

Figure 7.6. Immunity in Zindarou vs. immunity in Banizoumbou.

7.6 Conclusion

In order to mechanistically link hydrology and climate forcings to actual malaria circulation in the human host/mosquito vector system, a representation of human acquired immunity must accompany model simulation of parasite transmission between humans and mosquitoes. Otherwise, unrealistic estimates of prevalence response to variability in vectorial capacity would result. The simple model presented here reproduces the close match of observed malaria prevalence in Banizoumbou and Zindarou.

The presented immunity model also shows how memory of past variability in vectorial capacity can be observed in immunity level. Climatic variability brings about differences in vectorial capacity, and the resulting changes in rates of malaria inoculation boost immune response, which wanes slowly. Repeated years of high vectorial capacity bring about a high population immunity, and several years without high levels of transmission can cause immunity levels to wane. Such conditions can make populations very susceptible to devastating malaria epidemics when conditions shift back to promote more intensive biting pressure.

Chapter 8: Conclusions

A mechanistic modeling tool linking climate and malaria transmission has been developed, field validated, and applied to address questions of malaria transmission response to temporal climate variability and spatial hydrologic variability. This was done based on extensive field observations in Banizoumbou and Zindarou villages in the Niger Sahel. The new model, the Hydrology, Entomology, and Malaria Transmission Simulator (HYDREMATS) involves detailed representation of hydrology as a necessary intermediate between climate forcing, entomology and malaria transmission. In seasonal, water limited transmission environments such as the Niger Sahel, the formation and persistence of the breeding sites exploited by the dominant malaria vector mosquito, *Anopheles gambiae*, are predicted using high resolution rasters of vegetation type, soil type, and topography as hydrology model inputs. The persistence of these pools has been found to be a dominant control of mosquito population dynamics.

Using a novel approach, an agent-based entomology simulation is loosely coupled to the hydrology model output. Simulated pools allow mosquitoes to breed and emerge as adults. After eclosion (emergence as adults), mosquitoes move about the model domain and interact with their environment and human agents. The agent-based simulation tracks attributes of each agent (both mosquito and human) relevant to malaria transmission. These attributes can determine impacts of various types of perturbation scenarios on malaria transmission, while maintaining a spatially explicit structure. Relative positions of mosquitoes, breeding habitats, and human habitation are maintained. Mosquito population dynamics are thus mechanistically linked to environment and hydrology inputs. The model's spatial structure and incorporation of hydrologic response to precipitation represent an improvement over previous, correlation-based models linking environmental variability and mosquito population dynamics or malaria, because the detailed causative pathways connecting environmental influences to malaria transmission are explicitly represented.

The coupled model has proven effective for testing the impacts of various perturbation scenarios on mosquito abundance and malaria transmission. Chapter 4 considered in detail the mosquito population response to climate variability in the Banizoumbou village transmission environment. For this simulation, measured meteorological variables for the 2005 and 2006 wet seasons were the only difference between the two years, and this interannual difference in model forcing reproduced the interannual variability in mosquito abundance very well. In Chapter 5, the simulation was extended to nearby Zindarou village, and demonstrated the ability of HYDREMATS to incorporate spatial hydrologic variability to predict associated spatial variability in mosquito abundance and malaria transmission. In Zindarou, the model was used to simulate mosquito population dynamics during the 2005 and 2006 transmission seasons. Predicted interannual variability in Zindarou and predicted spatial variability between Zindarou and Banizoumbou matched field observations very well at the seasonal scale. The very wet conditions of Zindarou in close proximity to the more typically dry village of Banizoumbou presented a useful test scenario with which to isolate the effects of regional hydrologic variability on village-scale malaria transmission. Further application of the model involved climate shift scenarios in Banizoumbou, and was discussed in Chapter 6. Past climate shifts in the Sahel and the possibility that such shifts may occur again in the future were used as the climatological basis for these simulations. Measured meteorological data from two villages located in Mali and Benin to the north and south of Banizoumbou along the precipitation gradient were applied to the Banizoumbou environment, and the resulting changes in mosquito abundance and vectorial capacity were predicted. Taken together, the simulations and their predictions result in the general conclusions of this thesis:

- **The calibrated, field-validated coupled hydrology/entomology model that has been developed in this thesis (HYDREMATS), which operates at fine spatial and temporal resolution, accurately simulates the impacts of various environmental perturbations on malaria transmission, at the village scale and in water-limited environments.**

- **The model effectively reproduces observed mosquito population dynamics at seasonal and interannual time scales, as well as spatial distributions of clustering near breeding pools and human habitation.**
- **Spatial hydrologic variability controls local, village-scale mosquito abundance and vectorial capacity in areas of seasonal malaria transmission such as the Niger Sahel. Variability in malaria transmission can vary at small scales in the Sahel.**
- **Different modes of limitation of malaria transmission may dominate as a result of future climate shifts in the Sahel, depending on the direction of the shift (cooler and wetter conditions or warmer and dryer conditions). Malaria transmission response to climate shifts is less pronounced than precipitation or temperature alone may indicate. Also, changes in rainfall patterns and precipitation frequency associated with climatic shifts are shown to affect mosquito abundance nonlinearly, due to small-scale hydrologic processes influencing pool persistence.**
- **The simple acquired immunity model in HYDREMATS reproduces the close match of observed malaria prevalence in Banizoumbou and Zindarou. The presented immunity model shows how memory of past variability in climate-determined vectorial capacity can be observed in immunity level, and simulation results support various field observations of suppressed prevalence in areas of high biting pressure.**

The graduate study proposal leading to the research presented in this thesis stated four hypotheses. These are repeated and addressed here.

Hypothesis 1: For a given land cover type, a critical range of surface water body sizes exists which spans the dimensions of pools producing the vast majority of anophelines which plague the village.

The importance of pool sizes and their associated persistence was considered in Chapter 4, where it was noted that in Banizoumbou the most productive pools persist long enough to allow at least one cohort of adult mosquitoes to develop. Optimally productive pools

must also dry out periodically and then become re-wetted so that complex ecosystems with high predation rates and intense competition for limited nutrients do not develop. In other words, new water is the most dangerous for causing mosquito population increases. Without hydrology modeling, it is impossible to report an exact pool size or pool size range as yielding the most favorable persistence for mosquito development, because persistence depends on soil types, evaporation rates, infiltration losses, pool bathymetry, as well as precipitation patterns. Some pools of very large size may drain more rapidly than smaller pools with lower permeabilities in the pool substratum. Knowledge of hydrologic details is therefore important, and pool persistence is best evaluated with HYDREMATS, to determine pool productivity on an individual pool basis. Size ranges of the most productive pools can be determined for any particular location, but such a determination would be very site-specific and would assume similar pool bathymetries, stationarity in precipitation and other climate patterns, and unchanging land cover conditions.

Hypothesis 2: A critical distance from human habitation exists beyond which emerging anophelines do not significantly add to local malaria transmission.
HYDREMATS maintains the spatial structure of the mosquito populations. The spatial relationship of individual mosquitoes to breeding sites, human agents, and important components of the environment is thus maintained, and the model can address questions about critical distances from pools to human habitation. Sufficient information is maintained in each individual mosquito agent's attribute matrix to draw valuable conclusions. For example, Figure 8.1 shows the locations of adult mosquito eclosion for the 2006 Banizoumbou simulation. Each green circle represents a site where mosquitoes have emerged from pooled water, up to the present time in the simulation. The red circles are a subset of green circles that represent sites from which mosquitoes have emerged and have then gone on to cause at least one new malaria infection. Clearly, the mosquitoes that are ultimately responsible for malaria transmission in Banizoumbou village emerge from breeding habitat within or nearby the village. Beyond several hundred meters, very few emerging mosquitoes ultimately contribute to malaria transmission, even though more distant pools are very productive. Field larval surveys noting high larval abundance

in these pools may give the false impression that these water bodies are as hazardous as the equally productive within-village pools. This demonstrates the capability of the model to predict the locations of the most dangerous breeding sites, and distinguish those from other productive sites in the field which may be incorrectly implicated in exacerbating malaria transmission in the village. Threshold distances are site-specific and must be determined by model application to a particular site of interest. Such simulations are very useful for the design of environmental management scenarios.

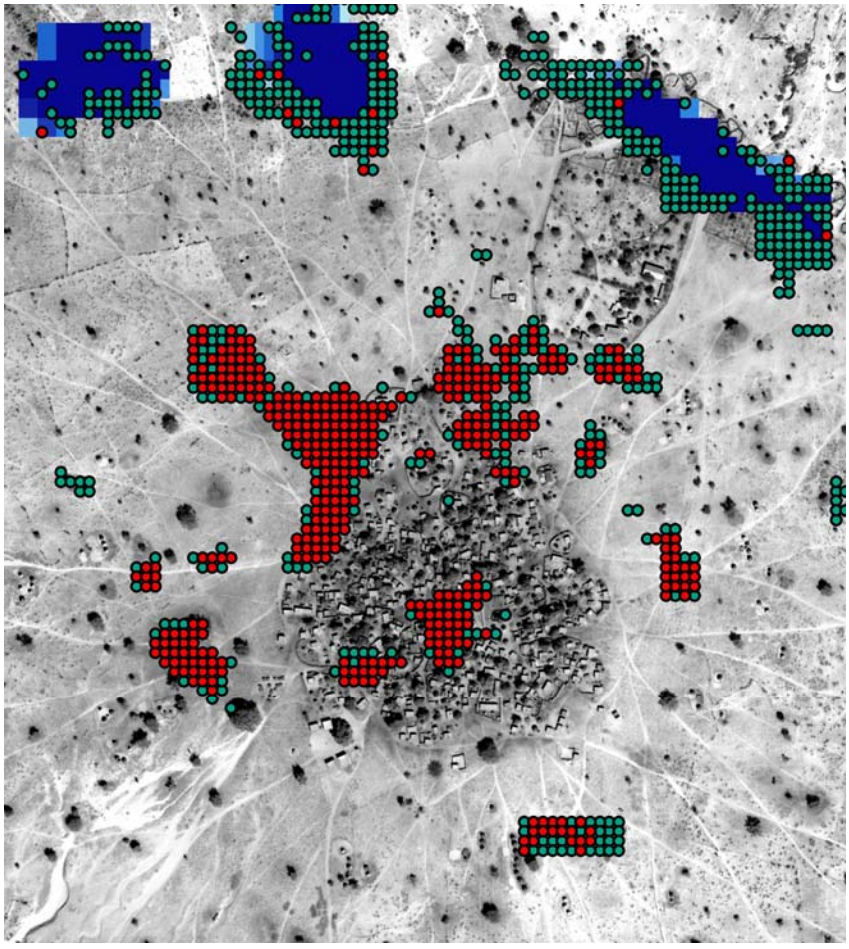

Figure 8-1. A depiction of model results addressing hypothesis 2 around Banizoumbou village. Green circles represent locations of adult mosquito eclosion (emergence) at some point during the 2006 Banizoumbou simulation. Red circles represent locations of adult mosquito eclosion for which at least one of the emergent mosquitoes ultimately caused at least one new case of malaria in Banizoumbou. Distant but equally productive pools may not contribute many transmitting mosquitoes. Thus the importance of pool proximity to human habitation for adding mosquitoes to the transmission system is clearly illustrated.

Hypothesis 3: Mean relative humidity and temperature range during the wet season and sudden transformation of these conditions at the onset of the dry season act as important controls of malaria transmission seasonality. Simulation of population response to change in dominant climate conditions will allow identification of the key governing variables of malaria transmission.

The seasonal variation in vectorial capacity depends on daily survival probability which is temperature-dependent. Daily survival reductions due to high temperature affect malaria transmission, as has been discussed in detail in Chapter 6 in the context of climate shifts. Relative humidity impacts on daily survival have not been built into HYDREMATS because no published model for survival as a function of humidity exists, but it seems likely that low humidity levels may severely stress mosquitoes and raise mortality. Details of this effect remain unknown, and this knowledge gap presents opportunity for further investigation.

Hypothesis 4: Efficacy of various intervention scenarios can be evaluated *a priori* using understanding of spatiotemporal determinants of village-scale malaria transmission.

Several intervention efforts have seen common usage in the fight against malaria, such as insecticide-treated bednets (ITN), indoor residual spraying (IRS), zooprophylaxis, and environmental management through source reduction. All of these directly intervene in the mosquito life cycle at various stages, with ITN and IRS aimed at reduction of adult survivability as well as interruption of human biting. Zooprophylaxis involves deployment of animals near human habitation to divert bites away from humans. Environmental management through source reduction involves identification of water bodies expected to contribute large numbers of mosquitoes, and elimination of those water bodies as viable breeding grounds. This can be accomplished with larvicides or by physical alteration of the microtopography such as pool filling or reshaping the bathymetry to make the pool less persistent or otherwise unfavorable for mosquito breeding. Model tests of altered pool bathymetries were carried out by Rebecca Gianotti and the results of these simulations are described in Gianotti et al. (2008a). Larviciding can be simulated by allowing water to pool in the original depression, but raising larval

mortality rates to reflect the larvicide's effects. Field tests were carried out using aqueous neem extracts during the 2007 wet season in Banizoumbou (Gianotti et al., 2008b). Modeling was not involved in this study, but the reduction of mosquito numbers resulting from larvicide applied to the most dangerous pools is clearly represented. Through computer modeling of the hydrology/entomology system in relation to human habitation, various intervention possibilities (i.e. combinations of the above techniques) can be tested with the model, and as a result an optimal intervention technique can be prescribed for each village. All of the relevant processes necessary to evaluate the effects of interventions are represented by the model.

The coupled model can be used to explore effects of land use change on malaria transmission. Land use changes in the Sahel have been noted with increasing population density. For example, Leduc et al. (2001) noted an unexpected rise in groundwater tables in southwestern Niger over the period of extended drought in the region in the last three decades. This apparently paradoxical result is attributed to land use changes associated with increasing rural population, and more land cleared for millet cultivation. This increases runoff coefficients to allow more runoff to reach topographic low points which in turn results in concentrated infiltration. Leduc et al. (2001) suggest that water distribution into pools is more dependent on land clearing by the rural population than on climate variability. This effect has obvious implications for pool persistence and associated mosquito breeding. With our hydrology model simulating overland flow over an infiltrating surface, such changes can be explicitly evaluated. High-resolution satellite multispectral images will allow the monitoring of such land use changes and assignment of distributed model parameters. Plant functional type assignments for model grid cells affect root zone uptake and vadose zone water redistribution. Water uptake from the root zone will influence infiltration and runoff from subsequent storms. Changes in root zone water uptake, soil crusting, and surface roughness associated with increased cultivated land will likely lead to pronounced variations in malaria prevalence. Future research using the presented model will address these questions.

Model representation of human immunity is an important component of the complete, simulated connection between climate forcing and malaria transmission. The HYDREMATS representation of immunity is simple, in that it groups a multitude of various complicated physiological mechanisms into one overall effect of increased immunity caused by high inoculation rates. The model's simplicity may have drawbacks in that certain processes are not explicitly represented. However, the simple model allows extension of predictive ability beyond environmental variability impacts on vectorial capacity, to malaria prevalence. Chapter 7 explored the use of the immunity model for predicting malaria prevalence and showed that predictions are consistent with various field observations of malaria transmission, in the study villages Banizoumbou and Zindarou as well as elsewhere in Africa. General assessments of increased or decreased malaria burden resulting from perturbations may be made with this model.

Future directions of the mosquito model within HYDREMATS involve refinement of the immunity and parasite transmission model. Variable parasite densities should be represented by the model. In addition, more sophisticated, mechanistic representation of the various effector mechanisms of immunity within human agents may lead to more accurate prediction of malaria prevalence and incidence. More research can address this question. The age structure of malaria prevalence in a population is often closely related to the force of infection for that transmission environment and can have implications on malaria burden of individuals. Age is presently not tracked for individual human agents in the model. An important future development of the HYDREMATS representation of malaria transmission in the human population is the inclusion of human population dynamics, including birth, death, and age advancement of individuals. Longer-term transmission simulations would thus yield valuable results of age distribution of malaria incidence. While general, non-age specific malaria prevalence results can be very informative yet somewhat ambiguous, age distribution can supply much information about force of infection and malaria burden in the population.

The hydrology component of the model involves much input data, and must operate at scales consistent with the characteristic scale of pools typically utilized by the

anophelines responsible for malaria transmission. A primary future direction of the HYDREMATS model development involves assimilation of satellite-derived topography and land cover into a large model domain, and predicting malaria transmission on a more extensive scale consistent with administrative regions. Such extensive simulations would require improved computing efficiency. Code parallelization would benefit simulation efficiency and speed.

HYDREMATS has only been tested and applied in Banizoumbou and Zindarou, Niger. The model is strictly applicable to water-limited environments where *Anopheles gambiae sensu lato* is the dominant malaria vector, such as the desert fringe areas of Africa. Testing and applying the model to other Sahel environments would reinforce the model's utility, as would model application to southern African epidemic zones, such as Botswana, for example. The model is not suitable for other disease vectors that do not share breeding habitat with *An gambiae*, such as the yellow fever vector *Aedes aegypti*.

References

Ahumada, J. A., LaPointe, D., and Samuel, M.D. (2004) Modeling the population dynamics of Culex quinqefasciatus (Diptera: Culicidae), along an elevational gradient in Hawaii. *Journal of Medical Entomology* 41 (6): 1157-1170.

Alberts, B., Johnson, A., Lewis, J., Raff, M., Roberts, K., and Walters, P. (2002). *Molecular Biology of the Cell; Fourth Edition*. New York and London: Garland Science.

Amani, A. and Lebel, T. (1996). Typology of rainfall fields to improve rainfall estimation in the Sahel by the area threshold method. *Water Resour. Res.* **32** (8). pp. 2473–2487.

Ameneshewa B., and Service, M. W. (1996). The relationship between female body size and survival rate of the malaria vector *Anopheles arabiensis* in Ethiopia. *Medical and Veterinary Entomology*. **10**:170–172.

Appawu, M., Owusu-Agyei, S., Dadzie, S., Asoala, V., Anto, F., Koram, K., Rogers, F.N., Hoffman, S.L., Fryauff D.J. (2004) Malaria transmission dynamics at a site in northern Ghana proposed for testing malaria vaccines. *Tropical Medicine & International Health* **9**(1). 164–170.

Baup, F., Mougin, E., de Rosnay, P., Timouk, F., and Chênerie, I. (2007). Surface soil moisture estimation over the AMMA Sahelian site in Mali using ENVISAT/ASAR data. *Remote Sensing of Environment* 109:473-481.

Bayoh, M.N., and Lindsay, S.W. (2004). Temperature-related duration of aquatic stages of the Afrotropical malaria vector mosquito Anopheles gambiae in the laboratory. *Medical and Veterinary Entomology* 18: 174-179.

Beier, J.C., Oster, C.N., Onyang, F.K., Bales, J.D., Sherwood, J.A., Perkins, P.V., Chumo, D.K., Koech, D.V., Whitmire, R.E., Roberts, C.R., Diggs, C.L., and Hoffman, S.L. (1994). *Plasmodium falciparum* incidence relative to entomologic inoculation rates

at a site proposed for testing malaria vaccines in western Kenya. *American Journal of Tropical Medicine and Hygiene* **50**:529-536.

Bouma, M.J. and van der Kaay, H.J. (1996) The El Niño Southern Oscillation and the historic malaria epidemics on the Indian subcontinent and Sri Lanka: an early warning system, *Tropical Medicine and International Health* **1** (1996), pp. 86–96.

Bouma, M.J., Poveda, G. and Rojas, W. (1997) Predicting high-risk years for malaria in Colombia using parameters of El Niño southern oscillation. *Tropical Medicine and International Health* **2**:1122–1127.

Bowden, J., and Church, B.M. (1973). The influence of moonlight on catches of insects in light-traps in Africa. Part 2. The effect of moon phase on light-trap catches. *Bulletin Entomology Research.* **63**. pp. 129-142.

Boyer, L. (2003). Rapport de Projet Pluridisciplinaire. Ecole Nationale des Sciences Geographiques. Marne-la-Vallee, France.

Bruce-Chwatt, L.J. (1963). A longitudinal survey of natural malaria infection in a group of West African adults. *West African Journal of Medicine* **12**:199-217.

Campbell, G.S. (1985). Soil physics with BASIC. Elsevier, New York.

Campbell, G.S. and Norman, J.M. (1998). Introduction to Environmental Biophysics. Springer Verlag, New York.

Casenave, A. and Valentin, C. (1992). A runoff capability classification system based on surface features criteria in semi-arid areas of West Africa. *Journal of Hydrology* **130**(1): 231-249.

Charlwood J. D., Kihonda J., Sama S., Billingsley P. F., Hadji H., Verhave J. P., Lyimo E., Luttikhuizen P. C., and Smith T. (1995) The rise and fall of *Anopheles arabiensis* (Diptera: Culicidae) in a Tanzanian village. *Bull. Entomol. Res.* . **85**:37–44.

Claussen, M. (1998). On multiple solutions of the atmosphere-vegetation system in present-day climate. *Global Change Biology* **4**:549-59.

Clements, A.N., (1963) The Physiology of Mosquitoes. Pergamon Press, New York.

Clerget B, Haussmann, B.I.G., Boureima, S.S. and Weltzien E., (2007) Surprising flowering response to photoperiod: Preliminary characterization of West and Central African pearl millet germplasm. *Journal of SAT Agricultural Research* 5(1).

Coluzzi, M., Sabatini, A., Petrarca, V., Di Deco, M.A. (1979) Chromosomal differentiation and adaptation to human environments in the *Anopheles gambiae* complex. *Transactions of the Royal Society of Tropical Medicine and Hygiene*, **73**: 483-497.

Costantini, C., Gibson, G., Sagnon, N., Della Torre, A., Brady, J., and Coluzzi, M. (1996a). Mosquito responses to carbon dioxide in a west African Sudan savanna village. *Medical and Veterinary Entomolgy,* **10** (3), 220-227.

Costantini, C., Li, S., Della Torre, A., Sagnon, N., Coluzzi, M., and Taylor, C.E. (1996b). Density, survival, and dispersal of *Anopheles gambiae* complex mosquitoes in a West African Sudan savanna village. *Medical and Veterinary Entomology* **10**:203-219

Costantini, C., Sagnon, N.F., della Torre, A., Diallo, M., Brady, J., Gibson, G., and Coluzzi, M. (1998) Odor-mediated host preferences of West African mosquitoes, with particular reference to malaria vectors. *American Journal of Tropical Medicine and Hygiene*. **58**: 56-63.

Craig, M.H., Snow, R.W., and le Sueur, D. (1999) A climate-based distribution model of malaria transmission in sub-saharan Africa. *Parasitology Today* **15**(3):105-111.

D'Amato, N. and Lebel, T. (1998). On the characteristics of the rainfall events in the Sahel with a view to the analysis of climatic variability. *International Journal of Climatology* **18**: 955-974.

Depinay, J. M., Mbogo, C. M., Killeen, G., Knols, B., Beier, J., Carlson, J., Dushoff, J., Billingsley, P., Mwambi, H., Githure, J., Toure, A. M., and McKenzie, F. E. (2004). A simulation model of African *Anopheles* ecology and population dynamics for the analysis of malaria transmission. *Malaria Journal* **3:**29

Desconnets, J.C., B.E. Vieux, B. Cappelaere and F. Delclaux, (1996) A GIS for hydrological modeling in the semiarid, Hapex–Sahel experiment area of Niger, Africa. *Trans. GIS* **1** 2 (1996), pp. 82–94.

Desconnets, J.C., Taupin, J.D., Lebel, T. and Leduc, C. (1997) Hydrology of Hapex-sahel central supersite : surface water drainage and aquifer recharge througt the pool systems *Journal of Hydrology* **188-189:** 155-178.

Detinova, T.S. (1962). Age Grouping Methods in Diptera of Medical Importance. Geneva: World Health Organization.

Detinova, T.S., and Gillies, M.T. (1964). Observations on the determination of the age composition and epidemiological importance of populations of Anopheles gambiae Giles and Anopheles funestus giles in Tanganyika. *Bull. World Health Organ.* **30**:23-28

D'Herbès, J.M., and Valentin, C., (1997). Land surface conditions of the Niamey region: ecological and hydrological implications. *Journal of Hydrology* 188-189: 18-42.

Diuk-Wasser, M.A., Bagayoko, M., Sogoba, N., Dolo, G., Touré, M.B., Traoré, S.F., and Taylor, C.E. (2004). *International Journal of Remote Sensing*. **25**(2):359-376.

Diuk-Wasser, M.A., Touré, M.B., Dolo, G., Bagayoko, M., Sogoba, N., Traoré, S., Manoukis, N., and Taylor, C.E. (2005). Vector abundance and malaria transmission in rice-growing villages in Mali. *American Journal of Tropical Medicine and Hygiene* **72**(6):725-731.

Diuk-Wasser, M.A., Brown, H.E., Andreadis, T.G., and Fish, D.(2006). Modeling the spatial distribution of mosquito vectors for West Nile virus in Connecticut, USA. *Vector-Borne and Zoonotic Diseases*. **6**(3): 283-295.

Duchemin, J.-B., Leong Pock Tsy, J. –M., Rabarison, P., Roux, J., Coluzzi, M., and Costantini, C. (2001) Zoophily of *Anopheles arabiensis* and *An. gambiae* in Madagascar demonstrated by odour-baited entry traps. *Medical and Veterinary Entomology* **15** (1): 50–57.

Eisele, T.P., Keating, J., Swalm, C., Mbogo, C.M., Githeko, Andrew K., Regens, J.L., Githure, J.I., Andrews, L., and Beier, J.C. (2003). Linking field-based ecological data with remotely sensed data using a geographic information system in two malaria endemic urban areas of Kenya. *Malaria Journal* **2**(44)

Foley, J.A., Coe, M.T., Scheffer, M., and Wang, G. (2003) Regime shifts in the Sahara and Sahel: Interactions between ecological and climatic systems in northern Africa. *Ecosystems* **6**:524-539.

Gagnon, A.S., Bush, A.B.G. and Smoyer-Tomic, K.E. (2001) Dengue epidemics and the El Niño Southern Oscillation, *Climate Research* **19**:35–43.

Gagnon, A.S., Smoyer-Tomic K.E. and Bush, A. (2002) The El Niño southern oscillation and malaria epidemics in South America, *International Journal of Biometeorology* **46**:81–89.

Giannini, A., Saravanan, R., and Chang, P. (2003). Oceanic forcing of Sahel rainfall on interannual to interdecadal time scales. *Science* **302**(5647)**:** 1027-1030.

Gianotti, R.L., Bomblies, A., and Eltahir, E.A.B. (2008a) Hydrologic modeling to screen potential environmental management methods for malaria vector control in Niger. *Submitted to Water Resources Research.*

Gianotti, R.L., Bomblies, A., Dafalla, M., Issa-Arzika, I., Duchemin, J-B., and Eltahir, E.A.B. (2008b). Efficacy of local neem extracts for sustainable malaria vector control in an African village. *Malaria Journal* **7**:138.

Gillies, M.T. (1961) Studies on the Dispersion and Survival of Anopheles Gambiae Giles in East Africa: By Means of Marking and Release Experiments. *Bull. Entomol. Res.* **52**: 99–127.

Gillies, M.T., and DeMeillon, B. (1968) The Anophelinae of Africa South of the Sahara. South African Institute of Medical Research, Johannesburg.

Gillies, M.T. (1980). The role of carbon dioxide in host-finding by mosquitoes (Diptera: Culicidae): a review. *Bulletin of Entomological Research*, **70**:525-532.

Gimnig, J.E., Ombok, M., Otieno, S., Kaufman, M.G., Vulule, J.M., and Walker, E.D. (2002). Density-dependent development of *Anopheles gambiae* (Diptera: Culicidae) larvae in artificial habitats. *Journal of Medical Entomology* **39**:162-172.

Gupta, S., Snow, R.W., Donnelly, C.A., Marsh, K., and Newbold, C. (1999) Immunity to non-cerebral severe malaria is acquired after one or two infections. *Nature Medicine* **5**(3):340-343.

Haddow, A.J. (1954). Studies of the biting habits of African mosquitoes: an appraisal of methods employed, with special reference to the twenty-four hour catch. *Bulletin of Entomological Research*. **45**: 199-242.

Hales, S., Weinstein, P., and Woodward, A. (1996) Dengue fever epidemics in the South Pacific region: driven by El Niño Southern Oscillation?, *Lancet* **348**:1664–1665.

Hales, S., Weinstein, P., Souares, Y., Woodward, A. (1999) El Niño and the dynamics of vectorborne disease transmission, *Environmental Health Perspectives* **107**:99–102.

Hay, S.I., Snow, R.W. and Rogers, D.J. (1998). Predicting malaria seasons in Kenya using multitemporal meteorological satellite sensor data. *Transactions of the Royal Society of Tropical Medicine and Hygiene* **92**(12).

Hay, S.I., Cox, J., Rogers, D.J., Randolph, S.E., Stern, D.I., Shanks, G.D., Myers, M.F., and Snow, R.W. (2002). Climate change and the resurgence of malaria in the East African highlands. *Nature* **415**:905-909.

Healy, T.P., and Copland, M.J.W. (1995) Activation of Anopheles gambiae mosquitoes by carbon dioxide and human breath. *Medical and veterinary entomology* **9:** 331-336.

Hoelzmann, P, Jolly, D., Harrison, S.P., Laarif, F., Bonnefille, R., and Pachur, H-J. (1998) Mid-Holocene land-surface conditions in northern Africa and the Arabian peninsula: A dataset for the analysis of biogeophysical feedbacks in the climate system. *Global Biogeochemical Cycles* 12(1):35-51.

Hoogmoed, W.B. and Stroosnijder, L. (1984) Crust formation on sandy soils in the Sahel. I. Rainfall and infiltration. *Soil Tillage Res.* **4**: 5–23.

Horsfall, W.R. (1943) Some responses of the malaria mosquito to light. *Ann. Ent. Soc. Amer.* **36**(1): 41-45.

Horuk, R., Chitnis, C.E., Darbonne, W.C., Colby, T.J., Rybicki, A., Hadley, T.J., and Miller, L.H. (1993). A receptor for the malarial parasite *Plasmodium vivax*: The erythrocyte chemokine receptor. *Science* **261**:1182-1184.

Hoshen, M.B. and Morse, A.P. (2004) A weather-driven model of malaria transmission. *Malaria Journal* **3**(32).

Huffman, G.J., Adler, R.F., Arkin, P., Chang, A., Ferraro, R., Gruber, A., Janowiak, J., McNab, A., Rudolf, B., and Schneider, U. (1997). The Global Precipitation Climatology Project (GPCP) combined precipitation data set. *Bulletin of the American Meteorological Society* **78**:5-20.

Ijumba, J. N., Mwangi, R. W., and Beier, J. C. (1990) Malaria transmission potential of *Anopheles* mosquitoes in the Mwea- Tebere irrigation scheme, Kenya. *Medical and Veterinary Entomology* **4**:425–32.

Irizarry-Ortiz, M., Wang, G., and Eltahir, E.A.B. (2003). Role of the biosphere in the mid-Holocene climate of West Africa. *Journal of Geophysical Research* **108(D2)**, 4042, doi:10.1029/2001JD000989.

Jepson, W.F., Moutia, A., Courtois, C (1947) The malaria problem in Mauritius: The bionomics of Mauritian anophelines. *Bull Entomol Res* **38**:177-208.

Kim, Y., and Eltahir, E.A.B. (2004) Role of topography in facilitating coexistence of trees and grasses within savannahs. *Water Resources Research* **40:** W075005, doi:10:1029/2003WR002578.

Kinsman, R., Sauer, F.D., Jackson, H.A., and Wolynetz, M.S. (1995). Methane and carbon dioxide emissions from dairy cows in full lactation monitored over a six-month period. *Journal of Dairy Science* **78:**2760-2766.

Kiszewski, A. and Teklehaimenot, A. (2004). A review of the clinical and epidemiologic burdens of epidemic malaria. *American Journal of Tropical Medicine and Hygiene*, **71** (Suppl 2):128-135.

Koella J. C., and Lyimo, E. O. (1996). Variability in the relationship between weight and wing length of *Anopheles gambiae* (Diptera: Culicidae). *Journal of Medical Entomology* . **33**:261–264.

Koenraadt, C.J.M., and Takken, W. (2003) Cannibalism and Predation among larvae of the *Anopheles gambiae* complex. *Medical and Veterinary Entomology* 17, 61-66.

Kuhn, K.G., Campbell-Lendrum, D.H., Davies, C.R. (2002). A continental risk map for malaria mosquito (Diptera: Culicidae) vectors in Europe. *Journal of Medical Entomology* **39**(4): 621-630.

Lal, W. (1998). Performance comparison of overland ow algorithms, *J. Hydr. Engrg*., ASCE, **124** (4).

Lamb, P.J. (1978). Case studies of tropical Atlantic surface circulation patterns during recent sub-Saharan weather anomalies: 1967 and 1968. *Monthly Weather Review* **106**(4)**:** 482-491.

Lambot, S., Javaux, M., Hupet, F., and M. Vanclooster (2002) A global multilevel coordinate search procedure for estimating the unsaturated soil hydraulic properties. *Water Resources Research*, **38** (11)

Le Barbé, L. and T. Lebel, (1997). Rainfall climatology of the Hapex–Sahel region during the years 1950–1990. *J. Hydrol.* **188-189:** 43–73.

Lebel, T., Sauvageot, H., Hoepffner, M.,Desbois, M., Guillot, B. and Hubert, P. (1992): Rainfall estimation in the Sahel: The EPSAT-Niger experiment. *Hydrol. Sci. J.,* **37:** 201–215.

Leduc, C., Favreau, G. and Schroeter, P. (2001). Long-term rise in a Sahelian water-table: the Continental Terminal in South-west Niger. *Journal of Hydrology* **243**: 43-54

Le Menach, A., McKenzie, F.E., Flahault, A., and Smith, D.L. (2005) The unexpected importance of mosquito oviposition behaviour for malaria: non-productive larval habitats can be sources for malaria transmission. *Malaria Journal* 4:23

Lindsay, S.W., Alonso, P.L., Schellenberg, J., Hemingway, J., Adiamah, J.H., Shenton, F.C., Jawara, M., Greenwood, B.M. (1993) A malaria control trial using insecticide-treated bed nets and targeted chemoprophylaxis in a rural area of The Gambia, West Africa. 7. Impact of permethrin-impregnated bed nets on malaria vectors. *Transactions of the Royal Society of Hygiene and Tropical Medicine*. **87**:45-51.

Loevinsohn, M.E. (1994) Climatic warming and increased malaria incidence in Rwanda.*The Lancet* **343:**714-718.

Loewenberg, S. (2006) Niger welcomes largest bednet distribution in history. *The Lancet*, **367** (9521): 1473-1473.

MacDonald, G. (1950). The analysis of infection rates in diseases in which superinfection occurs. *Tropical Disease Bulletin* 47:907-915.

Macdonald, G. (1957). The Epidemiology and Control of Malaria. Oxford: Oxford University Press.

Manguin, S. and Boussinesq, M. (1999) Remote sensing in public health: applications to malaria and other diseases. *Medecine et Maladies Infectieuses* **29**(5): 318-324.

Martens, W.J.M. (1997) Health Impacts of Climate Change and Ozone Depletion: an Eco-epidemiological Modeling Approach. Maastricht University.

Martin, P.H., and Lefebvre, M.G. (1995) Malaria and climate—sensitivity of malaria potential transmission to climate. *Ambio* **24**:200–207.

McGregor, I.A. (1987). Malarial immunity: current trends and prospects. *Annals of Tropical Medicine and Parasitology*. **81**(5): 647-656.

Minakawa, N., Mutero, C.M., Githure, J.I., Beier, J.C., and Yan, G. (1999). Spatial distribution and habitat characterization of anopheline mosquito larvae in Western Kenya. *Am. J. Trop Med. Hyg*., **61(6)**:1010-1016.

Minakawa, N., Seda, P. and Yan, G. (2002a). Influence of host and larval habitat distribution on the abundance of African malaria vectors in Western Kenya. *Am. J. Trop. Med. Hyg*., **67(1)**:32-38.

Minakawa, N., Sonye, G., Motoyoshi, M., Githeko, A., and Yan, G. (2002b). The effects of climate factors on the distribution of malaria vectors in Kenya. *Journal of Medical Entomology* **39**(6): 833-841.

Minakawa, N., Sonye, G., Mogi, M., and Yan, G. (2004) Habitat characteristics of *Anopheles gambiae s.s.* larvae in a Kenyan highland. Medical and Veterinary Entomology **18** (3):301–305.

Minakawa, N., Sonye, G., and Yan, G. (2005) Relationships Between Occurrence of *Anopheles gambiae* s.l. (Diptera: Culicidae) and Size and Stability of Larval Habitats *Journal of Medical Entomology* **42** (3):295–300.

Molineaux, L. and Gramiccia, G. (1980). The Garki Project. World Health Organization, Geneva, Switzerland.

Molineaux, L., Muir, D.A., Spencer, H.C., and Wernsdorfer, W.H. (1988). The epidemiology of malaria and its measurement. Wernsdorfer, W.H., McGregor, I. Eds. *Malaria, Principles and Practices of Malariology*. Edinburgh: Churchill Livingstone, 999-1089.

Muriu, S.M., Muturu, E.J., Shililu, J.I., Mbogo, C.M., Mwangangi, J.M., Jacob, B.G., Irungu, L.W., Mukabana, R.W., Githure, J.I., and Novak, R.J. (2008). Host choice and multiple blood feeding behaviour of malaria vectors and other anophelines in Mwea rice scheme, Kenya. *Malaria Journal* **7**:43.

Mutuku FM, Alaii JA, Bayoh MN, Gimnig, J.E., Vulule, J.M., Walker, E.D., Kabiru, E., and Hawley, W.A. (2006) Distribution, description, and local knowledge of larval habitats of *Anopheles gambiae s.l.* in a village in western Kenya. *American Journal of Tropical Medicine and Hygiene* **74**:44–53.

Nicholson, S.E. (2000) The nature of rainfall variability over Africa on time scales of decades to millenia. *Global and Planetary Change* **26**:137-158.

Nihei, N., Hashida, Y., Kobayashi, M., and Ishii, A. (2002) Analysis of malaria endemic areas on the Indochina Peninsula using remote sensing. *Japanese Journal of Infectious Diseases* **55**(5): 160-166.

Okech, B.A., Gouagna, L.C., Killeen, G.F., Knols, B.G., Kabiru, E.W., Beier, J.C., Yan, G., and Githure, J.I. (2003). Influence of Sugar Availability and Indoor Microclimate on Survival of *Anopheles gambiae* (Diptera: Culicidae) Under Semifield Conditions in Western Kenya. *J. Med. Entomol.* **40**(5): 657-663.

Pascual M, and Dobson A (2005) Seasonal Patterns of Infectious Diseases. *PLoS Med* **2(1)**:

Pascual, M., Ahumada, J.A., Chaves, L.F., Rodo, X., and Bouma, M. (2006) Malaria resurgence in the East African Highlands: temperature trend revisited. *PNAS* **103**(15)

Patz, J.A., Strzepek, K., Lele, S., Hedden, M., Greene, S., Noden, B., Hay, S., Kalkstein, L., and Beier, J.C. (1998). Predicting key malaria transmission factors, biting and entomological inoculation rates, using modeled soil moisture in Kenya. *Tropical Medicine and International Health* **3**(10): 818-827.

Peugeot, C., Cappelaere, B., Vieux, B.E., Seguis, L., and Maia, A. (2003). Hydrologic process simulation of a semiarid, endoreic catchment in Sahelian West Niger. 1. Model-aided data analysis and screening. *Journal of Hydrology*, 279, 224-243.

Pollard, D. and Thompson, S.L. (1995) Use of a land-surface-transfer scheme (LSX) in a global climate model: the response to doubling stomatal resistance. *Global and Planetary Change*, **10**: 129–161.

Poveda, G., Rojas, W., and Quinones M. (2001). Coupling between annual and ENSO timescales in the malaria climate association on Colombia, *Environmental Health Perspectives.* **109**:307–324.

Pratt, H.D. (1948) Influence of the moon on light trap collections of Anopheles albimanus in Puerto Rico. *Jour. Natl. Malaria Soc*. **7**: 212-220.

Rogers, D.J., Randolph, S.E. (2000) The global spread of malaria in a future, warmer world. *Science* **289**:1763–1766.

Ross, R. (1911). The Prevention of Malaria, 2nd edition. London: Murray.

Service, M.W. (1977). Mortalities of the immature stages of species B of the *Anopheles gambiae* complex in Kenya: Comparison between rice fields and temporary pools, identification of predators, and effects of insecticidal spraying. *Journal of Medical Entomology* **13:**535-545.

Service, M.W. (1993). Mosquito Ecology. Field Sampling Methods, 2nd edn. Elsevier Applied Sciences, London, UK.

Shaman, J., Stieglitz, M., Stark, C., Le Blancq, S., and Cane, M. (2002a). Using a dynamic hydrology model to predict mosquito abundances in flood and swamp water. *Emerging Infectious Diseases* **8**:6-13.

Sharpe, P.J.H., and DeMichele D. W. (1977). Reaction kinetics of poikilotherm development. *Journal of Theoretical Biology* **64**:649–670.

Shaman, J., Stieglitz, M., Stark, C., Le Blancq, S., Cane, M. (2002a) Predicting flood and swampwater mosquito abundances using a dynamic hydrology model. *Emerging Infectious Diseases*; **8:**6-13.

Shaman, J., Day, J.F., and Stieglitz, M. (2002b). Drought-induced amplification of Saint Louis encephalitis virus, Florida. *Emerging Infectious Diseases* **8**(6):575-580.

Shanks, G.D., Hay, S.I., Stern, D.I., Biomndo, K., Snow, R. (2002). Meteorologic influences on *Plasmodium falciparum* malaria in the highland tea estates of Kericho, western Kenya. *Emerging Infectious Diseases* **8**(12):1404-1408.

Singh, N. and Sharma, V.P. (2002). Patterns of rainfall and malaria in Madhya Pradesh, central India. *Annals of Tropical Medicine and Parasitology* **96**(4):349-359.

Smith, M.E. (Ed.) (1968) Recommended Guide for the Prediction of the Dispersion of Airborne Effluents, American Society of Mechanical Engineers, New York.

Snow, R.W., Omumbo, J.A., Lowe, B., Molyneux, C., Obiero, J.O., Palmer, A., Weber, M.W., Pinder, M., Nahlen, B., Obonyo, C., Newbold, C., Gupta, S., and Marsh, K. (1997). Relation between severe malaria morbidity in children and level of *Plasmodium falciparum* transmission in Africa. *Lancet* **349**(9066):1650-4

Snow, R.W., Craig, M., Deichmann, U., and Marsh, K. (1999) Estimating mortality, morbidity, and disability due to malaria among Africa's non-pregnant population. *Bulletin of the World Health Organization* **77**:624-640.

Snow, R.W., Marsh, K.E. (2002). The consequences of reducing transmission of *Plasmodium falciparum* in Africa. *Advances in Parasitology* **52**:235-264.

Struik, S.S., and Riley, E.M. (2004) Does malaria suffer from lack of memory? *Immunological Reviews* **201**:268-290.

Sutherst, R.W., (2004). Global change and human vulnerability to vector-borne diseases. *Clinical Microbiology Reviews* **17**(1): 136-173.

Takken, W. and Knols, B. (1999) Odor-mediated behavior of afrotropical malaria mosquitoes. *Annu. Rev. Entomol*. **44**: 133-157

Talbot, M.R., (1980). Environmental responses to climatic change in the west african Sahel over the past 20 000 years. in: "The Sahara and the Nile, quaternary environments and prehistoric occupation in northern Africa", 37-62. Balkema ed., Rotterdam, Netherlands.

Taylor, C. E., Touré, Y. T., Carnahan, J., Norris, D. E., Dolo, G., Traoré, S. F., Edillo, F. E., and Lanzaro, G. C. (2001). Gene flow among populations of the malaria vector, Anopheles gambiae, in Mali, West Africa. *Genetics*. **157**: 743-750.

Teklehaimenot, H.D., Schwartz, J., Teklehaimenot, A., and Lipsitch, M. (2004). Weather-based prediction of *Plasmodium falciparum* malaria in epidemic-prone regions of Ethiopia II. Weather-based prediction systems perform comparably to early detection systems in identifying times for interventions. *Malaria Journal* **3**:44

Thomas, C.J. and Lindsay, S.W. (2000). Local-scale variation in malaria infection amongst rural Gambian children estimated by satellite remote sensing. *Transactions of the Royal Societyof Tropical Medicine and Hygiene* **94**(2):159-163.

Thomas, C.J., Davies, G. and Dunn, C.E. (2004) Mixed picture for changes in stable malaria distribution with future climate in Africa, *Trends in Parasitology* **20:**216–220

Thomson, M.C., Connor, S.J., Milligan, P. and Flasse, S.P. (1997) Mapping malaria risk in Africa: What can satellite data do? *Parasitology Today* **13:**313.

Thomson, M.C., Connor, S.J., Ward, N.J., and Molyneux, D. (2004) Impact of climate variability on infectious disease in West Africa. *EcoHealth* **1**: 138-150.

Thomson, M.C., Doblas-Reyes, F.J., Mason, S.J., Hagedorn, R., Connor, S.J., Phindela, T., Morse, A.P. and Palmer, T.N. (2006). Malaria early warnings based on seasonal climate forecasts from multi-model ensembles. *Nature* **439**: 576-579.

Toutin, T., and Gray, L. (2000). State-of-the-art of elevation extraction from satellite SAR data. *ISPRS Journal of Photogrammetry and Remote Sensing*. **55:** 13-33.

Tucker, C.J., Townshend, J.R.G. and Goff, T.E. (1985). African land cover classification using satellite data. *Science* **227**:369.

Vandervaere, J.-P., Peugeot, C., Vauclin, M., Angulo Jaramillo, M., and Lebel, T. (1997). Estimating hydraulic conductivity of crusted soils using disc infiltrometers and mini tensiometers. *Journal of Hydrology* **188-189**: 203-223.

Walker, E.D., and Merritt, R.W. (1993). Bacterial enrichment in the surface microlayer of an *Anopheles quadrimaculatus* (Diptera: Culicidae) larval habitat. *Journal of Medical Entomology* **30**:1050-1052.

Wang, G., and Eltahir, E.A.B. (2000) Ecosystem dynamics and the Sahel drought. *Geophysical Research Letters* **27**:95-98

Wegbreit, J., and Reisen, W.K. (2000). Relationships among weather, mosquito abundance, and encephalitis virus activity in California: Kern County 1990-1998. *Journal of the American Mosquito Control Association* **16**(1): 22-27.

Weller, U. (2003). Land evaluation and land use planning for Southern Benin (West Africa) – BENSOTER. http://ibb.gsf.de/homepage/ulrich.weller/Diss/node289.html

White, G.B. (1974). Anopheles gambiae complex and disease transmission in Africa. *Transactions of the Royal Society of Tropical Medicine and Hygiene,* **68** (4), 278-301.

World Health Organization, 2005. World Malaria Report. http://rbm.who.int/wmr2005/html/1-2.htm, Geneva.

Ye-Ebiyo, Y., Pollack, R. J., Kiszewski, A., and Spielman, A. (2003) Enhancement of development of larval *Anopheles Arabiensis* by proximity to flowering maize (*Zea Mays*) in turbid water and when crowded. *Am. J. Trop. Med. Hyg*. **68(6)**: 748-752

Yeh, P., and Eltahir, E.A.B. (2003). Representation of water table dynamics in a land surface scheme. Part I: Model development. *Journal of Climate* **18**(12):1861-1880.